CHALMERS

Pedestrian timber bridges with glulam beams and LVL deck

Master's Thesis in the International Master's Programme in Structural Engineering

STEFANO BATTOCCHI
ANDREA POLASTRI

Department of Civil and Environmental Engineering
Division of Structural Engineering
Steel and Timber Structures
CHALMERS UNIVERSITY OF TECHNOLOGY
Göteborg, Sweden 2006
Master's Thesis 2006:12

Pedestrian timber bridges
with glulam beams and LVL deck

Master's Thesis in the International Master's Programme in Structural Engineering

STEFANO BATTOCCHI

Andrea Polastri

Department of Civil and Environmental Engineering
Division of Structural Engineering
Steel and Timber Structures
CHALMERS UNIVERSITY OF TECHNOLOGY
Göteborg, Sweden 2006

Pedestrian bridges with glulam beams and LVL deck

Master's Thesis in the International Master's Programme in Structural Engineering
STEFANO BATTOCCHI

ANDREA POLASTRI

Cover:
Pedestrian timber bridge designed and assembled by Moelven Töreboda AB

Pedestrian bridges with glulam beams and LVL deck
Master's Thesis in the International Master's Programme in Structural Engineering
STEFANO BATTOCCHI

ANDREA POLASTRI

Department of Civil and Environmental Engineering
Division of Structural Engineering
Steel and Timber Structures
Chalmers University of Technology

ABSTRACT

In the last 30 years pedestrian timber bridges have been used more and more both for principal roads and for urban traffic roads, thank to their availability, economic efficiently, good durability and pleasing external appearance. All these qualities could be achieved on one side thank to nowadays well-known technologies like glued laminated timber, and on the other side by adopting construction techniques, connection and assembling systems, and products for the protection of wood more and more efficient.

This thesis deals with pedestrian timber bridges, and in particular it focuses on the study of a new kind of bridge composed by two simple supported glulam beams and a deck in plywood that are glued together in order to form a composite section. The technical innovation is represented by the choice of timber product used for the deck. Panels of Laminated Veneer Lumber (LVL), which belongs to the family of plywood, are glued over the glulam beams. These boards are utilized as slab elements, and for this reason particular attention should be paid on the effects of concentrated loads applied over the deck since the planar shear strength is very low for these materials. An important aspect for this bridge is that it is entirely assembled in the factory; the structure can be built following a standard, economical and well-controlled procedure.

This thesis is divided in three parts. The first part describes different kind of problems concerning timber bridges, in order to relate them to the particular bridge object of our study. In the second part the design of the bridge is carried out. The verifications in the ULS and SLS are based on the EC5 and then compared to the Swedish Codes BKR2003 and BRO2004. The differences between the codes are commented in details. The last third part deals with the results of the finite element analysis performed by the computer programmes Abaqus® and SAP2000®. The aim of these investigations is both to have a confirmation that the simplified schemes adopted in hand calculations are correct and on the safe side, and to make a realistic analysis of the mechanical response either of the entire structures or its individual components, in the various significant load combinations. The pedestrian bridge is designed and built in order to respond to severe load caused by a service vehicle: the effects of this concentrated load that acts over the deck of the bridge can not be solved by simplified hand calculations, and finite element models must be developed to get a correct solution. The finite element models are described in details and possible future research studies and improvements for the bridge are suggested.

Key words: Timber bridge, glulam, plywood and LVL timber products, glued connections, loading wheel tread, mechanical slab behaviour.

II

Ponti pedonali in legno con travi lamellari e soletta in LVL
Master's Thesis in the International Master's Programme in Structural Engineering
STEFANO BATTOCCHI
ANDREA POLASTRI
Dipartimento di Ingegneria Civile ed Ambientale
Division of Structural Engineering
Steel and Timber Structures
Chalmers University of Technology

ABSTRACT

Negli ultimi trent'anni ponti e passerelle pedonali in legno hanno trovato largo impiego sia lungo importanti vie di comunicazione che in ambiente urbano grazie alla loro versatilità, economicità, buona durabilità e apprezzabile aspetto estetico. Tutto ciò, da un lato, in seguito all'impiego di materiali e tecnologie ormai assodate, come il legno lamellare, e dall' altra grazie all'utilizzo di tecniche di costruzione, sistemi di connessione e assemblaggio, prodotti per la protezione del legno sempre più efficienti, sicuri ed economici.

La tesi tratta il tema dei ponti in legno, e in particolare lo studio di un nuovo tipo di ponte pedonale composto da due travi lamellari in semplice appoggio e un impalcato in compensato incollati fra loro per formare una sezione composta a completa interazione di lunghezza 15m e larghezza 2,5m. L'innovazione tecnica è rappresentata dalla scelta del materiale usato per l'impalcato : pannelli di LVL. Questi pannelli sono utilizzati come elementi a piastra, e per questa ragione un'attenzione particolare deve essere rivolta allo studio degli effetti di carichi concentrati agenti sulla soletta, data la bassa resistenza a taglio della stessa in direzione ortogonale alle fibre. Va inoltre menzionato che il ponte è completamente assemblato in stabilimento; la struttura potrà quindi essere realizzata secondo una procedura standard economica e controllata attentamente nelle varie fasi di costruzione.

La tesi è divisa in tre parti. Inizialmente vengono descritte le caratteristiche e le problematiche che possono presentarsi durante il progetto, la realizzazione e la fase di esercizio dei ponti in legno, per poi focalizzare l'attenzione in particolare sulla passerella oggetto di questa tesi. Nella seconda parte viene sviluppato il progetto della struttura. Sono state eseguite le verifiche allo Stato Limite Ultimo e allo Stato Limite di Servizio, mettendo in luce le differenze riscontrate fra la normativa europea e quella svedese. Si presentano infine i modelli agli elementi finiti elaborati tramite i programmi Sap2000® e Abaqus®. Lo scopo di queste ultime analisi numeriche è stato avere conferma che i risultati ottenuti tramite schemi di calcolo semplificati fossero corretti e a favore di sicurezza. Si è reso necessario lo studio della struttura con complessi modelli tridimensionali per determinare in modo attendibile lo stato tensionale e deformativo del ponte nelle varie configurazioni di carico e in particolare nel caso di alti carichi concentrati asimmetrici dati dal transito di eventuali mezzi di servizio. I risultati ottenuti sono stati descritti in dettaglio e sono stati suggeriti possibili ricerche e sviluppi futuri.

IV

Contents

Preface

This master thesis was carried out from August 2005 to February 2006 at the Division of Structural Engineering, Department of Civil and Environmental Engineering at Chalmers University of Technology in Göteborg, Sweden.

This thesis was also written under the supervision of Professor Maurizio Piazza , University of studies of Trento, Faculty of Engineering, Department of Mechanical and Structural Engineering.

First of all, we would like to thank our supervisor Dr. Eng. Roberto Crocetti, engineer at MOELVEN Töreboda AB, Sweden, for proposing the subject of the thesis and assisting us throughout the work. We would like to thank him also for the possibility of visiting the factory and having the opportunity to take part of the design of the bridge, object of this thesis, completed and presented publicly in November 2005.

This master's thesis was a great opportunity to improve our knowledge about timber structures. In particular, it was interesting to complete this thesis in Sweden where timber is ordinary used as building material.

We would like to express our gratefulness to Professor Robert Kliger, examiner of this thesis, for his support and all the literature borrowed from him.

We would also like to thank Assistant Professor Mohammad Al-Emrani for his useful help and Kamyab Zandi Hanjari, our opponent, for his help and comments on the thesis.

This Thesis gave us the possibility to make a great international experience and to meet people from all over the world. We would like to thank all these people for the great time we spent together.

Our gratitude also goes to our parents and relatives for their support during all our stay in Sweden.

Göteborg February 2006

Stefano Battocchi

Andrea Polastri

Notations

Roman upper case letters

A	Area of cross-section
E_{GL32c}	Glulam beam modulus of elasticity
$E_{kerto-S®}$	Kerto-S® longitudinal modulus of elasticity
$E_{kerto-Q®}$	Kerto-Q® longitudinal modulus of elasticity
$E_{0,mean}$	Mean value of modulus of elasticity
F_n	Normal force
F	Point load
G_{GL32c}	Glulam beam shear modulus
$G_{kerto-Q®}$	Kerto-Q® shear modulus
$G_{kerto-S®}$	Kerto-S® shear modulus
I	Moment of inertia of the transformed section
L	Length of the bridge span
M	Bending moment
P	Wheel load
R	Reaction at the support
S_x	First moment of area of the shear plane at the level of consideration
V	Shear force
W	Width of the bridge

Roman lower case letters

a_{RMS}	Vertical acceleration
b_{beam}	Glulam beam width

b_{deck}	Width of the deck
b_{ef}	Effective width of the flange
$b_{kerto\text{-}S®}$	Kerto-S® width
f_{c0d}	Design compressive strength along the grain
f_{c90d}	Design compressive strength perpendicular to the grain
f_{md}	Design bending strength
f_n	Natural frequency
f_{td}	Design tensile strength along the grain
f_{t90d}	Design tensile strength perpendicular along the grain
f_{vd}	Design value of the longitudinal shear stress
h_w	Height of the web
k_{def}	Factor taking into account the increase in deformation with time
k_{mod}	Modification factor for duration of load and moisture content
n	Homogenization factor
m	Total mass of the bridge per unit length
q_g	Self weight distributed load
q_p	Permanent distributed load
q_v	Live distributed load
q_s	Snow distributed load
$t_{kerto\text{-}Q®}$	Thickness of the Kerto-Q deck
$t_{kerto\text{-}S®}$	Thickness of the Kerto-S strip
x	Neutral axis distance from the bottom side

Greek lower case letters

α	Angle
γ	Safety coefficient

γ_M	Partial factor for material properties
δ	Deflection
ρ	Density
σ_{11}	Design bending transversal stress
σ_{22}	Design compression stress
σ_{33}	Design bending longitudinal stress
τ_{12}	Design shear flatwise stress in 12 direction
τ_{12}	Design shear flatwise stress in 23 direction

1 General introduction on timber bridges

1.1 Problem description

1.1.1 Background

In the last 30 years pedestrian timber bridges have been used more and more both for principal roads and for urban traffic roads, thank to their availability, economic efficiently, good durability and pleasing external appearance. All these qualities could be achieved on one side thank to nowadays well-known technologies like glued laminated timber or the use of simple safe static systems, and on the other side by adopting construction techniques, connection and assembling systems, and products for the protection of wood more and more efficient.

The theme of this thesis work is the study of a new kind of concept for pedestrian bridges, which could be used even for traffic road bridges adopting suitable modifications. The structure is composed by two simple supported glulam beams and a deck in plywood that are glued together in order to form a composite π-section (see Figure 1.1).
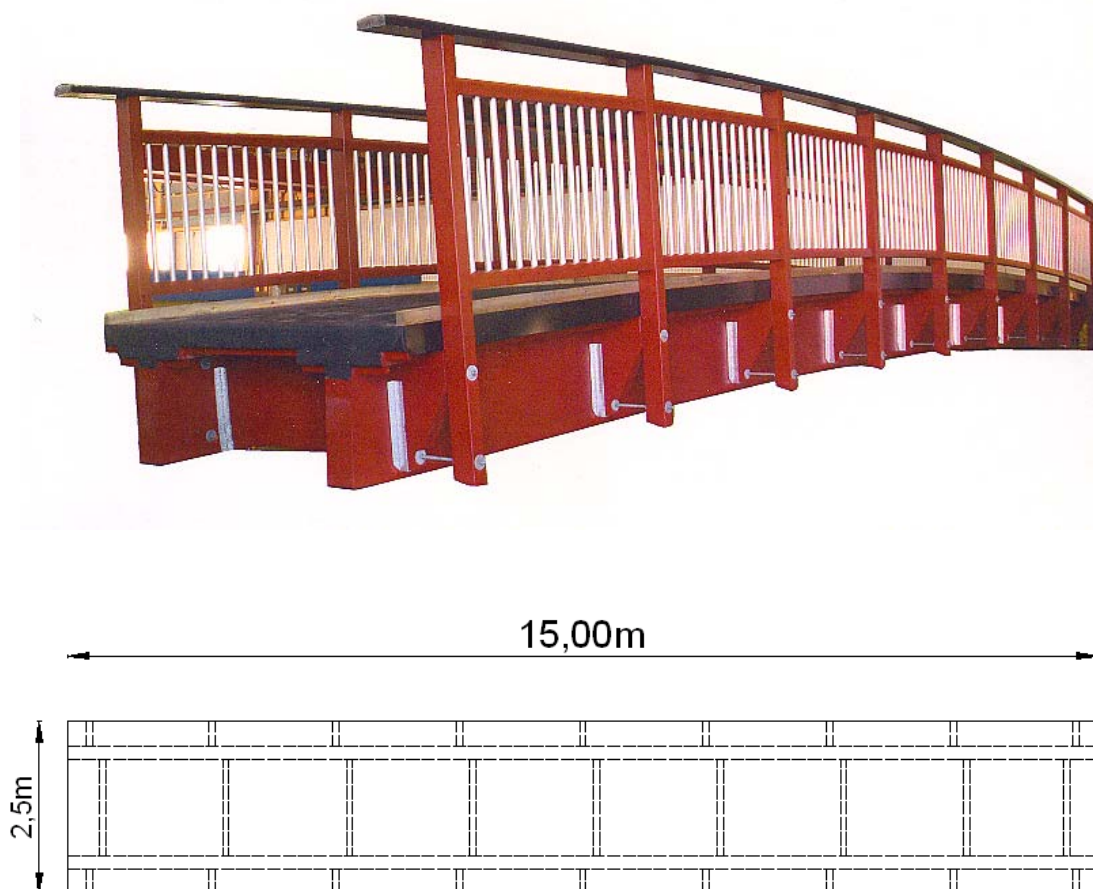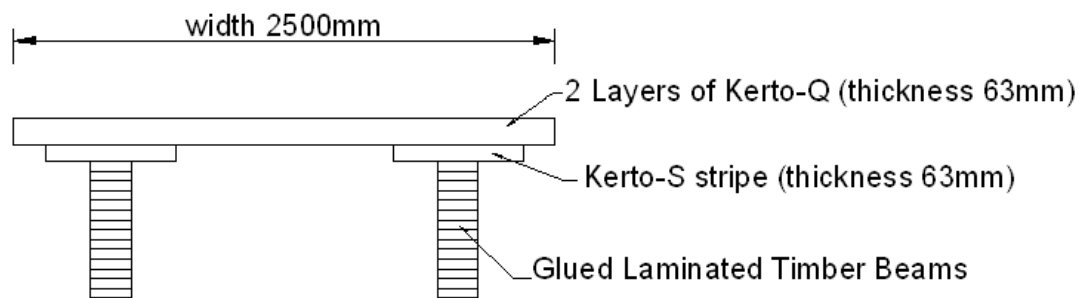
Figure 1.1   Picture of the complete bridge analysed in this thesis work, schematic drawings of the plan and the cross-section of the bridge, Moelven Törebode AB (2005)

The main characteristic of this kind of bridge is that it is entirely assembled in the factory, and then transported on the construction site where it is positioned by using cranes over the abutments previously arranged. In this way the construction period is extremely reduced. The assembling phase occurs under optimal conditions because the work is carried out inside the factory; for the same reason glulam beams and the deck are glued under control temperature and humidity.

The bridge analysed is quite innovative in the field of timber pedestrian bridges. Concerning the construction system, it can be considered as a prefabricated structure that a generic customer can find totally ready to be used. From the structural point of view the technical innovation is represented by the choice of timber product to use for the deck. Panels of Laminated Veneer Lumber (LVL), which belongs to the family of plywood, are glued to the glulam beams in order to form a composite section with full interaction between the two parts. Furthermore, the LVL panels are utilized as slab elements, in the flatwise mode, and for this reason particular attention should be paid on the effects of concentrated loads applied over the deck since the planar shear strength is very low for these materials.

The bridge is exposed to the surrounding atmospheric conditions, therefore special attention is paid to protect the structural timber members and guarantee an appropriate durability of the structure. This can be obtained covering the structural elements, adopting modern chemical additives to protect wood from biotic attacks, and taking care about construction details like mechanical joints and the supports.

1.1.2   Aims of the thesis and limitations

The subject of this thesis is to analyse a pedestrian bridge 2,5m wide and with a span of 15m, made of two simply supported glulam beams that form a composite section with the plywood deck whose dimensions are 15m x 2,5 m and 126mm thick. In the final design, the longitudinal profile of the bridge is slightly curved with a radius of curvature R = 86,37m.

The aim is to understand the structural behaviour of the bridge under different load combination, with particular attention to asymmetrical load configurations.

It will be interesting the study of the mechanical behaviour of the deck, which is made of a single plywood panel, concerning both local stress problems and the interaction with beams and transversal units.

The design of the bridge will be performed following Eurocode 5 (EC5, Anon. 2004). A basic assumption for this structure it has been supposed: there is a full interaction between the beams and the deck, and no slip occurs between the different parts of this composite section. In the first part special attention will be paid in order to find the load combination that maximizes the actions in the critical sections: in the middle span and at supports. Horizontal loads and their effects will not be analysed, because they are considered not important for this kind of bridge. A comparison between EC5 and Swedish codes BKR (Anon. 2003) and BRO (Anon. 2004b) will be carried out to understand accurately how loads, design values and Serviceability Limit State (SLS) verifications are defined. In particular, differences between the codes will be checked. Besides the design of the bridge of 15m span, in this part particular emphasis is given to understand the different stress distribution produced by different load combination in the plywood deck, which acts as a slab. Furthermore, bridges with similar section but longer span will be studied by simple hand calculations.

The structural system of the bridge is very simple, and in case of symmetrical load distribution it can be solved by using simple calculations. Nonetheless, since the composite section belongs to the group of glued thin-flanged T-section beams, it is important to know the realistic value of the effective flange width. The correct value of the effective flange width can be defined comparing the results obtained by models developed by Finite Element software with the hand calculation results.

Finally, problems due to asymmetrical load combination have been studied by using FE models. The curvature of the longitudinal profile of the bridge is not taken into account in the models, because the influence it has on the results is negligible. The service vehicle load represents a severe action for the bridge, and especially for the deck, because it causes, both locally and globally, high stress and deformations. The scope of the analysis is to understand the mechanical response of the deck, the mechanism of the load distribution from the top surface of the deck, where the load is applied, to the glulam beams below, and global deformation of the whole structure. The critical points where significant problems may occur due to the passage of the service vehicle will be highlighted.

A buckling analysis of the beams is not performed: the glued connection with the deck it is considered enough resistant to avoid buckling problems. Also local instability problems of the plywood slab are not analysed. Abutments and foundation of the bridge are not studied in this thesis; the effects of seismic loads on the structure have not been investigated.

1.1.3 Outlines

This thesis is divided in three parts. The first part (from Chapter 1 to Chapter 4) describes different kind of problems concerning timber bridges, in order to relate them to the particular bridge object of our study. Chapter 1 presents general problems related to timber pedestrian bridges like manufacturing, assembling and durability problems. Chapter 2 treats in details the materials typically used for such this kind of structures, first of all Glued Laminated Timber Beams. Typical materials used for the

deck are then analysed, focusing on LVL (Laminated Veneer Lumber) products, because these are the ones adopted for our particular bridge. In Chapter 3 the study of a classification of timber bridges based on the static system is carried out in order to point out the significant problems related to our bridge and the aspects that mostly influence the design. Chapter 4 introduces the particular bridge object of our study, trying to relate it to the information gathered in the beginning three chapters.

In the second part (Chapter 5) the design and verifications of the bridge is described. The calculations concerning design strengths of materials, loads acting on the bridge and significant load combinations, and verifications in the ULS and SLS are based on the EC5 and then compared to the Swedish Codes BKR and BRO. Divergences between the two codes have been found, especially regarding the definition of the design strength of materials. The differences between the codes are commented in details. The calculations in this Chapter are performed by hand calculations, and some simplifications have been assumed. The results are therefore compared to those found by finite element models of the bridge carried out with the commercial Finite Element programmes Abaqus® and SAP2000®.

The last third part (Chapter 6, 7 and 8) deals with the results of the finite element analysis performed by the computer programmes Abaqus® and SAP2000®. The aim of these investigations is both to have a confirmation that the simplified schemes adopted in hand calculations are correct and on the safe side, and to make a realistic analysis of mechanical response either of the entire structures or its individual components, in the various significant load combinations. The pedestrian bridge is design in order to respond to severe load caused by a service vehicle: the effects of this concentrated loads that acts over the deck of the bridge can not be solved by the simplified models adopted in Chapter 5, and finite element models were developed to get a realistic solution. In Chapter 6 the choice of the effective cross section is studied, since the composite section of the bridge is considered a glued thin-flanged section, in which shear lag or plate-buckling effects may occur. In Chapter 7 the local distribution of shear stresses among the deck of the bridge due to the service vehicle load is examined; also the benefits achieved by adding the Kerto-S® stripes between the glulam beams and the Kerto-Q® deck are evaluated. For these studies a very simple model of a transversal stripe of the bridge is used. In Chapter 8 the effects of concentrated loads acting over the deck and local stress distributions are treated adopting a complex model of the whole bridge. The finite element models are described in details and possible future research studies are suggested.

1.2 Advantageous and disadvantageous of timber bridges

Even if several studies have been developed in the last century, timber remains a material difficult to analyse and to use because it is not homogenous. For example, it has a modulus of elasticity that can vary depending on the principal directions. This is valid also for almost all its other mechanical properties. Even starting from the same tree, is possible to get different specimens with different characteristics, which influence and determine the resistance of the final structural product.

Nevertheless, timber is considered a very important building material for several reasons. It is light and easily transportable, so it can be handled very easily. It's easy to work with: it can be sawn, planed, nailed and screwed. It can well resist to knocks

and it is little influenced by fatigue problems. It has a good resistance both for compression and tension. Furthermore, it looks pleasing and its external surface does not need to be covered by other kind of products.

For many years, a limitation has been found in the use of timber in building constructions of large dimensions and large spans, but, with the invention of glued laminated timber, wood has started to be used also for large span structures. Glued laminate timber will be discussed in details in Chapter 2, and in particularly Section 2.1.

Pedestrian bridges are considered nowadays a good solution to traffic problems both in city areas and in the countryside. Especially in areas important from the historical or natural point of view pedestrian timber bridges are often evaluated as the first choice. Compared to bridges made by other kind of materials, the advantages of timber bridges can be summarized as follow:

- Timber structures are extremely light and could be almost totally assembled in the factory, so that the time to completely erect a whole structure is quite short.
- The assembling made by metal connectors allows easy assistance for maintenance problems.
- Glued laminated timber structures hold good capacity to respond to short-term loads.

1.3   General problems of timber bridges

1.3.1   Manufacturing and assembling phase

Historically, the size of trees determined the size of timber elements that may be produced. In the past it was possible to have members with cross-section up to 150mm x 450mm, and lengths up to 20m; nowadays this would not be realizable because it would not be economically advantageous. If larger sizes are needed, timber units can be combined together to form a composite member like for instance glulam member. Because timber is produced by nature, strength and stiffness properties are highly variable. Consequently large pieces of wood can be divided into smaller units and then rejoined together. In this way defects are distributed within the material. This type of timber elements are known as wood – based products (Anon. 1995a).

Wood is a material full of defects, so it's important from the beginning of the production process to pay a lot of attention to the level of quality of the specimen available. This aspect is as more important as the product to be obtained is made of elements of large size, because in this case it is higher the possibility of having more significant defects. Veneers, flakes, chips, fibres are the elements derived from a tree that are properly used to manufacture products like plywood, laminated veneer lumber, oriented strand board, particleboard, fibreboard.

Hence, from the manufacturing point of view, when producing all these different kind of timber products (it can be also logs and battens of sawn timber and glued laminated timber) it's very important to keep under control all the different steps of the production process, from the beginning inspection of the quality of raw product, discarding the worthless specimen, until the final product. Basically in the factory it is

possible to achieve optimum conditions for the production process, because for example temperature and humidity conditions can be perfectly controlled; furthermore, it is possible to lead the wood elements to a certain level of moisture content through drying processes. All the instructions described here are valid for all kind of timber structures, and obviously also for timber bridges.

A quite important problem that involves timber structures and timber bridges in particular is the assembling of the different parts that generate the whole structure. Timber structures are always made of many components of timber parts that have to be assembled together. Several types of connections are used to link together various kind of members, and all of them are to be carefully design both to guarantee the structural stability and to control the effects on timber of changes in the environmental conditions. The design of connections has to satisfy certain criteria like:

- Allow a simple assembling of the members of the structure.

- Avoid possible eccentricities of the forces involved in order to limit secondary effects whose consequences are not always easily predictable.

- Check the inclination of the forces respect to the direction of the wood fibres.

- Pay attention to the minimum distances between different members of the structure and the minimum thickness of the elements assembled.

Support devices should be design carefully since they have the important role of transferring the support forces to the ground through lateral abutments or internal supports. First of all their theoretical behaviour should be able to allow needed displacements of the members due to changes in the moisture content; they also must transmit forces avoiding settlements of the structure. The real behaviour of these support devices must fit as much as possible with the theoretical model studied in the design stage. See Figure 1.1.
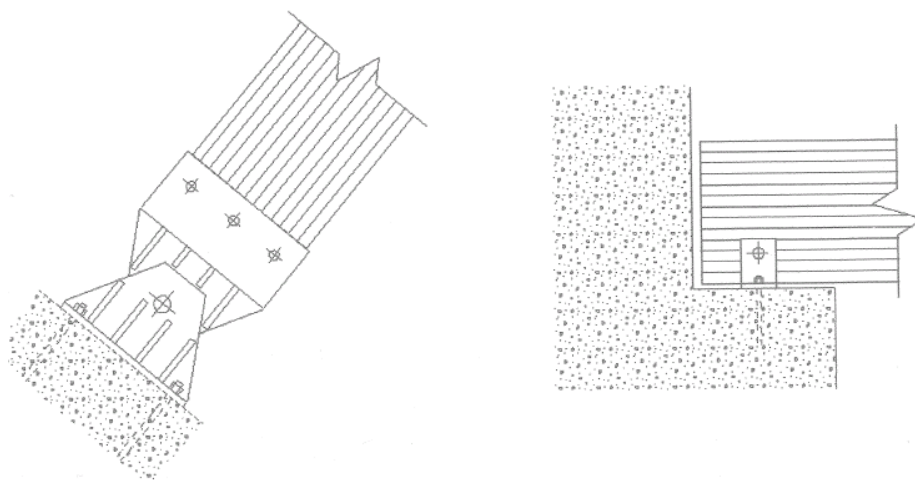

Figure 1.1 Examples of support devices (Bellumat, 2000)

For large span structures like timber trussed arches, a very important connection is the linking joint at the crown. They are made by welded steel elements that are attached to one ending face of the timber member. In this kind of connections (and in other connections that will be presented afterwards) it's important to check the resistance of both steel and timber elements. The verifications to check form the point of view of the steel parts are that all the elements should be verified for normal and shear stresses for the most unfavourable combination of loads (that eventually takes in account also seismic loads). Concerning the timber parts, verifications about tension and compression parallel or perpendicular to grain and regarding shear are to be checked in all the zones close to the joint (Bellumat, 2000).
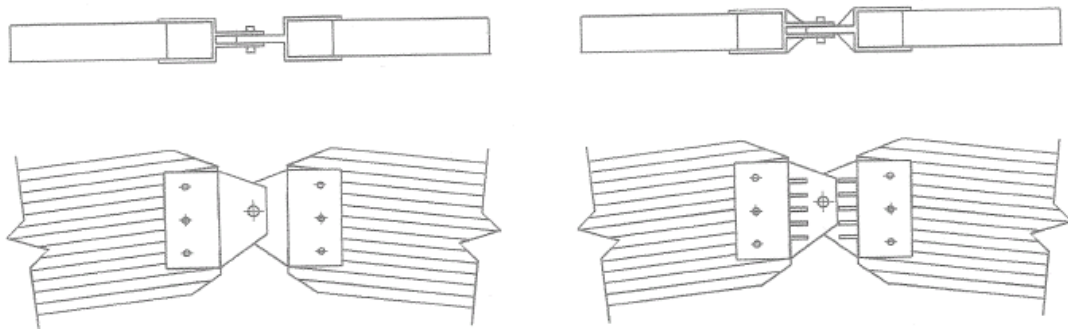
Figure 1.2 Example of a connection a the crown of the arch (Bellumat, 2000)

Similar verifications are to be checked also for all the connections that join together all other kind of members. Their aim is to guarantee the transfer of the forces that have been foreseen and quantified in the design stage. Nails, dowels, screws, shear-plates, single and double-sided toothed-plates, punch metal plate fasteners, joist hangers and framing anchors are the common timber connectors used in constructions. Some of them are shown in Figure 1.3.

Figure 1.3   Examples of timber connectors used in constructions: (a) nails; (b) screws; (c) shear-plates; (d) toothed-plates (Anon. 1995a).

Particularly, it is good to describe more in details the joist hangers connectors, since they are also used in the bridge that is studied in this thesis work (see Figure 1.4).

Figure 1.4 Joist hanger connectors (Anon. 1995a)

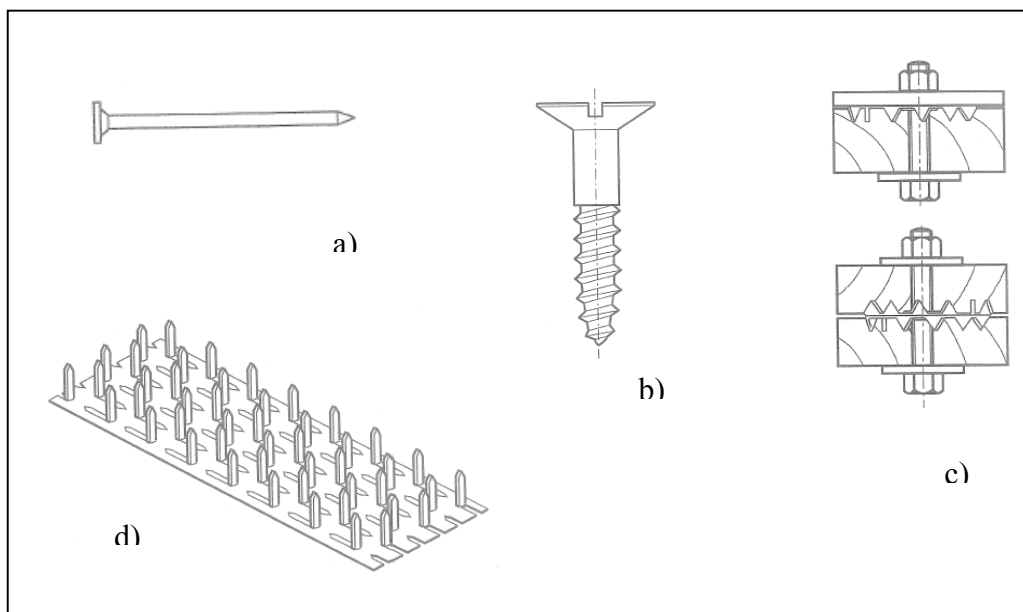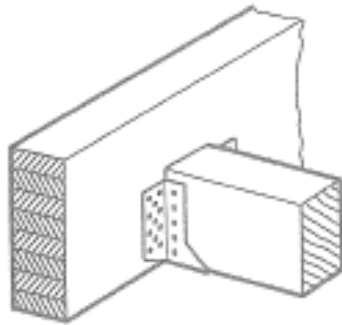It's a connection typically used to fix secondary members as bracing units or accessory parts to the main structure. The metallic plates they are made of are equipped with holes where to insert nails or screws to fix them to the timber member. They must be properly reinforced to avoid deformations or crushings due to knocks during the transportation or assembling stage. The main function of the joist hanger is to support the vertical force transferred by the joist itself to the main structure. The joist is supported both along its lateral surface through nails or screws, and by direct support on the bottom plate; therefore is necessary to verify the connection between the joist hangers and the joist itself, the connection between the joist hangers and the beam, and bending in the bottom plate (Bellumat, 2000).

A special attention should be paid about glue connections, since these have an important role in the bridge studied in this thesis work.

Structural wood adhesives are used to bind two or more wooden parts together in such a way that the products behaves as a static unit. The task of the adhesives is to fill the voids between the wooden members, and to produce adhesive bonds that are equally strong and durable as the cohesive forces within the members. In addition, the adhesive layer itself must have sufficient strength and durability to retain its integrity in the assigned service class throughout the expected life of the structure. The attraction forces between adhesive and wood are of the same type as the cohesion forces in the wood, i.e. electric attraction forces between molecules. The resulting bonds are mostly of the secondary bond type (hydrogen bonds and van der Walls bonds). Some primary bonds (covalent bonds) are also likely to be produced with some adhesives.

To completely achieved these kind of bonds, the two following steps of the bonding process must be attained:

Application of a liquid adhesive which wets the surface of both adherents so that attraction forces between adhesive molecules and wood molecules are created across the borderlines.

Transformation of the liquid adhesive (which fills the voids between the members) into a solid of sufficient strength and durability to retain its integrity throughout the service life of construction (Anon. 1995a).

1.3.2 Durability problems

Durability problems are very important for timber structures, especially when wood is directly exposed to the surrounding environment. Mechanical deterioration of wood is due to imposed geometrical variations (swelling and shrinkage) due to changes in the moisture content. Moreover degrade in the wood material can be caused by biotic attacks of insects or bacteria. For these reasons an accurate study in the design stage together with the use of covering products to protect wood and an appropriate maintenance are needed to control the structure when the material grows old.

Looking at the examples of the past, it's possible to distinguish two different groups of bridges: bridges uncovered or covered by a roof. For the first class of bridges the protection from rainfalls and snowfalls is guaranteed by the roof, whereas the second class needs special treatments and a particular care in designing details to protect the material.

If wood is directly in touch with the humidity contained in the surrounding air, then swelling and shrinkage take place in the timber elements due to the cyclic variations of the moisture content of the environment and, hence, of the wood itself. In fact the humidity in wood always tries to stay in equilibrium with the surrounding one. In this situation, if timber members are not free to deform by some external constraints, dangerous internal stresses develop, and might lead the structure to failure. A critical point to check in this context is represented by connections, where some fractures could take place between the dowels or bolts that are fixed in the wood but also to some undeformable steel plates. As an example it can be considered the picture in Figure 1.5: A deep beam is subjected to a decrease in the moisture content. Shrinkage takes place, and it is much greater across the grain than along the grain, leading to cracks if the member is restrained. The use of sliding connections can allow the shrinkage to occur.
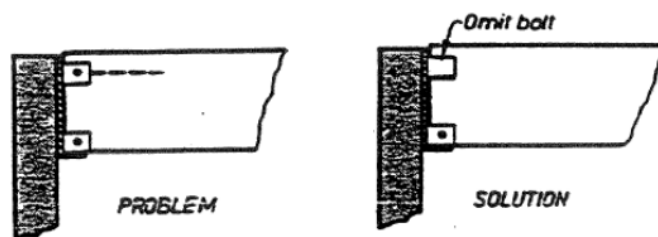
Figure 1.5 Potential shrinkage crack in a deep beam (Buchanan, 1992)

Nonetheless, the mechanical properties of wood are directly related to the value of moisture content, and essentially the moisture content will rise when the humidity increases. This behaviour is also taken into account when defining the value of design strength in the EC5, as it will be described in Chapter 5, and in particular Section 5.2. Figure 1.6 represents the strength values against percentile for matched samples of spruce in three different cases: element subjected to compression, a; tension, b;

bending, c. Low values of percentile are referred to low timber quality of the element, high values of percentile to timber of good quality. It is clear that in all cases low level of moisture (12%) is related to higher values in the resistance, while the curve that expresses the highest moisture (>28%) is the lowest in all the three graphs. Other derived information can be read from these graphs, like the fact that the influence of moisture content on compression strength is seen to be independent of timber quality, since the relative strength differences stay almost constant throughout the whole range of percentile values. Less coherent is the behaviour in case b (tension), where the strength values seem to vary much less against percentile. The more important case c (bending) is a mix of the two previous one, and still similar to case a (compression), but with larger differences of resistance against moisture content for high quality timber.
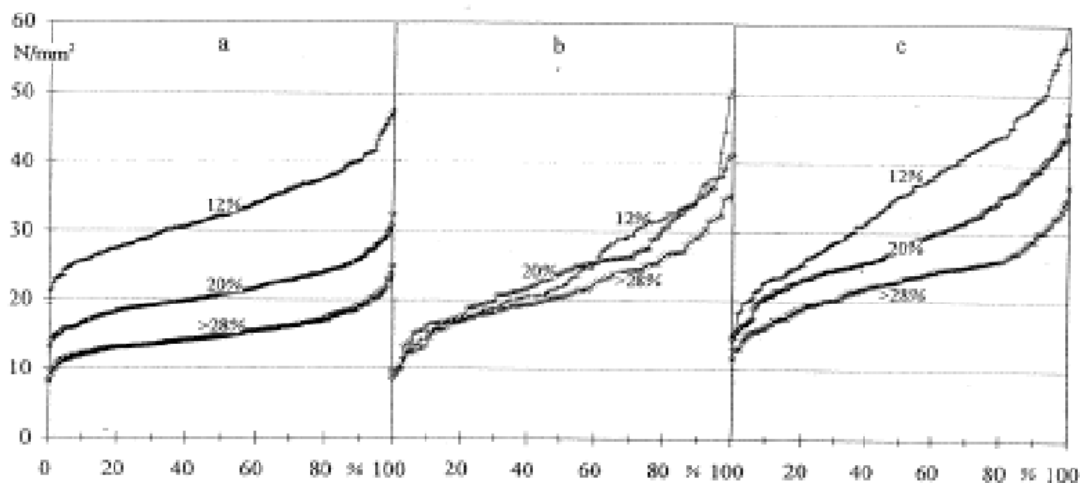

Figure 1.6   Strength against percentile for matched samples of spruce subjected to a: compression, b: tension and c: bending at moisture content levels 12%, 20% and >28% (Anon. 1995a).

If the climates conditions surrounding the timber bridge are characterized by intensive and frequent changes in the level of humidity, there is a higher risk of damage in glued laminated timber beams represented by the effect known as "glue line delamination". Delaminations between the lamella and fractures inside the lamella occur, and the resistance capacity of the beam decreases, especially concerning the characteristic shear strength. For the environmental conditions just defined particular care should be taken to protect glulam beams.

Besides forcing the element to strictly fallow the changeable level of moisture in the air, the direct action of wind and waterfalls on timber members will also accelerate the deterioration of the material combining erosion and wiping both of the external wood surfaces or the protecting covering. As a result cracking and an irregular surface develop, producing a decrease of the mechanical capacity of the member. Also the risk of possible biotic attacks rises.

The sun radiation has also a negative effect on timber because it can produce a chemical alteration of certain wood cells that can increase the capacity of the material to absorb water through its surfaces (Bellumat, 2000).

2 Materials and components of timber bridges

2.1 Glued laminated timber beams

Thank to this timber product, that has been developed with success during the last century, wood became a material good to be used also for large span structures in modern constructions. The bridge analysed in this thesis work would not exist if glued laminated timber beams had not been invented before.

Figure 2.1   Examples of structures that use glued laminated timber beams (Piazza, 2004).

Glulam beams are obtained gluing together under pressure timber battens of small size along their longitudinal surfaces. Still longitudinally, these battens are linked one to each other by use of several kind of joints; the most utilized is certainly the one known as "Finger joint", see Figure 2.2 and Figure 2.3.
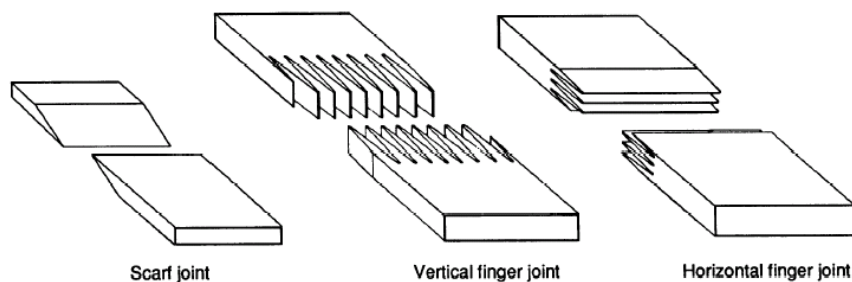

Scarf joint   Vertical finger joint   Horizontal finger joint

Figure 2.2 Types of lamination end joints used in glulam (Ritter, 1990)

Finger joint (l = finger length, p = pitch, b_t = tip width, l_t = tip gap).
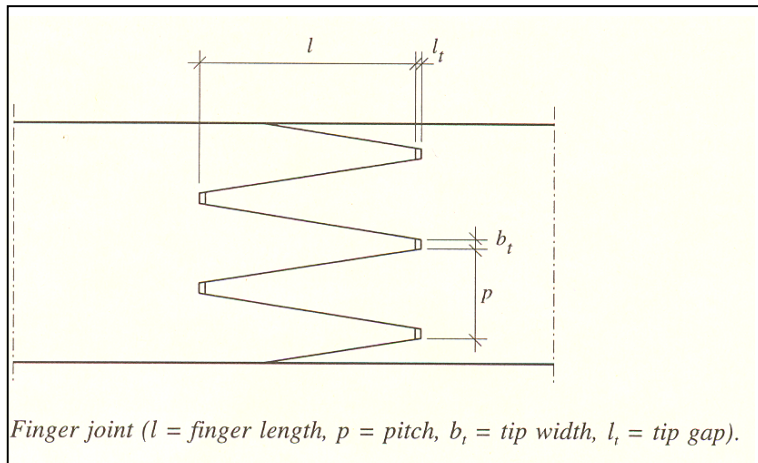
Figure 2.3 Detailed drawing of a vertical finger joint (Anon. 1995a)

In this way it is possible to get a timber member similar to solid wood, because the wood fibres are all in the same longitudinal direction, and with the advantage that the shape of the cross section can be chosen in a large variety of sizes. Moreover larger spans are achievable. At the same time the glulam beam obtained in this way is made of a less imperfect and more homogeneous material than a beam in solid wood, because made of many small pieces. Before joining the battens together, is possible to eliminate those parts with too many knots or too irregular directions of the fibres. All the battens can be set on a certain level of moisture content in advance, so that final member will reach a more uniform condition with the external environment that it will meet. At the same time, having all the battens arranged at the same level of humidity, the final member outcomes homogeneous, the global shrinkage outcomes uniform, and less internal stresses occur.

In the manufacturing stage an optimisation of the material can also be performed, arranging lower quality kind of wood in those parts were lower strengths are required (for example close to the neutral axis of the beam), and high quality laminates elsewhere. Furthermore, beams with uneven shapes can be easily achieved, like curved beam with constant cross-section or tapered and pitched cambered beams with variable cross-section along the longitudinal axis. See Figure 2.4 and Figure 2.5.
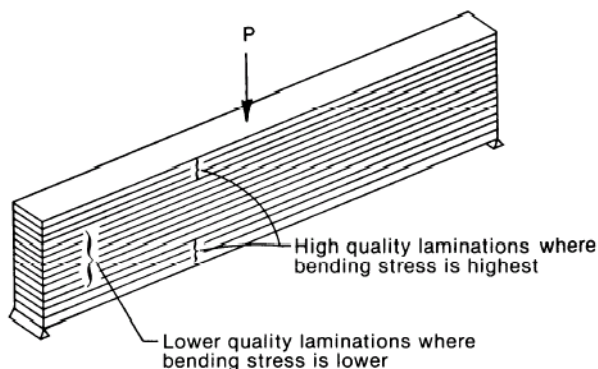

Figure 2.4   The quality of the lumber laminations is varied over the member cross section to provide higher strength where bending stress is higher (Ritter, 1990).
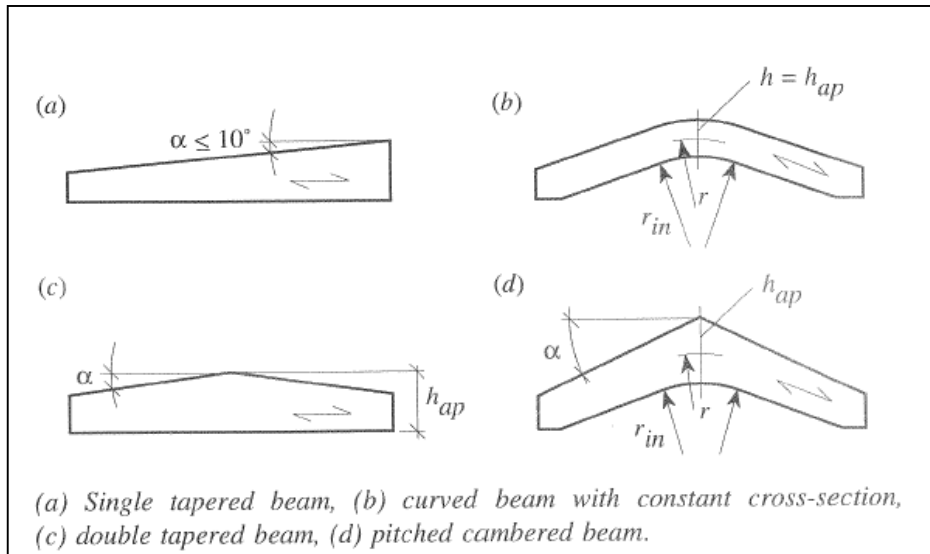
(a) Single tapered beam, (b) curved beam with constant cross-section,
(c) double tapered beam, (d) pitched cambered beam.

Figure 2.5 Glulam beams with uneven shapes (Anon. 1995)

The materials used to produce laminated timber products are wood and glues. Soft types of wood are generally used, because they are more malleable to work with, and their fibre directions are adequately straight. The battens created from these trees have some limitations in the size of their cross-section; the main reason for this is to avoid large deformations or stresses during the drying process. In Italy are commonly used battens 30-35mm depths, while in Sweden a depth of 45mm is also accepted. If the thickness is larger then the production costs are cheaper, because the total amount of glue per volume of glulam beam produced it's lower.

Adhesives for manufacturing glulam timber must meet minimum criteria for shear strength, resistance to delamination during accelerated exposure to wetting and drying and resistance to deformation under static load. Appropriate kind of glues are to be used: the phenol-phormaldehyde, resorcinol-phormaldehyde and phenol-resorcinol-phormaldehyde adhesives have an excellent record of long-term performance and durability in the field-over 50 years in the case of glulam timber. These adhesives are not attacked by biological organisms, do not emit formaldehyde or other vapours, and do not soften or melt even when exposed to direct flame. Since the strength of adhesion between these adhesives and wood is greater than the cohesive strength of the wood itself, test blocks bonded with these adhesives show over 75% wood failure when loaded to destruction (Cesaro and Piva, 2003).

In prEN 1194 (September 1993) five strength classes for glulam are defined, as it is described in Figure 2.6.

Strength class		GL 20	GL 24	GL 28	GL 32	GL 36
$f_{m,g,k}$	(N/mm^2)	20	24	28	32	36
$f_{t,0,g,k}$	(N/mm^2)	15	18	21	24	27
$f_{t,90,g,k}$	(N/mm^2)	0,35	0,35	0,45	0,45	0,45
$f_{c,0,g,k}$	(N/mm^2)	21	24	27	29	31
$f_{c,90,g,k}$	(N/mm^2)	5,0	5,5	6,0	6,0	6,3
$f_{v,g,k}$	(N/mm^2)	2,8	2,8	3,0	3,5	3,5
$E_{0,mean,g}$	(N/mm^2)	10 000	11 000	12 000	13 500	14 500
$E_{0,05,g}$	(N/mm^2)	8 000	8 800	9 600	10 800	11 600
$\rho_{g,k}$	(kg/m^3)	360	380	410	440	480

Figure 2.6 Strength classes for glued laminated timber (Anon. 1995a)

The bridge studied in this thesis work utilizes glulam beams GL32.

2.2   Materials used for the deck

The deck has the important structural function of supporting adequately the traffic load and transferring it to the bearing structure beneath. The type of deck traditionally used in timber bridges is similar to the one shown in Figure 2.7. Over the main beams, an interlace of joists and secondary beams act as a suitable support for the upper layer of wood battens. This system is still often used especially for pedestrian bridges.
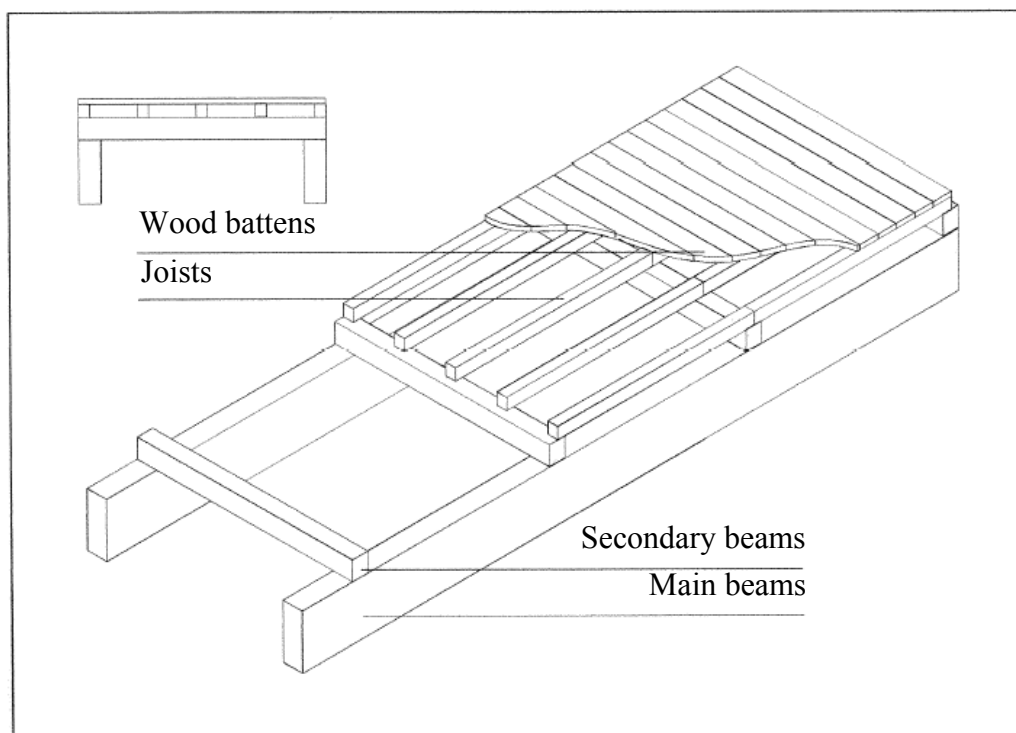

Figure 2.7   Example of a traditional batten deck used in timber bridges (Bellumat, 2000)

From the 70's new techniques regarding timber deck started to develop and became commonly used, like glued laminated and stress laminated timber decks.

Glued laminated timber decks (also simply called "Glulam decks") are constructed of panels manufactured of vertical laminated lumber. The panels are placed transverse to the supporting beams, and loads act parallel to the wide face of the laminations (see Figure 2.8). The two basic types of glulam deck are the non-interconnected deck and the doweled deck (see Figure 2.9). Non-interconnected decks have no mechanical connection between adjacent panels. Doweled decks are interconnected with steel dowels to distribute loads between adjacent panels. Both deck types are stronger and stiffer than conventional batten decks, resulting in longer deck spans, increased spacing of supporting beams, and reduced live load deflection (Ritter, 1990).
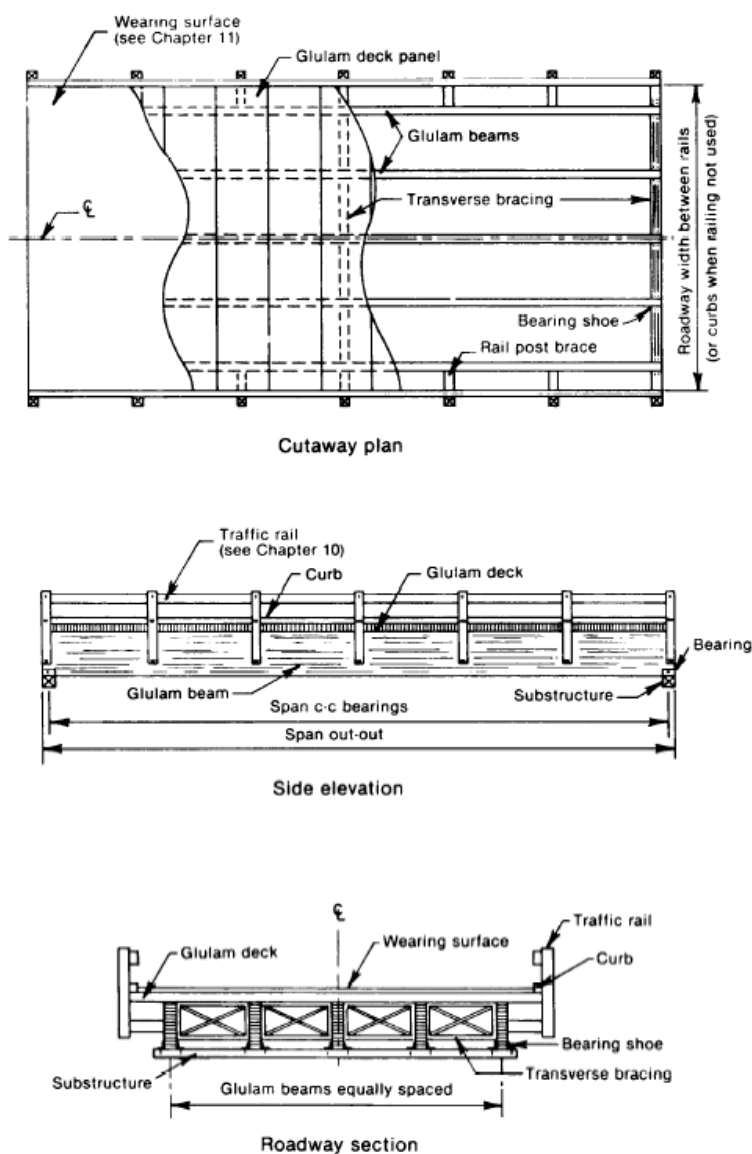

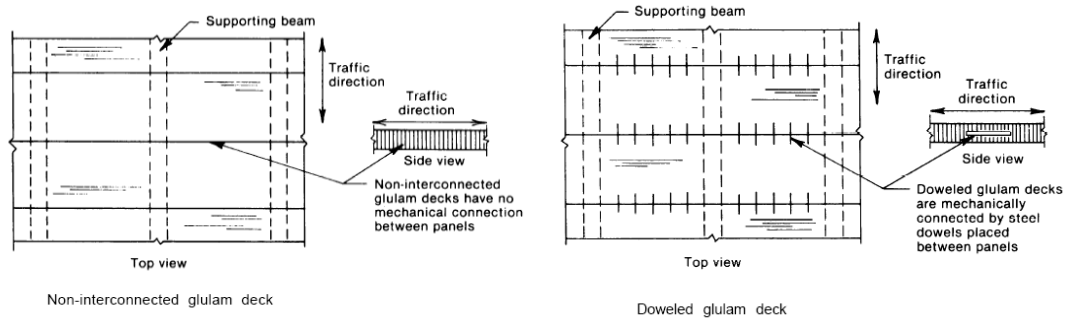*Figure 2.8 Typical glulam beam bridge configuration (Ritter, 1990)*

Figure 2.9   Configurations for non-interconnected and doweled glulam decks
             (Ritter, 1990)

Longitudinal stress-laminated deck superstructures consist of a series of lumber laminations that are placed edgewise between supports and are compressed transversely with high-strength prestressing elements (see Figure 2.10). The bridges are similar in configuration to glulam longitudinal decks previously discussed; however, with stress-laminated decks the load transfer between laminations is developed totally be compression and friction between the laminations, rather than by glue or mechanical fasteners. This friction is created by transverse compression applied to the deck using the same type of high-strength steel-stressing elements that are commonly used for prestressed concrete. These elements, which have historically been high-strength steel rods, are placed at regular intervals through prebored holes in the wide faces of the laminations and are stressed in tension using a hydraulic jack (Ritter, 1990).
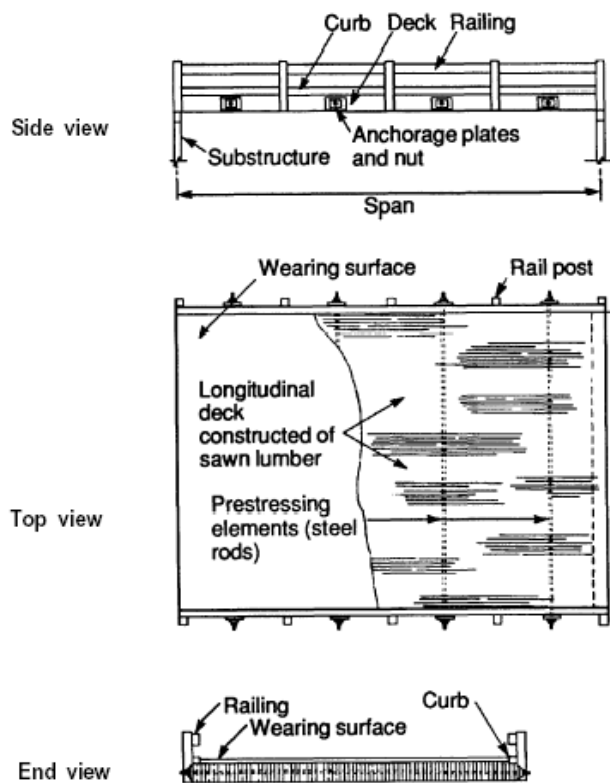

Figure 2.10 Typical configuration for a longitudinal stress-laminated lumber deck
            bridge (Ritter, 1990)

The techniques of stress-laminated and doweled glued laminated superstructure lead to obtain a 2-D deck that act as a continuous slab, with high stiffness both in the longitudinal and in the transversal direction.

If the design loads predicted for the bridge are relatively low (like it happens for pedestrian bridges), and the sizes of the structure are quite limited in width, it can be possible to utilize LVL panels for the deck. This is the idea that Moelven Töreboda AB designers have performed. An immediate advantage achievable by this method is that the panels can be very easily connected to the beam by use of glue connections. Furthermore, a composite section can easily be obtained and then assumed in design verifications, and the deck resistances can also be exploited to respond to the overall actions of the structure (bending and shear forces). Since LVL panels are a particular kind of plywood, it is good to star with the description of this important category of timber products.

2.2.1   Wood-based panels – Plywood

Plywood is a classic wood-based panel produced on the basis of a well-established technology and used for many structural components; a typical example is shown in Figure 2.11.

Figure 2.11 Example of a panel in plywood (Piazza, 2004)

Wood in thin layers, known as plies or veneers, has been used since ancient times for example by the Egyptians and Romans to finish wooden surfaces. Since the beginning of the 20th century, plywood has been industrially produced. Plywood as a building material consist as an odd number of layers (at least three) which are bonded using various types of adhesives.

Plies can be manufactured by rotary peeling, slicing or sawing. Plies for the structural plywoods used in building components are produced by the rotary peeling of steamed logs (see Figure 2.12).
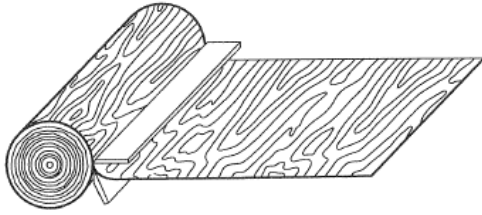
Figure 2.12 Production of an "endless" ply ribbon by rotary peeling (Anon. 1995a)

This procedure resembles the unwinding of the log to obtain a wooden ribbon of about 2mm to 4mm thickness. The next step is o cut the ribbon into sheets. After kiln drying and gluing, the veneers are laid up with an angle of 90° between the grain direction of adjacent layers and bonded under pressure. In this way shrinkage and swelling are strongly reduced because grains that want to shrink in their transversal direction (deformation caused by variations in moisture content are much bigger in the direction perpendicular to the grain than in the longitudinal one) are prevented by the close fibers perpendicular to them of the next layer. Figure 2.13 shows the layered composition of a plywood cross section (Anon. 1995a). The orientation of the board is determined by the fibre direction of the two external layers (also called "face veneers").
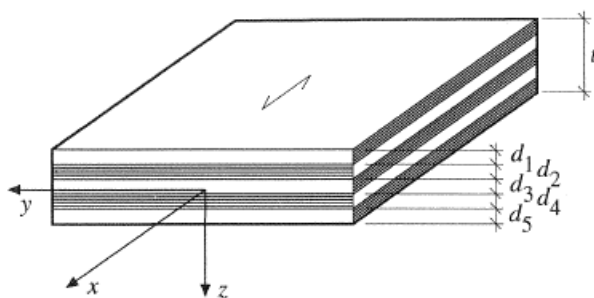

Figure 2.13 Composition of balanced, 5 layers plywood cross section. $d_4 = d_2$; $d_5 = d_1$ (Anon. 1995a).

Plywood is structurally suited for use as a panel material in various components, for example as the web or flange of beams, in diaphragms, as wall panels or as gussets in spaced columns and trusses.

Plywood density is generally higher than the density of the wood from which it was made, because it was compressed and pressured in the bonding stage of the production process.

Plywood is subjected to creep deformations slightly higher than solid timber, due to the glue lines.

When studying the structural properties of plywood, is very important to differentiate between bending perpendicular to the plane of the panel, also known as "Flatwise" (see Figure 2.14), and in-plane bending, also known as "Edgewise" (see Figure 2.15). These two cases are moreover divided in two other options to take in account the orientation of the board.
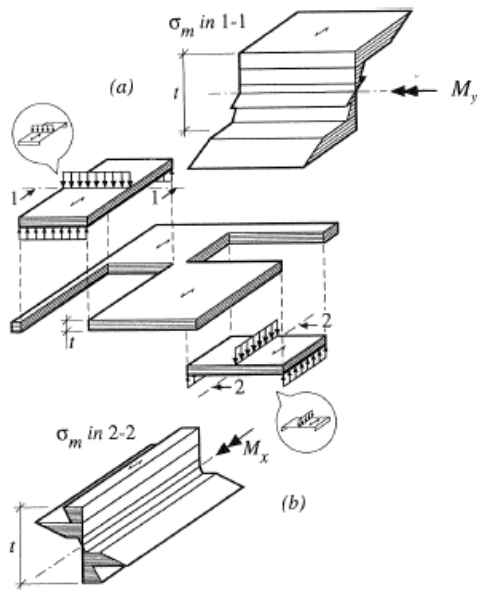
Figure 2.14 Bending perpendicular to the plane. (a) Parallel to the grain of face veneer, (b) perpendicular to the grain of face veneer (Anon. 1995a).
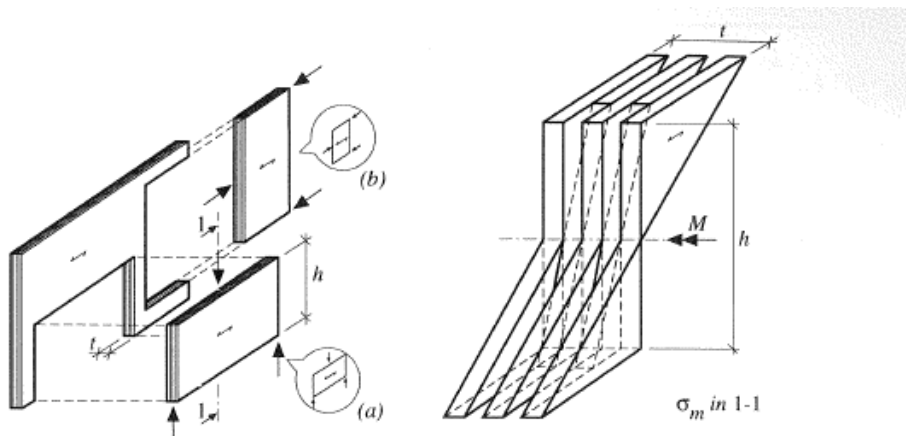

Figure 2.15   In plane bending (a) parallel and (b) perpendicular to the grain of face veneer (Anon. 1995a)

It is also very important to be aware of the fact that the resistance to shear of plywood is much lower when the panel is used in the modality flatwise than the edgewise. This is due to the fact that close layers with different fiber direction can slip each other. At a microscopic level of study, it is possible to imagine the wood fibers of a layer rolling over the wood fibers perpendicular to them. For this reason this behavior is called "Rolling shear" (or planar shear). This problem doesn't occur when the panel is used in the modality edgewise, and in this case the resistances result much higher. See Figure 2.16 and Figure 2.17.
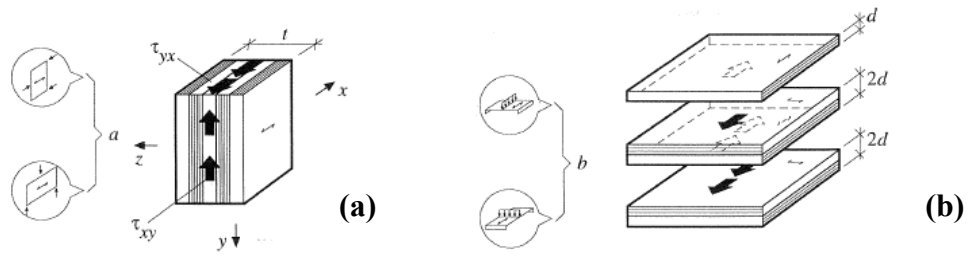
Figure 2.16   (a) panel shear (b) planar shear stress (normal stresses are not shown) (Anon. 1995a)

type of characteristic strength	S-plywood[1]		FIN-plywood[2]		US-plywood[3]		CAN-plywood[4]		D-plywood[5]
	t mm	f_k N/mm²	t mm	f_k N/mm²	t^6 mm	f_k N/mm²	t mm	f_k N/mm²	f_k N/mm²
$f_{m,0,k}$	12,0	23,0	12,0	37,2	12,5	23,5	12,5	19,0	$77k_1$
	24,0	21,6	24,0	34,8	21,0	14,8	25,5	15,8	
$f_{m,90,k}$	12,0	11,4	12,0	27,6	12,5	12,2	12,5	7,3	$77(1-k_1)/k_3$
	24,0	12,4	24,0	29,0	21,0	10,1	25,5	8,7	
$f_{t,0,k}$	12,0	15,0	12,0	38,9	12,5	13,6	12,5	9,9	$77k_2$
	24,0	15,4	24,0	37,2	21,0	10,5	25,5	10,6	
$f_{t,90,k}$	12,0	12,0	12,0	32,9	12,5	7,2	12,5	6,3	$77(1-k_2)$
	24,0	11,4	24,0	34,1	21,0	6,9	25,5	6,6	
$f_{c,0,k}$	12,0	15,0	12,0	19,9	12,5	13,9	12,5	12,6	$58k_2$
	24,0	15,4	24,0	19,3	21,0	10,6	25,5	14,1	
$f_{c,90,k}$	12,0	12,0	12,0	17,5	12,5	8,1	12,5	9,0	$58(1-k_2)$
	24,0	11,4	24,0	18,1	21,0	7,7	25,5	9,7	
$f_{v,k}$	12,0	2,9	12,0	9,8	12,5	3,2	12,5	3,2	8,0
	24,0		24,0		21,0		25,5		
$f_{r,k}$	12,0	0,9	12,0	2,5	12,5	0,9	12,5	0,9	3,0
	24,0		24,0		21,0		25,5		

Characteristic strength values in N/mm² and characteristic density values in kg/m³ according to EN TC 112.406 for established products.

1.   Swedish plywood P30, spruce, unsanded
2.   Finnish birch plywood, 1,4 mm veneer, sanded
3.   US plywood C-D, exposure 1, group 1, unsanded
4.   Canadian plywood, Douglas fir, regular or regular select sheathing, unsanded
5.   German beech plywood (for k_1, k_2, k_3 see Equations (17), (18) and (19))
6.   ≥ 5-layers

Figure 2.17   Characteristic strength values in N/mm² according to EN TC 112.406 for established products (Anon. 1995a)

LVL products (Laminated Veneer Lumber) are similar to plywood, but veneers are parallel (mostly) and larger dimensions are available.

2.2.2 LVL Kerto®

The idea of Moelven Töreboda AB designers was to have the deck of the bridge made by a LVL product called Kerto, which is produced in Finland. Two types of LVL Kerto have been used: two panels of Kerto-Q® 63mm thick are attached to each other and form the deck of the bridge. Two stripes of Kerto-S® 75mm thick are placed between deck and glulam beams and attached by glued connections to them (see Figure 2.18). In Kerto-Q®, some of the veneers are crossgrained, which permit the panel to act as a slab, with a relatively high stiffness even along its weak direction. In Kerto-S®, all veneers are parallel grained. The products are manufactured from spruce (*Picea abies*) or pine (*Pinus sylvestris*) veneers with a nominal thickness of 3mm, using an adhesive suitable for exterior conditions. The veneers are glued together using an adhesive suitable for exterior use. On one side of a veneer, phoenol-formaldehyde glue is spread evenly. For surface veneer melamine adhesive may be used. The veneers are scarf jointed using a phenol-formaldehyde or melamine adhesive.

Kerto-S®

Kerto-Q®

Figure 2.18   Example of panels in Kerto-S® and Kerto-Q® (© Finnforest Corporation – brochure about Kerto)

Depending on the thickness of the panel, the number and the disposition of veneers change. The lay-up of the cross section of Kerto-Q® is given in Table 2.1; as an explanation for the table, the first line says that a panel 21mm thick is made of 7 plies laid up in the following way: 3 central plies in the strong direction, 2 external plies in the strong direction and the two second plies starting from the external faces in the weak direction.

Table 2.1 Lay-up of Kert-Q® (Anon. 2005)

Nominal thickness mm	Number of plies	Lay-up
21	7	|—|||—|
21	7	||—|—||
24	8	||—||—||
27	9	||—|||—||
30	10	||—||||—||
33	11	||—|||||—||
39	13	||—|||—|||—||
45	15	||—||||—||||—||
51	17	||—|||||—|||||—||
57	19	||—|||—|||||—|||—||
63	21	||—|||—|||—|||—|||—||
69	23	||—||||—|||—|||—||||—||

The presence of cross-grain veneers in Kerto-Q® give a reasonable stiffness to the panel in the transversal direction. Considering the modulus of elasticity, the properties of Kerto-S® instead reproduce those of glued laminated timber. See Table 2.2.

Table 2.2   Mean values of Modulus of elasticity of Kerto-S® and Kerto-Q® (Anon. 2005)

Property	Symbol	Characteristic value, N/mm² or kg/m³		
		Kerto-S Thickness 21 - 90 mm	Kerto-Q Thickness 21 - 24 mm	Kerto-Q Thickness 27 - 69 mm
Mean values				
Modulus of elasticity:				
Parallel to grain	$E_{0,mean}$	13800	10000	10500
Perpendicular to grain, edgewise	$E_{90,edge,mean}$	430	2400	2400
Perpendicular to grain, flatwise	$E_{90,edge,mean}$	130	130	130
Shear modulus:				
Edgewise	$G_{0,mean}$	600	600	600
Flatwise	$G_{0,mean}$	600	-	-
Density	ρ_{mean}	510	510	510

Kerto-Q® and Kerto-S® have different resistances (see Table 2.3). Especially regarding the shear strength, Kerto-Q® results very weak for the flatwise mode (1,3 MPa). This low resistance may be a problem if the panel is used as a superstructure of a bridge when vertical traffic loads act on the deck. To prevent too high stresses in the Kerto-Q® panel, Moelven Töreboda AB designers had the idea of adding two stripes of Kerto-S®, whose flatwise shear strength is almost the double of the Kerto-Q®'s one, between the beams and the deck.

Concerning durability problems, it is recommended that Kerto products can be used in service class 1 and 2 as defined in EC5, which correspond to the hazard classes 1 and 2 as defined in EN 335-1. The product should not be used in service class 3 / hazard class 3 without additional protective treatment. The designers shall pay attention to

the details of the construction and to ensure that no water pockets will be formed (Anon. 2005).

Table 2.3 Characteristic values of Kerto-S® and Kerto-Q® (Anon. 2005)

Property	Symbol	Characteristic value, N/mm^2 or kg/m^3		
		Kerto-S Thickness 21 - 90 mm	Kerto-Q Thickness 21 - 24 mm	Kerto-Q Thickness 27 - 69 mm
Fifth percentile values				
Bending strength:				
Edgewise (depth 300 mm)	$f_{m,0,edge,k}$	44.0	28.0	32.0
Size effect parameter	s	0.12	0.12	0.12
Flatwise (thickness 21 to 90 mm)	$f_{m,0,flat,k}$	50.0	32.0	36.0
Tensile strength:				
Parallel to grain (length 3000 mm)	$f_{t,0,k}$	35.0	19.0	26.0
Perpendicular to grain, edgewise	$f_{t,90,edge,k}$	0.8	6.0	6.0
Perpendicular to grain, flatwise	$f_{t,90,flat,k}$	-	-	-
Compressive strength:				
Parallel to grain	$f_{c,0,k}$	35.0	19.0	26.0
Perpendicular to grain, edgewise	$f_{c,90,edge,k}$	6.0	9.0	9.0
Perpendicular to grain, flatwise	$f_{c,90,flat,k}$	1.8	1.8	1.8
Shear strength				
Edgewise	$f_{v,0,edge,k}$	4.1	4.5	4.5
Flatwise	$f_{v,0,flat,k}$	2.3	1.3	1.3
Modulus of elasticity:				
Parallel to grain	$E_{0,k}$	11600	8300	8800
Perpendicular to grain, edgewise	$E_{90,edge,k}$	350	2000	2000
Perpendicular to grain, flatwise	$E_{90,edge,k}$	100	100	100
Perpendicular to grain	$E_{90,k}$	-	-	-
Shear modulus:				
Edgewise	$G_{0,k}$	400	400	400
Flatwise	$G_{0,k}$	400	-	-
Density	ρ_k	480	480	480

3   Classification of timber bridges based on the type of static system

In the preliminary stage of the design the choice of the structural system to be used is important. Concerning timber bridges, four static systems can be defined: arch bridges, lattice structures and frame static systems, cable-stayed and suspension bridges and beam static system. Each of them has its particular advantages and disadvantages, and its significant problems that are to be known in order to have a realistic view of the aspects that mostly influence the design.

3.1   Arch bridges

In these structures the arch is the structural element that has the function of hanging the deck (in case the arch is situated above the traffic layer) or supporting it (in case the arch is entirely under the deck itself - see also Figure 3.1).

Figure 3.1 Different positions of the deck in arch bridges (Bellumat, 2000)

The deck instead must support the traffic loads and sometimes can stabilize transversally the structure. In fact an important aspect to take care of in this kind of structures is the possible buckling of the arch due to high compression stresses. Positive and negative bending moments act in different cross-sections of the arch, therefore buckling may occur both in the upper or in the lower part of the beam, and appropriate bracing units must be arranged to take care of this problem.

From the economic point of view arch structures are particularly efficient to cover long spans, because they can effort it by rather small sections. To limit the size of the cross-sections, positive and negative bending moments along the longitudinal axis must be minimized. This can be achieved as much as the curve of the arch axis coincides with the curve of compression for that arch; anyway, often the shape of the arch is already fixed from the beginning, like the circular one for example (Bellumat, 2000).

Another important point to study is the one concerning the lateral supports of the arch, because very high horizontal forces can occur in these positions. Finally, in case the arch is not a continuous beam, the joint at the crown represents an important point to be analysed.

3.2   Frame static systems and Lattice structures

Compared to the simple supported beam static system (that it will be analyzed in Section 3.4 of this chapter), a frame static system tries to reproduce the mechanical

behaviour of the arch, reducing shear forces and bending moment by increasing compression stresses in the structure. As a consequence, buckling problems are important to be checked in the various element of the structure.

Particular attention should be paid on the joints between the main beam and the inclined columns, because stresses perpendicular to the grain are acting on a section whose area might be reduced by a notch.

Timber bridges that use a truss for their structural system are very common. Some examples of this kind of structures can be found in Figure 3.3.
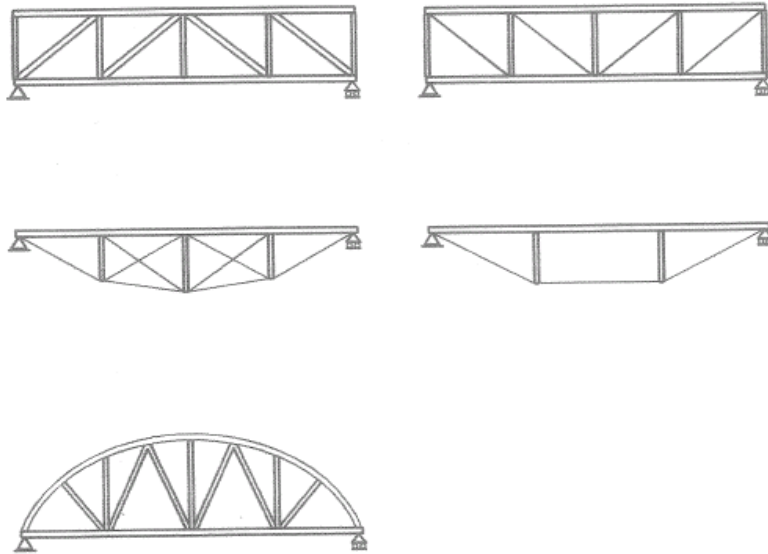

Figure 3.3 Examples of timber trussed bridges (Bellumat, 2000)

All the members of the truss are mainly subjected by pure compression or pure tension forces, except for the elements directly under external loads (usually the upper chord of the truss), in which a bending moment is also acting. When the geometry of the truss has been chosen, it is possible to get the forces acting in all the members, and therefore is possible to perform a better design of the members themself taking into account the buckling of the compressed elements. Now a new solution of the structure based on the previuos choices of the members has to be performed, and the members will be designed again. To be realistic this analysis must take in account also the rotational stiffnesses of the connections between the elements, because they can transfer a certain amount of moment. Especially in important structures like long span trussed arches the evaluation of the rotational stiffness must be well checked with several hypothesis and analysis, in order to get the correct solution. Connections are an important point to be studied in the design of such these kind of structures.

3.3   Cable-stayed bridges and suspension bridges

Timber suspension and cable-stayed bridges, other than as pedstrian bridges are relatively rare. Cables can be used to support a deck, removing the need for piers beneath the superstructure.

The cable-stayed bridges consist of a beam supported by a certain number of straight cables, fixed at a tower, which can be anchored to the deck or to the ground. There are a lot of different solutions that depend on the number of cables and their position (See Figure 3.4). The first solution (a) permits an easier connection of the cables in comparison to the second (b) where the cables converge to a single anchorage point. This second solution could produce a localized high concentration of stresses. In the first scheme (a) results compressed but subjected to bending moment too, in the second (b) the tower is compressed principally. The third solution is a mix between the first and the second.
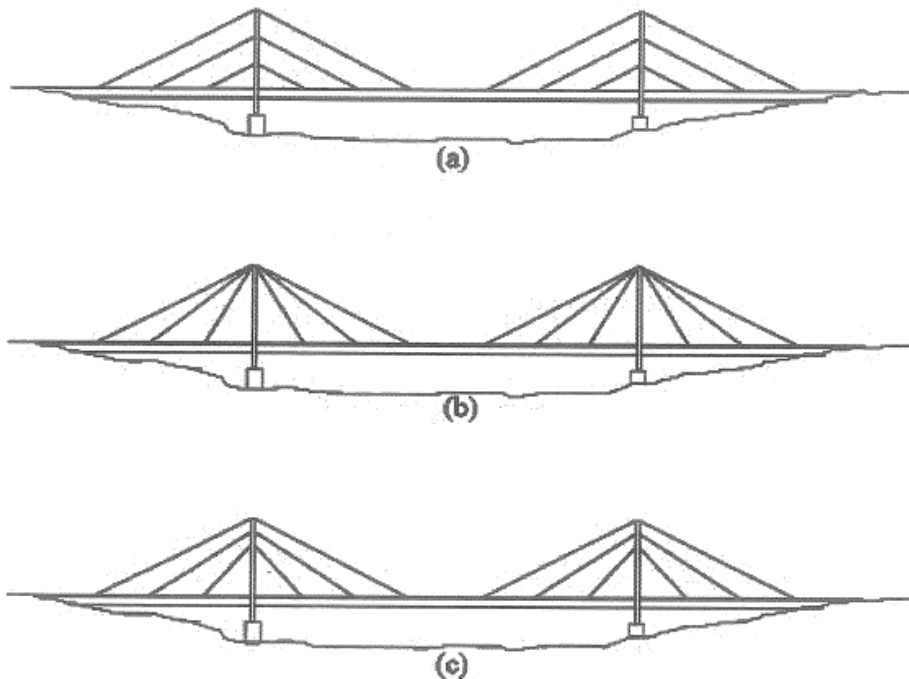

Figure 3.4 Cables-stayed bridges schemes (Cesaro and Piva, 2003)

The suspension bridges are characterized by a principal structure made up of cables set like a curved, usually parabolic, shape (see Figure 3.5). The deck is suspended up to these cables using a thick series of suspensions. Only a part of the loads is usually transmitted to the cables, another part is taken directly by the deck structure. So, a suspension bridge acts like a kind of a composite structure. The cables are connected to the bridge towers and then anchored to the ground.
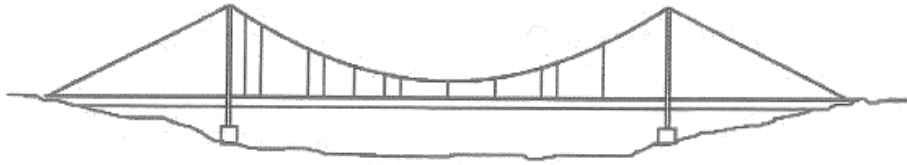
Figure 3.5 Suspension bridges scheme (Cesaro and Piva, 2003)

In both kind of structures, the structural scheme that should be used is one that causes tension in the main strings of the deck (see figure 3.6). That permits to avoid instability problems of these.
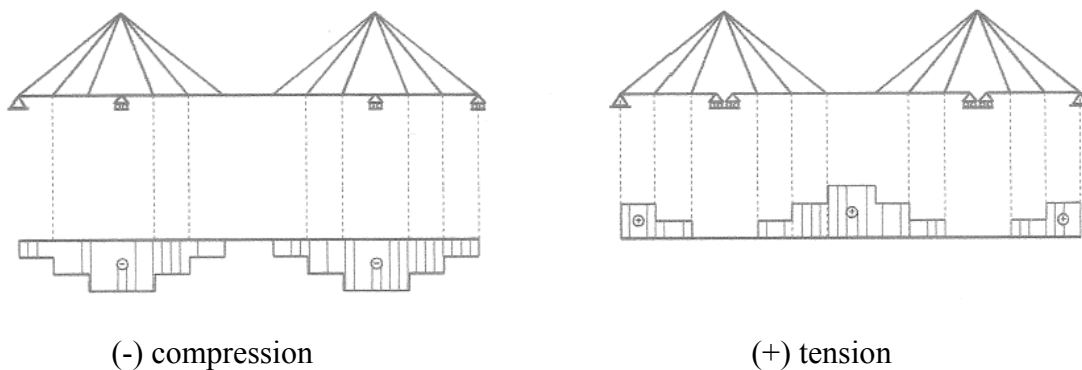

(-) compression   (+) tension

Figure 3.6   Distribution of axial forces in the string depending on the choice of restraints (Bellumat, 2000)

3.4   Beam static system

Compared to the examples treated previously in this Chapter, the main advantage of bridges that adopts the beam static system is their simplicity concerning manufacturing and assembling stages. This is the most common static system for timber bridges up to 30 meters spans, and it is also the one adopted for the bridge analysed in this thesis work.

The beam represents here the main bearing element for these structures, so that the design it's based on it. A first advantage is just the simplicity of the static system, which allows models and calculations to correspond to the real structure, so that the evaluations of actions and stresses result very realistic. At the same time, a first disadvantage could be the limitation in the span attainable for this kind of bridges, since bending moment increases with the span raised to the power of two.

Simple supported beams are used up to 20-30m spans. They are usully slightly precambered especcially in order to limit the deflection in the long-term and to allow a better evacuation of the water from the bridge.

The limitation of the span can be partially overtaken using a particular scheme of a simple supported beam known as Gerber beam. See Figure 3.7.
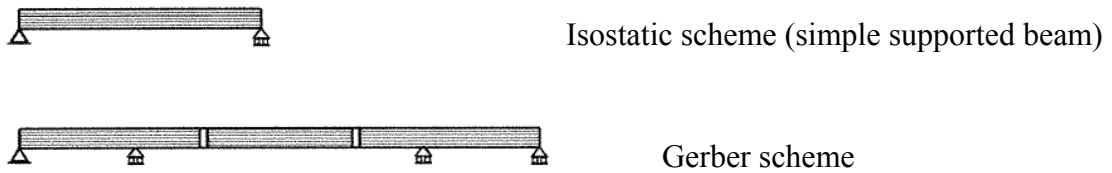
Figure 3.7 Isostatic scheme and Gerber scheme for timber bridges (Bellumat, 2000)

In a Gerber beam the structure is still statically determinated and it is possible to uniform the distribution of bending moment along the length of the bridge using a cantilever model for the lateral elements, and joining by use of simple pins the central beam to these two.

Also the scheme of the continous beam (see Figure 3.8) permits a better exploitation of the material compared to the simple supported beam, both varying the position of the supports and eventually the cross-section along the longitudinal axis. Since this model is not a statically determinated system, particular attention should be paid on the supports to avoid possible settlements, and therefore the growth of internal stresses (Bellumat, 2000).

Figure 3.8 Scheme of a continuous beam (Bellumat, 2000)
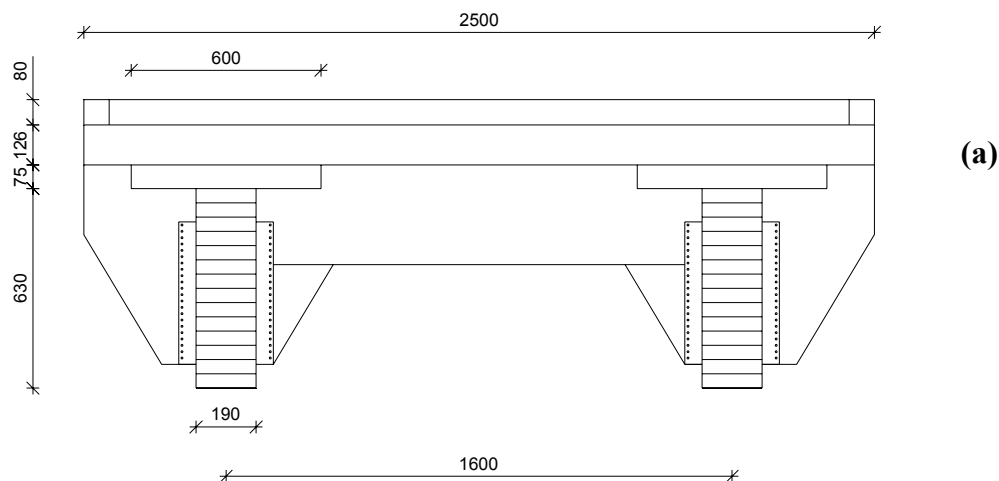
4 Introduction on the bridge studied

In the first three chapters general information about timber bridges, and in particular pedestrian timber bridges, have been resumed. Problems concerning manufacturing, erection, durability have been discussed, and advantages or disadvantages of different kind of timber bridges have been described. In this chapter the bridge analysed in this thesis work it's introduced, trying to relate it to the information presented previously.

The designers of the company Moelven Töreboda AB have performed the idea of this kind of bridge. In accordance with this company, the study has been concentrated on part of the aspects of this project, and other, generally also important, have been omitted. The subjects not analysed in this thesis work are:

- Abutments and supports of the bridge and geotecnical aspects

- Effects of variations in the moisture content in the members of the structure

- Effects of loads acting on the handrails

4.1 Description of the bridge

The bridge is a pedestrian bridge with glulam beams, Kerto-S® and Kerto-Q® deck. The static system is a simple supported beam. The length of the bridge is 15 meters; examples of 20 or 25 meters span could also be studied, taking into account an increase of the height of the beams. See Figure 4.1.

(a)

(b)

- Middle transversal Bracing Unit
- Layer of Asphalt (thickness 80mm)
- 2 Layers of Kerto-Q (thickness 63mm)
- Kerto-S stripe (thickness 63mm)
- Lateral transversal Bracing Unit
- Metal Joist Hanger
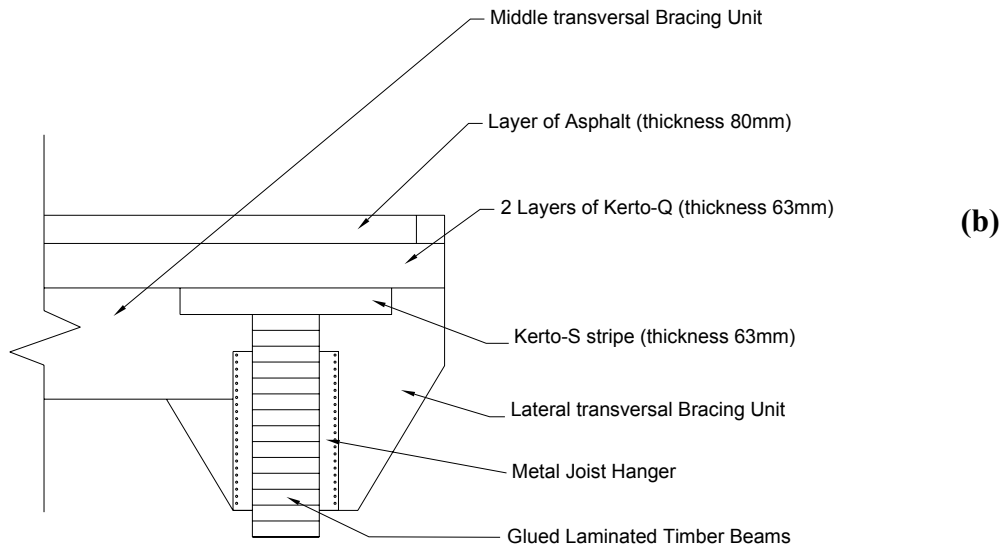- Glued Laminated Timber Beams

Figure 4.1 Transversal section of the bridge (a) and list of the different elements that form the section (b)

The bearing structure of the bridge is made of two Glued Laminated Timber beams assembled with a Kerto-Q® deck. The two stripes of Kerto-S® between the beams and the deck have been added to create a larger surface for transferring shear stress between the deck and the glulam beams. As it will be explained in this Chapter, the magnitude of this load is large enough to lead the Kerto-Q® material to failure because of the high shear stresses reached in the lateral part of the deck.

Glulam Beams, Kerto-Q® and Kerto-S® are glued together in their contact surfaces forming a connection that can be considered fully fixed. Therefore the whole section works as a composite section, without any slip between the different parts.

Above the timber deck there is a layer of asphalt 80mm thick that represents part of the permanent load acting on the structure. Every 1.80m in the longitudinal direction lateral transversal bracing units and middle transversal bracing units are located; they are tied to the beams by using some metal joist hangers. The middle transversal elements are also glued to the Kerto-Q® deck all the way through their upper surface. See Figure 4.2.

a)

- Lateral Transversal Bracing Unit
- Glued Laminated Timber Beam
- Middle Transversal Bracing Unit
- Kerto-Q deck
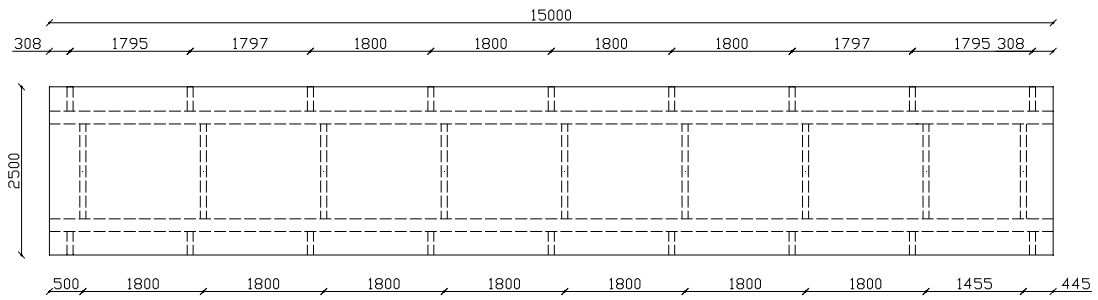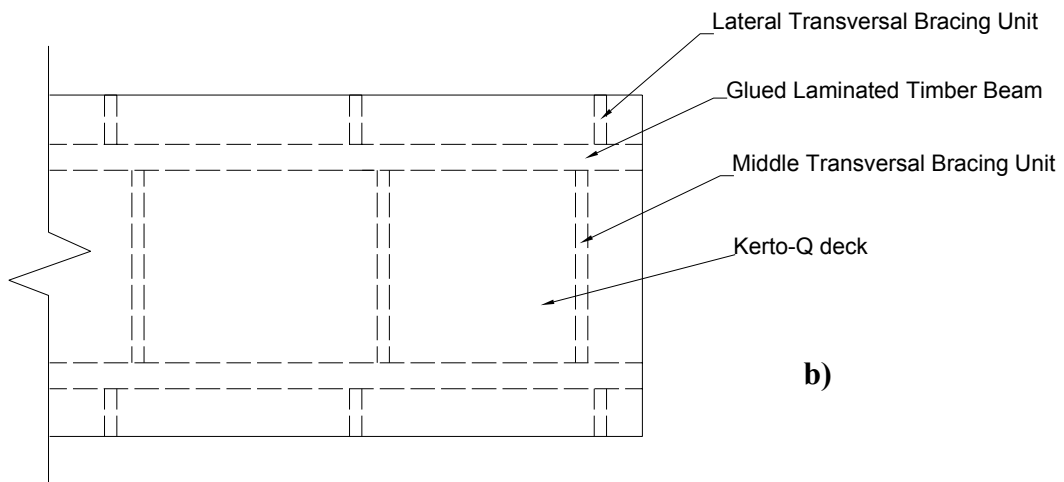
b)
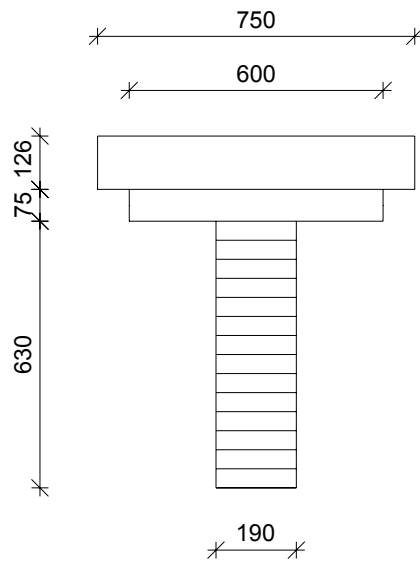
(c)

Figure 4.2 Plan of the bridge (a), list of the different elements that form the structure (b), effective section to assume in the calculations (c), Moelven Törebode AB (2005).

These three different parts are linked together by glue connections, so that complete interaction is garanteed and the hypothesis of composite section should be assumed (see Section 4.3 in this chapter for further details). In first approximation, an effective T-section symmetric about the vertical axis can be assumed in the calculations (see Figure 4.2 (c)).

It's practical to present here the notations regarding the coordinate system assumed for the structure, in order to comprehend better the studies that are described in the next chapters.
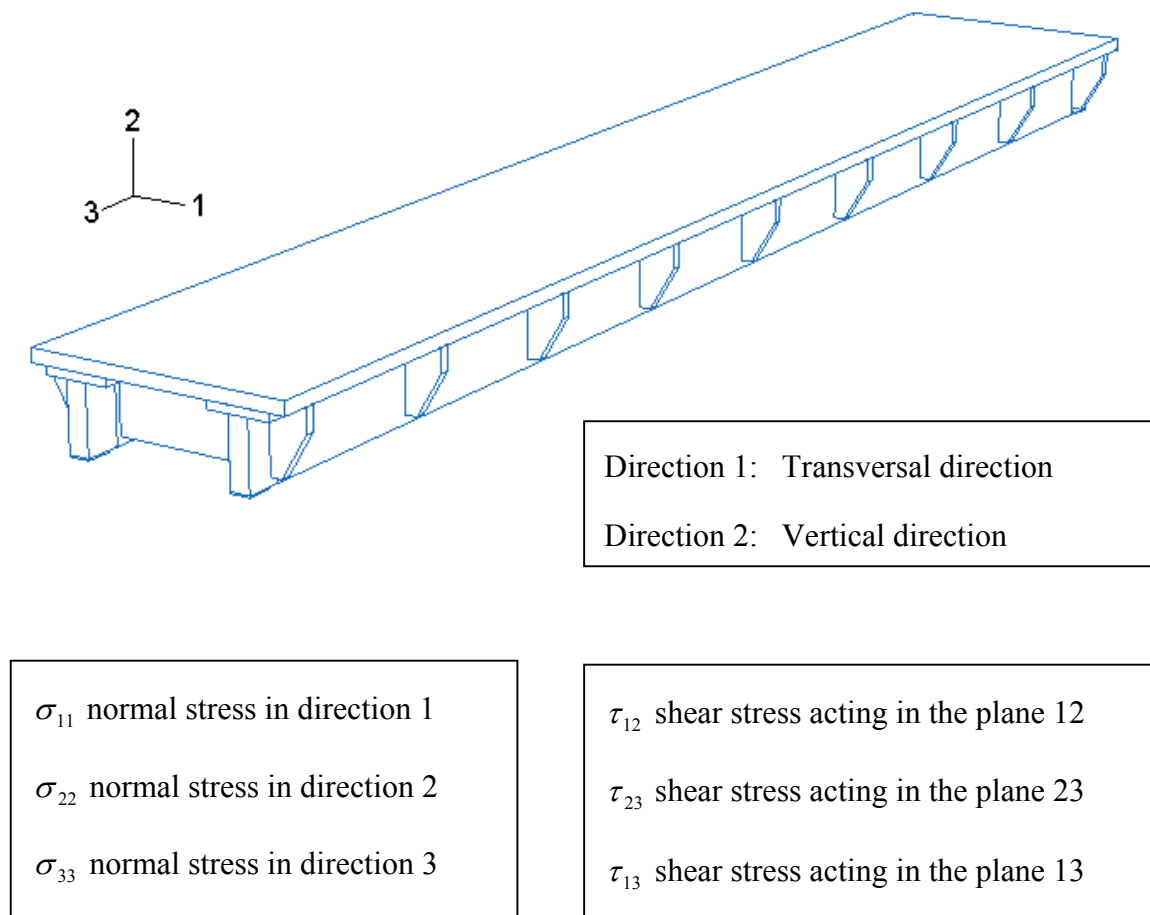

Direction 1:   Transversal direction

Direction 2:   Vertical direction

σ_{11} normal stress in direction 1	τ_{12} shear stress acting in the plane 12
σ_{22} normal stress in direction 2	τ_{23} shear stress acting in the plane 23
σ_{33} normal stress in direction 3	τ_{13} shear stress acting in the plane 13

Figure 4.3 Coordinate system assumed to analyse the bridge

4.2 Manufacturing and assembling phase

The bridge is made up with several timber elements: glued laminate timber beams, flat units of laminated veneer lumber for the deck, glued laminated timber for the internal and the external transversal elements (cross beams). All these components are produced in the factory, under strict and careful controls, so that the quality control of these products is guaranteed. Drying processes have been performed on these members in order to reduce as much as possible negative effects of variation in the moisture content in the materials when the structure will be placed in the construction site.

The significant advantage of this bridge is the fact that it is entirely assembled in the factory, and therefore in optimal conditions. When the assembling phase is finished, the bridge is placed on a proper truck, then transferred on the construction site, and in the end placed in its final position between abutments previously constructed by using an apposite type of crane.

The assembling process of the bridge in the factory is extremely simple. The main parts of the bridge (glulam beams and the LVL panels for the deck) are simply glued together; the transversal bracing units are connected to the main bearing structure by joist hanger metal connectors and glued connections in some parts. The detailed procedure is described as fallow:

Step 1

The two glulam beams are placed in the correct position: parallel to each other and at a appropriate distance. Note that the beams have a certain precamber (Figure 4.4).
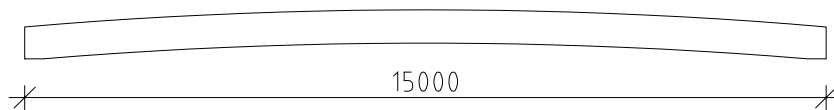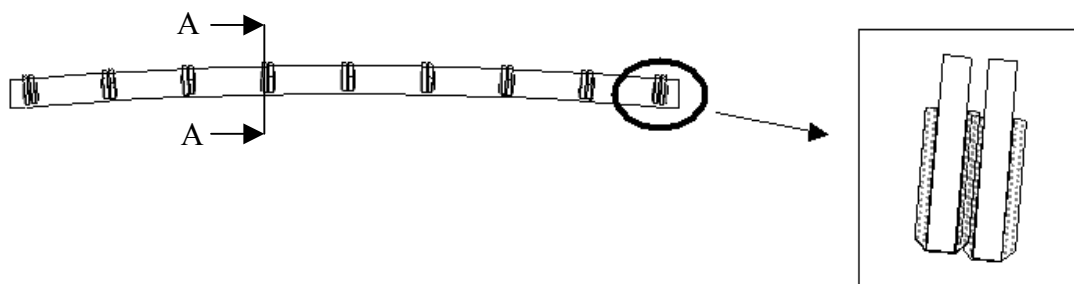

Figure 4.4 Step 1 in the assembling process of the bridge (Crocetti et al., 2005)

Step 2

Internal and external bracing units are attached to the two beams by using metal jois hangers connectors (Figure 4.5). The space between these bracing units is 1,80m.
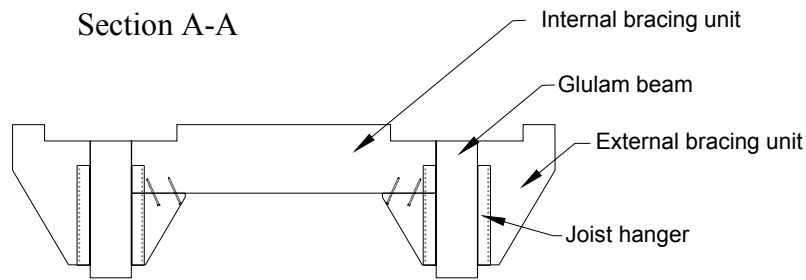
Figure 4.5 Step 2 in the assembling process of the bridge (Crocetti et al., 2005)

Step 3

The glue is spread over the upper surface of the two beams, and the stripes of the LVL Kerto-S® are placed over them. To guarantee a full connection a certain nember of screws are provided to keep these two members attached to each other until the glue has completely hardened. In fact the LVL Kerto-S® elements have to be slightly bent to follow the precambered shape of the glulam beams (Figure 4.6).
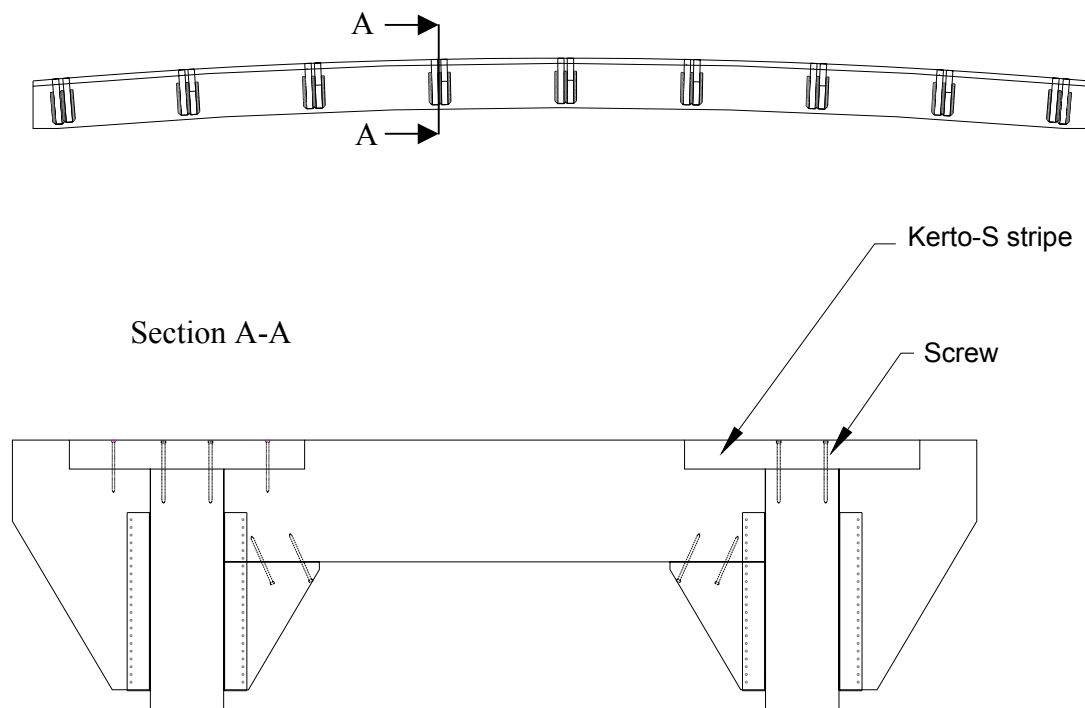

Figure 4.6 Step 3 in the assembling process of the bridge (Crocetti et al., 2005)

Step 4

In a similar way as in the previous step 3, now the LVL Kerto-Q® layers are placed over the structure. The glue is spread among all the upper surface of the Kerto-S® stripes and of the transversal bracing units as well. Is still necessary to provide a proper amount of screws to permit a full interaction while the glue is hardening (Figure 4.7).

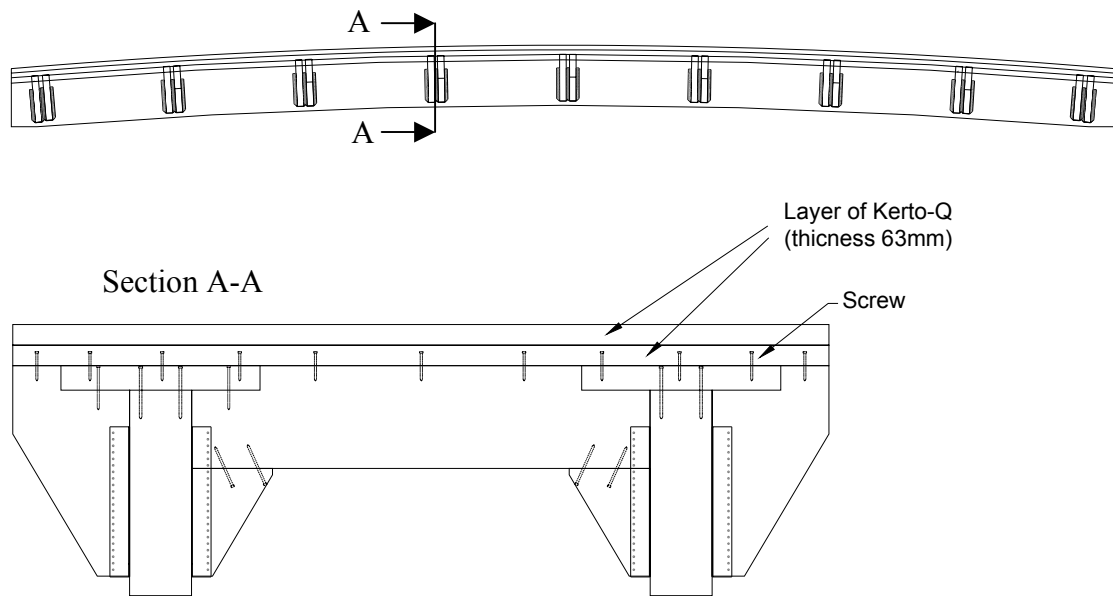Section A-A

Layer of Kerto-Q (thicness 63mm)

Screw

Figure 4.7 Step 4 in the assembling process of the bridge (Crocetti et al., 2005)

Step 5

Before adding the last components of the bridge (handrails and the elements of the wearing surfaces) a layer of an insulation mat to protect wood is provided all around the Kerto-Q® deck (Figure 4.8).
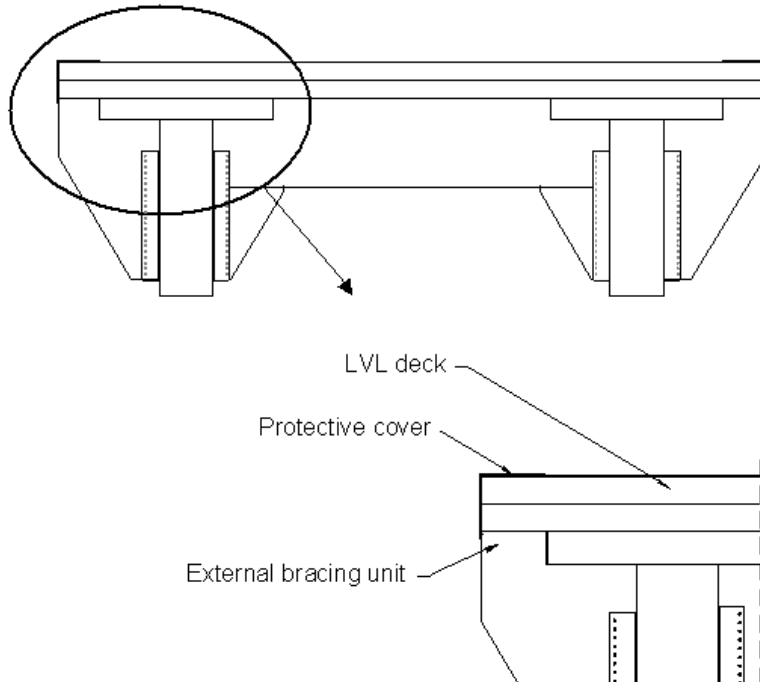

LVL deck

Protective cover

External bracing unit

Figure 4.8 Step 5 in the assembling process of the bridge (Crocetti et al., 2005)

Step 6

The handrail structure is then added to the bridge through connections in the nine sections where there are the external transversal elements. In each of these connetions metal connectors are arranged to provide enough resistance to the handrails against the actions considered in the ultimate limit state design (Figure 4.9)
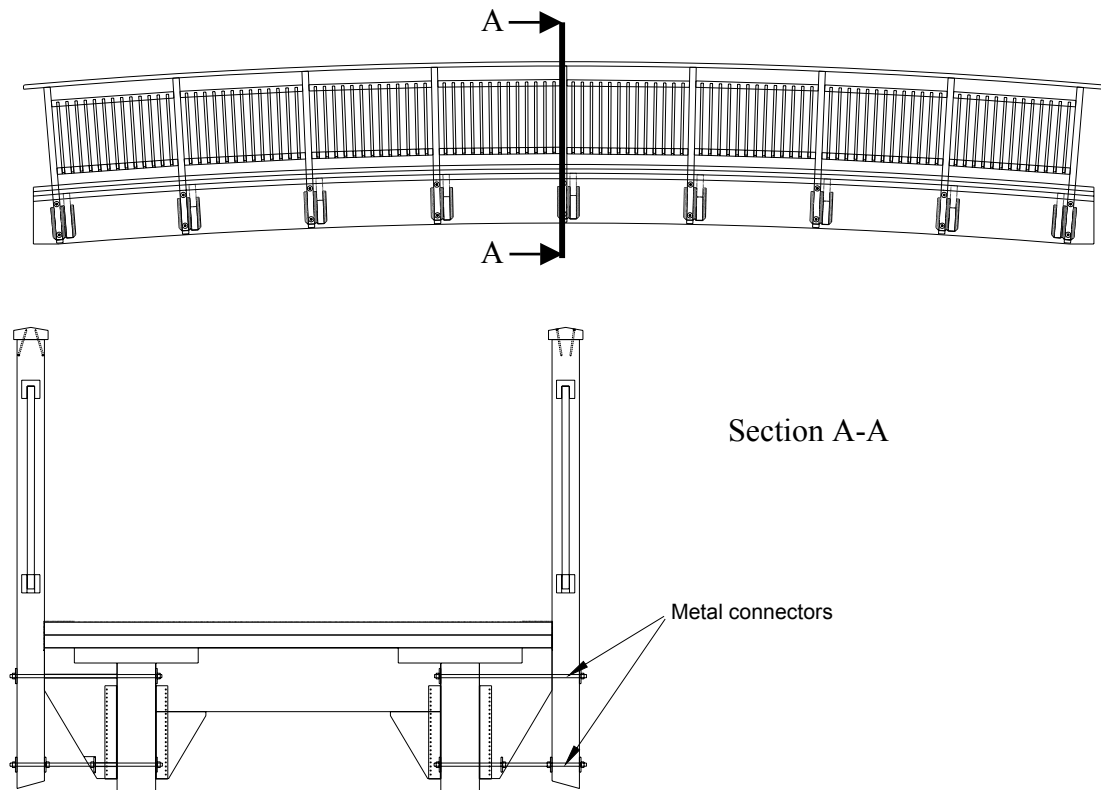

Figure 4.9 Step 6 in the assembling process of the bridge (Crocetti et al., 2005)

Step 7

Finally, the wearing surface over the deck is added (Figure 4.10).
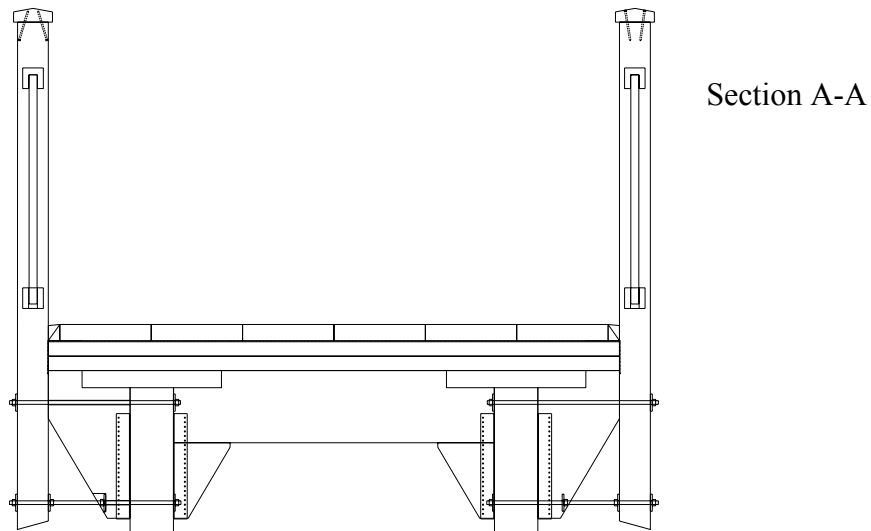
Section A-A

Figure 4.10 Step 7 in the assembling process of the bridge (Crocetti et al., 2005)

The bridge is now ready to leave the factory and to be transferred on site.

The market offers a large variety of suitable trucks to transport such type of structure; Bridges with spans larger than 15m and based on the same concept of the one analysed in this thesis could be available (increasing the height of the beams). Transportation does not represent a limit in this case: nowadays special trucks which could transport up to 40 m lengths are available. Limitations can be given instead by the type of road and the shape of the track that links the factory to the construction site.

Figure 4.11 Special truck used to transport large timber memebers (Holzbau Spa)

4.3   Durability problems

The risk correlated to durability problems are essentially related to the level of protection of wood from the surrounding humidity. These problems are also taken into account by the national and European construction codes, introducing some coefficients that reduce the characteristic strengths of timber. The value of these parameters depends on the service class that the structure belongs to (both EC5 and Swedish codes classify timber structures in three service classes, depending on the atmospheric conditions, especially humidity, expected in the place where the structure will spend its service life). The worse is the service class for that structure, the larger it is the reduction on the characteristic strength of materials. Besides the environmental conditions measured in the construction site, also the type of protection of its timber members determines the service class for that bridge.

It is possible to adopt valid techniques to protect the wooden parts, which consent to limit significantly durability problems for the bridge. An abstract of the article "Wearing Surfaces for timber Bridges (Anna Pousette, 1997)" is presented as follow.

"Traditionally, wearing surfaces for timber bridges were made of battens. Nowadays, asphalt or concrete paving is possible also on timber bridges. An asphalt pavement will protect the timber bridge deck from traffic abrasion and moisture as well as provide a smooth and skin-resistance surface. To avoid cracks and potholes in the asphalt paving, a stable deck with little deflection is required. A stress-laminated deck plate is the best choice, but glulam or nail-laminated decks are also suitable for paving.

Asphalt pavements are adapted to different traffic densities by using different thickness and configurations of the pavement. The insulation protects the supporting structure from moisture penetrating the asphalt, the protective layer protects the insulation and the binding layer is used to reduce cracking and provide a smoother deck for the wearing surface. The wearing surface is applied with a dense mixture. See Figure 4.11.
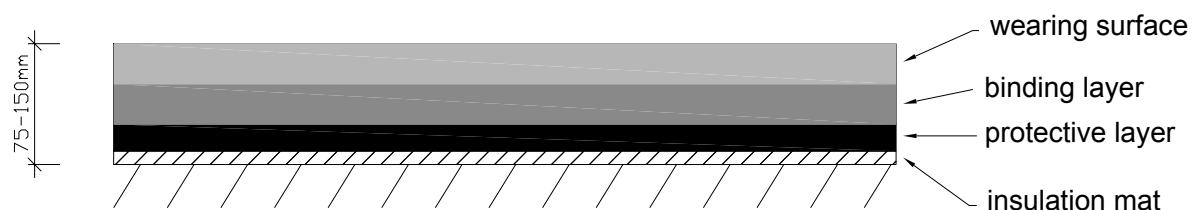

Figure 4.11 Configuration of asphalt pavement on concrete bridges for vehicle traffic (Anna Pousette, 1997)

For bridges, the insulation is an important part of the paving, and for timber bridges, the main purpose is to protect the timber against high moisture ratios, over 20%. Good insulation requires a smooth and even deck surface. The insulation must meet the following demands: water-tightness, adhesion to the deck in order to avoid blistering and assure shearing resistant fastening to deck and pavement.

Asphalt mastic or insulation floated asphalt is used together with a gas discharging glass fibre net, which will prevent blistering caused by moisture from the deck. Qualities at low temperatures are improved if the asphalt mastic is polymer-modified. Bitumen insulation mats consist of a body of glass fibre or polyester, and the upper side may be covered with sand, granulate or plastic foil. The bridge is pretreated with primer and the mat is fastened with bitumen or welded. Qualities at low temperatures are improved if the bitumen mat is polymer-modified.

The testing shows that welded insulation mat may be used on timber bridges, and blistering occurs in a lower amount than on concrete decks.

Adherence problems when using an insulating mat for insulation usually depends on blistering under the mat. For this reason it is important that the deck is dry on the surface when insulating. A planed or sanded surface provides the best adherence. Blistering may occur due to the heat when hot asphalt is spread on top of the insulation. However, hot asphalt must be used on the insulation mat to get adherence between the insulation mat and the asphalt as well as between layers of asphalt. A certain thickness of the protective layer is also required to get a good paying that covers seams, and the thinner the layer is, the easier it cools down. Blistering may also occurs due to heating by the sun later. Thicker pavement is considered to decrease the deck surface temperature, but that is less important for wood decks than concrete decks since wood has low heat conductibility.

Insulating may take place at a factory, for example when manufacturing smaller foot bridges that are transported assembled to the construction site. When the insulated bridge is brought to the construction site, it must be mounted at once and paved with a protected coating. Edge sealing along the bridge may be done with epoxy on top of the insulation mat.

Floated asphalt is made of a combination of well-graded aggregate and a high portion of asphalt binder. The aggregate is chosen to provide the smallest possible number of cavities and the amount of asphalt binder is adapted to fill cavities entirely."

4.4 Verifications of the hypothesis of composite section

The hypothesis of composite section is very important in the design of the bridge. If there was not fully interaction between the two components (beam and deck), the stresses due to bending in the beams would have been much higher since it would not have been possible to use the inertia of the composite section in the calculations.

In the gluing layer of interface shear and normal stresses are acting (tensile stresses due to particular non-symmetric loads may also occur). The glue has to provide enough strength to transfer shear stresses between adjacent elements.

The Moelven Töreboda AB designers assured that the bridge is entirely assembled in the factory, so the gluing process develops in a way comparable to the one use for the laminates in glued laminated timber. The glue connections can therefore be considered as rigid connections and they should not represent a problem during the service life of the bridge (Crocetti, 2005).

In addition if adhesives used to link together glulam beams and the LVL products has similar properties to the one utilized for manufacturing glued laminated timber, then the properties described in Chapter 2, Section 2.1 are still valid: the strength of adhesion between these adhesives and wood is greater than the cohesive strength of the wood itself, as test blocks bonded with these adhesives show over 75% wood failure when loaded to destruction (Cesaro and Piva, 2003).

Hence, it has been chosen to omit to study through the problems concerning the interface between glulam beams/Kerto-S® and Kerto-S®/Kerto-Q®.

5 Design and verifications of the bridge based on EC5

The bridge that is analysed in this Thesis work has been already presented in the previous Chapter 4. The information gathered and described in the first chapters together with the considerations formulated in Chapter 4 are useful also now that the design of the bridge is going to be developed. The coefficients for the load combinations, the safety factors for the materials, the service classes, the duration of loads assigned in the Eurocode (Anon. 1995b) and the characteristic strength of materials assigned in UNI-EN 1194 (1993) have been assumed. In this Chapter, Chapter 6,7 and 8 the orthotropic hypothesis for the materials of the deck is not considered; all the components of the bridge are simplified as isotropic materials.

This Chapter analyses in details the design of the bridge based on EC5. It is divided in 6 parts: 1) definition of the design values for the strength of materials, 2) definition of the loads acting on the bridge, 3) definition of the load combination, 4) calculation of the design moment and the design shear, 5) verifications in the ULS: stress verification, 6) verifications in the SLS: deflection and vibration verification.

The differences between EC5 and Swedish codes will also be examined, especially concerning loads, the resistance values of materials and partial safety factors for materials and load combinations.

Detailed information concerning analytical calculations and the differences between the two codes can be found in the appendices.

5.1 Design values for the strength of materials

For timber and wood-based materials the design strength in the ULS is calculated starting from the characteristic strength in the simple way:

$$f_d = k_{mod} \cdot \frac{f_k}{\gamma_m} \qquad (Eq.\ 5.1)$$

where γ_m is the material safety partial factor; for the timber γ_m is equal to 1.3 (see EC5, part 1-1, point 2.3.3.2)

To take in account the real mechanical behaviour of timber, when it is loaded by external actions, the introduction of the "Modification Factor" k_{mod} parameter it has been necessary.

This parameter depends on "Service class" and "Duration of loads" that have been assumed for the bridge studied: "Service class 2" and "Short loads". In this way k_{mod} becomes equal to 0,9.

The design values of the materials used in the bridge can be found in the Table 5.1:

Table 5.1 Design values of the materials used in the bridge

	fc [MPa]		fd [MPa]	
Glued Laminated Timber	f_{mk}	32.00	f_{md}	22.15
	f_{t0k}	24,00	f_{t0d}	16,62
	f_{t90k}	0,45	f_{t90d}	0,31
	f_{c0k}	29,00	f_{c0d}	20,08
	f_{c90k}	6,00	f_{c90d}	4,15
	f_{vk}	3,50	f_{vd}	2,42
	$E_{0,05}$	10800		
	E_{mean}	13500		
	$E_{90,mean}$	450		
	G_{mean}	845		
	$\rho_{k[kg/m^3]}$	440		
Kerto-S®	f_{mk}	36,00	f_{md}	24,92
	f_{t0k}	26,00	f_{t0d}	18,00
	f_{t90k}	0,00	f_{t90d}	0,00
	f_{c0k}	26,00	f_{c0d}	18,00
	f_{c90k}	1,80	f_{c90d}	1,25
	f_{vk}	1,30	f_{vd}	0,90
	$E_{0,k}$	8800		
	E_{mean}	10500		
	G_k	400		
	G_{mean}	600		
Kerto-O®	f_{mk}	50.00	f_{md}	34.62
	f_{t0k}	35,00	f_{t0d}	24,23
	f_{t90k}	0,00	f_{t90d}	0,00
	f_{c0k}	35,00	f_{c0d}	24,23
	f_{c90k}	1,80	f_{c90d}	1,25
	f_{vk}	2,30	f_{vd}	1,59
	$E_{0,k}$	11600		
	E_{mean}	13800		
	G_k	400		
	G_{mean}	600		

For more information see the Appendix C.

Remarks

BKR consider the plywood more influenced than the glued laminated timber by worse service classes. This distinguish is not present in the EC5. As a consequence, there is a difference of resistance for plywood of 38% between the two codes. The discrepancy between the two codes in the design resistances for Glulam results around 11%..

These considerations are clarified in the following Table 5.2:

Table 5.2 Comparison between BKR and EC5

		BKR		EC5	
Glued Laminated	Kr	0,85	kmod	0,9
	γm	1,15	γm	1,3
	γn	1,2		
	$\dfrac{k_r}{\gamma_m \cdot \gamma_n} =$	0,61	$\dfrac{k_{mod}}{\gamma_m} =$	0,69
	Discrepancy between the codes = 11 %				
Plywood	Kr	0,595	kmod	0,9
	γm	1,15	γm	1,3
	γn	1,2		
	$\dfrac{k_r}{\gamma_m \cdot \gamma_n} =$	0,43	$\dfrac{k_{mod}}{\gamma_m} =$	0,69
	Discrepancy between the codes = 38 %				

In the case of glulam, the difference of 11% can be quite reasonable, since it should be remind that the Eurocode imposes partial coefficient for permanent loads higher than the BKR (1.35 compared to 1.00 used in the Swedish codes – see Appendix D for more information).

Whereas the difference in the case of plywood is rather big. The reasons of this could depend on the different approaches adopted by the two codes: the BKR considers this LVL materials like Kerto-Q® and Kerto-S® very bad influenced by difficult environmental conditions in a stronger way than the EC5. These products are still quite new products and examples of long-term tests are not available yet.

Finally, we want to mention all the difficulties met during this thesis work due to the uncertainness of the characteristic values of these LVL products (Kerto-Q® and

Kerto-S®). The values shown in Appendix C refer to the certificate of the 24th October 2005; the certificate available before (VTT certificate NO 184/03, issued 24 March 2004) held very different characteristic resistance values. All the values related to the compressive strength perpendicular to the fibres and to the shear strength have been reduced. For instance, the value of f_{c90k} from 6 MPa decreases to 1.8 MPa. Previously this reduction had involved also glued laminated timber products but with a much lower percentage. Furthermore, the reduction of flatwise shear strength for Kerto-S® from 4.4 MPa to 2.3 MPa has been quite surprising. A modification of this amount can totally change the important aspects that have to be investigated in the design of such this kind of structures. Nonetheless, the new certificate holds just one value of flatwise shear resistance about the two different in-plane directions, while the previous VTT certificate considered two different values.

5.2 Loads acting on the bridge

The loads considered in the design of the bridge are:

1. **Live load**

The live load is a uniformly-distributed load acting on the bridge. The characteristic load given by Eurocode (Anon. 2004c) for a 15 meters span bridge is: $q_{vk} = 4.67 \dfrac{kN}{m^2}$

2. **Service vehicle load**

The pedestrian bridge has to be design also in respect to the loads caused by a service vehicle used for several services, like maintenance, assistance for people (it could be an ambulance for example), or other kind of functions (for example a vehicle used to clean the roads from the snow). The service vehicle load adopted is the one suggested by the BRO, point 21.2227; a full description can be found in the Appendix A.

$P_{front} = 40kN$ and $P_{rear} = 80kN$ are the characteristic values respectively of the front wheel axle and the rear wheel axle.

3. **Snow load**, it was assumed the characteristic value $s_k = 3.0 \dfrac{kN}{m^2}$.

The snow design value was calculated in the next way:

$$q_{sd} = 0.8 * 3.0 \frac{kN}{m^2} = 2.4 \frac{kN}{m^2}$$

4. **Self weight**

The self-weight load q_g comprehends the weight of all the elements of the structure that have a bearing role like the beams, the deck and the transversal

bracing units. The layer of asphalt above the timber deck, the railways, and the waterproof coverings are elements supported by the bearing structure, and are added to the self-weight in the combination of loads. It is good to collect them in a separate group of permanent loads q_p. The magnitudes of these loads based on the densities of materials (Eurocode 1 (Anon 1995b), part 2-1, section 4) included in the structure are:

$$q_g = 1.66 \frac{kN}{m^2} \qquad\qquad q_p = 2.34 \frac{kN}{m^2}$$

For more information concerning the loads see Appendix D.

5.3 Load combinations

To design the whole structure three different load combinations have been considered.

1. Self-weight + Permanent load + Live load

2. Self-weight + Permanent load + Service vehicle load (placed in the middle of the span)

3. Self-weight + Permanent load + Service vehicle load (placed over the support)

The load combination 1 must be considered in the design, even if it does not maximize the moment in the middle of the span. Furthermore, it is relevant in the design and verification of the deflection. Compared to this first group of loads, the load combination "Self-weight + Permanent load + Snow load" produce less unfavourable result, so that is not taken into account. The value of snow load ($q_{sk} = 2.4 kN/m^2$) is lower than the live load ($q_{vk} = 4.67 kN/m^2$) as it was explained in the previous paragraph.

The load combination 2 is the one that maximizes the moment in the middle of the span. The load combination 3 is the one that maximize the shear in the cross section. In the load combinations 2 and 3 the service vehicle is not placed symmetrically in the transversal direction, but close to the edge of the deck; in this way most of its weight is transferred to one of the two beams, and the most unfavourable load case is therefore taken into account.

An eventual fourth load combination: "Self-weight + Permanent load + Snow load + Service vehicle load" could also be considered, but in this case the vehicle load used to clean the bridge from the snow is not allowed to stay with its wheels at the edge of the deck because of the encumbrance of the snow shovel. For this reason this load combination produces less unfavourable effects than the other already considered. The explanation with calculations of this fact can be read in the Appendix E.

The values of the loads presented in the previous chapter are gathered in Table 5.3:

Table 5.3 Characteristic loads acting on the bridge

Self - weight	qg	1.66	kN/m²
Permanent load	qp	2,34	kN/m²
Live load	qv	4,67	kN/m²
Design veicle load	Pfront	40	kN
Design veicle load	Prear	80	kN
Snow	qv,s	2,40	kN/m²

These loads must be combined using appropriate partial factors γ and combination factors ψ, in the way presented as follow (Eurocode 1 (Anon.1995b), part1-1):

$$\sum_{i\geq 1}\gamma_{Gj}G_{kj}+\gamma_{Q1}Q_{k1}+\sum_{i>1}\gamma_{Qi}\psi_{0i}Q_{ki} \qquad \text{(Eq. 5.2)}$$

G_{kj} is the permanent action, Q_{k1} is the dominant variable action and Q_{ki} represents other variable actions.

In Table 5.4 the load combination coefficient used can be found.

Table 5.4   Coefficient used in the relevant load combinations

Load combination coefficient:	
γg	1.35
γq	1,5
ψ01	0,7

The only difference with the Swedish codes regards the value of the partial safety factor related to the permanent load γ_g: in the Swedish codes this value is decreased to 1.0.

The load combinations discussed at the beginning of this paragraph lead to the following design load values, Table 5.5:

Table 5.5 Load Combinations

Load Combination:			
1. Loads 1+2+3	qd1EC5	12,40	kN/m²
2. Loads 1+2+4 (middle span)	qd2EC5	5,40	kN/m²
3. Loads 1+2+4 (near support)	qd2EC5	5,40	kN/m²

$q_d = 15.50 \dfrac{kN}{m}$ is the total design load acting on both the two effective symmetric

sections of the bridge in the load combination 1;

$q_d = 6.75 \dfrac{kN}{m}$ is the design load acting on both the two effective symmetric sections

of the bridge in the load combinations 2 and 3 only due to the permanent loads; the additional vehicle load is to be added not sharing it equally on the two effective section because of its non-symmetry;

$q_d = 9.90 \dfrac{kN}{m}$ is the design load acting on both the two effective symmetric sections

of the bridge in a load combination that takes into account the permanent loads and the snow load.

5.4 Calculation of the Design moment and the Design Shear

To verify the structure in the Ultimate Limit State the values of design moment and design shear must be calculate; this calculation is done on a bridge with 15 meters span, whose transversal section is presented in Figure 5.1 without handrails and waterproof coverings:
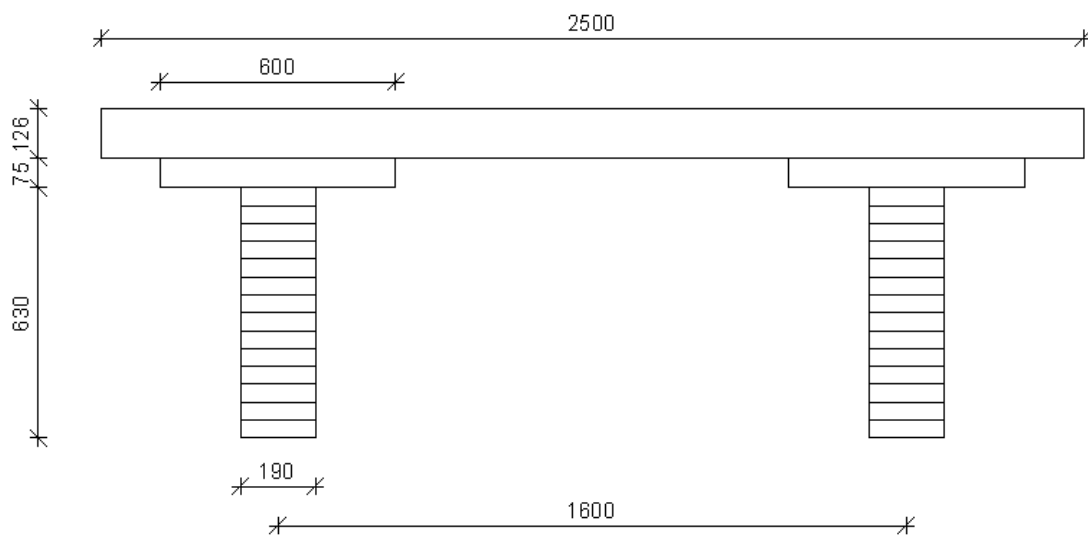
Figure 5.1 Cross section of the bridge without handrails and waterproof coverings

In this first step of design of the bridge simple models of the structure on the safe side will be used. The aim of the hand calculation contained in this paragraph is both to design and verify the bridge in the ULS, but also to start to understand the mechanical behaviour and the problems related to this bridge. In the case of "only distributed load", load combination 1, two single simply supported beams subjected to a linear distributed load $q_d = 15.50 \, \text{kN/m}$ and with a suitable effective section have been

verified. In Chapter 6 it will be explained how the effective section should be calculated.

Load combination 1:

Permanent and Live Load
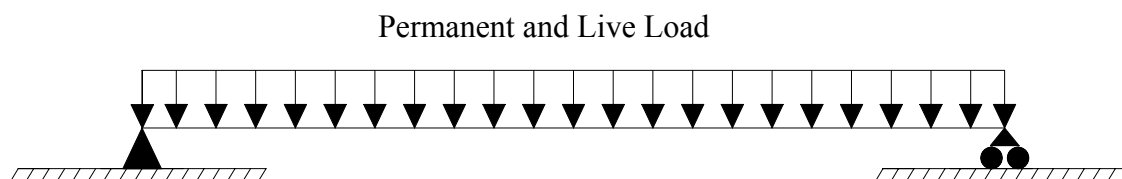
Figure 5.2 Load combination 1

Design moment and design shear result for load combination 1:

$$M = \frac{ql^2}{8} = 435.94 \text{ kNm} \qquad\qquad V = \frac{ql}{2} = 116.25 \text{ kN}$$

Load combinations 2 and 3:

As just mentioned, the load combinations that include the vehicle load give higher values for M and V. Firstly, a preliminary study has to be performed to take in account the non-symmetric position of this load in the transversal direction. In fact, if the vehicle is not placed in the middle on the road, but it is place on the edge of the deck with its wheels, very high stresses will be induced on one beam compared to the other, as it is shown in the Figure 5.3:

Load treads of the vehicle

Highly Loaded Beam
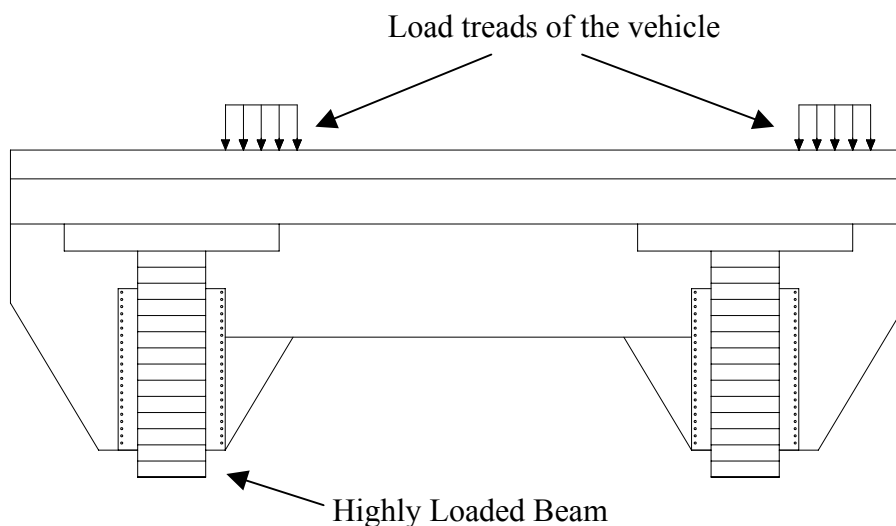
Figure 5.3   Position of the concentrated loads due to the service vehicle, view of the cross-section

In the real case, the vehicle has a certain encumbrance (see Appendix A), and it will always be placed at least 10cm from the external edge of the deck. In this preliminary study on the safe side, it is consider without encumbrance:
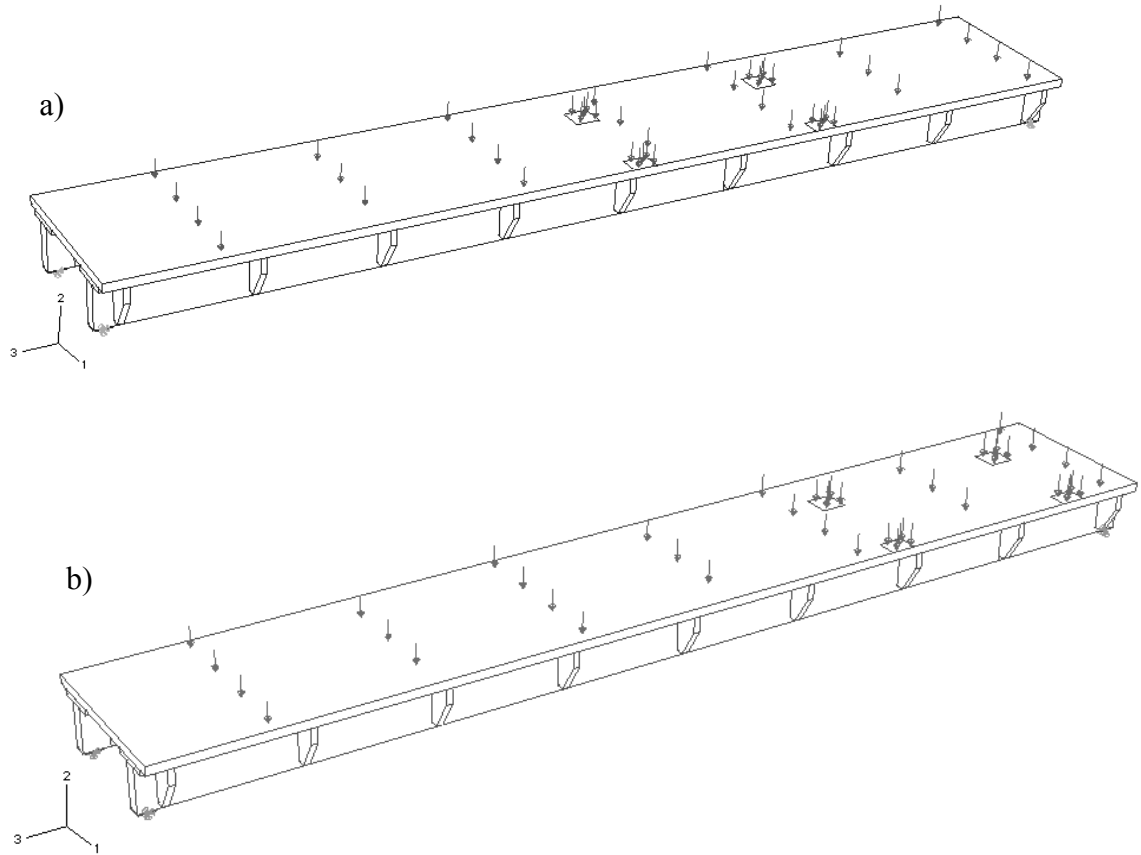
Figure 5.4   a) Load combination 2 b) Load combination 3

It's easy to understand from the picture above that the load combinations 2 and 3 are non-symmetric, both in the longitudinal and transversal direction. To solve the structure by hand calculations it has been necessary to model it as two independent longitudinal beams loaded in a different manner.

In the same way, in order to find how the load is divided transversally, a model was used of a simply-supported beam made with a stripe of the deck (e.g. of Kerto-Q®), where the supports are represented by the glulam beams, see Figure 5.6 and 5.5. The results obtained in this way will be on the safe side, The concentrated load will be divided on the two beams as it is shown in Figure 5.5, using the coefficient k.

.
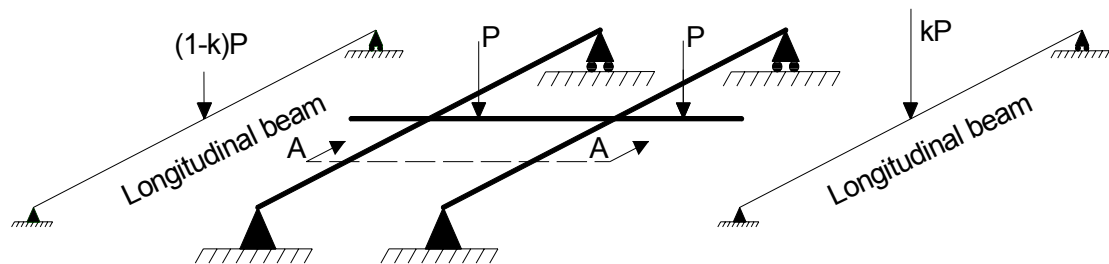
Figure 5.5 Model of the bridge in two directions to study the distribution of the non-symmetric loads P
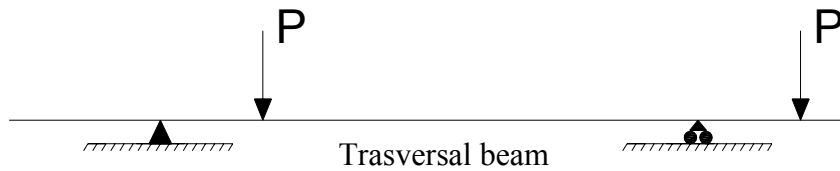
Figure 5.6   Section A-A referred to the Figure 5.5

Hence, referring to the Figure 5.7, the aim is to study the amount of load that will be transferred to each beam.
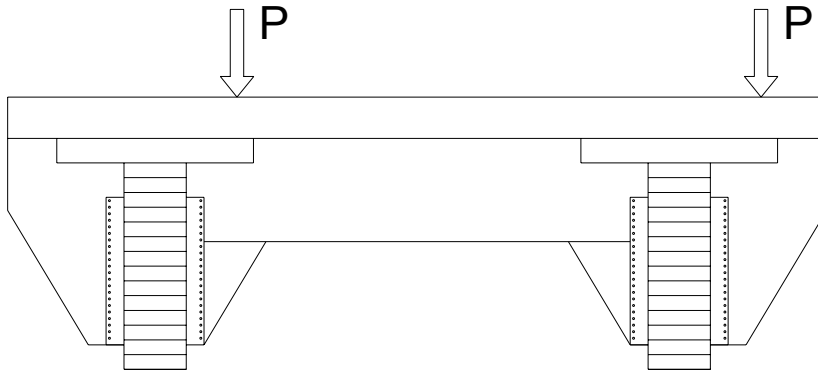
Figure 5.7 Cross-section and concentrated loads position

Using scheme of the transversal beam shown in Figure 5.8 is possible to determine the coefficient k. This coefficient permits to assign the percentage of load due to the service vehicle for each beam.
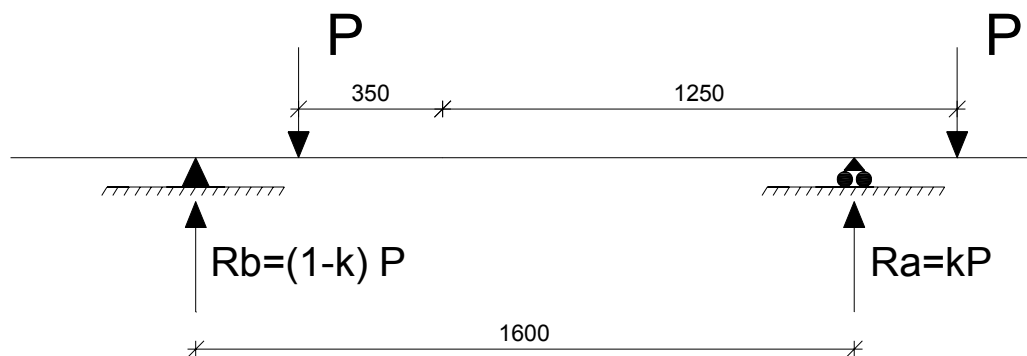
Figure 5.8 Scheme of the cross-section used in analytical calculations to find the k-coefficient

The reactions Ra and Rb represent the amount of load that is differently transferred to the two beams.

P = 60 kN

Ra * 1600mm= P *(1250mm+350mm) + P * 350 mm

$$Ra = \frac{2300mm}{1600mm} * P = 1,43 \ P \qquad\qquad Rb = 0,57 \ P \qquad\qquad k = 1,43$$

It was chosen to increase the most loaded beam by a factor equal to 1.43 compared to the situation with the vehicle in the centre of the road.

It is now possible to find the maximum moment and shear acting on the structure.

For more information concerning the method used to find the k-coefficient value of 1,43 see Appendix E.

Load combination 2:

To maximize the moment in the middle of the span, the vehicle should be placed in order to have its heavier wheel axle in the middle of the span.
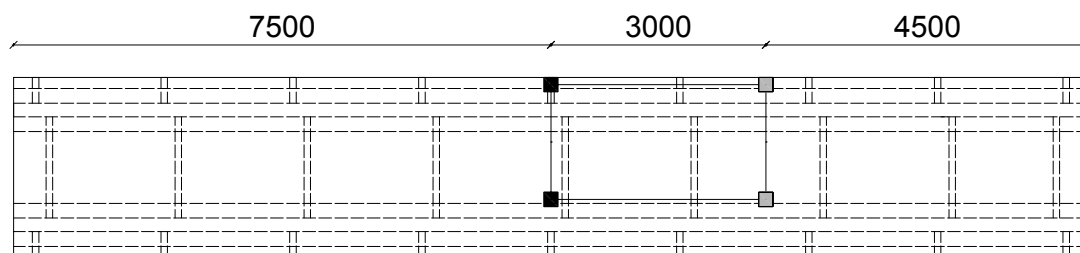
Figure 5.9 Plan view of the bridge: load combination 2

The load due to the heavier wheel axle is $P_{rear} = 80.00kN$. Being a variable load, it should be increased by a coefficient $\gamma = 1.5$. Since the non-symmetry in the transversal direction will be taken into account at the later stage, to consider its effect on just one beam it should be also divided by two:

$$P_{max} = \frac{P_{rear} \cdot 1.5}{2} = 60kN = P \qquad\qquad P_{min} = \frac{P_{front} \cdot 1.5}{2} = 30kN = \frac{P}{2}$$

Using the equilibrium equation is possible to obtain the values of M and V:

M = 608.12 kNm   V = 123.56 kN

Load combination 3:

In Chapter 7, using the models of the structure in Abaqus®, it will be shown the position of the service vehicle that maximizes the shear at the supports. This position is not the one with the heavy wheel axle exactly over the support, but when it's at a certain distance from it.

Following the EC5, part 1-1, point 5.1.7.1:the heavy wheel axle is then located at a distance of 2h from the support. The depth of the effective section is equal to 831mm.
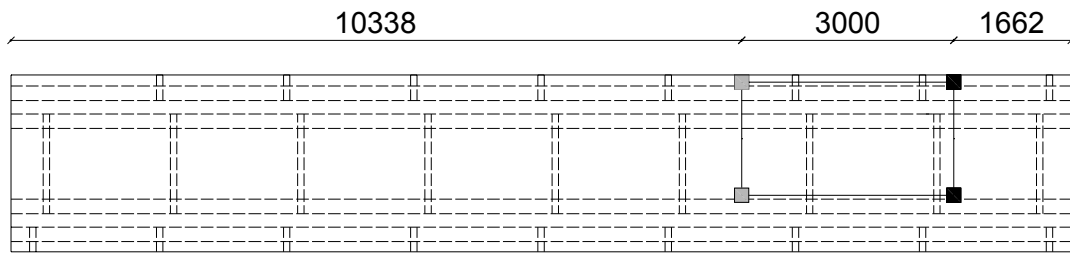
$2 \cdot h = 1662mm$

Figure 5.10 Plan view of the bridge: load combination 3

The maximum shear force V_B at the right support due to the service vehicle load results: V = 157 kN

The total moment in the middle span is: M = 361 kNm

Load combination 4:

It is here shown that this load combination produces lower shear and moment in the structure; the service vehicle is transversally set in middle of the road, so that moment and shear are not increased by the factor 1.43.
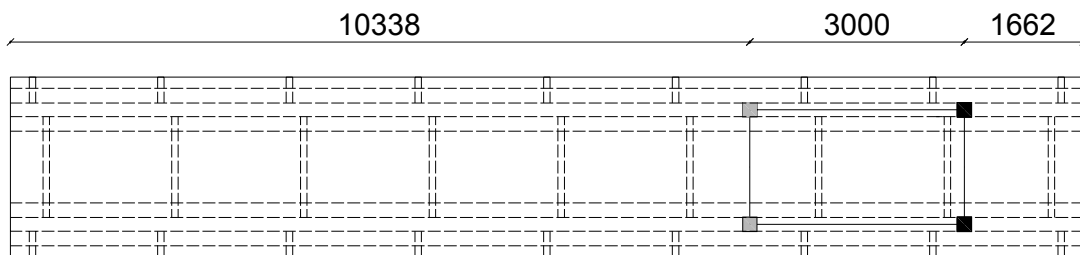

Figure 5.11   Plan view of the bridge: load combination 4

The shear results lower than the load combination 3:

The total shear force at the right support is: V_B = 148.25 kN

The moment in the middle of the span is: $M = 570 kNm$

Hence, it results lower than the one of the load combination 2.

The design Moment and the Design Shear on which the verifications must be based are summarized as follow:

M = 608.12 kNm   (load combination 2)

V = 157 kN   (load combination 3)

For more information concerning the methods used to find M and V in the different load combinations see Appendix E.

5.5 Stress Verifications

The effective cross section, which the stress verifications are based on, is presented in Figure 5.12 below:
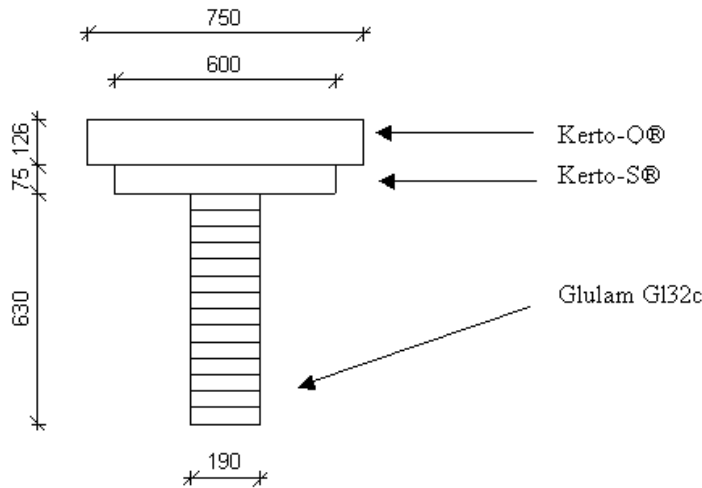
Figure 5.12   Effective cross section of the two beams of the bridge

The components of this section are the Glulam beam Gl32c, the whole stripe of Kerto-S®, and a part of Kerto-Q® deck for a width of 750mm. The section is symmetric about the vertical axis. In Chapter 6 the study of the effective width to take in account in hand calculations will be treated in details. At this step it can be enough to know that this section satisfies the restrictions imposed at point 5.3.2 of the EC5 about the choice of the effective cross section for glued thin-flanged beams; the non-uniform distribution of stresses in the flanges due to shear lag and plate buckling are taken into account.

The elastic modulus of the three materials of the composite section are:

Emean KertoQ	10 500	MPa
Emean KertoS	13 800	MPa
Emean Gl32c	13 500	MPa

It can be assumed that planar sections perpendicular to the beam axis in the undeformed shape remain so even after loading when the deformed shape is reached. To find the stress distribution over the section it's obviously necessary to take in account the different values of modulus of elasticity of the three different materials. This is done by the use of the modular ratios n of the transformed section; the modulus of elasticity chosen as reference is the one of the Kerto-Q® material:

$$n_1 = \frac{KertoQ}{KertoQ} = 1,00 \qquad n_2 = \frac{KertoS}{KertoQ} = 1,31 \qquad n_3 = \frac{GL32c}{KertoQ} = 1,29$$

Position of the neutral axis and the inertia of the effective section have been calculated for the design in the ultimate limit state. The calculations are reported in the Appendix F.

The value found for the position of the neutral axis is x =309.02mm; the inertia of the section is Isec=1.88E+10mm^4

In order to find the stresses in the section due to bending, the modular ratios must be introduced in the Navier formula: $\sigma = \dfrac{M}{I} y \cdot n$

where "y" is the distance of the general fiber from the neutral axis. The distribution of normal stresses is described in Figure 5.13.
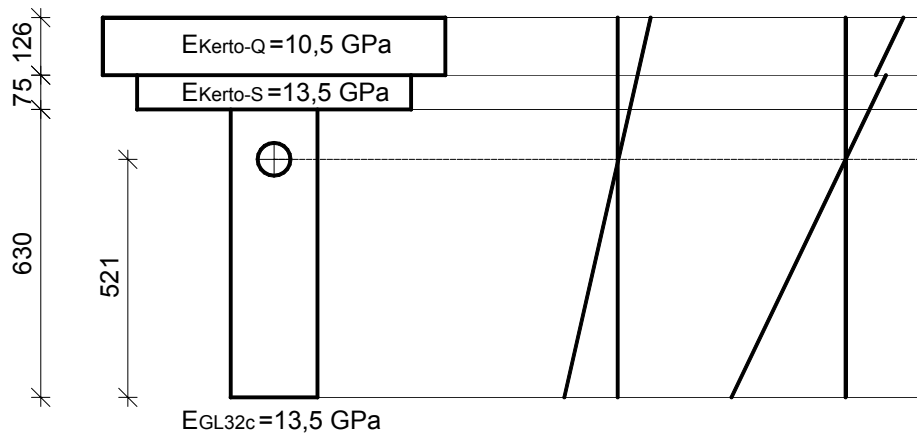

Figure 5.13   Distribution of normal stresses among the effective section

Jourawsky formula is used instead to find the distribution of shear stresses among the section: $\tau = \dfrac{V \cdot S}{b \cdot I}$

In the calculation of the moment of the first order $S = \dfrac{b}{2} \cdot \left(h_1^2 - h_2^2 \right)$ the centre of gravity of the transformed section is taken in account.

S beam n	3,10E+07	mm^3
S KertoS	2,99E+07	mm^3
S KertoQ	2,33E+07	mm^3
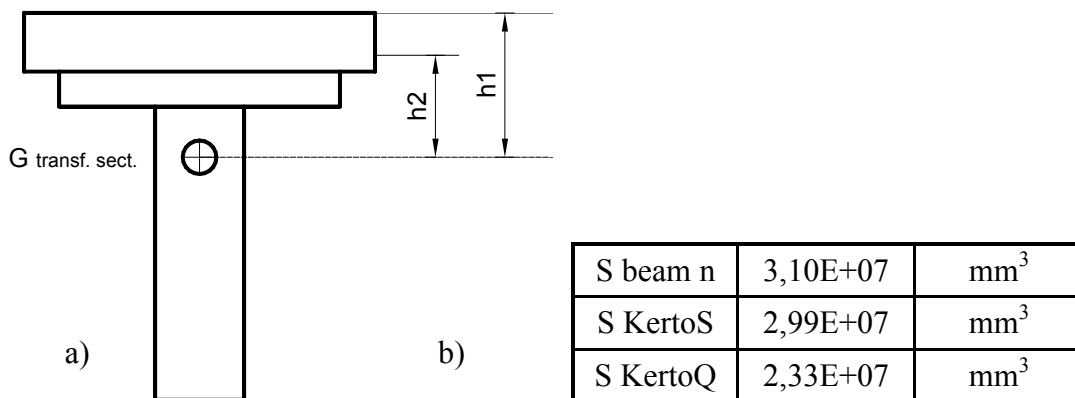
Figure 5.14   a)Cross section, b) Values of the first moment of inertia

Table 5.6 Values of normal stresses σ and shear stresses τ for the load comb 1,2 and 3

Load combination 1				
MsdEC5_1 [kNm]	435.94	VsdEC5_1 [kN]		116.25
		Stress [MPa]	fd [Mpa]	Utilization values [%]
Bending	σ Kerto-Q®	7,16	24,92	29
	σ Kerto-S®	5,58	34,62	16
	σ beam	15,56	22,15	70
Shear	τ Kerto-Q®	0,24	0,90	27
	τ Kerto-S®	0,97	1,59	61
	τ beam	1,01	2,42	41
Load combination 2				
MsdEC5_2 [kNm]	608.12	VsdEC5_2 [kN]		123.56
		Stress [MPa]	fd [Mpa]	Utilization values [%]
Bending	σ Kerto-Q®	9,99	24,92	40
	σ Kerto-S®	7,78	34,62	22
	σ beam	21,70	22,15	98
Shear	τ Kerto-Q®	0,25	0,90	28
	τ Kerto-S®	1,03	1,59	65
	τ beam	1,07	2,42	44
Load combination 3				
MsdEC5_3 [kNm]	361.44	VsdEC5_3 [kN]		157.02
		Stress [MPa]	d [Mpa]	Utilization values [%]
Bending	σ Kerto-Q®	5,94	24,92	24
	σ Kerto-S®	4,62	34,62	13
	σ beam	12,90	22,15	58
Shear	τ Kerto-Q®	0,32	0,90	36
	τ Kerto-S®	1,31	1,59	82
	τ beam	1,36	2,42	56

Table 5.6 shows the values of normal stresses σ and shear stresses τ for the fibres at the lowest edge of the beam (σ_{beam}, τ_{beam}), at the interface beam – Kerto-S® (σ_{KertoS}, τ_{KertoS}), at the interface between Kerto-S and Kerto-Q (σ_{KertoQ}, τ_{KertoQ}), for the three load combinations presented in the previous Section 5.5.

From the values of Table 5.6 it can be noticed that:

- All the values of stresses presented in Table 5.6 are respecting the design values based on EC5.

- The most important verification in the ULS it's the one concerning bending in the beam in load combination 2, where the 97% of the bending resistance of GL32c is reached.

- Looking at the stresses in Kerto-Q® deck, which represents the flanges of the "T" cross-section, it can be noticed that they are very low. This is due to two reasons: firstly the fact that in this kind of "T" section the position of the center of gravity is very close to the flange. Secondly, the fact that the Kerto-Q® material has a lower value of the modulus of elasticity. The bending capacity is not utilized in the Kerto-Q® deck.

- On the opposite, the shear stresses in the Kerto-S® for the load combination 3 are quite high: τ Kerto-S® =1,31MPa is smaller than 1,59 MPa. This rappresents 82% of the utilization factor.

  This aspect should be more considered since the characteristic values for these LVL materials are more or less uncertain, as it has been discussed in Chapter 5.2. As it will be shown at the end of this paragraph, the verification about the shear stresses for Kerto-S® based on the BKR is not satisfied.

5.5.1 Comparison between stresses found by analitical calculations and the models in Abaqus®

The values presented in Table 5.6 are now compared with the results of two kind of models developed by the using of the finite element program Abaqus®: the first model refers to a beam with the same "T" section considered in hand calculations, the second model represents the whole structure of the bridge. These two models will be described more in details both in Chapter 6 and Chapter 8.

- **Load combination 1**

Since the structure is subjected to a symmetric load, the hypothesis to consider the two beams separately is correct. This fact is supported also by the comparison between the maximum stresses calculated by hand and those given by the Abaqus® model of a simple beam with the same cross section and the Abaqus® model of the whole structure of the bridge.

Values found by hand calculations: σKertoQ® = 7,19 MPa and σbeam = 15,56 MPa

Values found by the Abaqus® model of a beam with a "T" cross section: σKertoQ® = 6,84 MPa and σbeam = 15,14 MPa

Values found by the Abaqus® model of the whole bridge: : σKertoQ® = 5,02 MPa and σbeam = 13,52 MPa

Differences of 5% concerning stresses in the beam and 2.8% concerning stresses in the deck can be observed between hand calculations and the model applied in Abaqus® of a beam with a "T" cross section. Differences of 13% concerning stresses in the beam and 30% concerning stresses in the deck can be observed between hand calculations and the model in Abaqus® of the whole bridge. This last large difference is due to the fact that a width of 750mm for the flange of the effective cross section is very much on the safe side. As it is explained in Chapter 6 it could be assumed an effective width of 1250mm (e.g. half of the total width of the bridge). In this case that difference decreased to 3% both for stresses in the beam and in the deck.

- **Load combination 2 and 3**

Both the assumption of analysing the bridge in the longitudinal direction as two separated beams and modelling the bridge like a stripe in the transversal direction are not realistic. These two assumptions do not take in account the 2D-behaviour of the deck, which works as a slab and not as two independent beams. The large thickness of the Kerto-Q® deck (126mm) plus the Kerto-S® stripes (63mm), compared with a rather small span of the deck (1410mm), it make sure that the "slab behaviour" of the deck is provided. Furthermore, adopting these two assumptions is not possible to define the real local distribution of stresses in the various elements of the bridge when the service vehicle is placed over the deck. A 3D model in Abaqus® is necessary to investigate the global and local behaviour of the structure and obtain realistic results when high non-symmetric loads are acting on the bridge.

Values found by hand calculations: σKertoQ® = 10,00 MPa and σbeam = 21,71 MPa

Values found by the Abaqus® model of the whole bridge: σKertoQ® = 7,57 MPa and σbeam = 16,50 MPa

Differences of 24% concerning stresses in the beam and 24% concerning stresses in the deck can be observed between hand calculations and the model in Abaqus® of the whole bridge. Finally, is good to notice that hand calculations show values larger than the one produced by Abaqus®: this confirms that hand calculations are on the safe side.

Comparison with the Swedish codes BKR

To compare the stress verifications based on the EC5 with the BKR is necessary to check the utilization factor of resistance used (e.g. the highest stresses reached with respect to the correspondent design strength). In this way both the partial factors used to define the design strengths and the design values of loads in the ULS are taken into account. As it is mentioned in Section 5.1 and 5.2, the values of these coefficients are quite different for the two codes. Three valuable considerations can be made:

- Looking at the bending stresses in the beams in the load combination 1:

EC5 $\implies$ σbeam = 15,56 MPa   < 22,15 MPa Utilization factor = 70%

BKR $\implies$ σbeam = 12,36 MPa   < 20,33 MPa Utilization factor = 60%

The difference is rather large; the reason is firstly the difference between the two characteristic values of live load: $q_{vk} = 4.67 \frac{kN}{m^2}$ for EC5 and $q_{vk} = 4 \frac{kN}{m^2}$ for BKR. Secondly is higher using value of partial factors γ for the permanent loads in the load combination in the ULS. EC5 uses $\gamma = 1.35$ than BKR, $\gamma = 1.00$.

As a confirmation of this, the comparison of bending stresses in the beams in the load combination 2 can be observed; in this case the vehicle load, whose characteristic values are the same for the two codes, is acting on the bridge instead of the live load, and the differences between the two codes are very small:

EC5 $\implies$ σbeam = 21,71 MPa   < 22,15 MPa Utilization factor = 97%

BKR $\implies$ σbeam = 19,65 MPa   < 20,33 MPa Utilization factor = 96%

- Looking at bending stresses in Kerto-Q® or Kerto-S® in the load comb 2:

EC5 $\implies$ σKerto-Q® = 10,03 MPa   < 24,92 MPa Utilization factor = 45%

BKR $\implies$ σKerto-Q® = 9,4 MPa < 15,52 MPa Utilization factor = 60%

The percentage values are very different in this case. The reason of this is the large difference in the design values of strengths obtained for plywood products in service class 2: as it was discussed in Section 5.1, the Swedish codes considers the plywood more influenced than the glued laminated timber by worse service classes, so that the resistance of Kerto-Q® and Kerto-S® must be further decreased by a factor equal to 0.7.

- Looking at the shear stresses in Kerto-S® in the load combination 3:

EC5 $\implies$ τKerto-S® = 1,31 MPa < 1,59 MPa   Utilization factor = 82%

BKR using the characteristic value given by VTT certificate NO 184/03, issued 24 March 2004 $\implies$ fvvk, Kerto-S® = 4,4MPa

BKR $\implies$ τKerto-S® = 1,35 MPa < 1,9 MPa   Utilization factor = 71%

BKR using the characteristic value given by VTT certificate NO 184/03, revised 24 October 2005 $\implies$ fvvk, Kerto-S® = 2,3MPa

BKR $\implies$ τKerto-S® = 1,35 MPa > 0,99 MPa   Utilization factor = 136%

The verification of the shear stresses based on BRO is not satisfied if the VTT certificate NO 184/03, revised 24 October 2005 is adopted for the characteristic

values of Kerto-S®. The verification was satisfied using the old VTT certificate NO 184/03, issued 24 March 2004, because it provided a resistance of 4.4 MPa.

It is still mentioned that the value of $\tau_{Kerto-S}$ = 1.35 is obtained from a simplified calculation and it is highly on the safe side. A detailed analysis of the distribution of stresses τ and σ will be presented in Chapter 8.

5.6 Design in the SLS

In timber structures, especially bridges, verifications in the SLS are very important and often, as for the bridge studied in this thesis, also the strictest one. To support this statement, it can be useful to analyse the contents of the following Table 5.7:

Table 5.7   Comparison of mechanical properties between glued laminated timber and other materials

Material	E/f
Concrete (Rck300)	≈ 1250
Steel Fe430	≈ 480
Glued laminated timber (GL20-GL36)	≈ 470

Deflection and vibrations are important aspects when designing timber structures and, hence, in the pedestrian bridge analysed. This fact is confirmed once again observing the values contained in table 5.7. The parameter in the right column E/f takes in account the risk of large deformation in the structures: the higher is this quantity, the lower is the risk of large deflections.

When f is high it means that the referred material has high resistances, and that the resultant structure is slender. As a consequence, this structure will also be characterized by small Inertia for its sections. Therefore a small value of the quantity E/f is also related with a small value of the bending stiffness $(E \cdot I)$. Looking at the formula to calculate the deflection for a simple supported beam under a uniformly distributed load $\delta = \dfrac{5}{384} \cdot \dfrac{q \cdot l^4}{E \cdot I}$ it's easy to notice that $(E \cdot I)$ is the denominator. As a conclusion, low values of E/f can be related with large deflections.

The values of E/f for steel and timber are still very similar and much lower than the one for concrete; that's the reason why the SLS often results the strictest verification for timber structures.

5.6.1 Verification of Deflection

Eurocode (Anon. 2004c), part 2 treats only vibration problems concerning design in SLS for bridges. These aspects are treated in the general part 1-1 of EC5, section 4. Since the limitations here specified seem to be little strict, it has been chosen to verify the bridge following the BKR, and compare these verifications with those obtained following the Eurocode.

The verifications about the SLS are still based on the composite section showed in Figure 5.12. Therefore the results are once again on the safe side as it is proved by the analysis of the model of the whole bridge in Abaqus® that is treated in Chapters 6 and 8.

The calculations of deflection are based on theory of elasticity. Usually for materials as steel and concrete the amount of deformation due to shear is negligible; this is not acceptable for timber because its value of shear stiffness (G = 800 MPa) is much lower than the one it would have if it was an Isotropic material (about G = 5000 MPa using the formula: $G = \dfrac{E}{2 \cdot (v+1)}$). Therefore deformations due to shear, which represents about 10% of the deformation due to bending, should be considered in the calculations. The load combination to adopt in the design in SLS is define as follow (EC5, point 4.1):

Combinations of actions for serviceability limit state should be calculated from the expression:

$$\sum G_{k,j} + Q_{k,1} + \sum_{i>1} \psi_{i,1} Q_{k,1}$$

where the partial coefficients:
$\gamma_G = 1.00$
$\gamma_Q = 1.00$
$\Psi_{1,1} = 0$

The same load combination in SLS is found following BKR, Table 2:321

Swedish codes BKR

The deformation of a timber member is influenced by creep and moisture. In the calculations this is taken in account reducing the mean value of the modulus of elasticity by the factor k_s, which depends on the service class and the load duration class (BKR, 5:322):

$$E_d = \frac{\kappa_s \cdot E_k}{\gamma_m} \tag{Eq. 5.3}$$

$\gamma_m = 1$ in the serviceability limit state

The values of k_s to use for the two types of load and the three different materials involved are:

	Kerto-Q®	Kerto-S®	Glulam
P loads :	0,5	0,5	0,45
C loads :	0,9	0,9	0,9

The modulus of elasticity E_d to use in the calculation of the deflection becomes:

	Kerto-Q®	Kerto-S®	Glulam
$E_{k,mean}$ [MPa]	10500	13800	13000
E_d - C loads [MPa]	5250	6900	5850
E_d - P loads [MPa]	9450	12420	11700

Three final deflections δ_p, δ_l and δ_v must be calculate.

δ_p is the final deflection due to permanent loads

δ_l is the final deflection due to variable live loads

δ_v is the final deflection due to variable service vehicle load

All of them must not be greater than the maximum value allowed $\delta_{max} = \dfrac{L}{400} = 37.5mm$, where Leaving out at the moment the amount of deflection due to shear, δ_p and δ_l are verified:

$\delta_p = 36.34mm < 37.50mm$ OK   96.91%

$\delta_l = 18.98mm < 37.50mm$ OK   50.63%

$\delta_v = 22.68mm < 37.50mm$ OK   60.48%

The verifications of the deflections have been verified. It's important to notice that $\delta_p = 36.34mm$ is very close to the limit value 37.50mm; considering that the contribution due to shear is not taken into account, this is in fact the most significant verification for the pedestrian bridge. As it was already mentioned in Section 5.5, the simple models of the bridge used by hand calculation are on the safe side, and this is proved by the results given by finite element analysis made by Abaqus® of the bridge (which is treated in Chapter 6 and 8). This is actually more tangible concerning the maximum values of the stresses than the values of maximum deflection. The models adopted in this Chapter to estimate the deformations by hand calculation seem to be more realistic than those used to get the stresses in the ULS.

Finally, it should be mentioned that the bridge has a considerable precamber that can have a favourable effect on the calculation of the final deflection. This benefit is not taken into account in the Swedish codes, but only in the Eurocode.

See Appendix G for more information regarding analytical calculations of the deflection based on BKR.

All the calculations about analytical calculations of the deflection based on EC5 can also be found in Appendix G.

5.6.2   Verification regarding vibrations

Pedestrians' traffic represents a dynamic load that can cause vibrations of the bridge. If the eigen frequency of the bridge is close to the frequency of the dynamic load, movements in the structure are produced. The magnitude of these vertical displacements is increased by the effect of resonance, causing an unsafe and uncomforting feeling to the pedestrians. The bridge will not be considered a safe structure by the people that use it, even if the verifications in the ULS are largely satisfied. Hence, it is important to verify vibration.

Also for the SLS regarding vibrations it has been followed the BKR, but this time the comparison with the Eurocode is not performed since the verification will result to be largely satisfied.

Swedish codes BRO

To avoid large movements of the structure, the natural frequency of the bridge must be higher than 3.5 Hz. The formula in details is:

$$f_n = \frac{\pi}{2 \cdot l^2} \cdot \sqrt{\frac{EI}{m}} \geq 3.5 Hz \qquad \text{(Eq. 5.4)}$$

where:

E is the E_{mean} value for load-type C,

I is the inertia of the bearing cross section,

m is the mass of half bridge considering self-weights and permanent loads expressed in Kg/m,

l is the length of the bridge.

If this condition is fulfilled, no further verifications should be done. The formula is based on Theory of Elasticity (particularly in case of Isotropic and homogeneous material) and it's valid for a simple supported beam.

Considering the same cross section showed in Figure 5.12 with an effective length of 750mm it results:

$$f_n = 4.44 Hz$$

This result is confirmed by the dynamic analysis of the model of the bridge performed by the finite element program SAP2000® described in Chapter 8. This analysis produced a value $f_n = 4.87 Hz$. Therefore the bridge provides a sufficient level of comfort against vibrations.

Considerations about problems in bridges with the span larger than 15m

It's very interesting the different problems that will involved bridges with the same kind of cross section as the one studied in this thesis work, which is made by a slab 126mm thick of Kerto-Q® plus two stripes 75mm thick of Kerto-S®, but with spans larger than 15m. This is obtained by increasing the depth of the glulam beams for an appropriated amount (therefore the only changes in the cross section regard the height of the beams; the width of the beams always remain 215mm).

- It can be observed that for spans larger than 25m the SLS verifications, and especially the one regarding vibrations, are the strictest and most significant. Just as information, concerning ULS verifications is good to know that the load which maximizes the normal stresses in the middle of the span is the service vehicle load only up to 27m span; for larger spans, the bending moment is maximized by the distributed live load.

  Considering a span of 25m, beams 855mm height are sufficient to fulfil ULS verifications, but to respect vibration limits imposed by the formula seen above, beams 1260mm height are necessary.

  By the way, a span of 25m is still acceptable (it is good to remind that theoretically it is possible to transport bridges with a span up to 35m if we look at the Swedish limitations about transportation traffic); but in this case it is recommended a more detailed dynamic analysis, for instance applying formulas given by Eurocode (Anon 2004c), or performing finite element dynamic models of the bridge.

- Considering a span of 30m, the ULS design would be satisfied by depths of 1035mm, but the vibration verifications and deflection verifications need beams 1800mm and 1500mm depth respectively.

  This considerations lead to the conclusion that a limitation of the bridge studied in this Thesis is that it can be used for rather small spans, up to 30m, because the SLS design imposes extremely height beams compared to the level of stress reached in the section. The material capacities would not be properly exploited, and the result would be a bridge economically disadvantageous.

- For large spans of 30m or more, it is possible to change the geometry of the cross section or totally change the static system of the structure.

- The addition of another slab of Kerto-Q® 63mm thick will not solve the problems mentioned before.

- The important problem of high shear stresses in the deck and in the Kerto-S® stripes related to the bridge studied in this thesis (see Chapter 8), are not badly influenced by the increase of the span. Instead, these values are lower when the span is larger, because shear stresses at supports remain more or less the same (the load is almost all given by the service vehicle load), the neutral axis moves away (downwards) from the layer of Kerto-S® since the height of the beams is bigger, and because lower stresses are generally acting in the section since the SLS verifications influence the design, as it has just been explained. Also local problems of high shear stresses in the deck do not increase whit the span, just because they are local problems and therefore not related to the dimensions of the whole structure.

5.7   Conclusions

The following conclusions can be drawn for this Chapter:

- The proposed cross-section with a flange 750mm wide (see Figure 5.12) satisfies all the verifications given by EC5 in the ULS and SLS design.

- The strictest verifications in the ULS design are those related to the normal stresses and shear stresses in the load combination 2.

- The strictest verification in the SLS design is:the long-term deflection for permanent loads based on BRO.

- Bridges with longer spans may have problems in the SLS design especially regarding vibration verifications.

- Some divergences have been found between Eurocode and Swedish codes concerning the definitions of design strength values for plywood materials.

6   Analysis of the effective cross-section

In the previous Chapter 5, and particularly Section 5.6, the bridge has been verified concerning the stresses in the ULS. In order to carry out those verifications it has been necessary to assume the effective width shown in Figure 5.11. This Chapter investigates the correct effective cross-section to use to design the bridge. At first, the choice of the effective width is checked with the regulations of EC5. Afterwards, some results of numerical simulations performed by Abaqus® and SAP2000® are analysed to improve the choice of the effective width. The aim is to prove that the whole π-section could be assumed for stress verifications. This will be done first studying the bridge loaded by symmetrical loads, and then by asymmetrical loads in the transversal direction.

6.1   Calculation of the effective cross-section based on EC5

At point 5.3.2 of EC5, the problem of the effective width for glued thin-flanged I-section beams is treated (see Figure 6.1). Since the directives of EC5 will be largely satisfied, and since the EC5 does not specified anything about glued thin-flanged T-section beams, the regulations at point 5.3.2 for the T-section are applied.
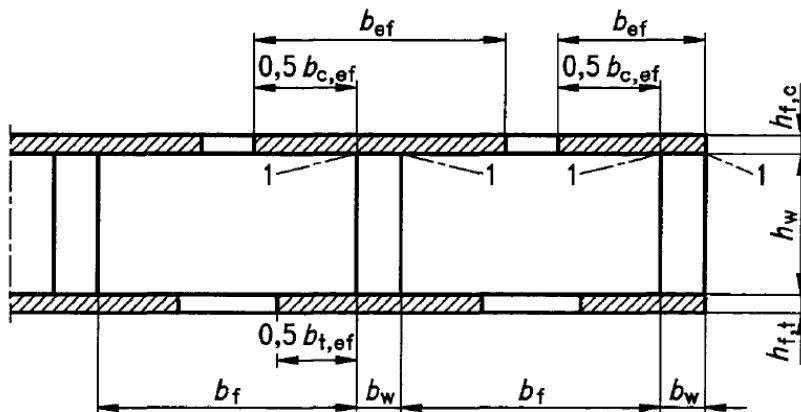
Figure 6.1 Figure taken from EC5, Section 5.3.2

The EC5 takes into account two different phenomena that limit the effective width of the flanges of a I or T-cross section:

- Shear lag

- Plate buckling

The first one takes into account the reduction of normal stresses at the points of the flange far away form the web (compared to the values of stresses attained where the webs are situated) caused by deformations due to secondary shear stresses. This reduction can involve both the compressed and the tensioned flange. Therefore, is not generally correct to consider a uniform distribution of stresses along the width because this would lead to results not on the safe side; The second effect takes in account the potential local instability of the compressed flange. In the T-section the

flange will be compressed, and it can buckle in the regions far from the webs. In the regions close to the web the stability is provided by the webs themselves, that represent some stiffeners for the flange. Where the flange buckles, there is a sudden lack of resistance, and this region of the flange does not contribute anymore with its normal stresses to the strength of the whole structure. EC5 reduces the cross section using the Table shown in Figure 6.2.

Flange material	Shear lag	Plate buckling
Plywood, with grain direction in the outer plies:		
— parallel to the webs	0,1l	25h$_f$
— perpendicular to the webs	0,1l	20h$_f$
Oriented strand board	0,15l	25h$_f$
Particleboard or fibreboard with random fibre orientation	0,2l	30h$_f$

Figure 6.2   Table adopted by EC5 to calculate the value of b_{ef} in case of glued thin-flanged beams

The values for the bridge studied in this thesis: $l = 15m$ and $h_f = 126mm$ (only Kerto-Q® deck is considered). Kerto-Q® has plies with grain direction in the face veneers parallel to the webs, so the value of effective width is the smaller between:

$$b_{ef,shearlag} = 0,1 \cdot l = 1,5m$$

$$b_{ef,buckling} = 25 \cdot h_f = 3,15m$$

Both these two values are higher than half width of the deck of the bridge studied:

$$b_{deck} = \frac{2,50m}{2} = 1,25m$$

This means that the whole deck can be taken into account in the calculation of the effective width. The two following considerations are taken into account:

The symmetry of the T-section ceases if the width is assumed larger than 900mm, as it is showed in Figure 6.3. This could represent a negative aspect to chose an effective section larger than 900mm.
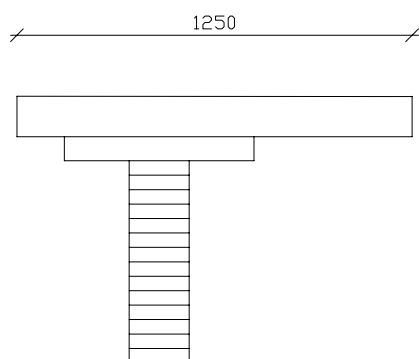
Figure 6.3 Effective section when $b_{ef} = 1250mm$; the section is not symmetric

The bridge cross-section is not only made of Kerto-Q® deck and glulam beams, but stripes of Kerto-S® are placed in the middle of these two parts.

In stress verifications carried out in Chapter 5, the symmetric section showed in Figure 5.11. At points (6) and (7) of Section 5.3.2 of the EC5 are defined the stress verifications that have to be checked:

P(6): For sections 1-1 in Figure 6.1 it should be verified that:

$$\tau_{mean,d} \leq f_{v,90,d}$$

where $\tau_{mean,d}$ is the design shear stress at the sections, assuming a uniform distribution, and $f_{v,90,d}$ is the design planar (rolling) shear strength of the flange.

P(7): The normal stress in the flanges must be lower than the respective design strength.

Both these two verifications are carried out in Chapter 5, Section 5.6, and particularly Figure 5.13. The verification defined at point P(7) is largely satisfied; the verification described at point (6) is much more strict instead. In the stripes of Kerto-S® shear stresses up to 1.31 MPa are achieved, compared to a flatwise design strength of 1.59 MPa.

Nevertheless, in order to have more realistic results, it is possible to assume $b_{ef} = 1250mm$ (see Figure 6.4).
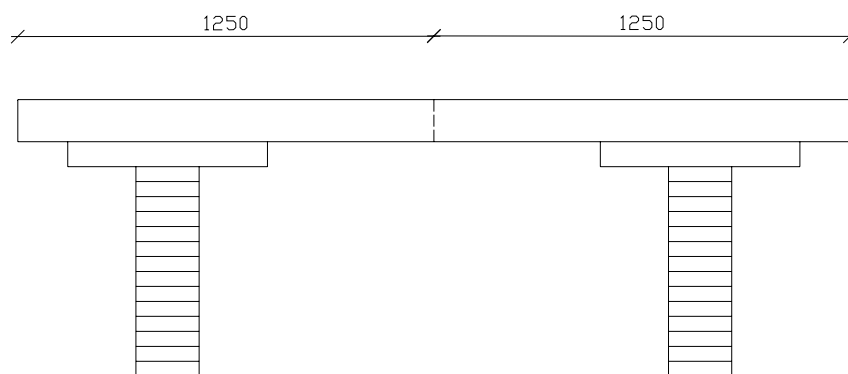
Figure 6.4 The whole section can be assumed for stress verifications

This assumption can be considered on the safe side for the following reasons:

The EC5 permits this assumption, as it has been described before.

Between glulam beams and Kerto-Q® deck two stripes of Kerto-S® have been placed; these two elements allows a better distribution of the stresses.

Models performed by using computer programs Abaqus® and SAP2000® confirm this assumption.

However, deformations and stresses found by hand calculations are over-estimated if an effective width of 750mm is assumed, because:

The effective span is slightly smaller than 15m: as it is showed in Figure 6.7 the support devices are made of two steel plate 250mm wide, so that the real span of the simple supported beams is reduced from 15,00m to 14,75m. As a result, stresses and deflections found by hand calculations are 3% and 6% lower respectively.

The 3D structure of the bridge has been simplified in the analysis of two separate stripes (one longitudinal and one transversal): the results obtained in this way are strongly on the safe side (see Chapter 5, Section 5.5 for detailed information).

The choice of an effective width of 750mm is largely on the safe side as it has been previously described, and as it is assured by the models carried out with the computer programs Abaqus® and SAP2000®.

6.2 Analysis of the effective cross-section using numerical simulations with Abaqus® and SAP2000®

6.2.1 Case of symmetric load (Load combination 1)

In the first part of this section the analysis with the computer program Abaqus® of a T-section simply supported beam will be performed; afterwards, a more realistic models of the bridge in 3D is studied.

The results found by hand calculations (already presented in Chapter 5) are compared with the results given by the model of a simple T-section beam with 750mm effective width and two different kinds of edge-supports (with or without steel plates). These models are described in Figures 6.5, 6.6 and 6.7 below:
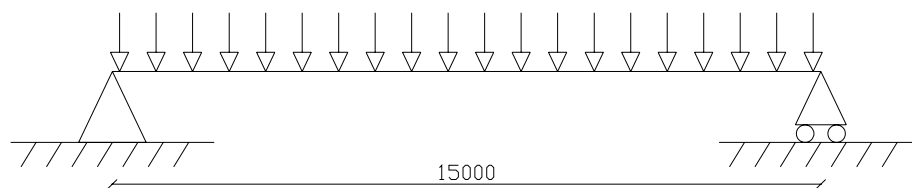
Figure 6.5 Scheme adopted in hand calculations; the beam is simply supported.
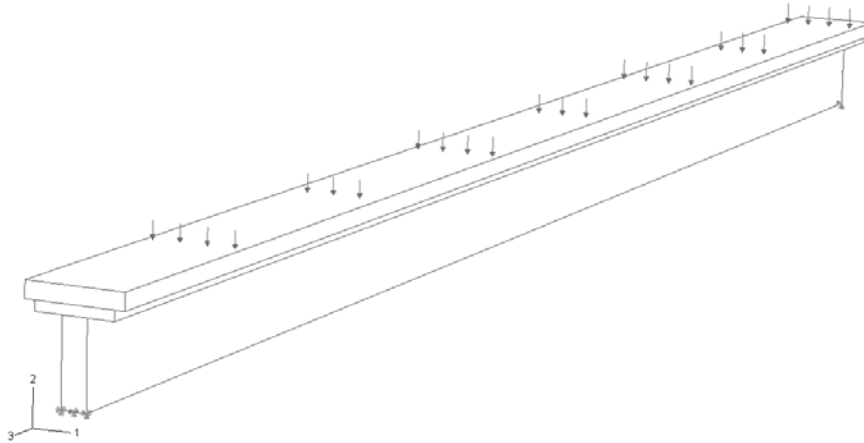
Figure 6.6 Model performed by Abaqus® of a T-section beam under a uniformly mdistributed load, without steel plates at the support
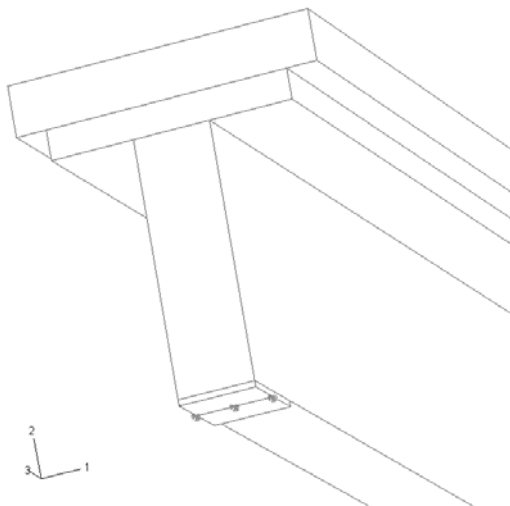
Figure 6.7 Model performed by Abaqus® similar to the one in Figure 6.6, but equipped with steel plates at the supports

The load applied to the beam shown in Figure 6.5 is given by load combination 1, calculated in Chapter 5, Section 5.4, which gathers together self-weight, permanent load and live load. The value of this load is 15,50 kN/m. Coherently, the beams in Figure6.6 and 6.7 are loaded by a pressure found spreading the linear load of 15,50 kN/m over a width of 750mm.

In the following Table 6.1 the results by the model in Abaqus® are compared with those found by hand calculations.

Table 6.1 Comparison between values of stresses and deflection given by the model in Abaqus® and by hand calculation

	Hand Calculation for b_{ef} = 750mm	Model in Abaqus® with supporting steel plates	Comparison with hand calculation	Model in Abaqus® without supporting steel plates	Comparison with hand calculation
G [mm]	521,37				
Inertia [m^4]	1,88E+10				
$\sigma_{33,beam}$ [MPa]	15,56	13,52	(-) 13,1%	14,99	(-) 3,7%
$\sigma_{33,KertoQ}$ [MPa]	7,19	6,4	(-) 10,9%	6,73	(-) 6,3%
Deflection [mm]	51,81	46,9	(-) 9,5%	53	(+) 2,2%

Focusing the attention on the principal stresses in the beams and the deck collect in Table 6.1, it is possible to draw the following conclusions: comparing hand calculation results with those found by the Abaqus® model without the steel plates (span 15m), there is an increase of stresses of about 4% in the beam and 6% in the deck. If the comparison is carried out with the Abaqus® model provided by steel plates (span 14,75m) the same percentages increase to 11% and 13% respectively. In any case, with or without steel plates, the longitudinal normal stresses given by the Abaqus® models are lower than the hand calculation results of about 5-10%. The non-realistic hypothesis assumed concerning the hand calculation results is that the structure of the supports is not considered and the boundary effects on the stress distribution are not taken into account. Close to the edges of the beam there is a different stress distribution from the one provided by the Linear Elastic Theory of De Saint Venant. The region influenced by these boundary effects is quite large since the beams are rather high (831mm) and because of the presence of the steel plates. For these reasons, in general, there is a decrease of values of the longitudinal stress in the reality compared to the theoretical hand calculation results. As a confirmation of the influence of these boundary effects, two problems will be discussed (see Figure 6.8 and 6.9).
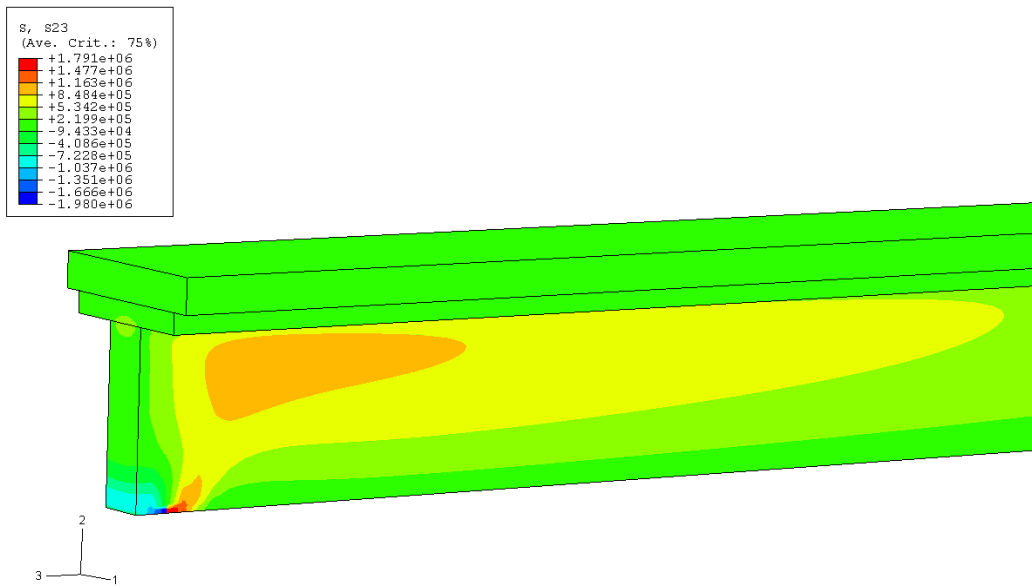
Figure 6.8 Distribution of shear stresses τ_{23} *for the beam described in Figure 6.7*

Besides the local concentration of shear stresses close to the supporting steel plate, which are not realistic, it can be notice in Figure 6.8 above that the distribution of shear stresses differs from the one expected from the simple solution by hand calculation because the maximum shear at the level of the neutral axis has slightly shifted from the edge face of the beam.
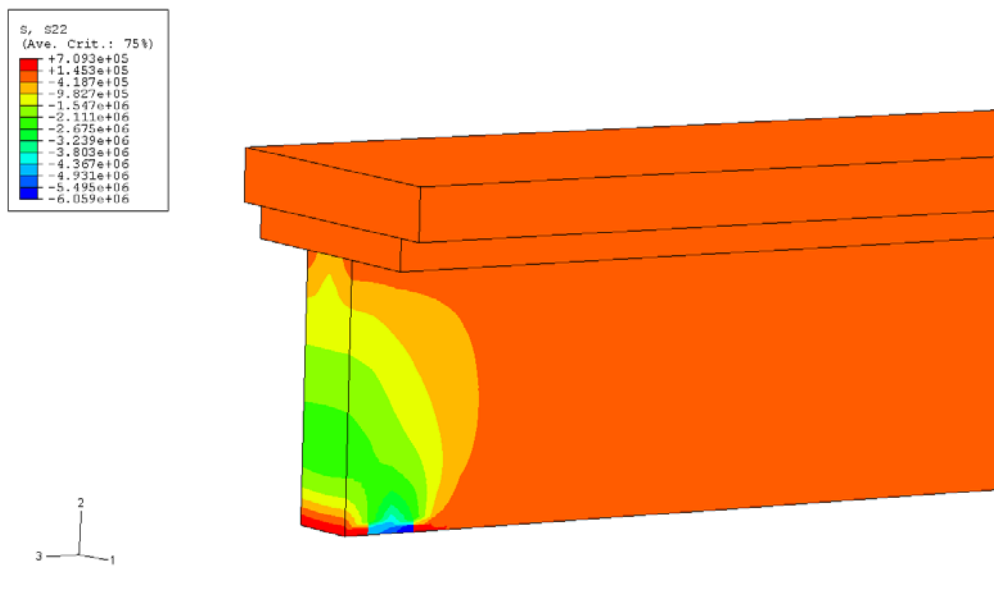
Figure 6.9 Distribution of normal stresses σ_{22} *close to the support for the beam described in Figure 6.7*

Figure 6.9 shows that a rather large region close to the support is involved by high normal stresses σ_{22} that are not taken into account in the simple solution by hand calculation.

Concerning the values of deflection collect in Table 6.1, the result by hand calculation differs respectively by 10% and 2% from those found by the Abaqus® model with and without the steel plates. These differences can be caused by the variations in the span, which is a quantity rise to power of 4 in the formula used to calculate the deflection.

$$\delta = \frac{5}{384} \cdot \frac{q \cdot l^4}{E \cdot I}$$ (6.1)

The conclusion of this first part of Section 6.2.2 is that the models described in Figure 6.8 and 6.9 confirm that the simple results by hand calculation (on which the verifications are based) are correct and on the safe side in view of the fact that they do not take into account the real supports and the boundary effects.

Now comparisons between results found by hand calculations and a complete model of the bridge in 3D are carried out in order to prove that the simplified scheme of the bridge in two separate beams with 750mm effective width are on the safe side, and effective widths up to 1250mm could be assumed.

The distribution of normal stresses σ_{33} among the middle cross-section for the load combination 1 are calculated for the values of effective width b_{ef} = 750; 800; 900; 1050; 1250mm. In the model transversal elements and four steel plates 250mm wide at supports are considered; the effective span is 14750mm (see Figure 6.10).
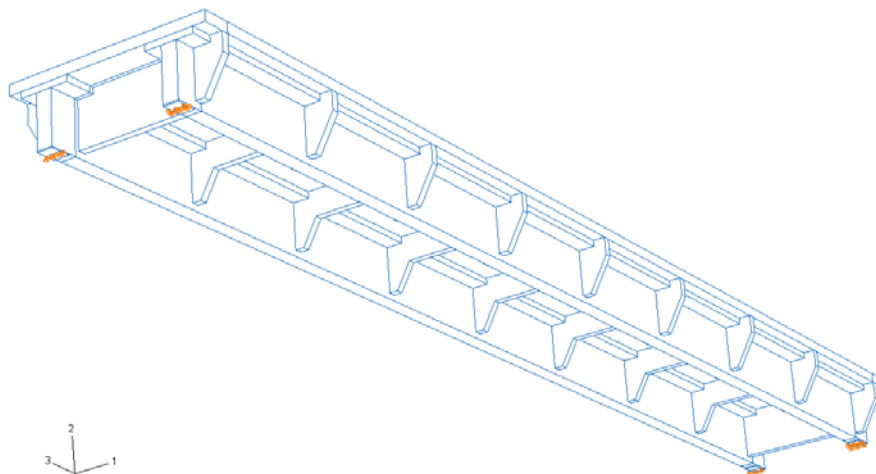
Figure 6.10 Complete model in 3D of the bridge performed by Abaqus®

The graphs in Figure 6.11 represent the distribution of normal stresses σ_{33} among the section for all the different choices of effective width and the case of the Abaqus® model. The distances in the vertical axis of the graph starts from the bottom face of the beam; the line at a distance of 630mm corresponds to the interface layer between glulam beams and Kerto-S® stripes, whereas the line at a distance of 705mm corresponds to the interface layer between Kerto-S® stripes and Kerto-Q® deck.
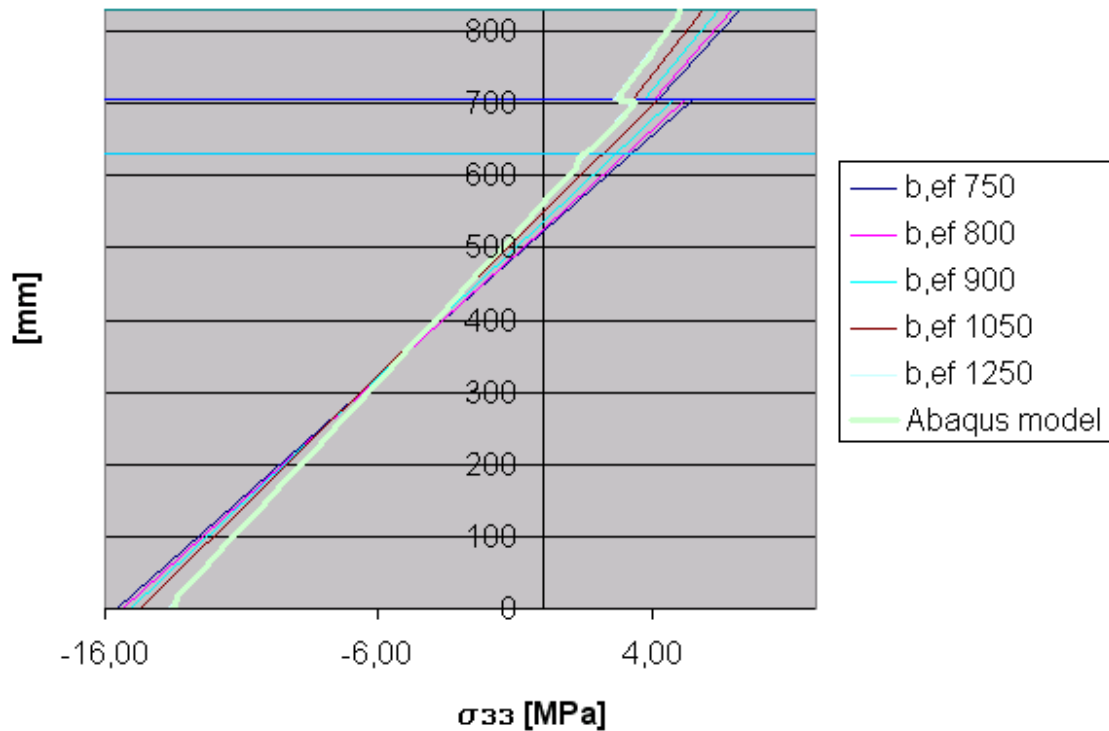
Figure 6.11 Distribution of normal stresses σ_{33} in the middle cross-section of the bridge for different values of effective width and the Abaqus® model

The significant values for the graphs of Figure 6.11 are also shown in Table 6.2. The table contains the maximum stresses in the three elements of the structure (glulam beams, Kerto-S® and Kerto-Q®) and the maximum deflections for all the cases of different effective widths and the Abaqus® model of the bridge. The quantity G is the distance of the neutral axis from the bottom face of the beams for the various cases.

Table 6.2 Values of stress and deflection found by hand calculation for different effective widths and found performing the numerical model

	Effective width b_{ef} [mm]					Abaqus model
	750	800	900	1050	1250	
G [mm]	521,4	526,34	535,7	548,5	563,5	
Inertia [m^4]	1,88E+10	1,92E+10	1,99E+10	2,09E+10	2,2E+10	
$\sigma_{33,KertoO}$ [MPa]	7,19	6,93	6,47	5,90	5,29	5,12
$\sigma_{33,KertoS}$ [MPa]	5,48	5,23	4,77	4,20	3,60	3,55
$\sigma_{33,beam}$ [MPa]	15,56	15,39	15,10	14,72	14,33	13,88
Deflection [mm]	51,81	50,78	48,93	46,61	44,15	41,32

It can be easily noticed how the position of the neutral axis is obviously moving upwards when the effective width increases; at the same time the stresses decrease, especially in the Kerto-Q® deck. It's also easy to note that the discontinuity in the interface between Kerto-S® and Kerto-Q® is much more marked than the one between glulam beams and Kerto-S®: this is due to the fact that the modulus of elasticity for Kerto-Q® is much lower than those of glulam and Kerto-S®, which are quite similar instead (see Chapter 5, Section 5.2 for detailed values of the mechanical properties of these materials).

Looking at Figure 6.11 it can be observed that passing from the case of $b_{ef} = 750$mm to $b_{ef} = 1250$, the differences in the stresses and in the deflection get closer to the Abaqus® model curve. The graph related to the value of 1250mm of the effective width is almost coincident with the graph of the Abaqus® model.

Comparing the deflection and the stresses in the beam and in the deck found by analytical calculations (case $b_{ef} = 1250$mm) with those found by numerical calculations of Table 6.2, the following differences can be found:

		Comparison with the model in Abaqus®
$\sigma_{33,beam} =$	15,56 MPa	(+) 13,1%
$\sigma_{33,KertoQ} =$	7,19 MPa	(+) 30,2%
Deflection =	51,81 mm	(+) 19,32%

Also the values by hand calculation for the beam with $b_{ef} = 1250$mm are compared to the Abaqus® model:

		Comparison with the model in Abaqus®
$\sigma_{33,beam} =$	14,33 MPa	(+) 5,6%
$\sigma_{33,KertoQ} =$	5,28 MPa	(+) 4,9%
Deflection =	44,12 mm	(+) 5,2%

Considering $b_{ef} = 750$mm the differences with the results by the Abaqus ® model are rather high (15-30%). The differences in case of $b_{ef} = 1250$mm are just around 5%. This means that the assumption of $b_{ef} = 750$mm is not correct because too much on the safe side, and the case $b_{ef} = 1250$mm leads to results much more realistic instead.

Furthermore, a confirmation of the fact that the case $b_{ef} = 1250$mm gives more realistic results comes from the data included in the graph of Figure 6.12, which shows the deflection against different values of effective width. Both the curves of the deflection for a span of 15m and a span of 14,75m are presented, but this second one is the most correct. When the value of the effective width increases, the deflection

decreases, and when b_{ef} = 1250mm the deflection is almost coincident with the one given by the Abaqus® model of the bridge.
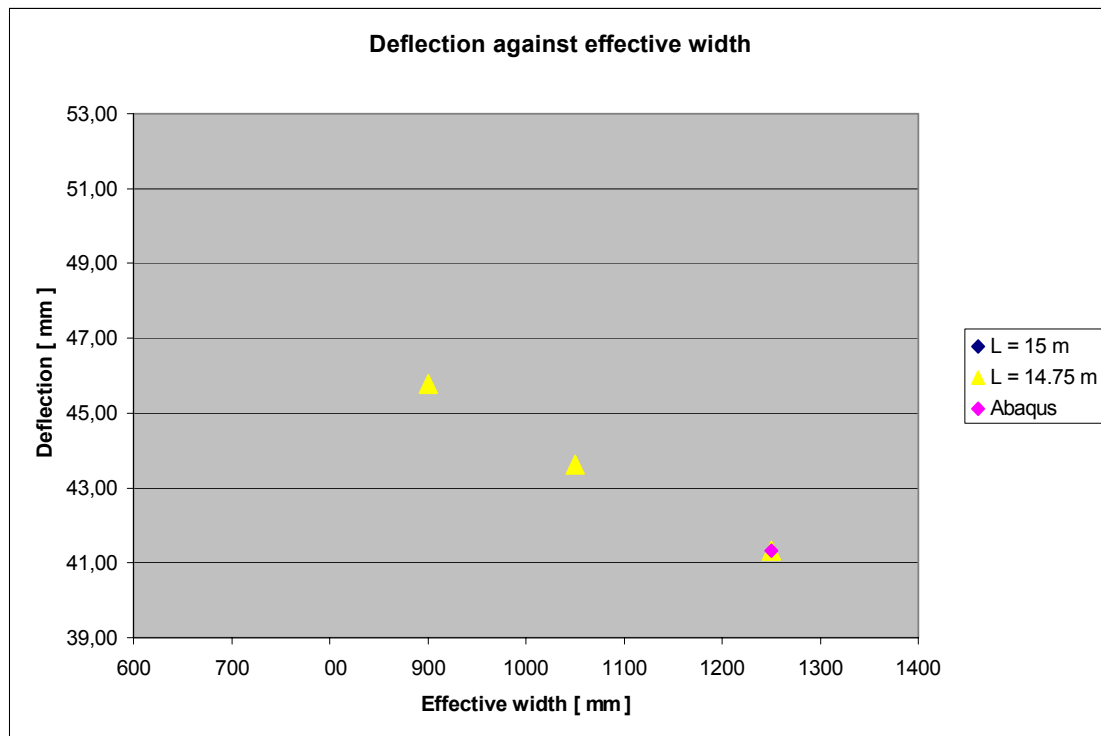
Figure 6.12 Deflections against different values of effective width

The confirmation that the assumption b_{ef} = 1250mm is correct comes from the results of the model of the bridge performed by using the computer program SAP2000® (see Chapter 8, and in particular Section 8.1). In fact this analysis gives values of the longitudinal stress σ_{33} almost coincident with those found by hand calculation of a stripe with b_{ef} = 1250mm. The differences are about 1%.

6.2.2 Case of non-symmetric load (Load combination 2)

When the bridge is loaded by a non-symmetric load the results found by hand calculation of two separated stripes become less realistic, even when an effective width b_{ef} = 1250mm is chosen, and the differences with the results of the model in Abaqus® of the whole bridge increase. Especially the normal stresses in the beam σ_{33} found by hand calculation result 17% greater than those given by the Abaqus® model (see Figure 6.13 and Table 6.3).
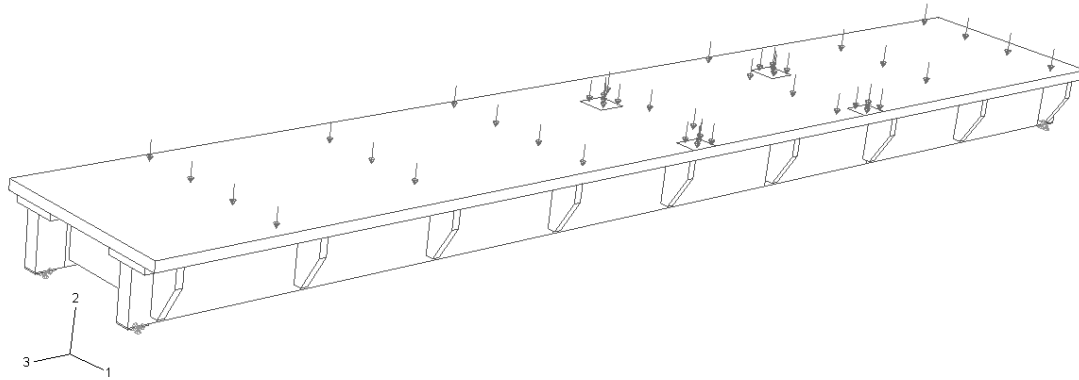
Figure 6.13 Model of the bridge performed by Abaqus® in load combination 2; the wheels of the service vehicle are placed close to the longitudinal edge of the deck

Table 6.3 Stresses and deflection in load combination 1 for the Abaqus® model and for the scheme of the bridge in two separate stripes with b_{ef} = 1250mm

	Model in Abaqus®	Hand Calculation for b_{ef} = 1250mm	Comparison with Abaqus® model
$\sigma_{33,beam}$ [MPa]	16,5	19,9	(+) 17,1%
$\sigma_{33,KertoQ}$ [MPa]	6,9	7,2	(+) 4,2%
Deflection [mm]	46,6	46,5	(-) 0,2%

Hence, the simple scheme of two separate stripes adopted in the verification of the bridge is not realistic and largely on the safe side. When choosing an effective width b_{ef} = 750mm, stresses σ_{33} =21,7 MPa are reached in the beams (see Figure 5.13 in Section 5.6 of Chapter 5). Many remarks have already been made about the problems caused by these simplifications of the structure when the bridge has been verified in the ULS design (see Chapter 5, Section 5.6).

Since the choice of the section of the glulam beams is based on the values of normal stress σ_{33} calculated in the ULS design, a reduction of the height of the beams could maybe be done basing on the values given by the Abaqus® model (σ_{33} = 16,5 MPa) instead of those calculated by hand (σ_{33} = 19,9MPa). However, the reduction of the height of the glulam beams is not possible because of the SLS verifications: in this case the long-term deflection is caused by permanent loads, and it has been demonstrated that the results obtained with the scheme by hand calculation are very similar to those given by the Abaqus® model. The SLS verifications require the height of the beam to be at least equal to 630mm.

Finally, a further confirmation that the hypothesis of the composite section is valid is presented. Figure 6.14 shows the stress distribution among the cross-section of the bridge in load combination 1 calculated by the Abaqus® model. It's easy to notice how the stresses σ_{33} are uniformly-distributed among the Kerto-Q® deck.
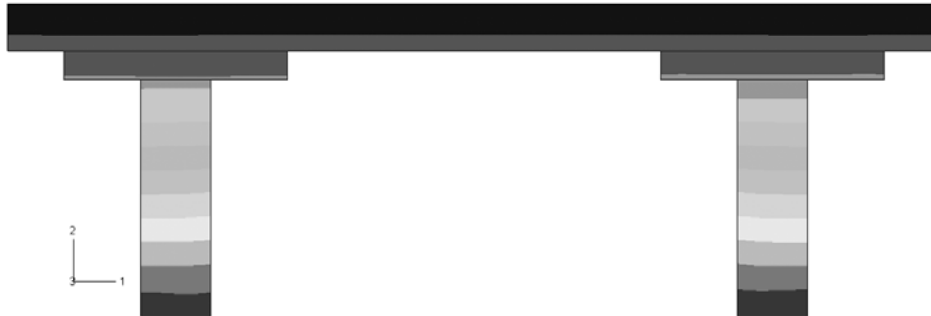
Figure 6.14 Distribution of normal stresses σ_{33} among the cross-section of the bridge in load combination 1 calculated by the Abaqus® model

To demonstrate this fact, the distribution of normal stresses σ_{33} along the upper and the lower edge line in direction 1 of the Kerto-Q® deck referred to the middle cross section of the bridge is shown in Figure 6.15. The straight line represents the average value of these stresses.
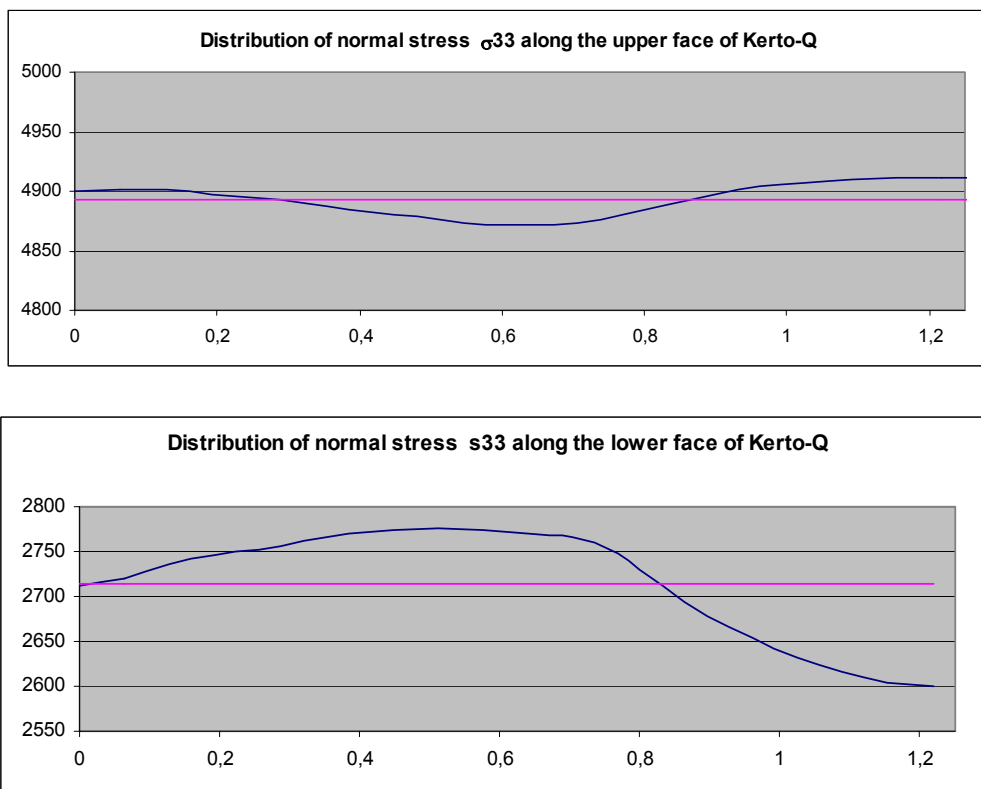
Figure 6.15 Distribution of normal stresses σ_{33} [in kPa] along the upper and the lower edge line [in meters] in direction 1 of the Kerto-Q® deck referred to the middle cross section of the bridge

In both cases the differences of values of stress σ_{33} compared to the average are very small. Along the inferior face there are differences of about 0,2 MPa between the region close to the web and the one close to the middle of the deck (the difference is about 6% respect to the average value $\sigma_{33} = 2{,}71$MPa). Moving upwards throughout the thickness of the deck the stresses spread homogenously and become almost constant and equal to $\sigma_{33} = 4{,}89$MPa.

6.2.3 Consideration about shear stress in the cross-section

As it has been specified in the previous Section 6.2.2, the linear elastic Theory of De Saint Venant leads to correct results only in regions far from the supports. The beams related to the bridge studied in this thesis are 831mm high (glulam beams + Kerto-S® + Kerto-Q®), and for a large area at the edges they have a distribution of stress different from the one expected by hand calculation. In particular, in the regions close to the supports there are compression stresses up to 2 MPa (see Figure 6.16 (d)). In all the pictures of Figure 6.16 it can be noticed how much complex the stress distribution it is close to the supports compared to the central part of the span. In those regions shear and compression stresses are important, and stresses due to bending are negligible. Looking at the minimum principal stress (Figure 6.16 (b)) which represents the value of principal compression, it is possible to notice that, moving towards the support from the middle span, normal stresses due to bending slightly evanish and shear stresses becomes more and more important, because the principal stresses get more and more inclined and become almost vertical just above the support. The picture related to shear τ_{23} (Figure 6.16 (c)) confirms that the shear stress becomes normal compressive stress just above the support.
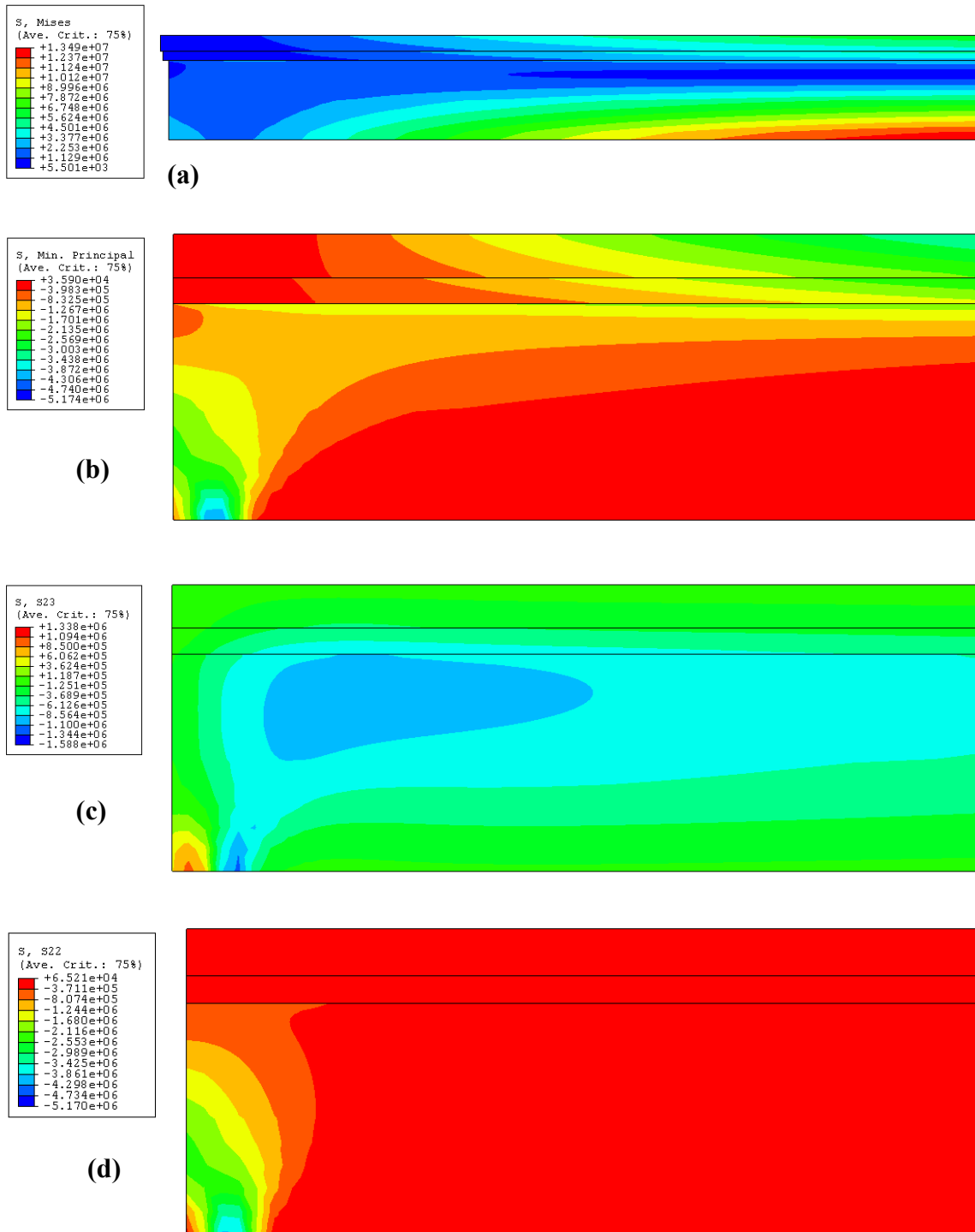
Figure 6.16 Numerical simulation of a part of the bridge close to the left support: (a) Von Mises stress for half of the bridge; (b) minimum principal stresses in the region close to the supports; (c) shear stresses in the region close to the supports; (d) compressive stresses σ_{33} in the region close to the supports

Figure 6.17 shows the value of shear stress τ_{23} at the level of the neutral axis along the beam, starting from the left support. For each section, the neutral axis is the point where the shear is the highest, following the linear elastic Theory of De Saint Venant.

It's easy to see that the maximum value is not at the external face of the beam, but has shifted of 375mm from the support towards the middle of the span.

Distribution of shear stress in the longitudinal direction
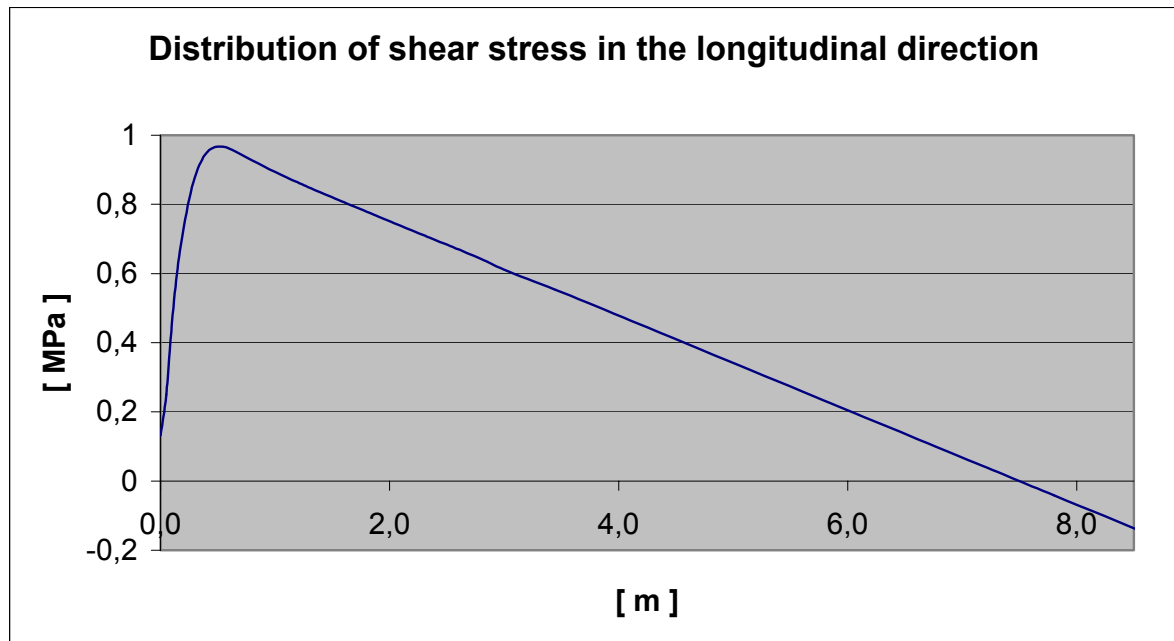
Figure 6.17 Distribution of shear stress along the beam in load combination 1

Referring to the section where the shear is the greatest, at a distance of 375mm from the support, it is interesting to check the distribution of shear stress among the section itself (see Figure 6.18). The effective width is b_{ef} = 750mm and the structure is in case of load combination 1. The curve is calculated using Eq. (6.2).

$$\tau = \frac{V \cdot S}{b \cdot I} \tag{6.2}$$

The curve has a parabolic shape. And the maximum is positioned at the level of the neutral axis (G = 521mm starting from the lower face of the beam). The discontinuity in the diagram is due to the variation in the width *b* of the cross-section, which results at the denominator of Eq. (6.2).
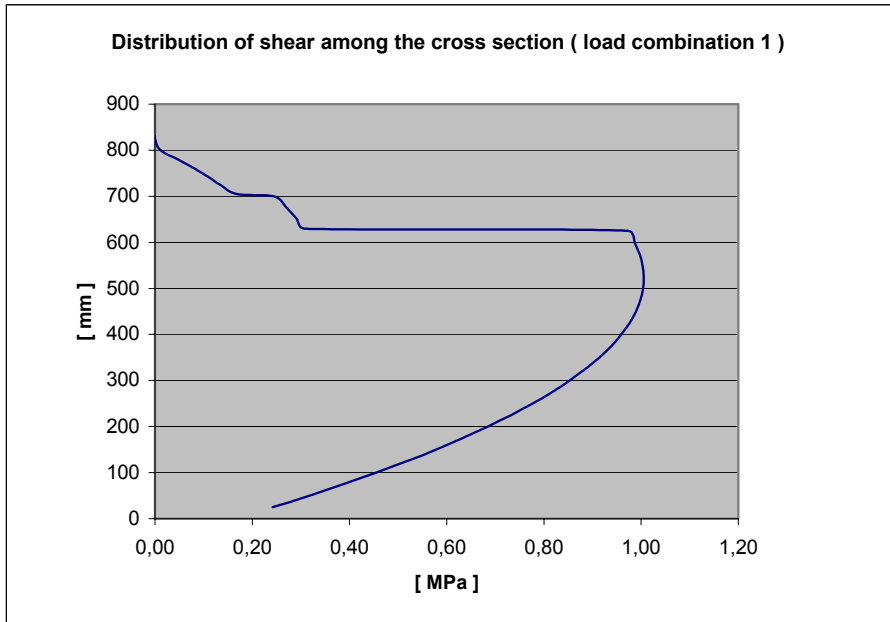
Figure 6.18 Distribution of shear stresses τ_{23} among the cross-section at a distance of 375mm from the support.

The comparison between the distribution of shear stresses found by hand calculation of Figure 6.18 with the one given by the Abaqus® model is shown in Figure 6.19. The two curves are very similar to each other; the maximum values of shear stress reached at the level of the neutral axis (G = 521mm) differ just for 0,048 MPa (see Table 6.4).
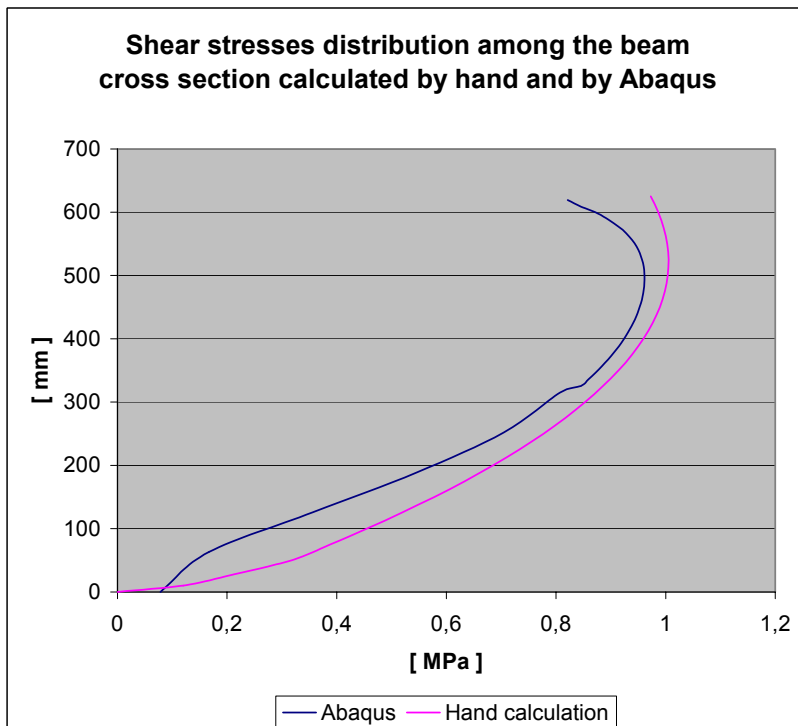
Figure 6.19 Distribution of shear stress found by hand calculation and the one given by Abaqus® model

Table 6.4 Maximum value of shear stress τ_{23} found by hand calculation and by the Abaqus® model

Hand calculation	Abaqus® model	Difference
$\tau_{23} = 1,01$ MPa	$\tau_{23} = 0,962$ MPa	4,7 %

6.3   Conclusions

The conclusion of this Chapter can be resumed as follow:

- The results found by hand calculation, used for the design of the bridge in the ULS and SLS, have been confirmed by the numerical analysis performed by FE programmes. These results are largely on the safe side especially if the effective width is chosen equal to 750mm.

- An effective width of 1250mm (half width of the bridge) can be assumed for the design. This is allowed by the regulations of EC5 at point 5.3.2. Also the results of the numerical simulations confirm this assumption.

Even for the assumption of maximum effective width ($b_{ef} = 1250$mm), the analytical results in case of asymmetrical loads are on the safe side. Compared with hand calculation results, the Abaqus® model (that will be described in details in Chapter 8) shows stresses at the bottom edge of the section (in the glulam beam), and at the upper edge of the section (in the Kerto-Q® deck) about 17% and 4% lower respectively.

7 Evaluation of the benefits achieved by adding the Kerto-S® stripes – Finite Element Model of a transversal stripe of the bridge

The approach that was adopted in the finite element modelling is to develop firstly very simple models and add later on several other hypotheses always comparing the new results with the previous one to obtain a reasonable model without getting far from the real solution. Simple models of a small part of the structure are replaced by the more complex geometry of the whole bridge with and without transversal bracing units.

The aim of this chapter is to perform some simple FE models of a transversal stripe of the bridge to investigate the distribution of shear stresses τ_{12} due to the wheel load of the service vehicle, and check the benefits given by adding the Kerto-S® stripes.

7.1 Description of the Abaqus® Model

As it was shown in the general design of the bridge, the main problems related to such a kind of timber bridges are the high values of the shear stress that occur through out the Kerto-Q® deck when the load due to the weight of the special service vehicle is acting. For this reason the original design of the bridge with only the Kerto-Q® deck was modified into a new one provided with two longitudinal stripes of Kerto-S® between deck and beams to better resist to the high shear τ_{12}.
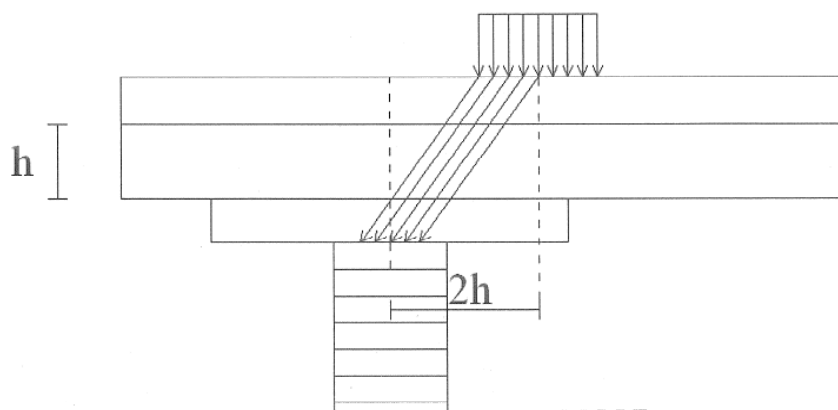
Figure 7.1   The vertical load due to the vehicle's wheel is transferred to the beam just partly with a pure compression.

If the models with SAP2000® were useful to describe the global longitudinal moment and shear distribution among the bridge (both in the glulam beams and the deck), they are not suitable when the distribution of stresses inside the cross section (the shear τ_{12}) is to be investigated.

The simple reason for this is the fact that the deck is there modelled using shell elements, which can only calculate the average value of shear among the cross section.

To fulfil our aims a model in Abaqus® using solid elements should be used. The basic properties (how the elements are connected and the input data like the material properties) of the simple models treated in this Chapter are the same as the ones of the model of the whole bridge described in Chapter 8. Therefore, more information can be found in Chapter 8, Section 8.2.

In this firs step some simple introductive models will be developed. The goals of these first rough analyses are to quantify the values of shear stress in the deck (preferably on the safe side), to localize their highest values and eventually an approximate "critical path" through the thickness where these highest values are set, and to check the improvements achieved by adding the Kerto-S® stripes.

The model is a transversal stripe of the bridge 360mm wide supported in the two contact surfaces with the glulam beams. The width of 360mm represents also the dimension of the loading tread of the vehicle's wheel defined in the Swedish codes Bro 2004 (See Appendix A). In this way it is considered the smallest transversal stripe that can contain a whole load of a train of wheels. Being on the safe side, is not considered the capacity of the deck to transfer the loads even to the transversal bracings in the longitudinal direction.

The position of the vehicle that maximizes the stresses is when the external edge of the wheel is coincident with the edge of the deck.

Note that this case will be formally not realistic during the service life of the bridge because the presence of the handrails will force the vehicle to stay at a certain distance to the edge of the deck. Furthermore, it must be mentioned that the position of the load when the wheels of the vehicle are placed in the middle of the cross section (which would maximize the stresses in the deck) is negligible since the width of the vehicle (1.80m) is almost comparable with the width of the deck (2.50m). See Figure 8.34 in Chapter 8.

7.2   Model with fix supports

In this model fix boundary conditions are applied to the 360mm deck's stripe. The deformed shape and the distribution of stresses τ_{12} are presented in Figure 7.2. Note that the maximum values of the shear stresses are reached at the external edge of the right supports;
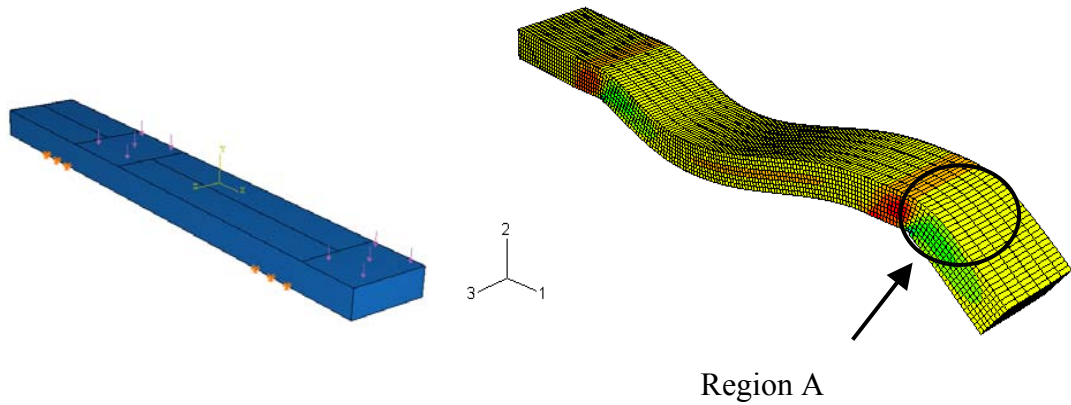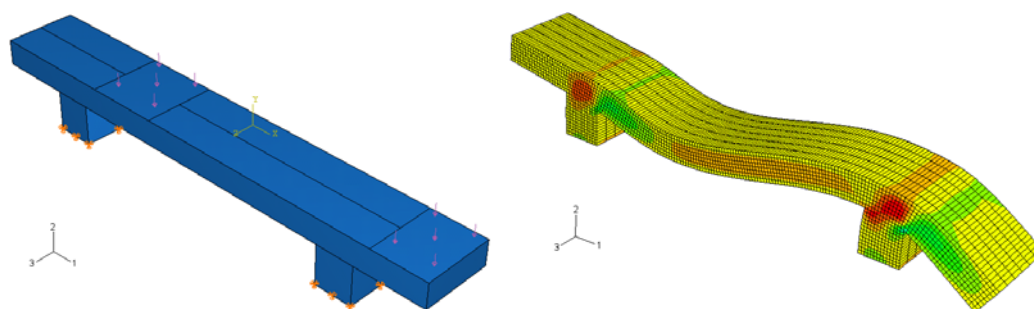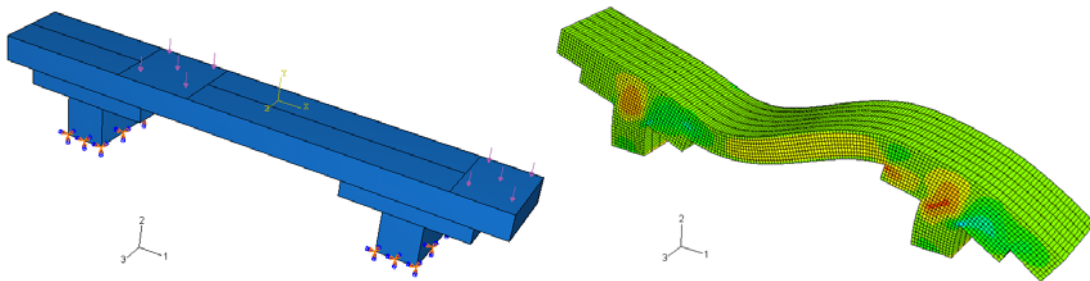
Figure 7.2   Position of the load applied to the deck's stripe, distribution of the shear
stresses τ_{12} , deformed shape, and localization of the region where these
stresses are higher.

A detailed 3D analysis of the distribution of shear stresses around the region A of this model leaded us to find the path on which the highest values of stress are set (see figure 7.3). It is a path in the vertical transversal plane 12 that has its origin point in the external edge of the support on the lower surface of the deck, and it has an inclination of about 45° with respect to the horizontal plane.
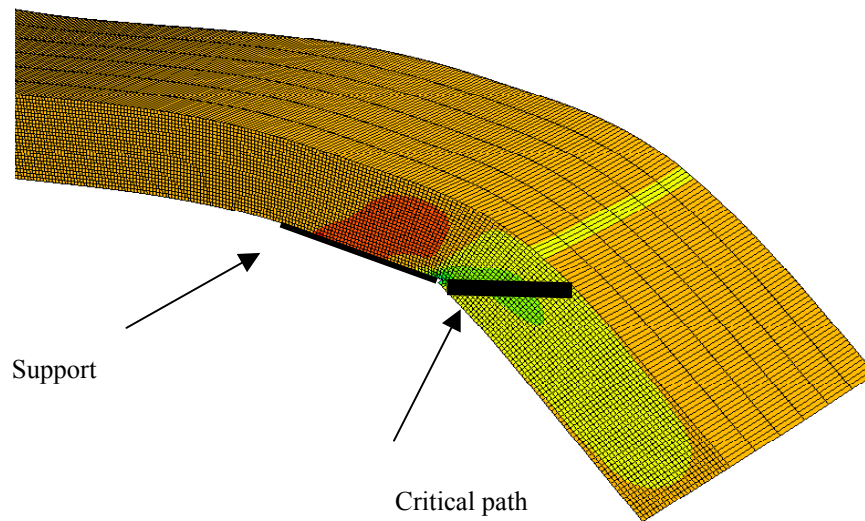
Figure 7.3   Distribution of shear τ_{12} in the deck's stripe and shape of the critic path
where the highest values are set

Figure 7.4 shows the values of the shear stress τ_{12} along the critical path; these values are plot with respect to the y-coordinate of the incline critical path. Close to the lower surface of the Kerto-Q® deck very high values of shear stress are reached (more than 8 MPa): this is due to a typical problem in modelling with a linear-elastic analysis when geometries with sharp angles between different surfaces are used. So these values are not physical acceptable and to get reasonable values one should start to

look from a certain distance to the edge. The values decrease quickly moving upwards through the deck and they are almost constant in all the central region and contained in a range of (1.00,2.00 MPa).
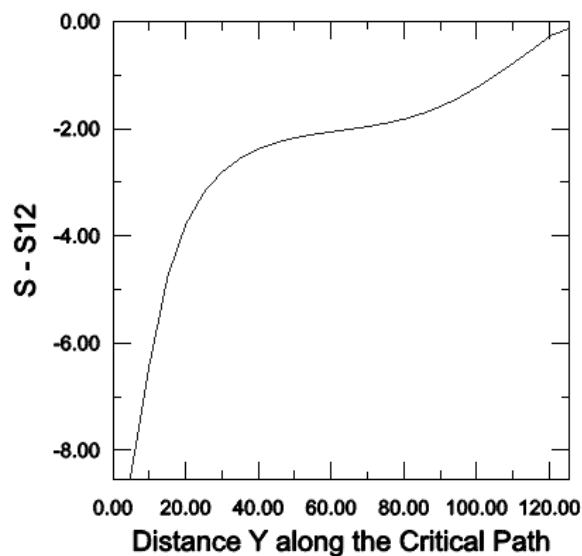
Figure 7.4 Shear stress τ₁₂ respect to the Y coordinate along the critical path.

It's important to point out again that this model doesn't lead yet to realistic results for our bridge. As an example the real behaviour of the beams is not described at all, because the fix supports do not allow them neither to deflect independently nor to rotate in the transversal plane. On the other hand, it is satisfactory to describe the local effects of the concentrated loads regarding the shear stresses. For instance the position and the shapes of the regions and the paths where the shear stresses τ₁₂ are the highest.

7.3   Model with fictitious beams

A good choice to get a more realistic model consists in adding the two beams below the deck, to allow a certain rotation of the contact surfaces with the deck around the longitudinal axis. The glulam beams have a section showed in Figure 7.5 (See also Chapter 4 and 5). In this model the boundary conditions are applied to the lower surface of the beams. The rotation of the beams that is obtained in such this way would be excessive, so to represent more realistically their deformation is better to take just a portion of them. A depth of 200mm it has been chosen. See Figure 7.5.

Section of the Glulam Beam
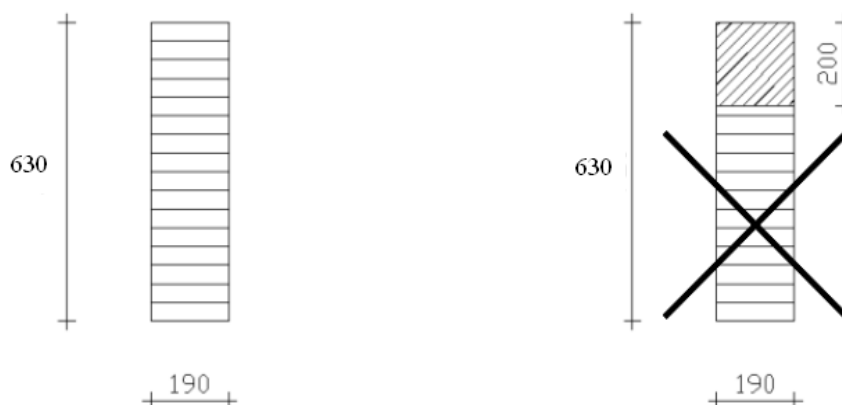
Figure 7.5 Section of the glulam beam and the region chosen for the model

The results of this model say that the region and the critical path where the stresses are the highest is still the same (see Figure 7.6).

Figure 7.6   Position of the load applied to the deck's stripe, distribution of the shear stresses τ_{12} , deformed shape.

The shape of the curve representing the shear stress τ_{12} is very similar to the one shown in Figure 7.4 (see Figure 7.7).
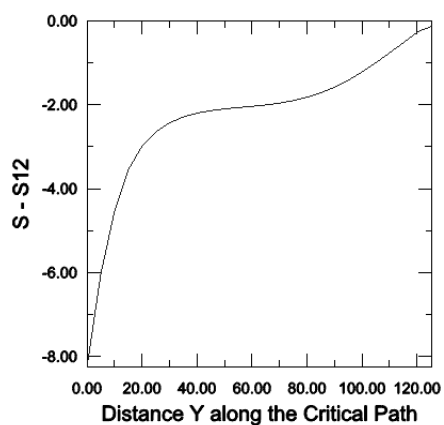
Figure 7.7 Shear stress τ_{12} respect to the Y coordinate along the critical path

7.4   Model with Kerto-S® stripes

The previous models show that the stresses in the deck are quite high compare with the design strength of the Kerto-Q® material. This stresses can be smartly reduced adding a stripe of Kerto-S® material (whose flatwise shear strength is much higher than the one of Kerto-Q®) between the deck and glulam beams. The new critical path is very similar to the old one; it is still contained in the vertical plane XY with an inclination of about 45° respect to the horizontal plane, whereas the origin point it is in the external edge of the beam on the lower surface of the Kerto-S®. In Figure 7.8 it can be seen that the distribution of shear stresses and the deformed shape is coherent with the results exposed in Section 7.1.

Figure 7.8   Position of the load applied to the deck's stripe, distribution of the shear stresses τ_{12} , deformed shape.

Looking at the distribution of stresses τ_{12} along the critical path (see Figure 7.9) it is possible to see that a large decrease of stress is properly localized in the Kerto-Q® deck (the thickness of the Kerto-S® stripe it is 75mm); the stresses τ_{12} are here lower than 1.2 MPa. The local problem of high stresses close to the origin point is still present; these values are much lower than those found before because it has been used a coarse mesh compared to the previous models.
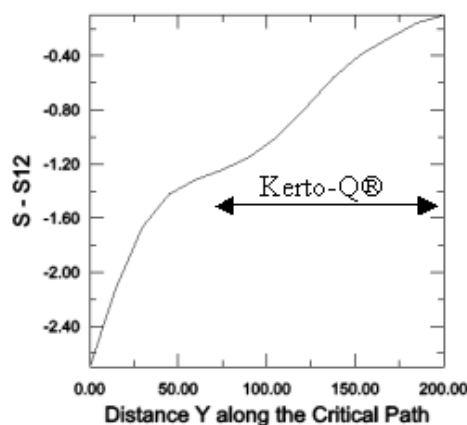
Figure 7.9 Shear stress τ_{12} respect to the Y coordinate along the critical path

7.5   Conclusions and limitations of the FE models

The models show that the suggestion of adding the Kerto-S® stripes is a good solution to decrease the values of shear stress in the Kerto-Q® deck. The highest values of shear stress occur in the Kerto-S® stripe itself, whose design flatwise shear strength is higher than the one of Kerto-Q®.

Anyway, the peak values of shear strength given by the models in both the LVL materials result higher than the design shear strengths. The cause is due to a limitation of the models: a short transversal stripe of the bridge does not properly describe the real mechanical response of the deck when subjected to concentrated loads. The model of the whole bridge presented in Chapter 8 behaves as a slab, with comparable stiffness in the two directions of the plane of the deck. The problem should be studied in 3D, because the vertical loads can be transferred in both planar directions 1 and 3 of the deck down to the glulam beams.

8 Analysis of the structure by using FE computer softwares Abaqus® and SAP2000®

The problems related to the bridge studied in the previous chapters are:

- Problems related to the materials used, especially concerning LVL elements.

- Technical problems related to manufacturing, assembling and transportation stages, techniques adopted to provide a good durability of the structure.

- Problems related to the two different codes EC5 and Swedish codes.

- Problems related to ULS design and SLS design of the bridge.

The aim of this Chapter is to analyse and solve the problems related to concentrated loads and non-symmetric loads respect to the longitudinal direction due to the service vehicle acting over the deck of the bridge. The stress distributions produced by such this load are not solvable by the simplified models adopted in Chapter 5, when the bridge has been designed.

A model by Abaqus® of the whole bridge (see Figure 8.1) was developed in order to study local effects of high concentrated loads. This model is described in details in Section 8.2 of this Chapter.
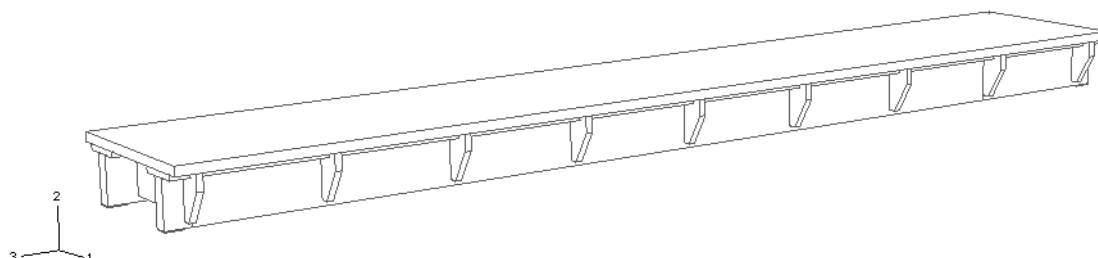
Figure 8.1 Model by Abaqus® of the whole bridge

Previously, a simpler 3D model of the bridge was performed by using the computer program SAP2000® (see Figure 8.2), but it has revealed to be inappropriate for load combinations 2 and 3.
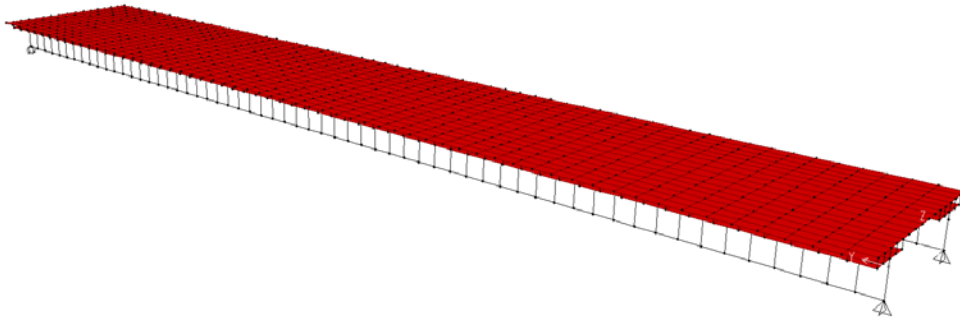
Figure 8.2   3D model of the bridge performed by using the computer program SAP2000®

It's good to remember that load combination 2 is the one that maximizes bending moment in the beams; in this case the vehicle is positioned in order to have its heavier wheel axis in the middle of the span (see Figure 8.3).
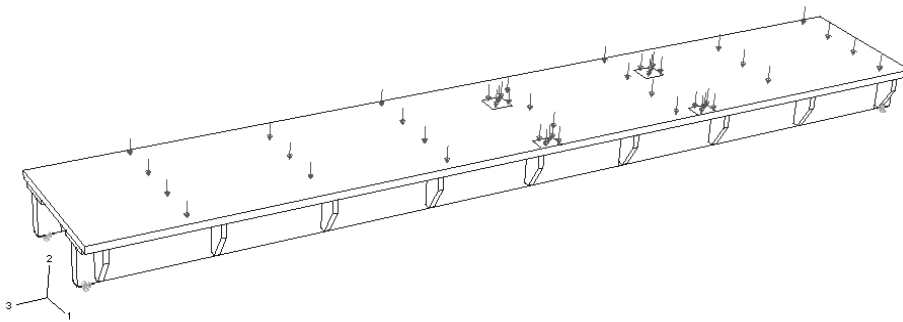
Figure 8.3 Configuration of load combination 2

Load combination 3 is the one that maximizes shear at the supports; in this case the vehicle is positioned in order to have its heavier wheel axis close to the support (see Figure 8.4).
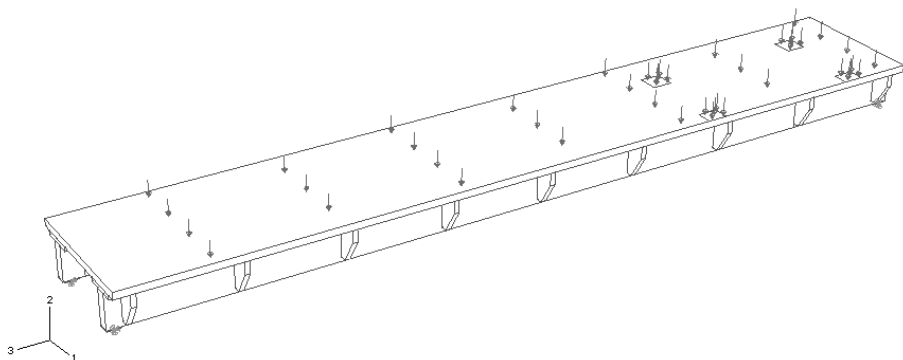
Figure 8.4 Configuration of load combination 3

The simplified model adopted in hand calculation analyses separately two effective sections, and do not take into account properly the collaboration between them when non-symmetric loads are acting. The glulam beams are in fact linked together by transversal bracing units placed at a distance of 1,8m in the longitudinal direction, and

especially by the Kerto-Q® deck. Essentially the deck provides the interaction between the beams.

(a)

(b)
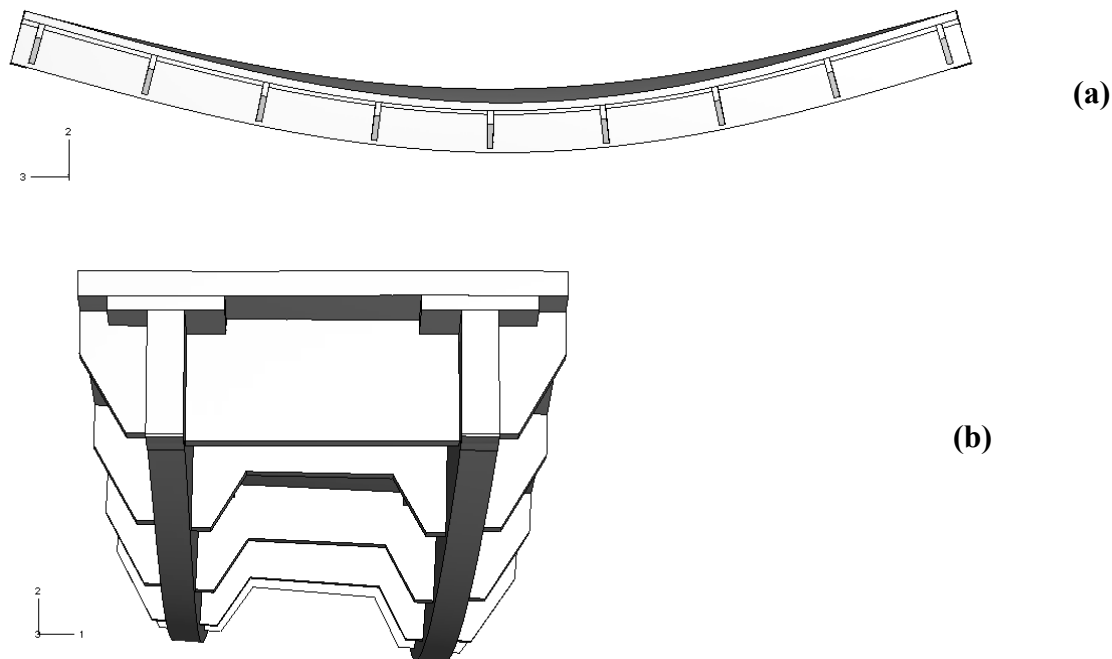
Figure 8.5   Side view (a) and frontal view (b) of the deformed shape of the bridge in load combination 2

As it is showed in Figure 8.5, when the bridge is asymmetrically loaded, the beams deflect different amounts, but not independently one from each other. The function of the transversal elements is not to increase the torsional stiffness of the structure, but to provide regular supports for the Kerto-Q® deck. Transversal bracings are positioned every 1,80m to limit the transversal deflection of the LVL panel and facilitate the transferring of loads in the longitudinal direction. A deep analysis of the mechanical slab behaviour of the deck is necessary to be developed for the design of this bridge since the simplified analysis of the deck in two different stripes is not realistic and too much on the safe side. Moreover, discrepancies in the values of design strength for plywood have been found between EC5 and BKR. Usually, LVL elements are employed in the edgewise mode. However for the bridge studied in this thesis they are used as a slab, in the so-called "flatwise" mode. Consequently, one more problem is represented by the low planar shear strength of these Kerto® materials (see also Chapter 5, Section 5.2).

The previous Chapter 7 has demonstrated that:

- Between the deck and the glulam beams is necessary to place a stripe of Kerto-S® to facilitate the spread of the concentrated loads due to the service vehicle.

- The simple FE model of the bridge as a short transversal stripe leads to values of shear stress τ_{12} higher than the design strength of the materials, because this kind of model disregards the benefits given by the mechanical slab behaviour of the deck. Figure 8.6 shows the typical slab behaviour of the deck that will be described in details later on in this chapter.
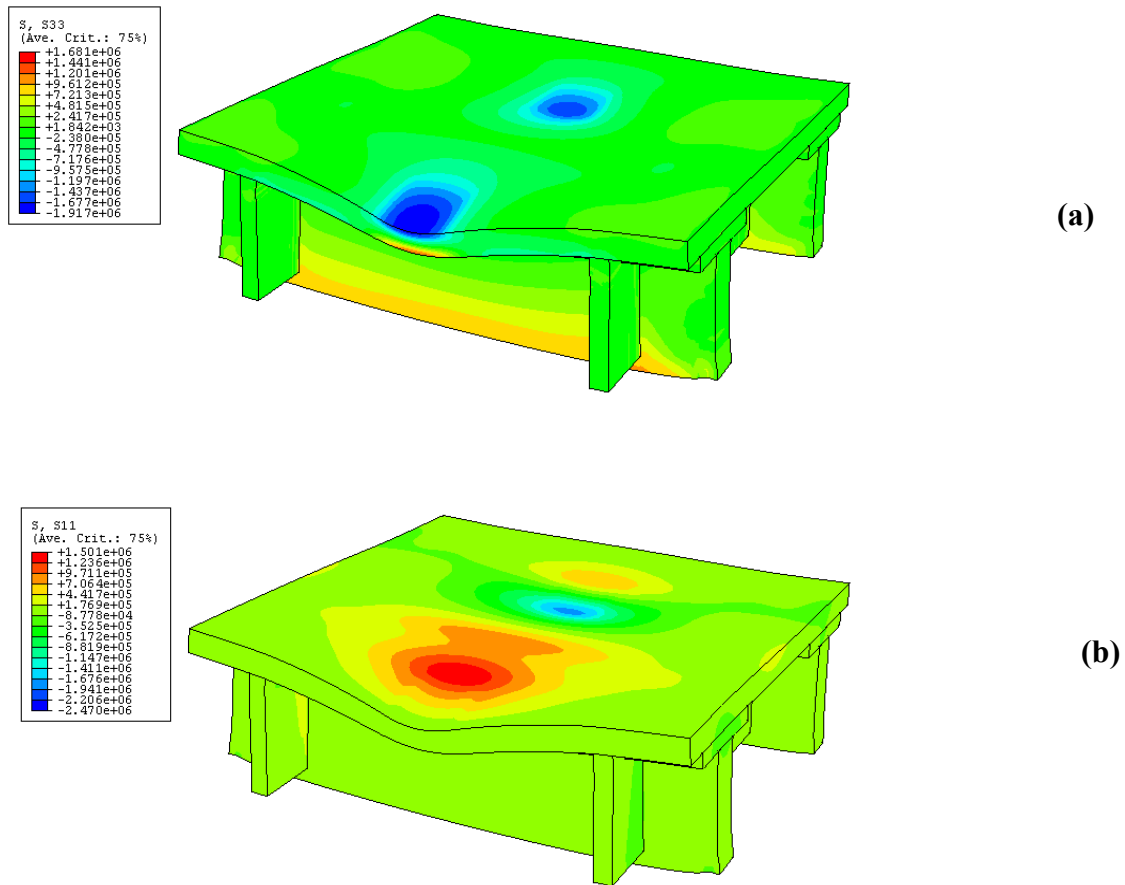
Figure 8.6 Deck mechanical slab behaviour: distribution of normal stress σ_{33} (a) and normal stress σ_{11} (b)

The regions where there are the main structural problems for this bridge are:

- Just under the load tread when the vehicle moves along the external edge of the deck, loading the part of the deck schematically described as a cantilever beam. Kerto-Q® and Kerto-S® materials are subjected to high shear stress τ_{12} and τ_{23}.

- In the region close to supports, where global shear stress τ_{23} are already maximum due to permanent loads. The Vehicle load increases these values up to the design strength of materials.
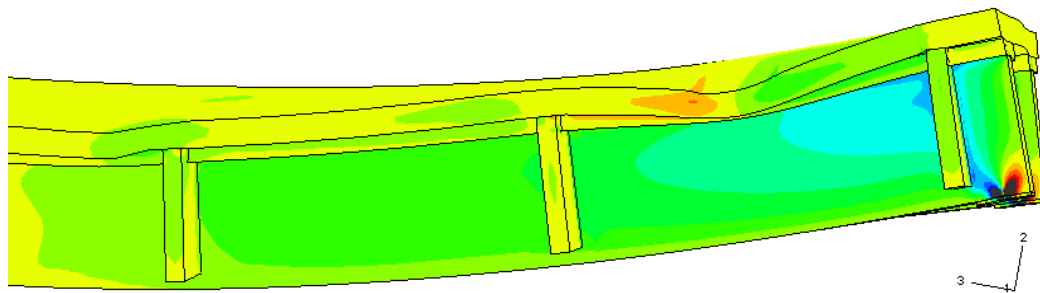
Figure 8.6 Deformed shape of the part of the bridge close to the right support under the vehicle load

The LVL material used for the deck has high values of flexural design strength, but is not subjected to high bending moment. On the contrary, it is subjected to high shear forces, which produce shear stress τ_{12} and τ_{23} close to the resistant values.

8.1   Software SAP2000®

8.1.1   Description of the model

The FE model performed by the software SAP2000® confirmed the results obtained by hand calculation. In particular it is helpful to understand the significant problems of the bridge for the various load combinations. In fact, one of the advantages achievable by this software is its practicality in defining and combining different loads (for the software Abaqus® this aspect is inconvenient since a new elaboration has to be run from the beginning every change of the load configuration). For this bridge it is developed the standard kind of model described as follow:

- Beams modelled as frame elements placed in their gravity centre.

- Shell elements used to model Kerto-Q® deck.

- Shell elements used to model the Kerto-S® stripes (see Figure 8.7).

KertoQ® deck = el shell

Transversal joint = el frame

Fictitious elements = el frame

Glulam beam = el frame

KertoS® strip = el shell
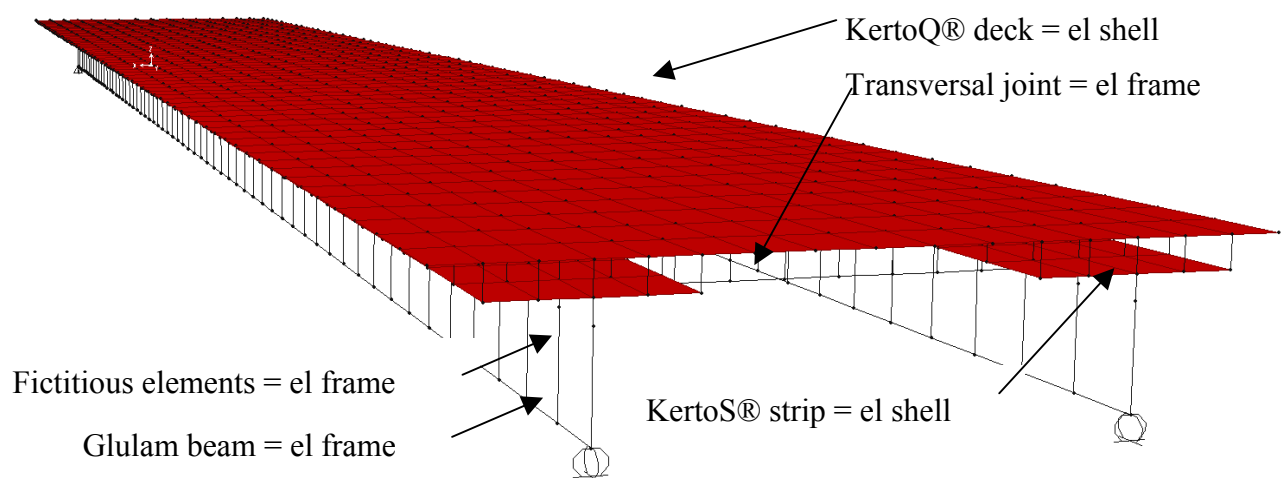
Figure 8.7 Different kind of element used to model the bridge

The three different parts are linked together by using fictitious frame elements, perpendicular to the deck and the beam axis, as it is showed in Figure 8.8.
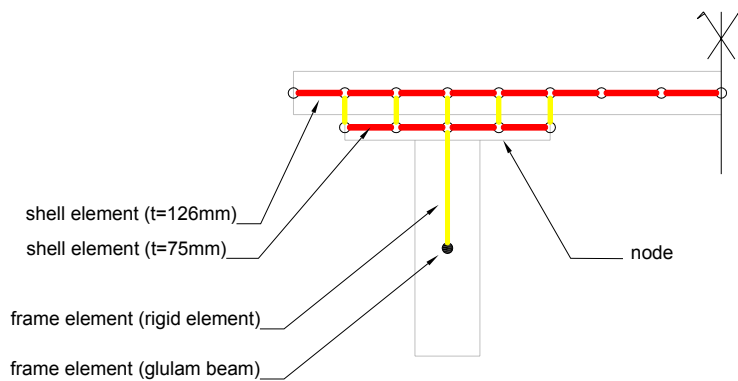
Figure 8.8 Detail of different kind of elements used to model the bridge

The fictitious frame elements that link together the two shell layers and the glulam beams with the shell layer which represents the Kerto-S® stripes, are elements without weight and with a very high stiffness (almost rigid). In the points of connection they form rigid nodes, and they reproduce the behaviour of the glue (used in the reality to assemble the elements of the bridge) so that the structure respect the hypothesis of composite section with full interaction between the different parts. Referring to the deformed shape, the generic cross-section of the bridge remains planar like it was before loading. The use of these fictitious elements is helpful also to obtain shear and axial stresses that develop in the beam and the deck of the composite section (see Figure 8.16 (b) and (e)).

The model is partially able to describe the mechanical slab behaviour of the deck. The shell elements are not suitable when the effects of concentrated load are to be investigated; they are appropriate to study problems of plane stress or in bending-plates. In particular, for the problem related to this bridge, deformations and shear stresses τ_{12} and τ_{23} out of plane are very important, and they can not be described properly using shell elements. To comprehend better the effects of concentrated loads acting over the deck, a model by the software Abaqus® has been performed (see Section 8.2 of this Chapter).

8.1.2 Material properties

To execute the model is necessary to define the material properties. The materials are assumed to be isotropic; the essential properties to define are: Elastic modulus E, Poisson coefficient ν, and density γ. See Table 8.1.

Table 8.1 Material properties defined in the Sap2000® model

	E [MPa]	ν	γ[kN/m^3]
Glulam GL32c	13500	0,2	6
Kerto S®	13800	0,2	6
Kerto Q®	10500	0,2	6
Material for the fictitious element	10000000	0,2	0

Afterwards, is necessary to define the section to assign to the frame elements (see for example the case of frame element that represents the glulam beam in Figure 8.9) and to the shell elements (see the case of Kerto-S® in Figure 8.10).
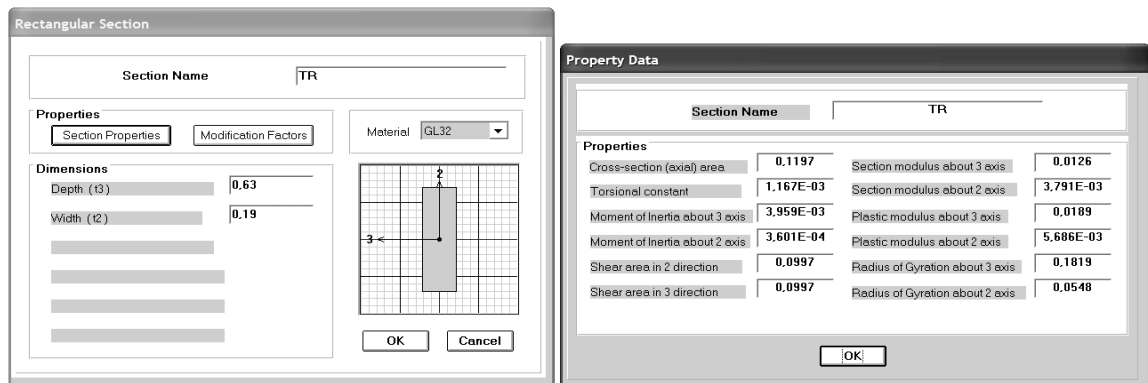
Figure 8.9 Definition of the section properties, the glulam beams
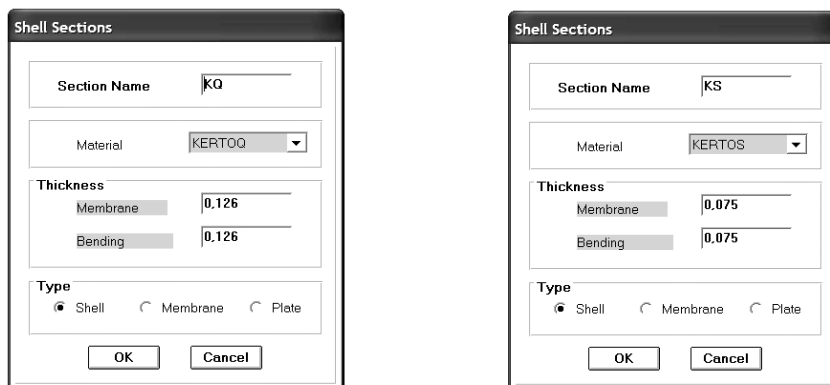
Figure 8.10 Definition of the section properties, Kerto-S® stripes

8.1.3 Boundary conditions

The structure has been fixed to the ground locking the right degrees of freedom at the beam's end. Just one support has been represent by a pin (free rotation and translation locked in all the three direction). The other one has been schematised like showed in the Figure 8.11. In this way the structure is globally an isostatic body in the 3D space.
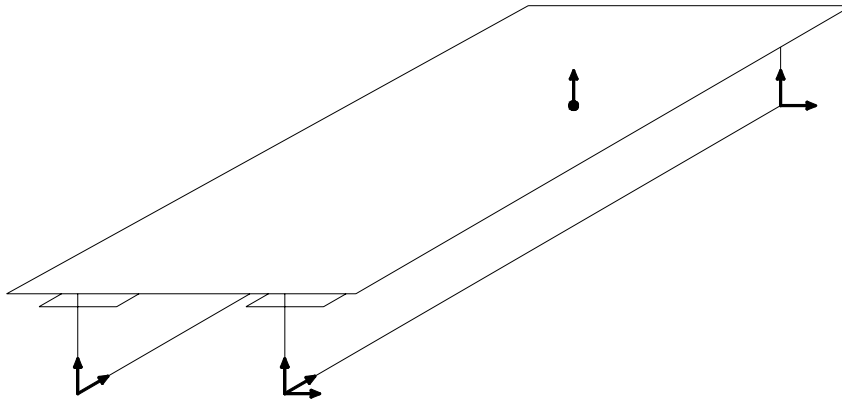
Figure 8.11   Boundary conditions: the arrows refer to the degrees of freedom that are locked

8.1.4 Mesh

To create a model in Sap2000® it is necessary to define the mesh at the beginning when the elementary unit will be created. Afterwards, coping and moving that small part the whole model will be generated.

Models with different mashes have been studied: Coarse meshes were used in the beginning models, more defined meshes were adopted afterwards (see Figure 8.12).
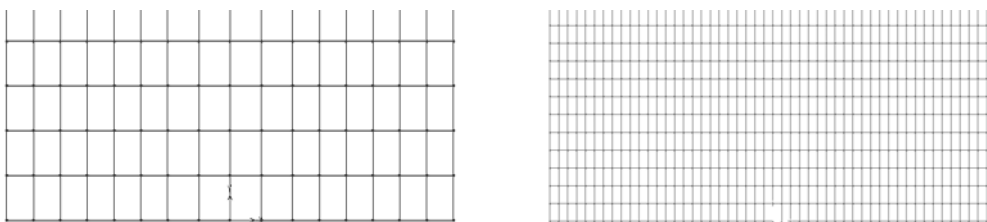
Figure 8.12 Different mesh adopted for the deck; on the right the more defined mesh used in the final model

8.1.5 Results of the model

The model used to study the structure in load combination 2 and 3, that take in account the service vehicle load, is showed in Figure 8.13.
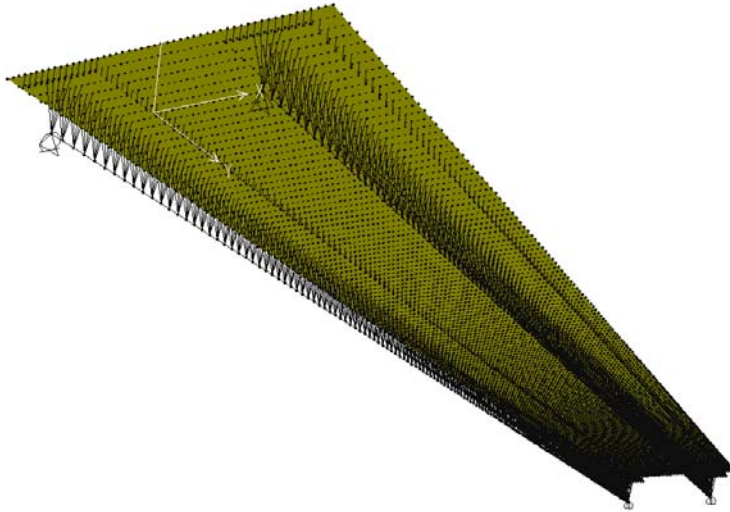
Figure 8.13 Bottom view of the model used to study load combination 2 and 3

This model can reproduce very well the hypothesis of composite section, and correctly describe the interaction between the beams and the deck, because glulam beams and Kerto-S® stripes are linked together using 5 fictitious frame elements (see Figure 8.14).

Figure 8.14 Element used to model the bridge, view of the cross-section

Although the model properly reproduces the full interaction between deck and beams, it is not able to describe correctly the distribution of shear stress in the regions of the deck directly on top of the glulam beams. In the reality shear stresses τ_{23} spread among the whole width of the deck, as it will be shown in the Section referred to the Abaqus® modelling. In the model with SAP2000® these shear stresses remain restricted in a small area over the glulam beams, reaching values extremely high (higher than 1MPa in Kerto-Q® deck, whereas hand calculations give values around 0,3MPa in the same region). The distribution of shear stress is showed in Figure 8.15 below.
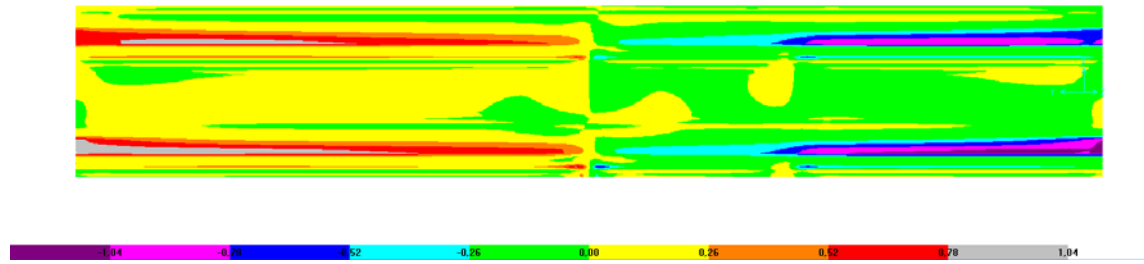
Figure 8.15 Distribution of shear stress τ_{23} in the deck for load combination 2

The results obtained in load combination 1 are presented in Figure 8.16.

(a)

(b)

(c)

(d)

(e)
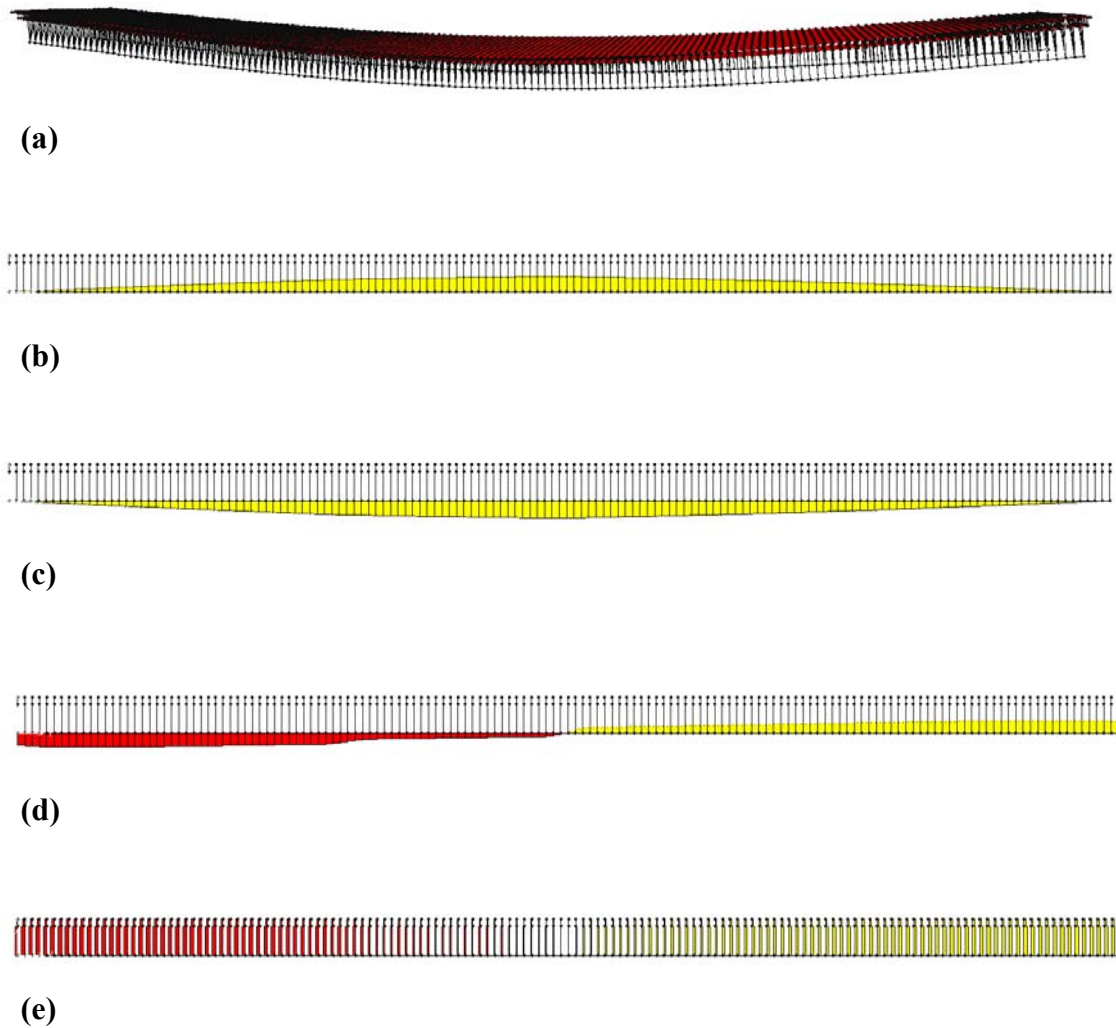
Figure 8.16   Results obtained by the model in load combination 1: (a) deformed shape, maximum deflection vmax = 44 mm; (b) distribution of axial force in the glulam beam Nmax=754 kN; (c) distribution of bending moment M in the frame glulam beam Mmax=100 kNm; (d) distribution of shear force V in the glulam beam Vmax= 58,96 kN; (e) distribution of shear force V in the frame fictitious elements Vmax= 3,52 kN

Comparing the results found by SAP2000® with the results by hand calculation in case of effective width b_{ef} = 750mm and b_{ef} = 1250mm, it is confirmed another one time how the choice of b_{ef} = 1250mm is the most realistic (see also Chapter 6). These values are shown in Table 8.2.

Table 8.2 Comparison between hand calculation and results of Sap2000® model

		Hand calculation	
	Sap2000® Model	beff = 750mm	beff = 1250mm
vinst [mm]	31	36,8	30,86
σ_{33MAX} beam [MPa]	14,25	15,56	14,33
σ_{33MAX} Kerto-Q® [MPa]	5,28	7,16	5,3

To get the values of normal stress σ_{33} for the model developed by SAP2000® it is used the Navier formula (8.1):

$$\sigma = \frac{N}{A} + \frac{M}{I} \cdot y \qquad (8.1)$$

Figure 8.17 shows the distribution of normal shear σ_{33} for the load combination 1 and 2. In load combination 2 the stress distribution is asymmetric and the stresses are very high in the regions close to wheel's treads. Figure 8.18 shows the distribution of stresses σ_{11} and τ_{12} in the deck due to the vehicle load. In all the pictures of Figure 8.17 and 8.18 there are peaks of values of the stress at the support edges of the deck. These peaks are due to problems in the boundary conditions caused by the rigid fictitious elements that link the glulam beams to the deck.
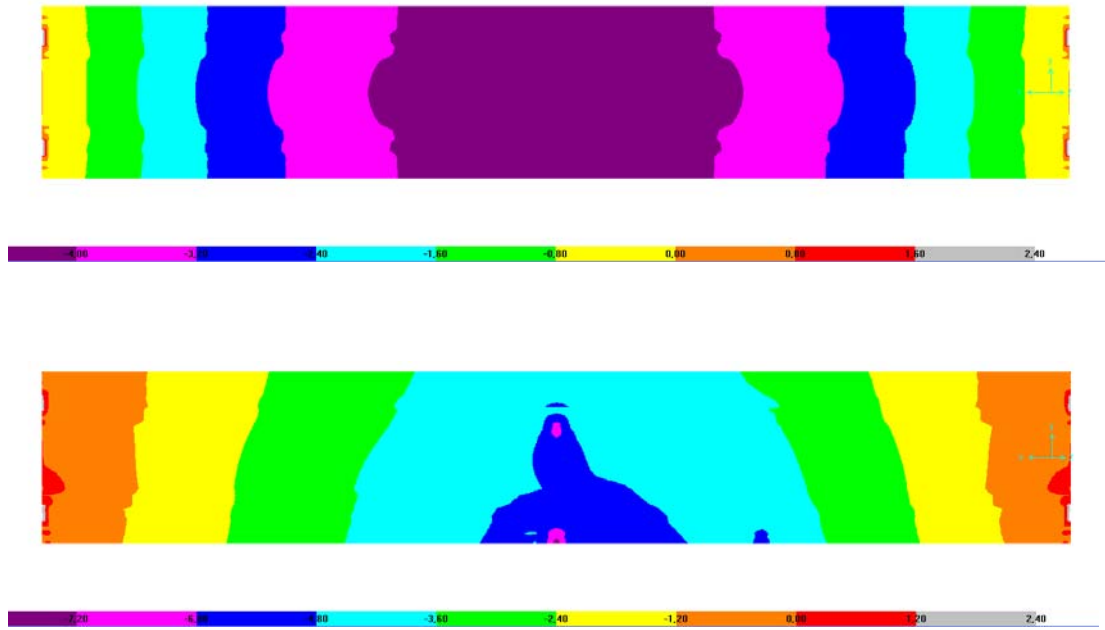
Figure 8.17 Distribution of normal stress σ_{33} in the load combination 1 $\sigma_{33MAX} = 5,5$ MPa (above), and in the load combination 2 $\sigma_{33MAX} = 7,5$ MPa (below)
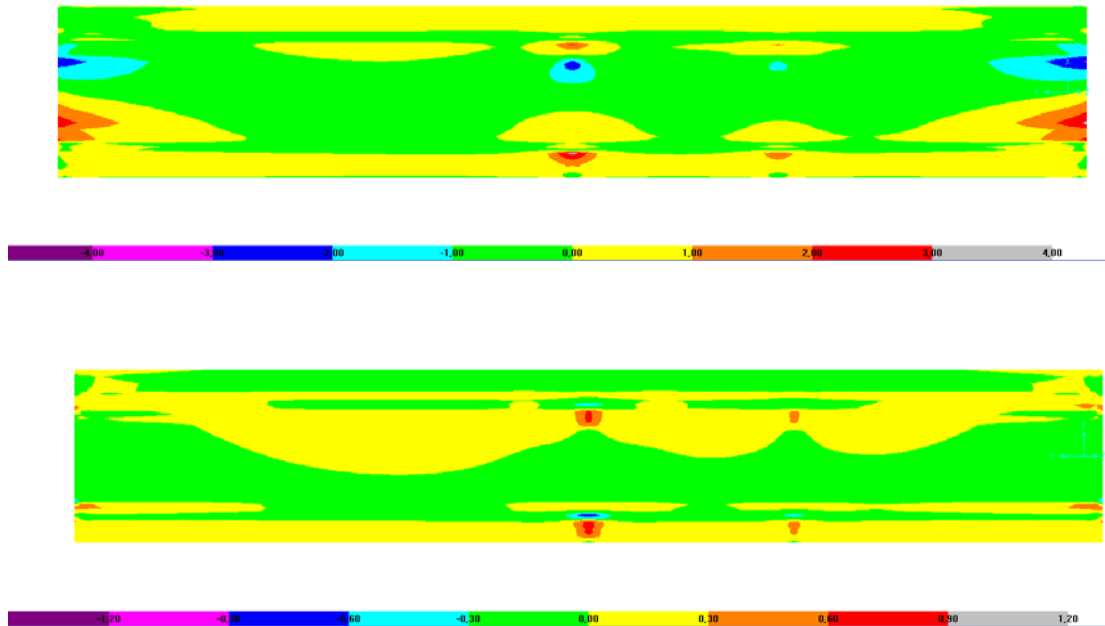
Figure 8.18 Distribution of normal stress σ_{11} in the load combination 2 $\sigma_{11MAX} = 3,5$ MPa (above), and of shear stress τ_{12} in the load combination 2 $\tau_{12MAX} = 0,7$ MPa (below)

The loading tread due to the service vehicle is a square 200mm x 200mm.The loading tread to apply over the timber deck is a rectangular 360mm x 280mm, because the layer of asphalt spread the loads on a larger area (see Appendix A and B). Figure 8.19 describes the geometry of the loading tread. Figure 8.20 shows the distribution of shear stresses τ_{12} and τ_{23} in the deck of the bridge in the regions around the concentrated load.
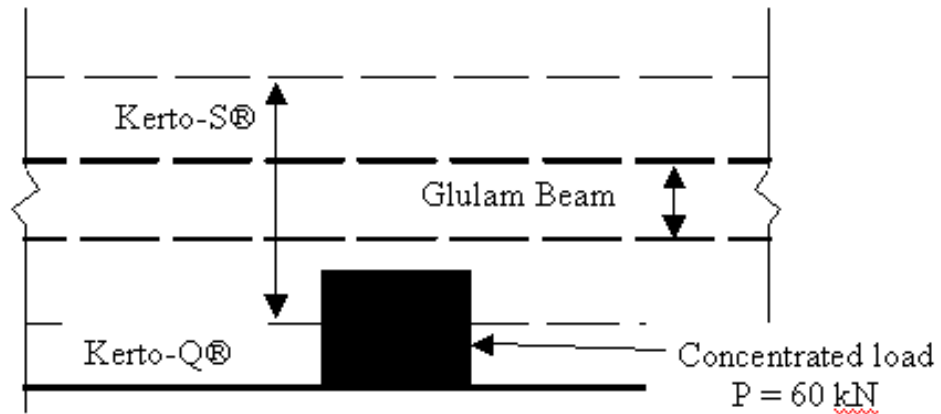
Figure 8.19 Position of the concentrated load on the deck
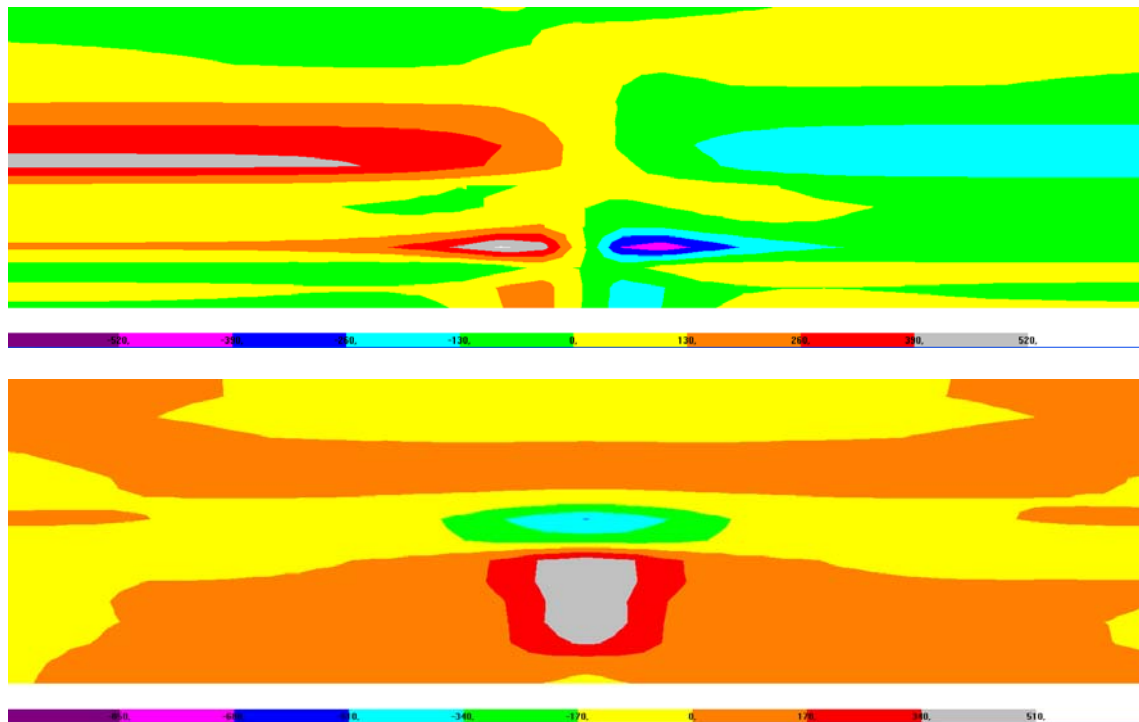
Figure 8.20   Distribution of shear stress τ_{23} in the load comb 2 $\tau_{23MAX} = 0,8$ MPa (above); distribution of shear stress τ_{12} in the load comb 2 $\tau_{12MAX} = 0,7$Mpa (below)

It can be noticed that:

- The concentrated load is spread longitudinally because it passes from an area 360mm long in the superior surface, to an area nearly 1 meter long in the contact face between the deck and glulam beam (see graph in Figure 8.21).

- Both shear stress τ_{12} and τ_{23} are comparable, and almost equal to 0,8Mpa. This fact demonstrates that the model of a stripe described in Chapter 7 is not correct because it does not take into account the slab behaviour of the deck.

The graph in Figure 8.21 reports the pressure between glulam beams and Kerto-S® stripes along a path in the longitudinal direction of the deck. The wheel 360mm wide is positioned at a distance of 7,5 m from the support. The values of pressure have been found dividing the normal force in the fictitious rigid frame elements by the correspondent area.
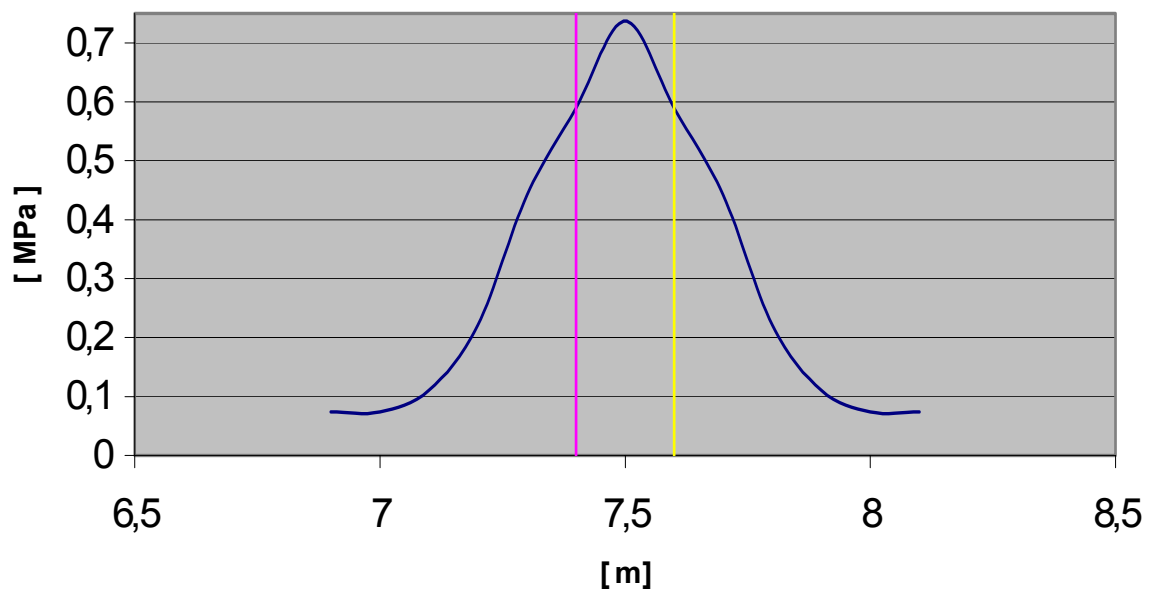
Figure 8.21 Distribution of the pressure between the Kerto-S® stripe and the glulam beam along a path in the longitudinal direction

A similar graph can be found plotting the pressure in the interface between glulam beam and Kerto-S® stripe for the Abaqus® model (that is described in Section 8.2 of this Chapter). In this case the origin of the longitudinal path is placed in the middle of the wheel loading tread, and in fact the load is completely spread at a distance of 0.5m (see figure 8.22).
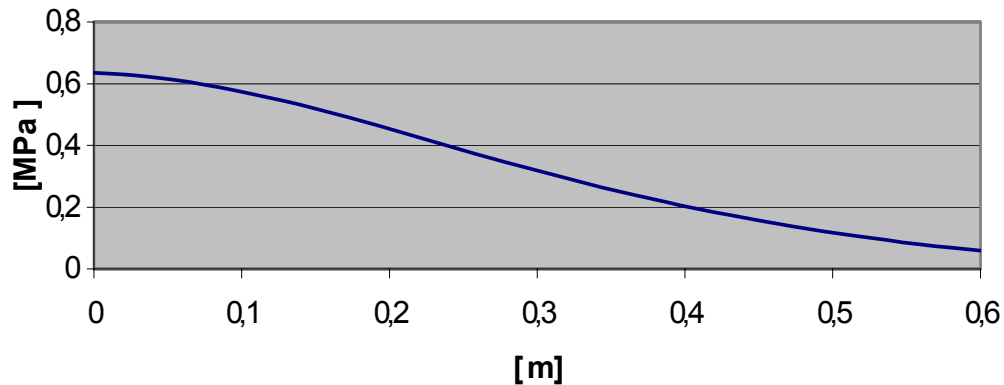
Figure 8.22 Distribution of the pressure found by Abaqus® between the Kerto-S® stripe and the glulam beam along a path in the longitudinal direction

The model SAP2000® described in this section has calculated a value of eigenfrequency for this structure equal to $4,87 s^{-1}$.

8.2 Software Abaqus®

8.2.1 Description of the model

The FE model performed by the software Abaqus® it is a 3D model of the bridge made with solid elements. The use of solid elements is necessary because the simplified models like the SAP2000® model previously described are not able to analyse properly the distribution of shear stress in the deck due to the passage of the service vehicle.

The model strictly reproduces the bridge designed by Moelven AB. The bridge has a curved longitudinal profile of a radius equal to 86,37m, but the model is made with straight elements. The differences in the results of these two models should be negligible. Handrails, layer of asphalt and the elements that protect the glulam beams are not included in the model, but are considered just as distributed loads acting on the structure. See Figure 8.22.
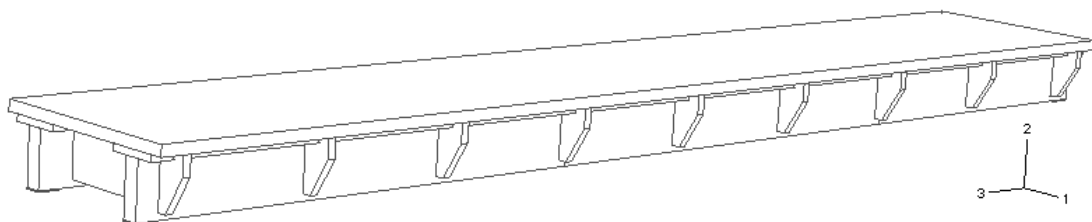
Figure 8.22 Model of the bridge performed by Abaqus®

The model is made by the following parts:

- 2 Glulam beams (190mm x 630mm x 15000mm ; GL32c)

- 2 Kerto-S® stripes (600mm x 75mm x 15000mm; Kerto-S®)

- 1 Kerto-Q® deck (2500mm x 126mm x 15000mm; Kerto-Q®)

- 7 Transversal Central Joists (90mm x 315mm x 1410mm; GL32c)

- 2 Transversal Final Joists (90mm x 630mm x 1410mm; GL32c)

- 18 External Element (see Figure 8.23; GL32c)

- 4 Supporting steel plates (190 mm x 15mm x 250 mm ; steel)
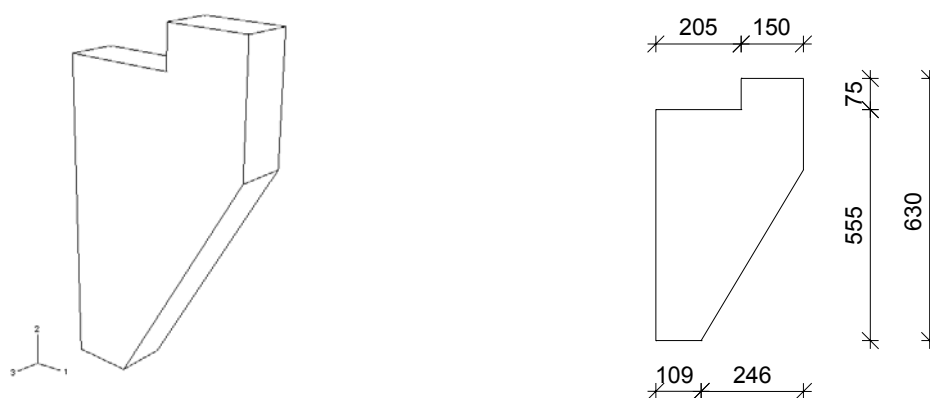
Figure 8.23 External elements

The different parts of the model are joint together using glued connections. This kind of connections is modelled by using a constraint known as "Tie connection".

8.2.2 Material properties

To execute the model is necessary to define the material properties. The materials are assumed to be isotropic; the essential properties to define are: Elastic modulus E, Poisson coefficient ν, and density γ. See Table 8.2.

Table 8.1 Materials properties defined in the Abaqus® model

	E [MPa]	ν	γ[kN/m^3]
Glulam GL32c	13500	0,2	6
Kerto S®	13800	0,2	6
Kerto Q®	10500	0,2	6
Steel	210000	0,3	78

8.2.3 Boundary conditions

The structure has been fixed to the ground locking the right degrees of freedom at the beam's end in the same way as for the model in Sap2000®. Just one support has been represent by a pin (free rotation and translation locked in all the three direction). The other one has been schematised like showed in the Figure 8.11. In this way the structure is globally isostatic in the 3D space.

The supports of the glulam beams have been modelled as two steel plates 190mm x 250mm and 15 mm thick. The boundary conditions are applied along a line placed in the middle of the lower surface of the steel plate. Displacements and rotations of the nodes along this line are locked (see Figure 8.24). In this way the stress distribution that is generated in the region over the support is similar to the one that there is in the reality for the bridge (see Figure 8.25). In an area of the glulam beam over the support, the compressive stress perpendicular to grain is higher than the design resistance value. This aspect has not been considered in this thesis work; if the real distribution of stresses in the glulam beam over the supports is to be investigated, the supporting steel plates should be modelled even more in details. In Figure 8.26 is shown the stress distribution at supports when the boundary conditions are just applied directly to the nodes of the short external side of the glulam beam. The results in this case reach high peaks, and a strong discontinuity in the values is noticed.
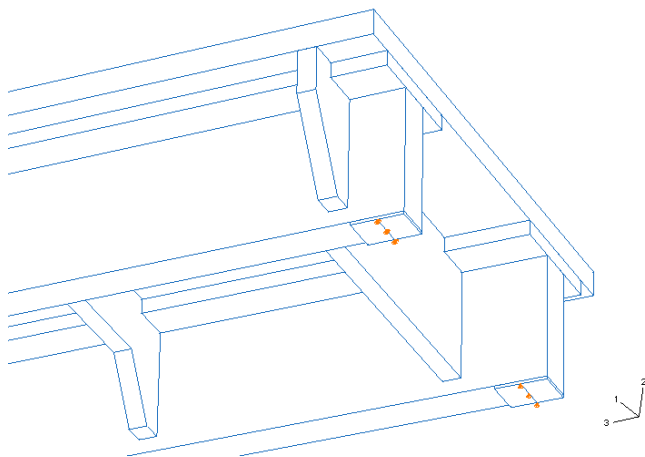
Figure 8.24   Boundary conditions applied along a line placed in the middle of the lower surface of the steel plate
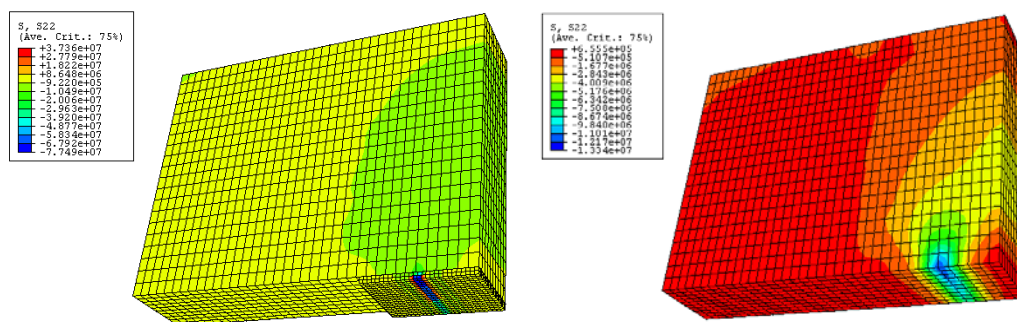
Figure 8.25   Distribution of compressive stress in the region of the beam close to the support modelled with a steel plate
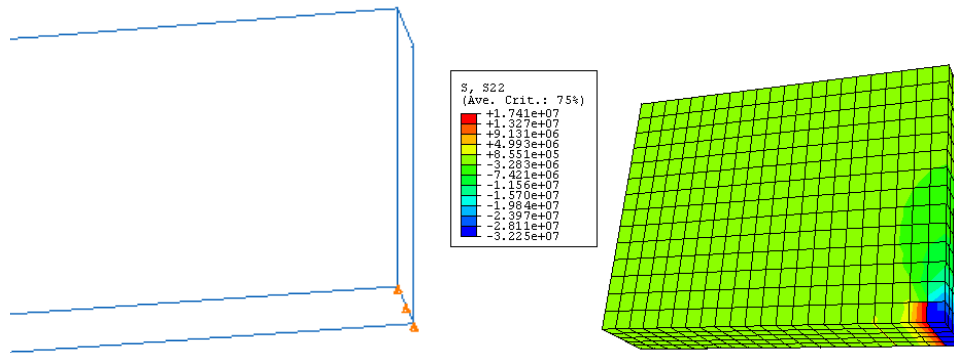
Figure 8.26   Stress distribution at supports when the boundary conditions are just applied directly to the nodes of the short external side of the glulam beam

8.2.4 Loads

Two types of load have been applied to the structure:

- Self-weight: it is defined as a gravity load inside the software; the density of the different kind of materials is defined.

- Permanent load and service vehicle load: the regions where these loads are applied and the magnitude of the pressure of these loads are defined (see Figure 8.3 and 8.4).

8.2.5 Mesh

The standard solid elements 8-node linear brick have been used for the mesh. At first, meshes with the same size of elements all along the bridge were adopted (see Figure 8.27). This fact caused an elongation for the time needed by the software to solve the analysis; at the same time, it caused problems in the region of the model where steep stress variations are predicted.
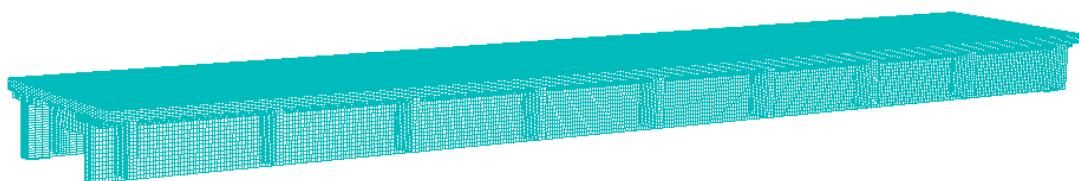
Figure 8.27 Mesh with the same size of elements all along the bridge

Hence, meshes more defined in those regions of the structure where more interesting results were expected have been performed. The part of the bridge directly under the load of the service vehicle have been generated with a define mesh in the model. The same thing was done for the regions close to the supports. The width and the height of the solid elements is everywhere the same; the thickness in the high-defined elements is around 20-30mm, whereas in the other parts of the bridge it is set around 100mm (see Figure 8.28).
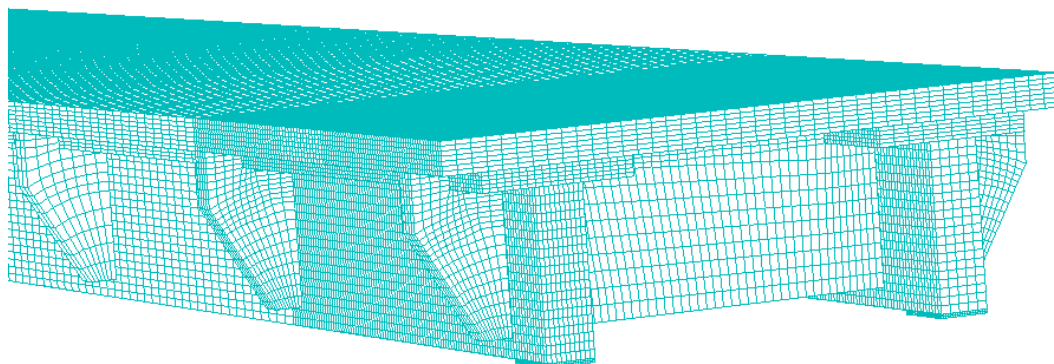
Figure 8.28   More defined meshes in those regions of the structure where more interesting results are expected

8.2.6 Results

The results are presented in three different groups: firstly the mechanical slab-behaviour of the deck is discussed, secondly the load-transfer mechanism between the deck and the beams is explained, and finally problems of local distribution of stresses at the passage of the service vehicle are investigated.

Mechanical slab behaviour of the deck

The following Figure 8.29-33 shows the results of stress distribution for the whole bridge modelled by Abaqus®.
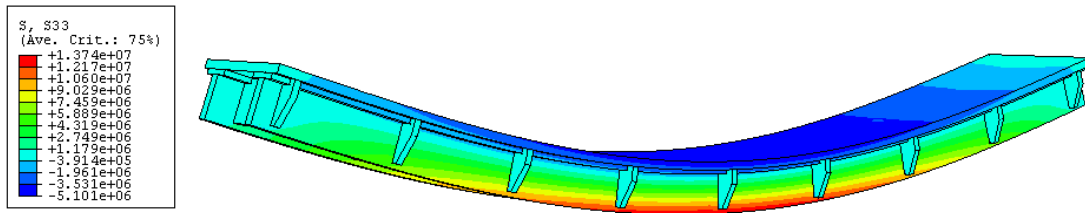
Figure 8.29 Distribution of bending stress in the whole bridge σ_{33} in load combination 1
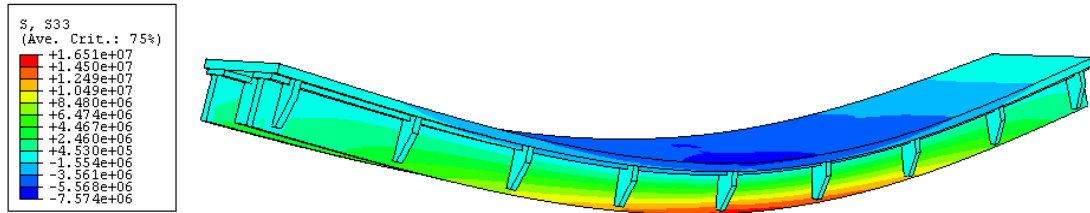
Figure 8.30 Distribution of bending stress in the whole bridge σ_{33} in load combination 2
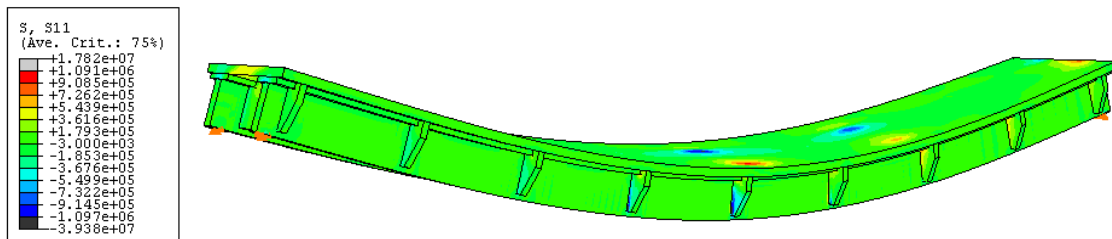
Figure 8.31 Distribution of transversal bending stress in the whole bridge σ_{11} in load combination 2
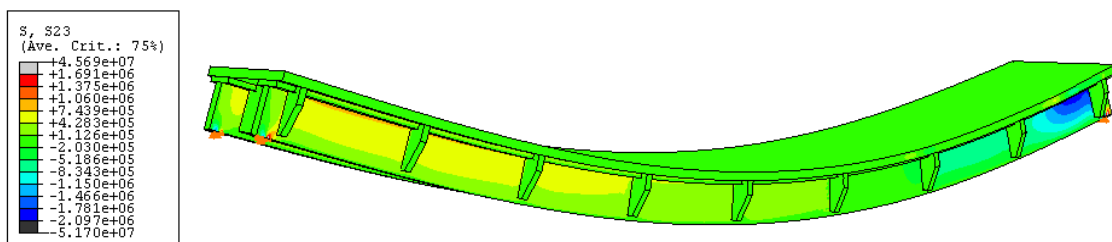
Figure 8.32 Distribution of shear stress in the whole bridge τ_{23} in load combination 3
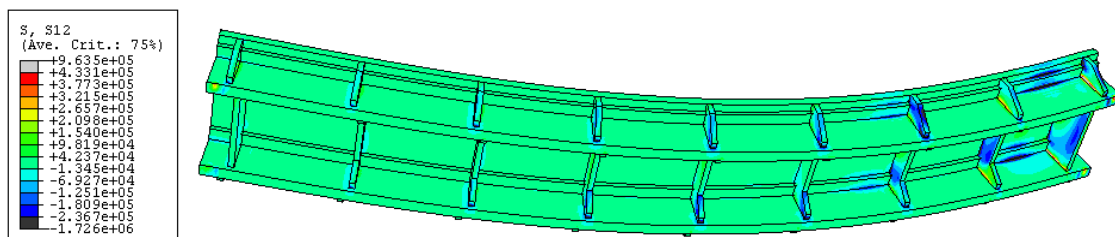
Figure 8.33 Distribution of shear stress in the whole bridge τ_{12} in load combination 3

The position of the service vehicle can be far or close to the transversal units (see Figure 8.34).
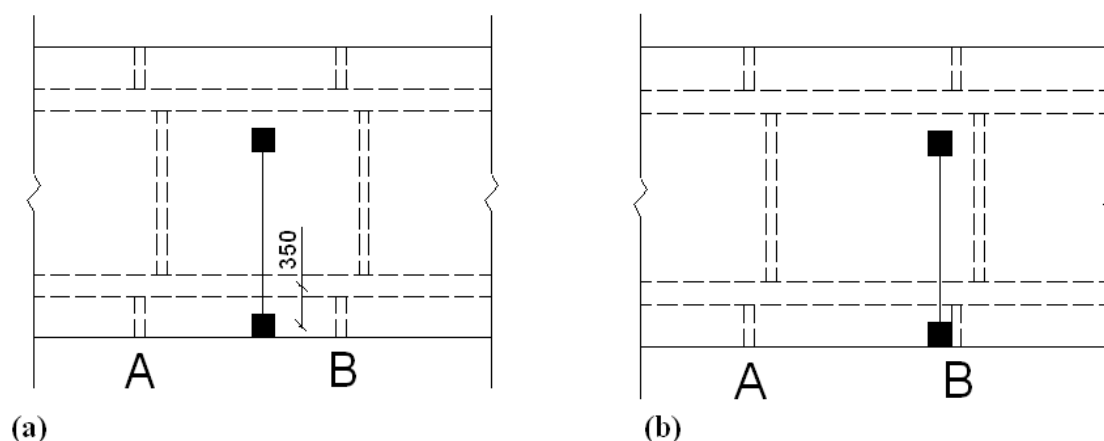
Figure 8.34 Transversal position of the concentrated loads: (a) far from the transversal units, (b) close to the transversal units

As it is shown in the previous figure, the maximum distance between glulam beams and the wheel in the transversal direction can be equal to 350mm. It is not possible to have a concentrated load transversally in the middle of the deck (see Appendix B).

Hence, especially in case (a) of Figure 8.34, a large amount of load is transversally transferred from the deck to the beams by compression or flexural bending of the deck itself (see the next paragraphs of this Section). In case (a) of Figure 8.34 only 15% of load of the external wheel is transferred to the two external elements A and B; the remaining 85% is directly transferred from the deck to the beams. In case (b) of Figure 8.34, almost half of the total load of the wheel is transferred to the external element B. In this case a large shear stress is reached in the Kerto-Q® deck (see the last part of this Section for more details).

The next Figures 8.35-37 prove the mechanical slab behaviour of the deck; they plot the distribution of normal stress σ_{11} in transversal section of the bridge with different longitudinal lengths (0,36m, 1,00m, 2,60m). The longer is the transversal section, the clearer is the mechanical slab behaviour of the deck. The transversal stripe of 1,00m gives values of normal stress σ_{11} 50% higher than the real case; the transversal stripe of 0,36m gives values of normal stress σ_{11} 300% higher than the real case.
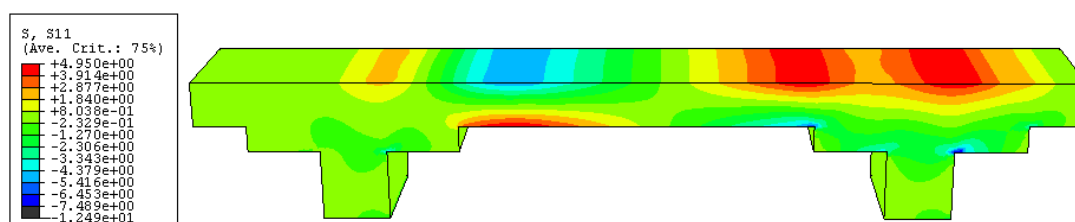

Figure 8.35   Distribution on normal stresses σ_{11} for a transversal stripe 0,36m long (the stress values in the table are in MPa)
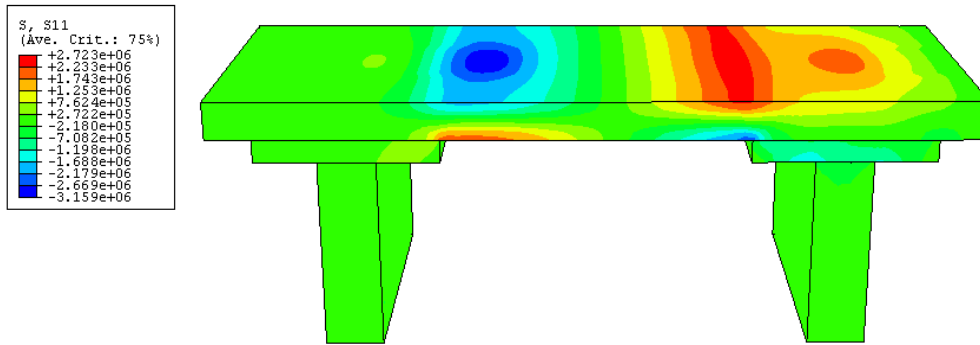
Figure 8.36 Distribution on normal stresses σ_{11} for a transversal stripe 1,00m long
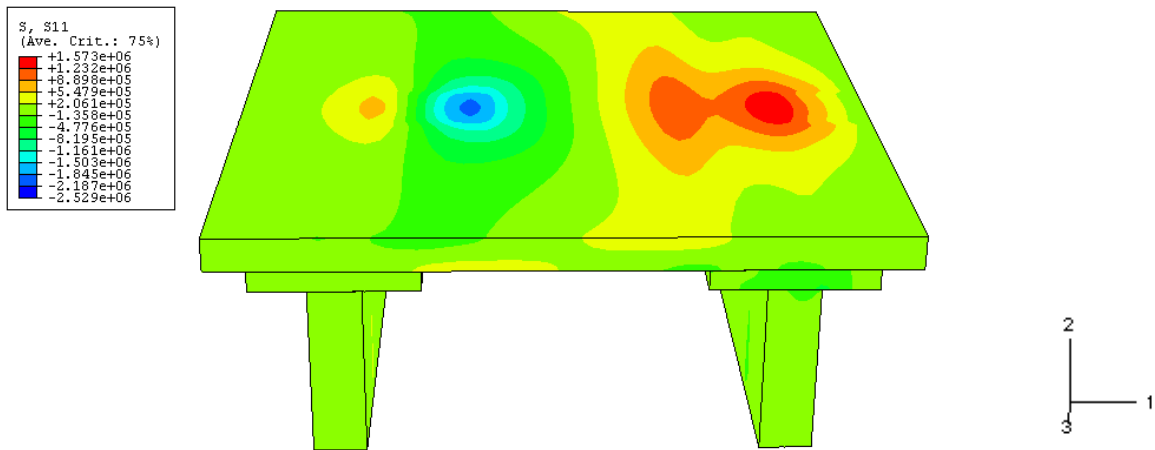

Figure 8.37 Distribution on normal stresses σ_{11} for a transversal stripe 2,60m long

The following Figures 8.38-40 show various results of the model of Figure 8.35, from different views.
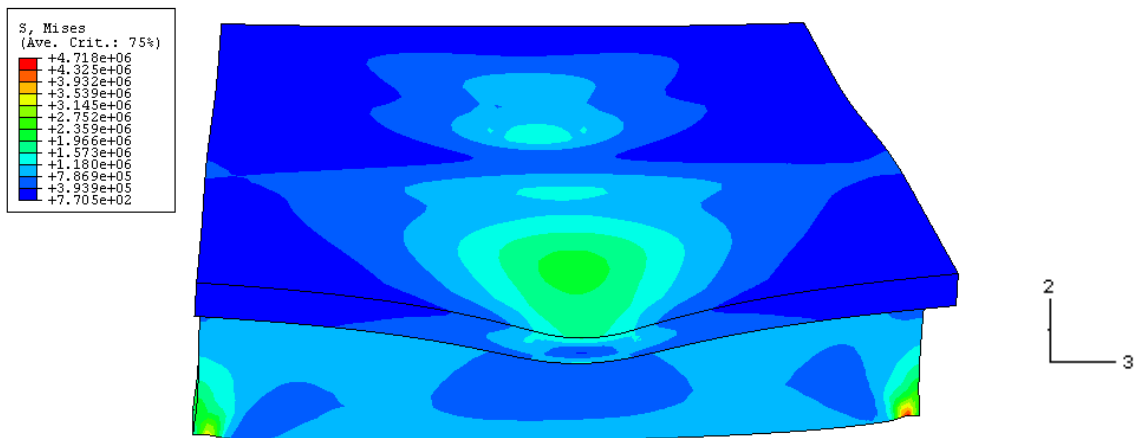

Figure 8.38   Von Mises stresses for the model of Figure 8.37 rotated of 90 degrees about the vertical axis 2
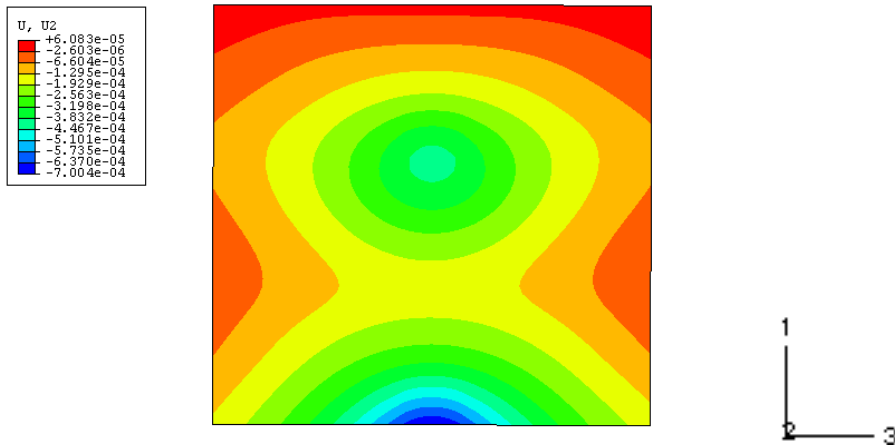
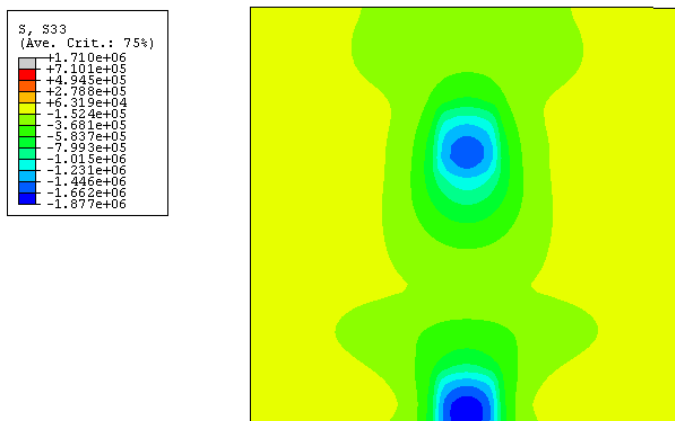*Figure 8.39 Vertical displacements u_2 of the deck (plan view of the model of Figure 8.37)*

Figure 8.40 Distribution on normal stresses σ_{33} among the deck (plan view of the model of Figure 8.37)

The following Figures 8.41-42 describe the different distribution of stresses σ_{11} among the deck for the bridge with and without the transversal units caused by the service vehicle load. It can be noticed how the concentrated load can be completely transferred to the beams within a region 1,50m wide.
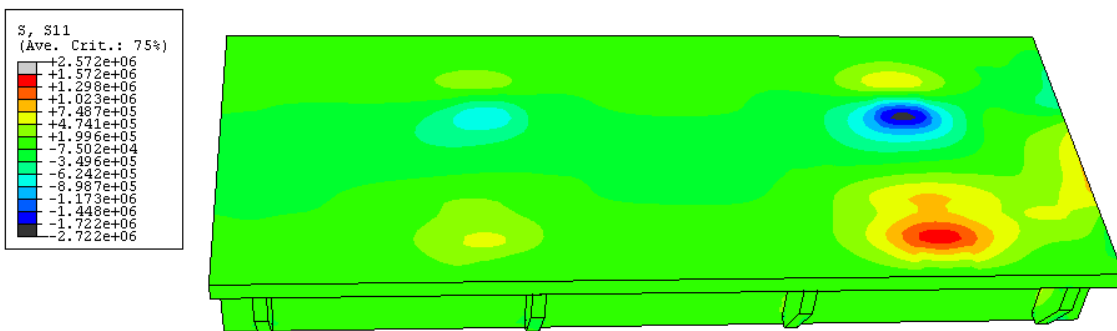
Figure 8.41 Distribution of normal stress σ_{11} among the deck for the bridge wit transversal units in load combination 3
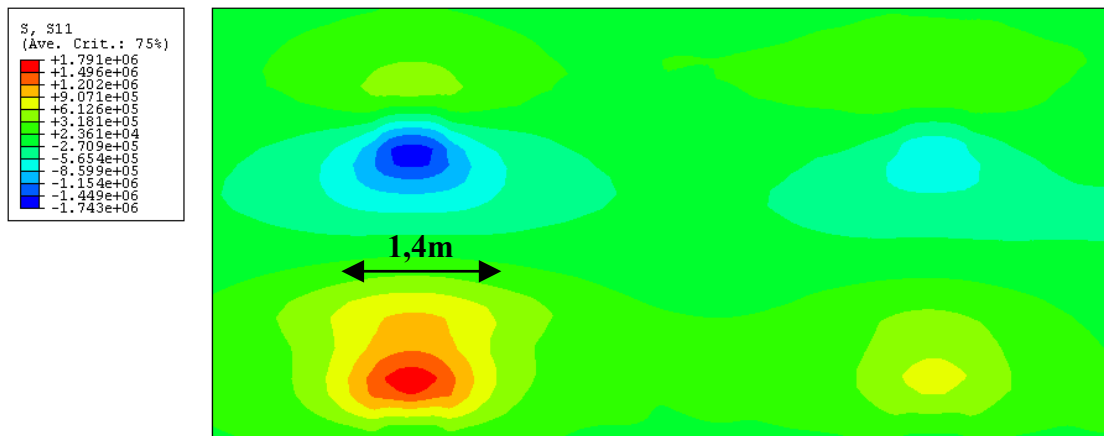
Figure 8.42   Distribution of normal stress σ_{11} among the deck for the bridge without transversal units in load combination 2

Load-transfer mechanism between the deck and the beams

The following Figure 8.43-45 show howo the loads produced by the wheels of the service vehicle can be transferred from the deck to the glulam beams. This transfer occurs by direct compression of the elements, by shear and by flexural bending of the deck.
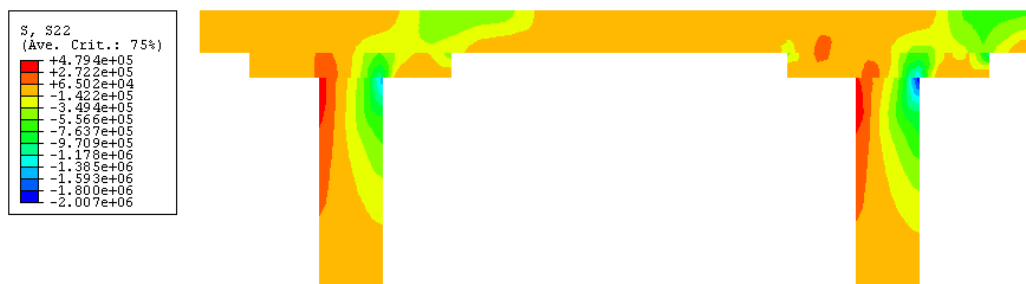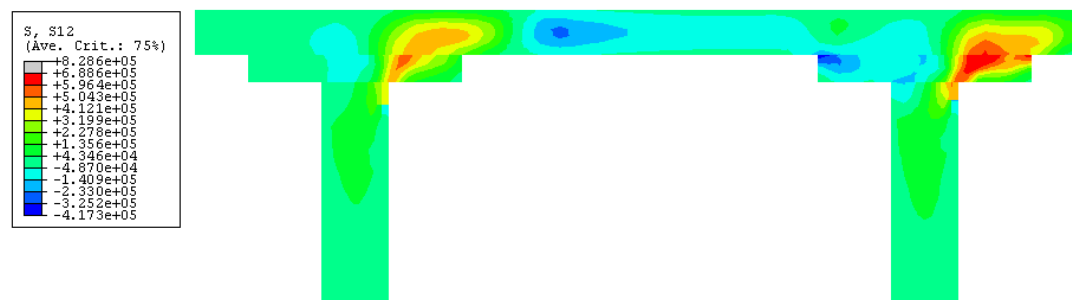

Figure 8.43 Distribution of compressive stress σ_{22}

Figure 8.44 Distribution of shear stress τ_{12}; note the similarities with the results of the model of the short stripe of the bridge treated in Chapter 7
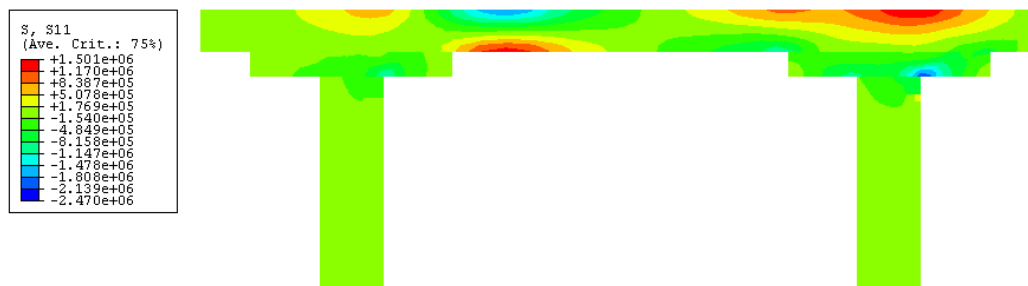
Figure 8.45 Flexural bending of the deck; distribution of normal stresses σ_{11}

Problems of local distribution of stresses at the passage of the service vehicle

The description of these problems it is divided in two parts: at first considerations are developed regarding the case when the loading wheel tread is positioned far from the transversal units, and afterwards problems caused by the wheel positioned over the transversal unit are treated.

The shear stress generated in the deck by the wheel load must be added to the global distribution of shear due to permanent load and self-weight. Close to the supports the shear stress is very high, equal to 0,8 MPa (the design strength for Kerto-Q® is f_{vd} = 0,9 MPa). To study the local distribution of stresses in case of wheel placed between two transversal units, a model of a part of the bridge is analysed (see Figure 8.46).
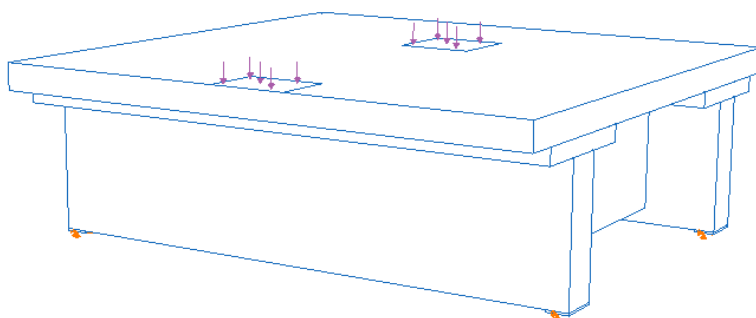

Figure 8.46 Model used to describe local distribution of stresses when the wheel is placed far from the transversal units

The model is symmetric in the longitudinal direction and it has the same boundary conditions described in Section 8.2.3; the length is 2,60m and the longitudinal distance of the transversal units is 1,80m, like for the real bridge. The results are described in Figure 8.47-51.
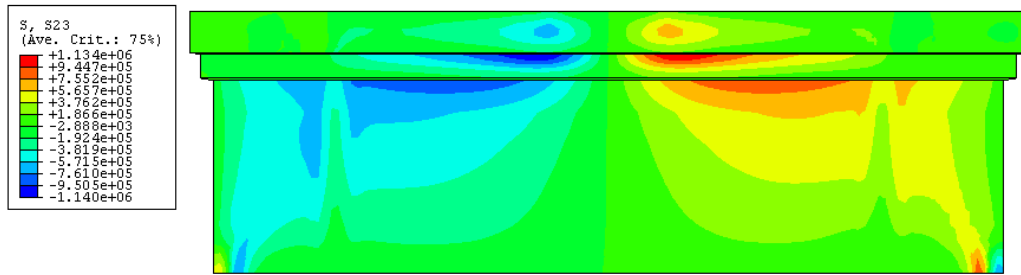
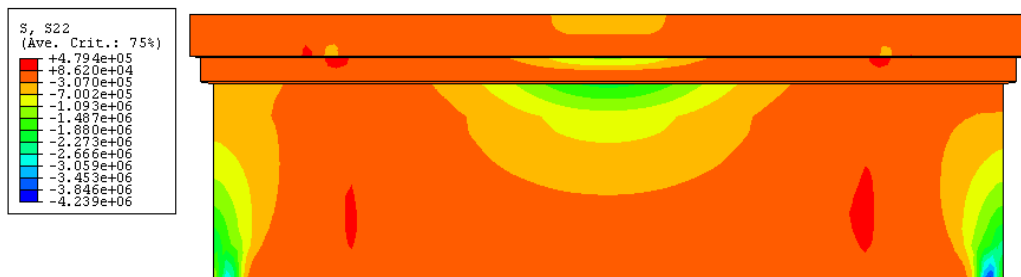*Figure 8.47 Distribution of shear stress τ_{23} for both the deck and the beams*

Figure 8.48 Distribution of vertical normal stress σ_{22} for both the deck and the beams
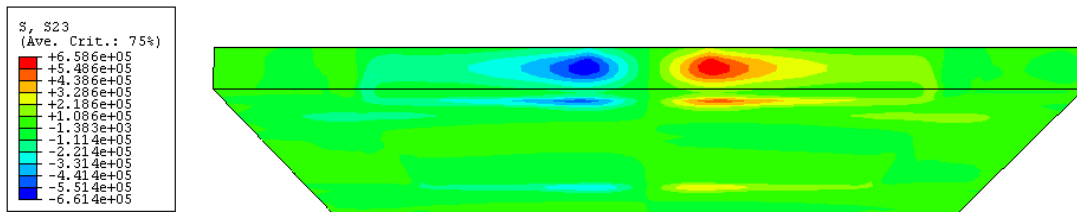

Figure 8.49 Distribution of shear stress τ_{23} in the Kerto-Q® deck

Figure 8.50 Distribution of shear stress τ_{23} in Kerto-Q® and Kerto-S® (view of the cross section); the high value around the sharp edge of the Kerto-S® stripe is due to a computational problem of the FE model,
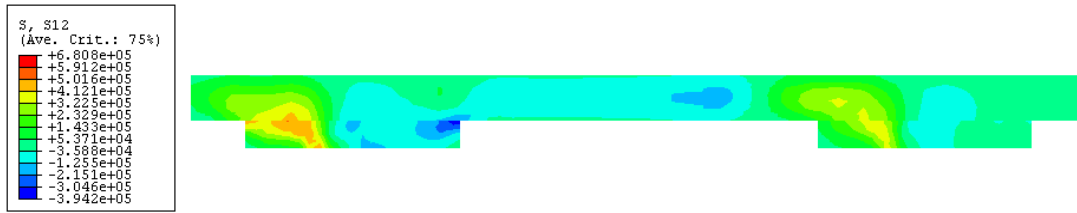
Figure 8.51   Distribution of shear stress τ_{12} in Kerto-Q® and Kerto-S® (view of the cross section)

When the vehicle load is positioned close to the supports, the global shear τ_{23} has to be added to the shear due to the service vehicle load. The shear τ_{23} is equal to 0,8 MPa in the Kerto-Q® deck (see Figure 8.52-53).
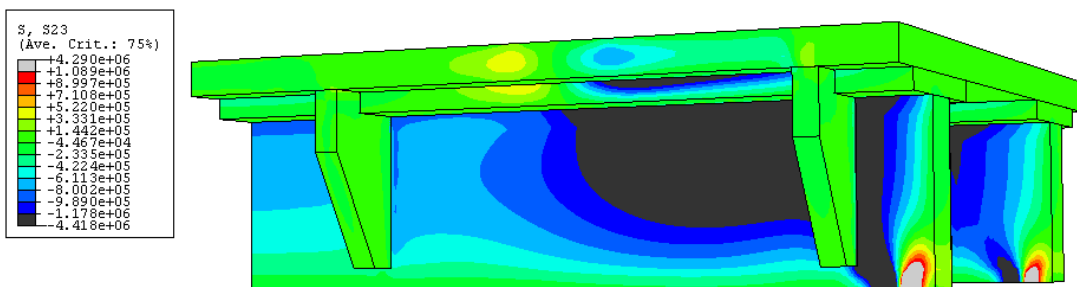

Figure 8.52   Distribution of shear stress τ_{23} for both the deck and the beams for the region of the bridge close to the supports
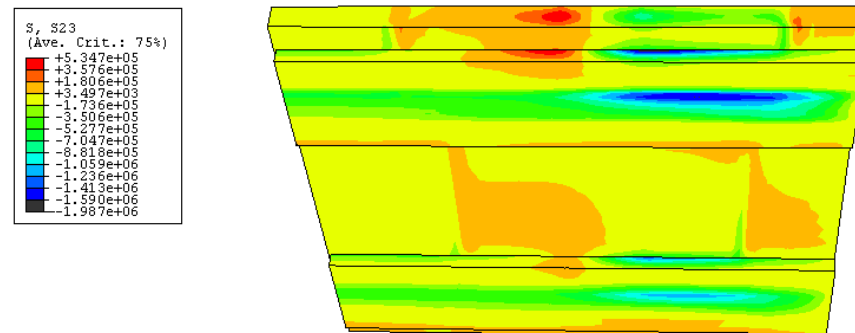

Figure 8.53   Distribution of shear stress τ_{23} for the same part of the bridge of Figure 8.52 referred only to the Kerto-Q® deck and Kerto-S®; the maximum value reached in Kerto-Q® deck is equal to 0,8 MPa

Now the configurations of loads with the wheel positioned over the transversal units are investigated. In this case it is possible to notice very high values of shear stress, larger than the design shear strength of the Kerto® materials in small regions over the transversal units.

The function of the transversal units is to support the deck in many points and limit its deflection. The external transversal units are placed to limit the deflection of the cantilever part of the deck. When the wheel is close to the external transversal units,

almost half of the whole load given by the wheel (60 kN) is transferred from the deck to the external bracing unit (see Figure 8.54-58).
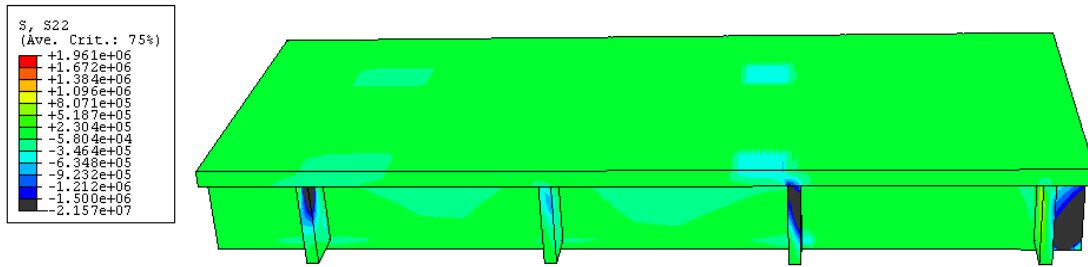

Figure 8.54   Vertical normal stress σ_{22} in the external transversal units when the wheels are placed close to them in a large view of the bridge
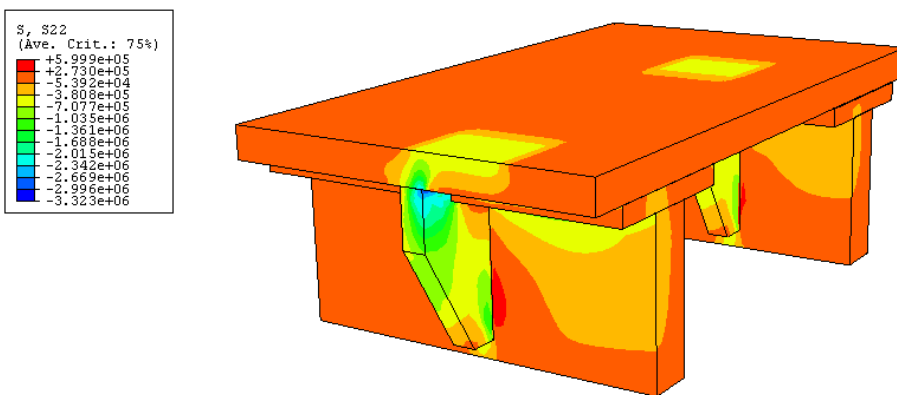

Figure 8.55   Vertical normal stress σ_{22} in the external transversal units when the wheels are placed close to them in a detailed view close to the external unit
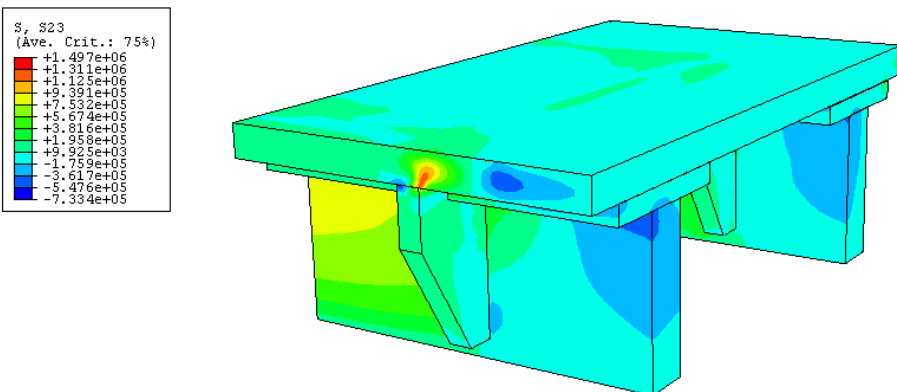

Figure 8.56   Distribution of shear stress τ_{23} when the wheel is placed close to the external unit; the shear stress in Kerto-Q® is equal to 1,18 MPa (more than the design strength)
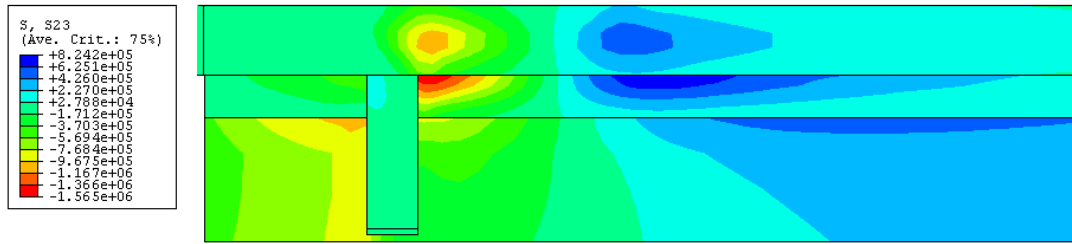
Figure 8.57 *Distribution of shear stress τ_{23} when the wheel is placed close to the external unit in case of not full-interaction between Kerto-Q® deck and external unit; just normal stresses and not shear stresses can be transferred from the Kerto-Q® deck to the external transversal unit*

Figure 8.58 *Distribution of shear stress τ_{23} among the cross-section when the wheel is placed over the external unit; the black spots in the Kerto-Q® deck are regions where the value of shear stress is higher than the design value of flatwise shear strength*

9 Final remarks

9.1 Conclusions

- The bridge of 15m span, with glulam beams 190x630mm, Kerto-S® and Kerto-Q® glued together to form a composite section respects the verifications imposed by EC5

- The Kerto-Q® deck is able to transfer the concentrated loads due to the service vehicle to the glulam beams either through direct compression and working as a slab. The stress verifications based on EC5 are verified.

- The cross beams act as supports for the deck, and they transfer to the glulam beams a relatively small amount of load when the wheel is far from the cross beams. If the wheel is directly over them, high peaks of shear stress occur in a local region under the wheel tread in the deck.

- Bridges with span longer than 15m and the same type of cross-section may be built. However, more detailed analysis regarding vibrations and deflection must be performed. For bridges with span longer than 30 m the static scheme should be changed.

9.2 Limitations

- More detailed study for bridges with span larger than 15m should be carried out.

- Experimental tests should be done on the bridge to have confirmations on the results of the analytical and numerical calculations.

- Mechanical tests should be performed on the Kerto® materials in the flatwise mode in order to check the correct value of characteristic planar shear strength.

- Numerical analysis should be studied taking into account the orthotropic properties of the materials.

9.3 Future research

Finally, some aspects related to this Thesis that could be investigated more in detail are suggested as follow:

- The hypothesis of Isotropic material adopted to model the LVL elements of the bridge contain some limitations. Taking into account the orthotropic behaviour of the Kerto-Q® and Kerto-S® materials, the distribution of stresses among the deck of the bridge should slightly vary. The maximum values of stress reached should not be very different, whereas large differences are expected for the way the loads are transferred through the different parts of the structure. The stiffness of the LVL elements in certain directions (for example in the transversal direction) would be highly reduced, increasing the amount of load transferred along these stiffener paths. At the same time, the magnitude of the stresses related to these stiffener directions would also

increase. Furthermore, in order to carry out analysis based on the use of orthotropic materials, a detailed study on LVL timber products should be done to find the correct values of material properties to be used.

- Problems regarding possible high tensile stresses perpendicular to grain in the glued interface between glulam beams and Kerto-S® stripes might be investigated. These stresses occur due to the bending of the deck in the transversal section caused by the asymmetric service vehicle load (see Figure 8.59).
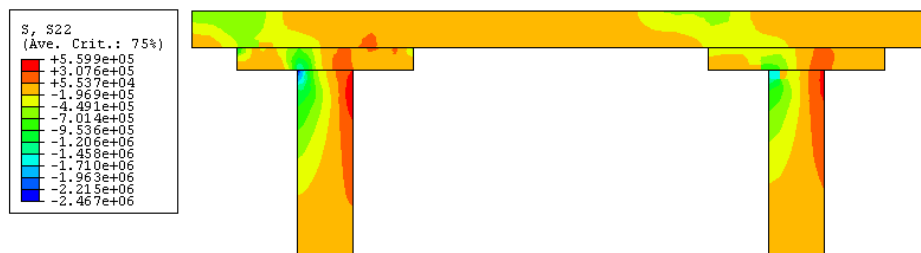

Figure 8.59 Vertical normal stress distribution in the cross section in load combination 2

- Possible different solutions of the geometry for the bridge may be analysed. For example, it could be possible to increase the space between the longitudinal glulam beams, and consequently decrease the cantilever region of the deck, which causes the highest values of shear stress. In this way, the load due to the service vehicle load would be transferred to the beams mainly trough compression (see Figure 8.60-61).
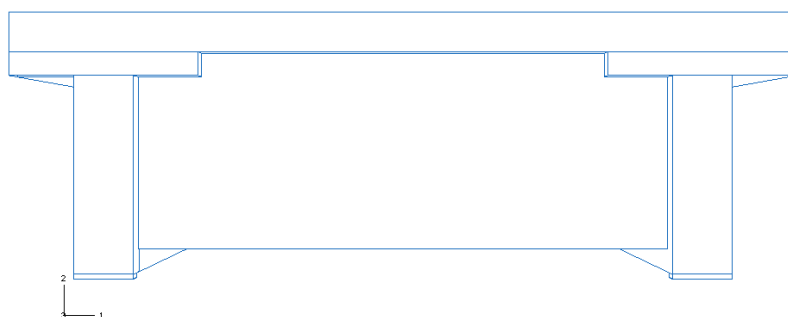

Figure 8.60 Geometric solution of the bridge with increased space between the longitudinal glulam beams, front view
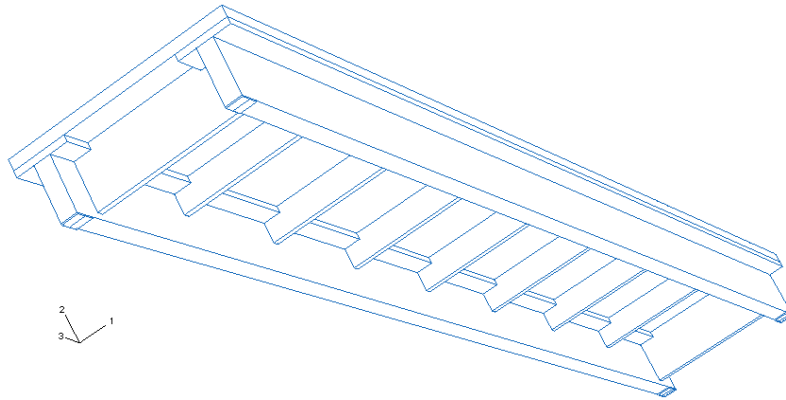
Figure 8.61 Geometric solution of the bridge with increased space between the longitudinal glulam beams, general view

- Furthermore, a solution of the bridge without transversal units could be studied, since these elements produce high values of shear stress in the deck at the passage of the service vehicle (see Figure 8.62), as it was described in Section 8.2.6 of this chapter.

Figure 8.62 Geometric solution of the bridge without transversal joists

- The aspects not considered in this Thesis, clarified in Section 1.1.2 of Chapter 1 may also be analysed. First of all a detailed study of the supports of the bridge and a detailed dynamic analysis of the structure should also be performed.

10 References

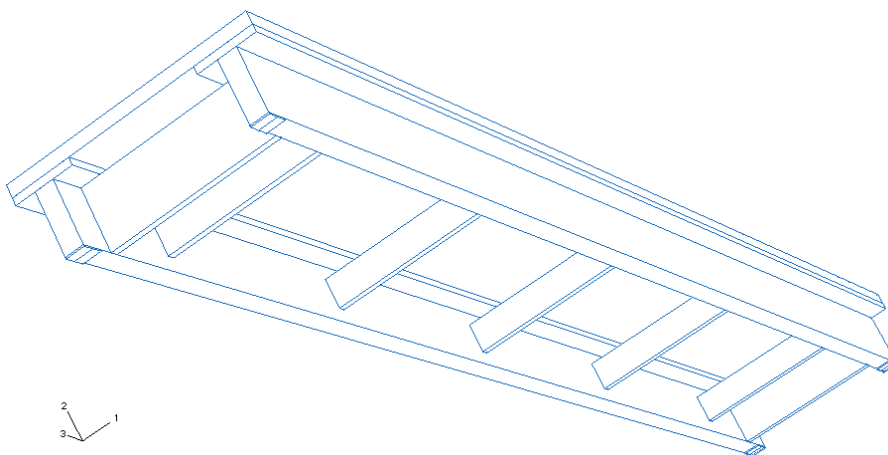Anon. 1995a : Blass H.J., et al, Timber Engineering STEP 1, 1995

Anon 1995b: Eurocode 1 Basis of design and actions on structures (ENV 1991-2-1:1995).

Anon. 2003: *Design regulations BKR*. Boverket, BFS 1998:39.

Anon. 2004a: *Eurocode 5: Design of timber structures Part1-1: General-Common rules and rules for buildings* (EN 1995-1-1:2004).

Anon. 2004b: *Bro 2004* (Swedish Building Code. In Swedish).

Anon 2004c: *Eurocode 5 – Design of timber structures – Part 2: Bridges*. European Committee for Standardization, Brussels.

Anon. 2005: VTT Certificate Revised No 184/03, 20 October 2005

Bellumat (2000): *Ponti e passerelle in legno lamellare incollato. Delaminazione e durabilita'*. Final thesis. Faculty of Engineering, Civil department, University of Trento (Italy)

Buchanan Andrew H. (1992): *Splitting in timber structures*. University of Canterbury.

Ormarsson S. (1999): *Numerical Analysis of Moisture-Related Distorsions in Sawn Timber*. Thesis for the degree of doctor in engineering, Chalmers University of Technology, Publication no. 99:7, Göteborg, Sweden.

Piazza M. (2004), Lectures of the course "Tecnica delle Costruzioni 3", Faculty of Engineering, Civil department, University of Trento (Italy)

Pousette Anna (1997), Nordic Timber Bridge Project, *Wearing Surfaces for Timber Bridges*. Trätek-Swedish Institute for Wood Technology Research, 1997

Ritter Michael A. (1990): *Timber bridges: Design, Construction, Inspection and Maintenance*. Washington, DC: 944p.

Cesaro G., Piva F. (2003): Timber Bridges – Design and Durability. Master's thesis. Department of Structural Engineering, Steel and Timber Structures, Chalmers University of Technology, Publication no. 03:5, Göteborg, Sweden, 2003.

Kliger R. (2005), Lectures of the course "Timber Structures", Department of Structural Engineering, Steel and Timber Structures, Chalmers University of Technology, Göteborg, Sweden.

(Crocetti et al., 2005): Drawings of the bridge made by Moelven Töreboda AB designers.

APPENDIX A: service vehicle load

The concentrated load acting among the deck of the bridge is due to the weight of a service vehicle similar for example to the one shown in Figure A.1.
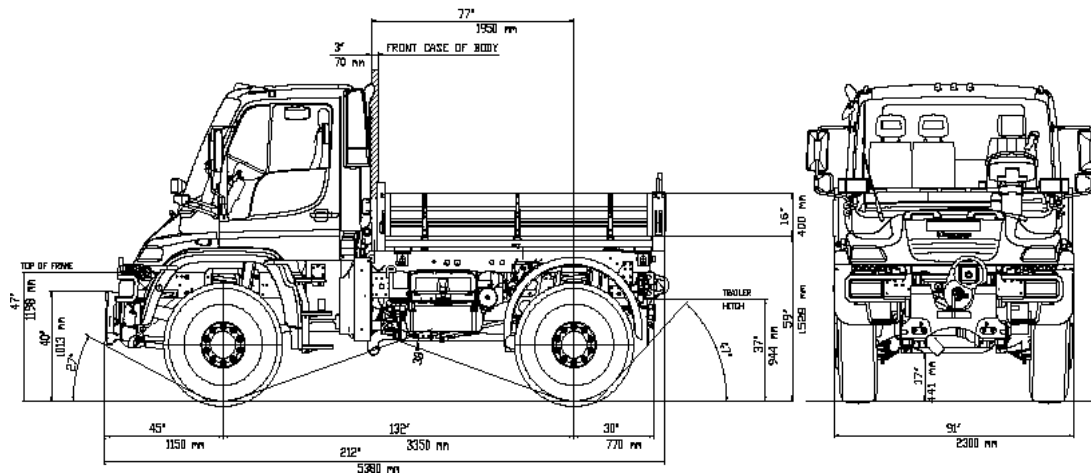
Figure A1   Typical service vehicle generally used on pedestrian and open-to-traffic bridges

This vehicle could be used for several services, like maintenance, assistance for people (it could be an ambulance for example), or other kind of functions (for example a vehicle used to clean the roads from the snow).

If detail information are not available from the customer or other official authorities, the Eurocode 1 suggests the use of a pre-defined service vehicle that is reported as follow:

Figure A2   Geometry of the Load-Group due to the service vehicle (Eurocode 1, Part 1-3)

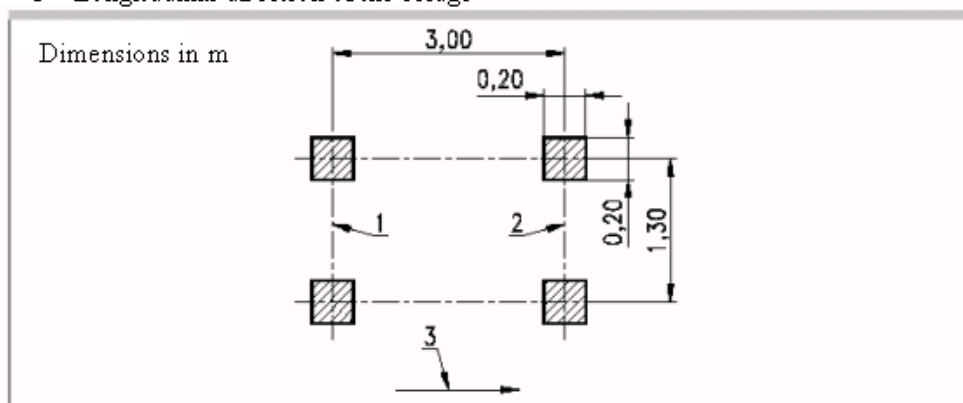The group of loads consists in 2 axis loads of 80kN and 40 kN with a longitudinal distance of 3.00m and a transversal distance between the axes of 1.30m between the wheels. The load's tread it is a square 0.20m side.

The pre-defined load due to the service vehicle imposed by the Swedish codes Bro 2004 it is described in Figure A3. The size of loads is the same as in the Eurocode; the difference regards the transversal distance of the wheels, which is increased up to 1.60m. Furthermore, the encumbrance of the vehicle is here taken into account, so that the load's trade will always be inside the edges of the deck for a distance of at least 0.1m.

Longitudinal Direction   **Transversal Direction**
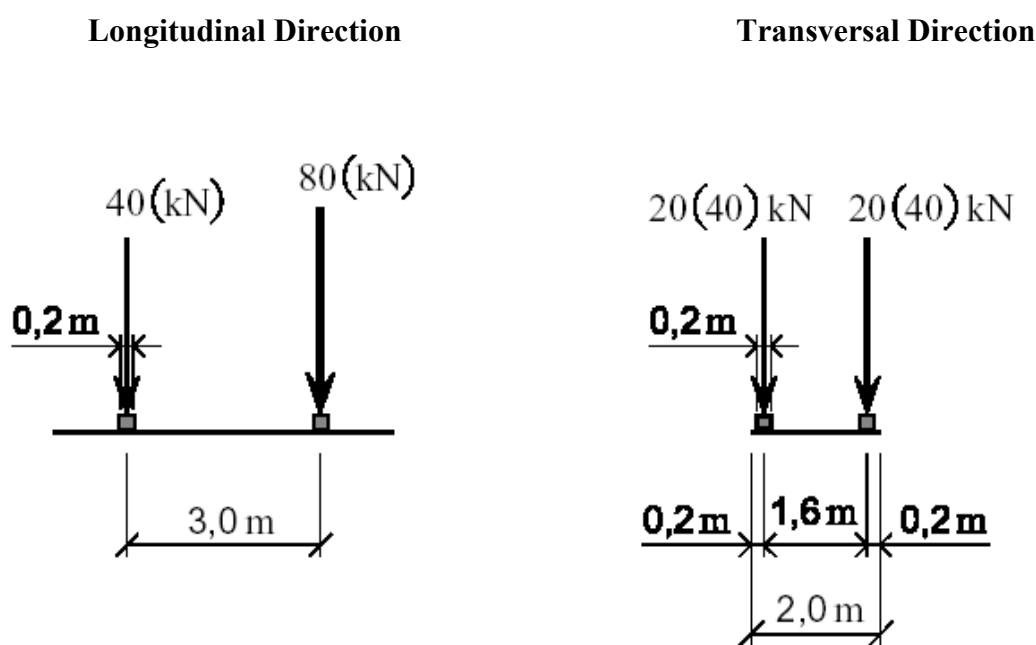
Figure A3   Geometry of the Load-Group due to the service vehicle (Swedish codes Bro 2004)

In order to study the effects of the vehicle load, as a reference in this thesis, it has been followed the geometry of the Load-Group described by the Swedish codes without the encumbrance of the vehicle for the preliminary design of the bridge on the safe side.

As it is discussed in chapter 5 the most unfavorable vehicle load would be the one defined in the Eurocode 1 because it gets the highest shear stresses τ_{12} and τ_{23}, due to the fact that the distance between the axes of the wheels is smaller.

APPENDIX B: numerical tests to investigate the most unfavorable position of the service vehicle load

In order to find the most unfavourable position assumed by the vehicle's load to maximize the shear stresses τ_{12} in the KertoQ deck, an analysis with Abaqus of a stripe of the bridge has been developed. The geometry of the load's tread produced by the wheels of the vehicle is a square with 200mm sides. The layer of asphalt has a thickness of 80mm.Thanks to this layer of asphalt the load's tread that will effectively act on the upper surface of the KertoQ deck will be bigger, because the stresses will be spread out passing through thickness above. The expansion of stresses takes place with an inclination of 45° (see Eurocode 1-3 point 4.3.6). The larger area of the load tread can be easily calculated (see figure B1).
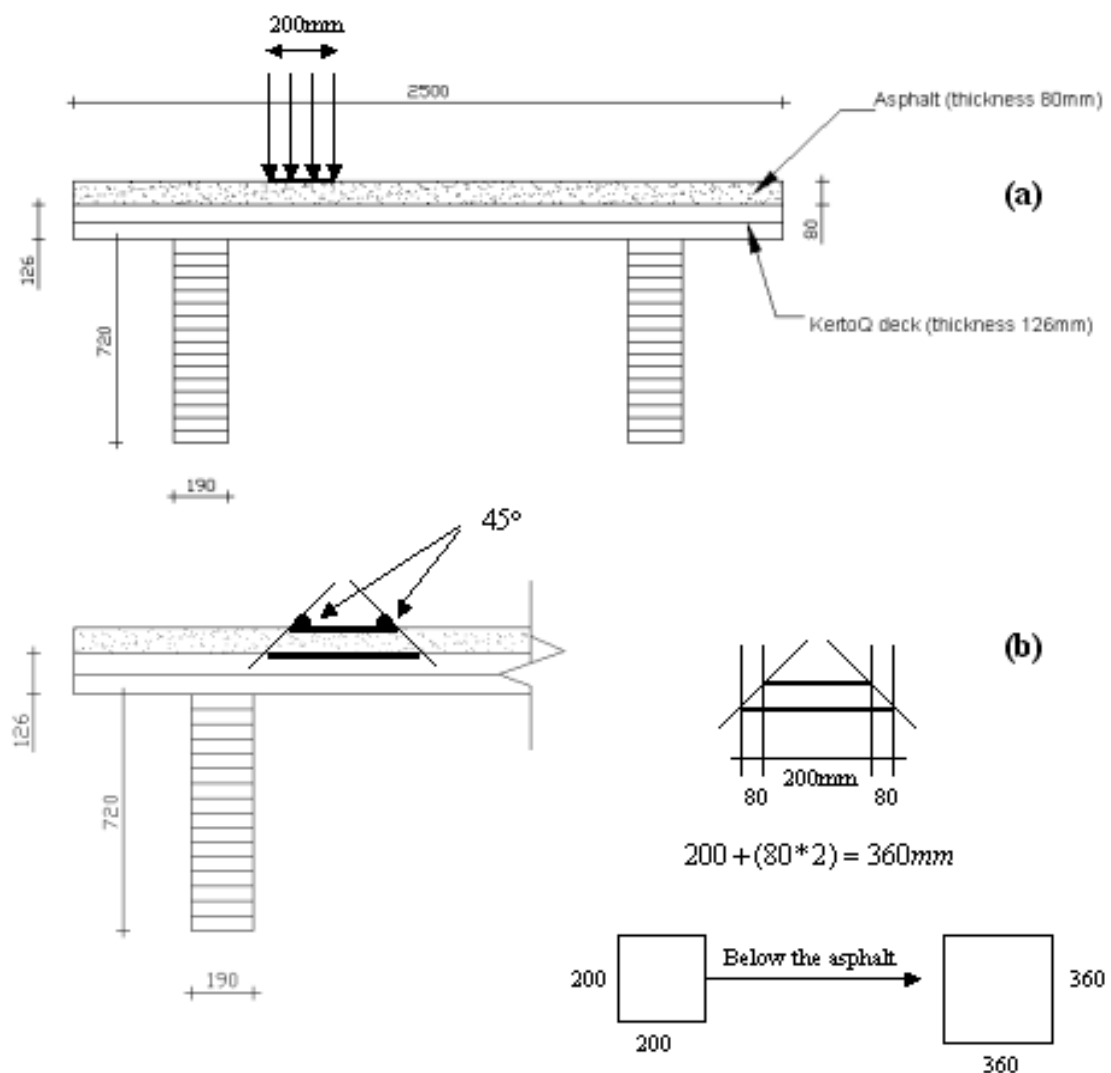

Figure B1   Transversal section of the bridge and load's tread due to the vehicle load (a) ; extension of the load tread passing from the upper surface of the asphalt to the surface of KertoQ below (b).

It has chosen to study four different cases related to four different positions of the loads that should maximize the shear stresses τ_{12} in the deck. They are described in the pictures below. It should be mentioned that the distance between the axes of the two beams is the same as the distance between the axes of the two wheels and equal to 1.6m (see Appendix A). The vertical axis of the coordinate system xy it always cross the point O, on the internal edge of the left beam. All the measures are in [mm].
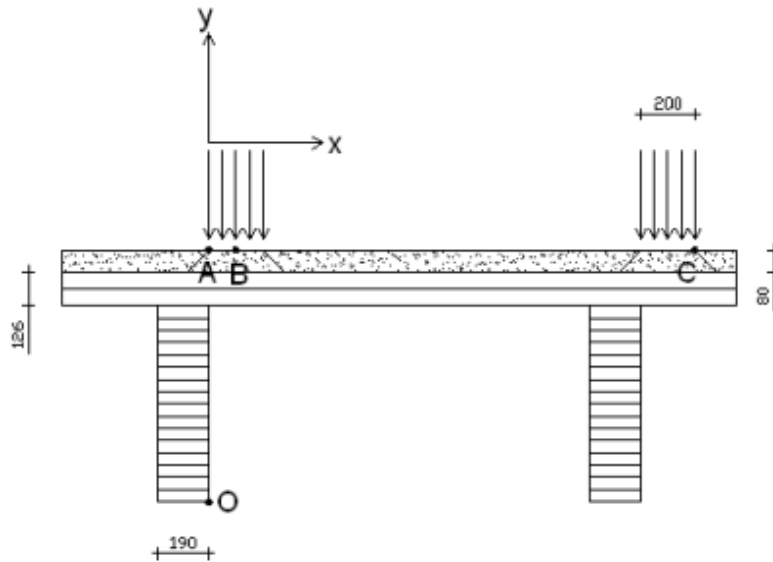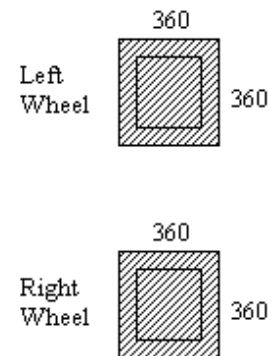
$$P_{1wheelaxis} = 80kN$$

$$P_{1wheel} = \frac{P}{2} = 40kN$$

$$A = 360 * 360 = 129600\,mm^2$$

p = 40kN/0,1296m^2 = 309kN/m^2
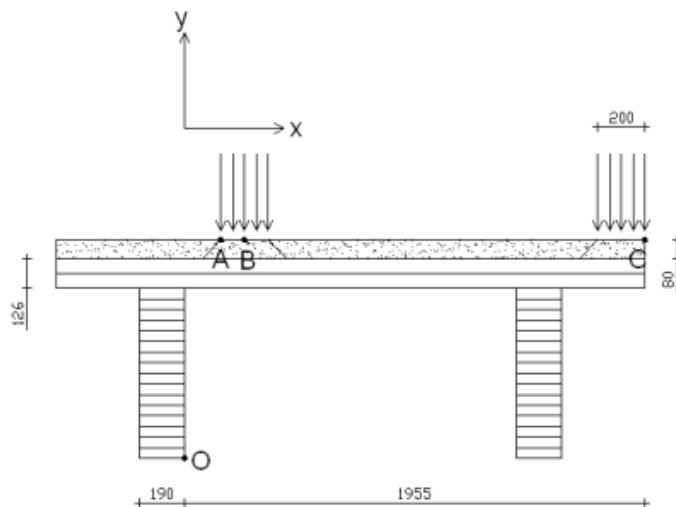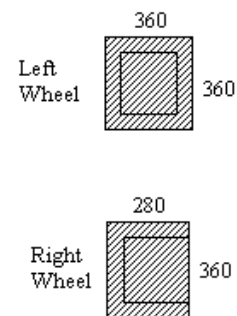
$$P_{1wheelaxis} = 80kN$$

$$P_{1wheel} = \frac{P}{2} = 40kN$$

$$A = 360 * 360 = 129600\,mm^2$$

$$A = 360 * 280 = 100800\,mm^2$$

p-left = 40kN/0,1296m^2 = 309kN/m^2

p-right = 40kN/0,1008m^2 = 397kN/m^2
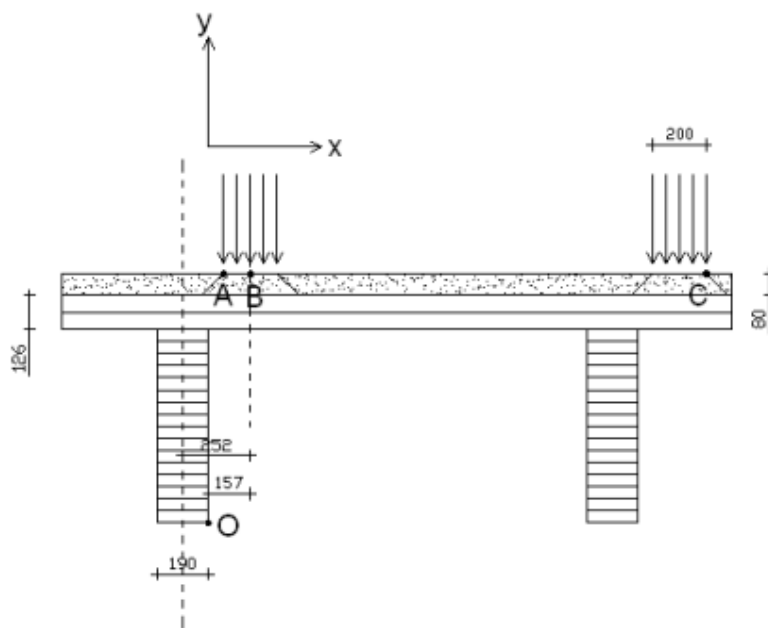
Case 3 (E.C.5)

Point B in X=157

Left Wheel

Right Wheel
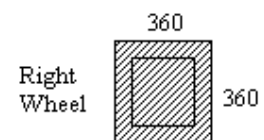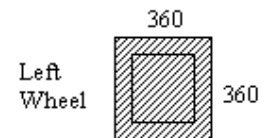
$$P_{1wheelaxis} = 80kN$$

$$P_{1wheel} = \frac{P}{2} = 40kN$$

$$A = 360 * 360 = 129600\,mm^2$$

$$\sigma_{left} = \frac{40000\,N}{0.1296\,m^2} = 308642\,Pa = 0.309\,MPa = \sigma_{right}$$
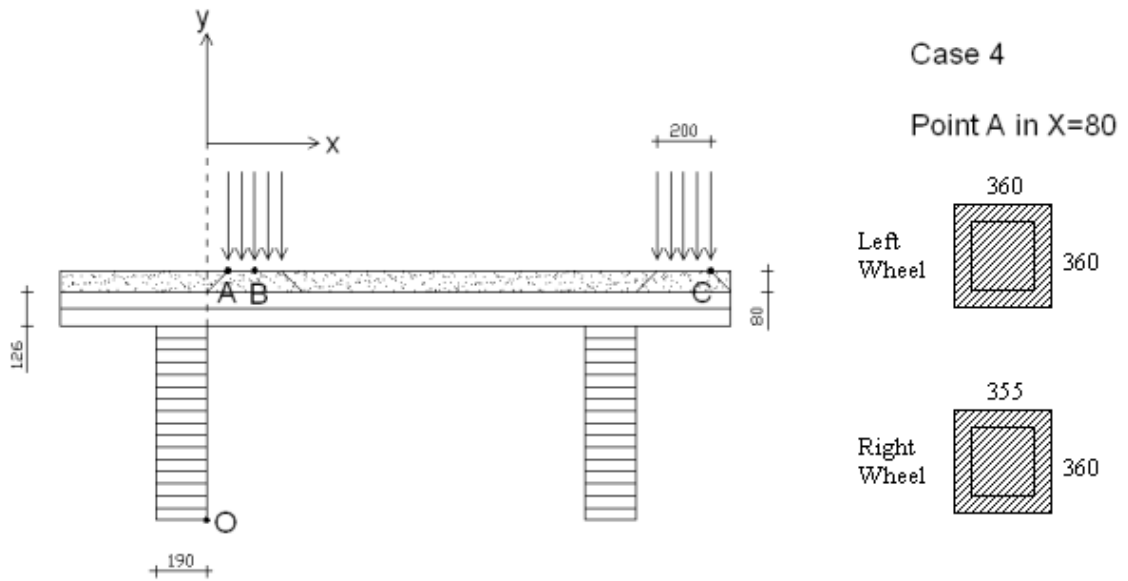
$P_{1wheelaxis} = 80kN$

$P_{1wheel} = \dfrac{P}{2} = 40kN$

$A = 360*360 = 129600\,mm^2$

$A = 360*355 = 127800\,mm^2$

p-left = 40kN/0,1296m² = 309kN/m²

p-right = 40kN/0,1278m² = 313kN/m²

In all the four cases the highest shear stresses τ12 are located in the lower surface of the deck where the KertoQ meets the edges of the beams. See the picture below. The region L is close to the internal wheel and the region R is close to the external wheel.
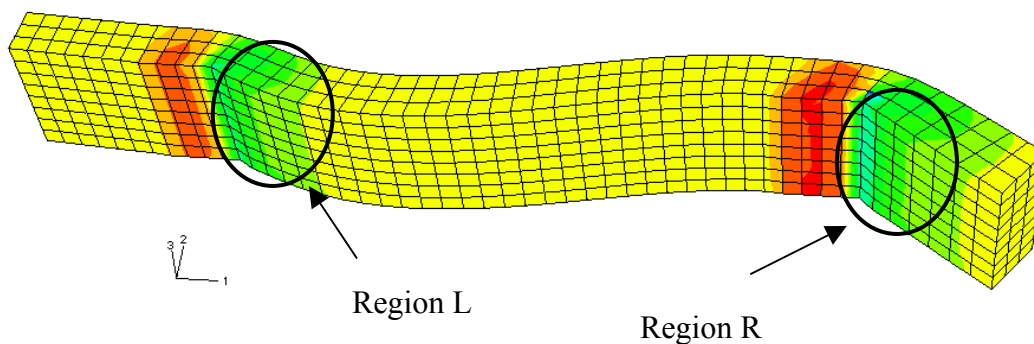
Figure B2   Regions where the stresses τ12 are higher.

The maximum shear stresses τ_{12} that have been found in those four cases are reported in Table A1.

Table A1   Maximum values of the shear stresses τ_{12} for the four Load-cases 1,2,3,4, both in Region L and in Region R.

	Region L Stress τ_{12} [MPa]	Region R Stress τ_{12} [MPa]
Case 1	1.21	1.69
Case 2	1.87	2.79
Case 3	1.55	2.25
Case 4	1.43	1.97

The values related to the region R are always higher than those related to the region L. The critical area of the deck is in the external part, which can be represented by a cantilever model. In the internal part of the deck the stresses τ_{12} are lower because the wheel load can be transferred to the support both in the x-positive direction and in the x-negative direction. In the model of the whole structure of the bridge the load can be transferred also to the transversal bracing units in the longitudinal direction. The worst case considered is case 2. It is now possible to know where to place the vehicle's load and which region of the deck is to be studied if one is interested in the maximum shear stresses τ_{12}. These results are also valid if the KertoS is taken into account, and in the model of the whole structure of the bridge.

APPENDIX C: design values for the strength of materials

The design strength in the ULS of common types of materials used in building constructions like concrete and steel is calculated starting from the characteristic strength in the simple way:

$$f_d = \frac{f_k}{\gamma_m}$$

where γ_m is the partial coefficient for material properties that depends on the specific material considered.

For timber and wood-based materials it has been introduced a new coefficient in the previous formula, that becomes:

$$f_d = k_{mod} \cdot \frac{f_k}{\gamma_m}$$
where γ_m is equal to 1.3 for timber (see E.C.5, part 1-1, point 2.3.3.2)

As it was mentioned also in Chapter 1 and 2, wood is a quite complex material from the mechanical point of view. To take in account the real mechanical behaviour of timber, when it is loaded by external actions, the introduction of the "Modification Factor" k_{mod} parameter it has been necessary.

This parameter depends on "Service class" and "Duration of loads"

The mechanical properties of wood are strongly influenced by its level of moisture content, which is directly related to environmental conditions of the structure. Generally it is reasonable to say that the higher it is the average surrounding humidity, the more the mechanical strength will be reduced.

Definition of Service Class by Eurocode5 (E.C. 5, part 1-1, point 3.1.5)

The Eurocode provides 3 different service classes that must be defined for every structure analysed:

3.1.5 Service classes

P(1) Structures shall be assigned to one of the service classes given below[17]:

P(2) Service class 1: is characterized by a moisture content in the materials corresponding to a temperature of 20 ⬚C and the relative humidity of the surrounding air only exceeding 65 % for a few weeks per year[18].

P(3) Service class 2: is characterized by a moisture content in the materials corresponding to a temperature of 20 ⬚C and the relative humidity of the surrounding air only exceeding 85 % for a few weeks per year[19].

P(4) Service class 3: climatic conditions leading to higher moisture contents than in service class 2[20].

[17] The service class system is mainly aimed at assigning strength values and calculating deformations under defined environmental conditions.
[18] In service class 1 the average moisture content in most softwoods will not exceed 12 %.
[19] In service class 2 the average moisture content in most softwoods will not exceed 20 %.
[20] Only in exceptional cases would covered structures be considered to belong to service class 3.

In addition, the duration of loads acting on the structure is important in the definition of the resistance of timber members. Any wood element can reach the failure for to large deformation of its fibres, that are produced not only by the instantaneous elastic deformation, but also by a long-term deformation due to creep. In other words, a constant long-term load acting on a wood element will continue to increase its deformation. Eurocode 5 classifies the loads in five Load-Duration-Classes (see E.C.5, part 1-1, point3.1.5):

Table 3.1.6 — Load-duration classes

Load-duration class	Order of accumulated duration of characteristic load	Examples of loading
Permanent	more than 10 years	self weight
Long-term	6 months — 10 years	storage
Medium-term	1 week — 6 months	imposed load
Short-term	less than one week	snow[a] and wind
Instantaneous		accidental load
[a] In areas which have a heavy snow load for a prolonged period of time, part of the load should be regarded as medium-term		

At point 3.1.1 of the Eurocode 5, part 2, it is specified that Service Class 3 should be assigned to all those bridges that are not directly protected by the rain. The bridge analysed in this thesis is not protected by any kind of roof, but the designers of Moelven Company has ensured that the products and the techniques used to protect the timber parts are good enough to assume the Service Class 2 for the bridge.

When it comes to the duration of loads, four loads presented here will act on the structure:

- Self-weight of structural elements → Permanent Load

- Self-weight of bared elements → Permanent Load

- Live load → Short-term Load

- Service vehicle load → Short-term Load

Using this information it is possible to define the value of the modification factor k_{mod} to assume in the calculation of the design strengths. This can be done with Table 3.1.7 at point 3.1.7 of the Eurocode 5, part 1-1:

Table 3.1.7 — Values of k_{mod}

Material/load-duration class	Service class		
	1	2	3
Solid and glued laminated timber Plywood.			
Permanent	0,60	0,60	0,50
Long-term	0,70	0,70	0,55
Medium-term	0,80	0,80	0,65
Short-term	0,90	0,90	0,70
Instantaneous	1,10	1,10	0,90

For the beams in glued laminated timber and the elements of the deck in plywood, the value assumed for the modification factors is 0.9, following the instruction explained in Eurocode 5, part 1-1, point 3.1.7 (2): "If a load combination consists of actions belonging to different load-duration classes a value of k_{mod} should be chosen which corresponds to the action with the shortest duration [...]".

Note that glued laminated timber and plywood are put together in the same group in the table above. This aspect will be relevant when the comparison with the Swedish code will be done later in this section. First of all, it's good to present the design values of the materials used in the bridge. The characteristic values have been certified by UNI-EN 1194 (1993) concerning the glued laminate beams, and VTT certificate NO 184/03, revised 24 October 2005 concerning Kerto-Q® and Kerto-S® materials. These values are shown in the Figure below a):

a)

Property	Symbol	Characteristic value, N/mm^2 or kg/m^3		
		Kerto-S Thickness 21 - 90 mm	Kerto-Q Thickness 21 - 24 mm	Kerto-Q Thickness 27 - 69 mm
Fifth percentile values				
Bending strength:				
Edgewise (depth 300 mm)	$f_{m,0,edge,k}$	44.0	28.0	32.0
Size effect parameter	s	0.12	0.12	0.12
Flatwise (thickness 21 to 90 mm)	$f_{m,0,flat,k}$	50.0	32.0	36.0
Tensile strength:				
Parallel to grain (length 3000 mm)	$f_{t,0,k}$	35.0	19.0	26.0
Perpendicular to grain, edgewise	$f_{t,90,edge,k}$	0.8	6.0	6.0
Perpendicular to grain, flatwise	$f_{t,90,flat,k}$	-	-	-
Compressive strength:				
Parallel to grain	$f_{c,0,k}$	35.0	19.0	26.0
Perpendicular to grain, edgewise	$f_{c,90,edge,k}$	6.0	9.0	9.0
Perpendicular to grain, flatwise	$f_{c,90,flat,k}$	1.8	1.8	1.8
Shear strength				
Edgewise	$f_{v,0,edge,k}$	4.1	4.5	4.5
Flatwise	$f_{v,0,flat,k}$	2.3	1.3	1.3
Modulus of elasticity:				
Parallel to grain	$E_{0,k}$	11600	8300	8800
Perpendicular to grain, edgewise	$E_{90,edge,k}$	350	2000	2000
Perpendicular to grain, flatwise	$E_{90,edge,k}$	100	100	100
Perpendicular to grain	$E_{90,k}$	-	-	-
Shear modulus:				
Edgewise	$G_{0,k}$	400	400	400
Flatwise	$G_{0,k}$	400	-	-
Density	ρ_k	480	480	480
Mean values				
Modulus of elasticity:				
Parallel to grain	$E_{0,mean}$	13800	10000	10500
Perpendicular to grain, edgewise	$E_{90,edge,mean}$	430	2400	2400
Perpendicular to grain, flatwise	$E_{90,edge,mean}$	130	130	130
Shear modulus:				
Edgewise	$G_{0,mean}$	600	600	600
Flatwise	$G_{0,mean}$	600	-	-
Density	ρ_{mean}	510	510	510

	GL24	GL28	GL32	GL36	correlazioni	
$f_{m,k}$	24	28	32	36		
$f_{t,0,k}$	18	21	24	27	$f_{t,0,k} = 0.75 f_{m,k}$	
$f_{t,90,k}$	0.35	0.45	0.45	0.45		
$f_{c,0,k}$	24	27	29	31	$f_{c,0,k} = 3 f_{m,k}^{0.65}$	
$f_{c,90,k}$	5.5	6	6	6.3		
$f_{v,k}$	2.8	3	3.5	3.5	$f_{v,k} = 0.7 f_{m,k}^{0.45}$	
$E_{0,mean}$	11000	12000	13500	14500	$E_{0,mean} = 4.8\, \rho_k^{1.3}$	
$E_{0,05}$	8800	9600	10800	11600	$E_{0,05} = .8\, E_{0,mean}$	
$E_{90,mean}$	370	400	450	480	$E_{90,mean} = E_{0,mean}/30$	
G_{mean}	690	750	845	900	$G_{mean} = E_{0,mean}/16$	
ρ_k	380	410	440	480		

b)

Figures above: Characteristic strengths of Kerto-Q® and Kerto-S® by VTT certificate NO 184/03, revised 24 October 2005 (a), Characteristic strengths of glued laminated timber certificated by UNI-EN 1194 (1993) (b).

In the structure studied, Kerto-Q® and Kerto-S® are only used in the modality "flatwise", never in the "Edgewise".

Comparison with the Swedish Codes

For general design values of material properties, the following formula is used:

$$f_d = \frac{k \cdot f_k}{\eta \cdot \gamma_m \cdot \gamma_n} \qquad (5.3)$$ BKR 2003, point 2:322

where η can be assumed equal to 1.0.

For timber structures in the design in the ultimate limit state, the formula becomes:

$$f_d = \frac{k_r \cdot f_k}{\gamma_m \cdot \gamma_n}$$ BKR 2003, point 5:3121

k_r is the equivalent of the modification factor k_{mod} of the Eurocode5,

γ_m is a partial factor which takes account of the uncertainty in determining resistance: for timber is taken equal to 1.15.

γ_n is a partial factor which takes account of the safety class in ultimate limit state. The safety class are define in this way at the point 2:115 of the Swedish codes BRO 2003:

With regard to the extent of injury to persons which the failure of an element of structure may cause, this shall be assigned to one of the following safety classes:
– Safety Class 1 (low), little risk of serious injury to persons
– Safety Class 2 (normal), some risk of serious injury to persons
– Safety Class 3 (high), great risk of serious injury to persons.

The bridge belongs to the safety class 3; in this case the value of γ_n is 1.20.

k_r depends on the service class and the duration of loads, in the same way as the factor k_{mod} in the Eurocode. The service classes are defined in the Swedish codes in a similar way than those in the Eurocode; in the BRO 2003 - point 5:21 four service classes are defined:

5:21 Service classes

In designing timber structures, consideration shall be given to the effect of moisture on resistance and stiffness. This shall be done by assigning the elements of structure to one of the following service classes and using the appropriate factors in determining the design values.

Service Class 0 is characterised by an environment in which relative humidity exceeds 65% for only a few weeks each year and, on average, does not exceed 40%.

Service Class 1 is characterised by an environment in which relative humidity exceeds 65% for only a few weeks each year and at no time reaches 80%.

Service Class 2 is characterised by an environment in which relative humidity exceeds 80% for only a few weeks each year.

Service Class 3 is characterised by an environment which produces in the materials a higher moisture content than that corresponding to Service class 2.

The load-duration classes defined in BRO 2003 - point 5:21 are almost the same as those in the Eurocode:

Table a. Classification of actions in view of their duration

Load duration Class	Cumulative duration of action	Example of action[1]
Permanent load		
Load type P	more than10 years	Self weight of permanent parts of the building.
Variable load		
Load type A	between 6 months and 10 years	The fixed portion of the imposed. load.
		Snow load of frequent value.
Load type B	between 1 week and 6 months	The free portion of the imposed load.
		Wind action of frequent value. Snow load of characteristic value.
		Actions on concrete formwork and similar temporary structures.
Load type C	less than 1 week	Wind action of characteristic value.
		Single concentrated load on a roof.

[1] The above examples are intended only as general recommendations.

Using these classifications is finally possible to calculate the value of the k_r; Differently form the Eurocode, the Swedish codes adopts two separated tables a) and b) belowe. Table a. for glued laminated timber ("L40" is the reference name for GL 32c), and Table b. for Plywood ("P40" is the reference name for Kerto-Q® and Kerto-S®).

Table a. Modification factor κ_r for calculation of the resistance of structural timber and glued laminated timber in Service Classes 0, 1 and 2 [1].

Strength classes	Action of shortest duration in a combination of actions [2]		
	P or A	B	C
f_m, f_t, f_c, E_R, G_R			
L40, K35	0.60	0.75	0.85
L30, K30, LK30	0.65	0.80	0.90
K24, LK20	0.70	0.85	1.00
K18, K12	0.75	0.90	1.00
$f_{t\,90}$			
all strength classes	0.40	0.60	0.80
$f_{c\,90}, f_v$			
all strength classes	0.60	0.75	0.85

(BFS 1998:39)

[1] For Service Class 3, the values are to be multiplied by a further factor of 0.85.

[2] The values refer to that action in a combination of actions which is of the shortest duration. P, A, B and C denote load duration classes in accordance with Subsection 5:22.

Table b. Modification factor κ_r for calculation of the resistance of K plywood in Service Class 1 [1].

Plywood strength class	Action of shortest duration in a combination of actions [2]		
	P or A	B	C
f_m, f_t, f_c			
P40	0.60	0.75	0.85
P30	0.65	0.80	0.90
P20	0.70	0.85	1.00
$f_{t\,90}, f_{c\,90}, f_p, f_v$			
all strength classes	0.60	0.75	0.85
E_R, G_R			
P40, P30	0.60	0.75	0.85
P20	0.70	0.85	1.00

[1] In Service Class 0 the values may be raised by 10% in relation to the values in Service Class 1. In Service Class 2 the values are to be multiplied by a factor of 0.7 and in Service Class 3 by a factor of 0.6. For tension parallel to the grain, the value of this factor may be put at 0.9 and 0.75 respectively.

[2] The values refer to that action in a combination of actions which is of the shortest duration. P, A, B and C denote load duration classes in accordance with Subsection 5:22.

k_r for Glulam should be assumed equal to 0.85 (it's already valid for service class 2). For plywood the value 0.85 should be further reduced multiplying it by a factor of 0.7 to take in account the service class 2: finally it results equal to:
$$k_r = 0.85 \times 0.7 = 0.595$$

APPENDIX D: loads

The analysis on the loads acting on the structure follows the directives of EC 1-3 (Eurocode1, part 3), in particular the Section 5:

Eurocode 1-3, point 5.3.2.1 **Live load**

The live load is a uniformly distributed load acting on the bridge. The characteristic load given by Eurocode is: $q_{vk} = 5 \dfrac{kN}{m^2}$

For spans longer than 10 meters it is possible to reduce this value by the use of the formula:

$$2.5 \frac{kN}{m^2} \leq q_{vk} = 2.0 + \frac{120}{L_{sj} + 30} \leq 5 \frac{kN}{m^2} \qquad (5.3)$$

where L_{sj} is the span in [m]. In our case the span is 15m, that means a live load of

$$q_{vk} = 4.67 \frac{kN}{m^2}$$

The Swedish codes instead assumes a constant value of $4 \dfrac{kN}{m^2}$ for the live load.

Eurocode 1-3, point 5.3.2.2 **Concentrated load**

For local verifications it is important to check the effects of concentrated loads especially over the deck of the bridge. Eurocode specifies a concentrated load Q_{vk} of 10 kN acting on a square surface of 0.1m side, to be place in the positions that get the most unfavourable effects. This concentrated load is not to be included if a service vehicle load is already considered for the bridge. In this project the service vehicle is taken into account as it is described in the following paragraph.

Eurocode 1-3, point 5.3.2.3 **Service vehicle load**

The pedestrian bridge has to be design also in respect to the loads caused by a service vehicle used for several services, like maintenance, assistance for people (it could be an ambulance for example), or other kind of functions (for example a vehicle used to clean the roads from the snow). The characteristics of this vehicle (geometry, weight) should be defined by the client.

Both the EC5 and the Swedish Codes suggest the use of a standard typology for this vehicle in case that there are not detailed information from the customer. Concerning this project, the Moelven Company could represent the client. Basically, the service vehicle load adopted is the one suggested by the Swedish codes BRO 2004, point 21.2227; a full description can be found in the Appendix A. This vehicle load is to be considered as a normal variable load and not as an accidental load; hence, the

coefficient γ of this load in the load combination shall be equal to $\gamma = 1.5$ and not $\gamma = 1.0$.

$P_{front} = 40kN$ and $P_{rear} = 80kN$ are the characteristic values respectively of the front wheel axle and the rear wheel axle.

Eurocode 1, part 2-3   **Snow Load**

The snow produces a distributed vertical load q_s that acts on the surface of the deck. The formula used to calculate it is:

$$q_s = \mu_i \cdot C_e \cdot C_t \cdot s_k$$

where the value of C_e and C_t, respectively expose and thermal coefficient, can be generally chosen equal to 1.0.

Concerning this bridge, the significant combination of loads is the one with a uniformly-distributed load, so the value of the shape coefficient is taken equal to 0.8.
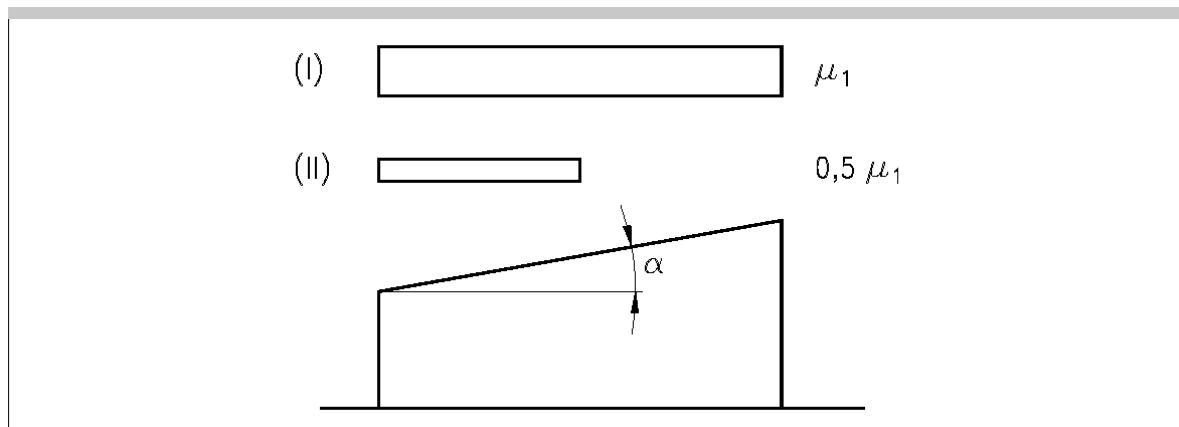

Roof Inclination	$0° \leq \alpha \leq 30°$	$30° < \alpha < 60°$	$\alpha \geq 60°$
Shape coefficien μ_1	0,8	0,8 (60 - α)/30	0,0

This bridge can be considered as a mono-pitched roof with an angle $\alpha = 0$ since the deck is horizontal. This consideration is still valid when the cambering of the bridge is considered, so that: $\mu = 0.8$.

The characteristic value of the snow load at the ground level s_k depends on the geographic position of the bridge. Sweden is divided in 6 regions respect to different levels of risk of snow: 1.0; 1.5; 2.0; 2.5; 3.0; 4.0. (see figure belowe).

As a reference it can be assumed the region 3.0, which has a quite high risk of large snowfalls; the value of s_k related to this region is $3.0 \dfrac{kN}{m^2}$.
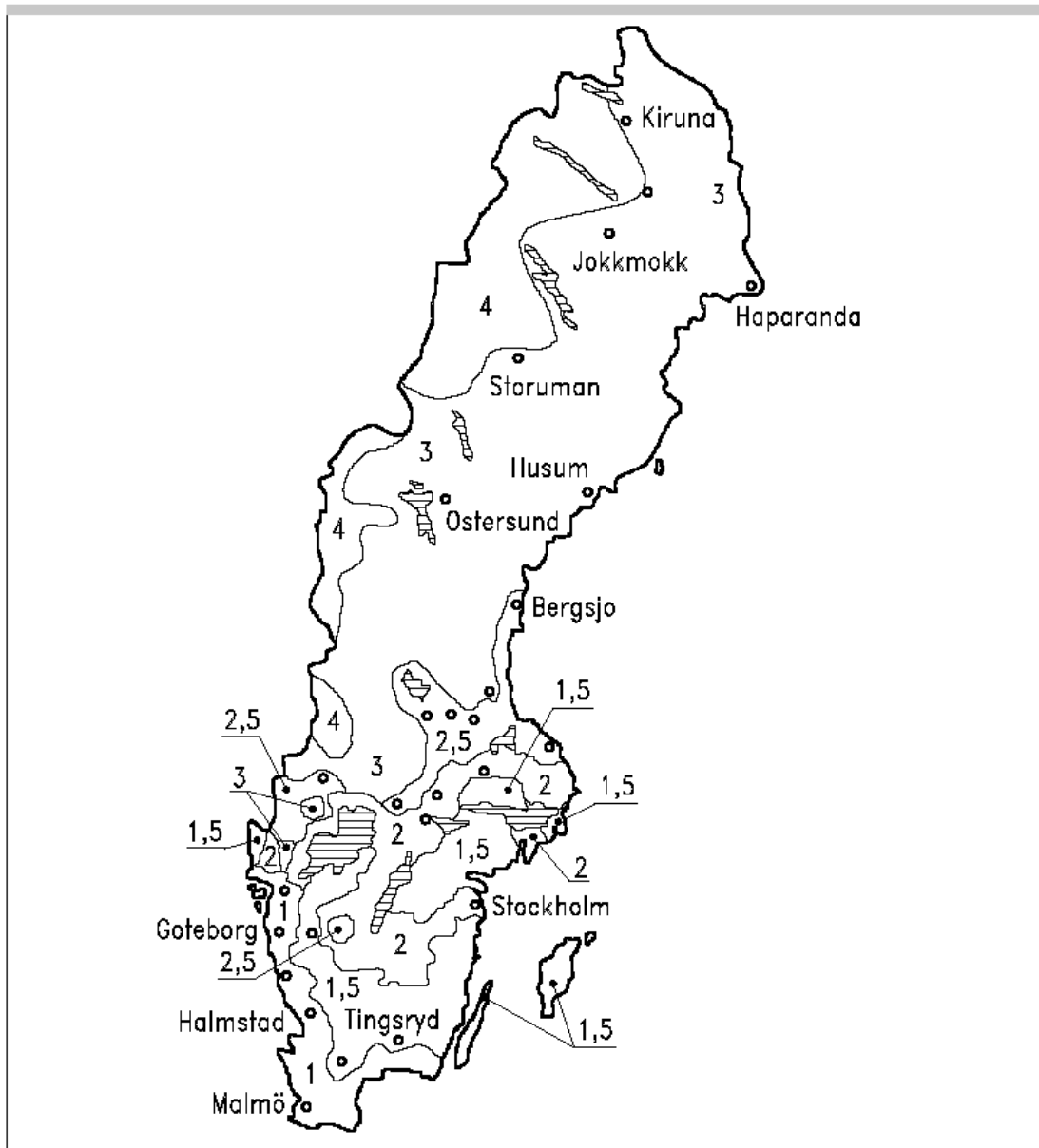
Finally it is possible to calculate the value for the snow load:

$$q_{sd} = 0.8 * 3.0 \frac{kN}{m^2} = 2.4 \frac{kN}{m^2}$$

It could be interesting to compare the characteristic value of snow load at the ground level just assumed for Sweden with the Italian one. In Italy the value of s_k depends also on the altitude of the geographic position considered. For the north part of Italy,

in the regions close to the Alps (National zone 1, see Figure 5.8), the value of $3.0\frac{kN}{m^2}$ is reached at an altitude of 670m above the sea level.

Figure above Different zones of Italy with different characteristic values of the snow load at the ground level s_k

Eurocode 1-3, point 5.4   **Horizontal loads**

The worst case of the following two situations is to be considered when the horizontal loads are studied:

- A magnitude equivalent to the 10% of the total vertical uniformly-distributed load;

- A magnitude equivalent to the 60% of the total vertical load caused by the service vehicle;

These horizontal loads act along the longitudinal axis of the deck and they are applied on the superior surface of the deck. Furthermore, they must be combined with the vertical loads that produce the horizontal loads themselves. Nevertheless, more investigation should be done in this context, especially to design the supports of the bridge.

The wind is an action that produces horizontal load in the transversal direction. The same considerations made about the loads discussed above are still valid, so that it is also not taken into account. The deck made of KertoQ® and KertoS® materials has enough stiffness to stabilize the structure in the transversal direction and avoid the buckling of the beams, Crocetti (2005).

Eurocode 1-3, point 5.6.1, point 5.6.2 **Accidental load**

There are two different types of accidental load to take into account related to pedestrian bridges: 1) Accidental car crash due to the presence of road under the bridge that could produce impact forces against some bearing elements of the structure. 2) Accidental presence of a track on the pedestrian bridge.

This first situation is not taken into account in this thesis work; the second one is not to be considered since the bridge allows the presence of a service vehicle load.

Eurocode 1-3, point 5.7 **Dynamic effects caused by the pedestrians users**

Vibrations and dynamic effects caused by the steps of users of the bridge are not considered in this thesis work. Also the dynamic effects due to the service vehicle are not studied. Nevertheless, a verification of the whole bridge concerning vibrations in the serviceability limit state has been performed following the Swedish codes.

Eurocode 1-3, point 5.8 **Actions on the handrails**

The load of 1 kN/m defined in Eurocode 1-3, point 4.8.1(1) shall be considered to design the railings of pedestrian bridges. Still these loads are not taken into account in this thesis work.

Self weight

The self-weight load q_g comprehends the weight of all the elements of the structure that have a bearing role like the beams, the deck and the transversal bracing units. The layer of asphalt above the timber deck, the handrails, and the waterproof coverings are elements supported by the bearing structure, and are added to the self-weight in the combination of loads. It is good to collect them in a separate group of permanent loads q_p. The magnitudes of these loads based on the densities of materials (Eurocode 1, part 2-1, section 4) included in the structure are:

$$q_g = 1.66 \frac{kN}{m^2} \qquad\qquad q_p = 2.34 \frac{kN}{m^2}$$

APPENDIX E: calculations for load combination 2 and 3

The load combinations 2, 3 and 4 are non-symmetric, both in the longitudinal and transversal direction.

To solve the structure by hand calculations it has been necessary to model it as two independent longitudinal beams loaded in a different manner.

In the same way, in order to find how the load is divided transversally, a model was used of a simply-supported beam made with a stripe of the deck (e.g. of Kerto-Q®), where the supports are represented by the glulam beams. The results obtained in this way will be on the safe side, so that they will be used to divide the loads on the two beams.
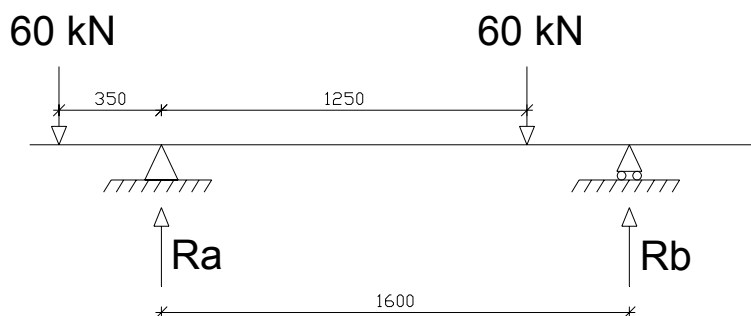
Referring to the picture below, the aim is to study the amount of load that will be transferred to each beam.
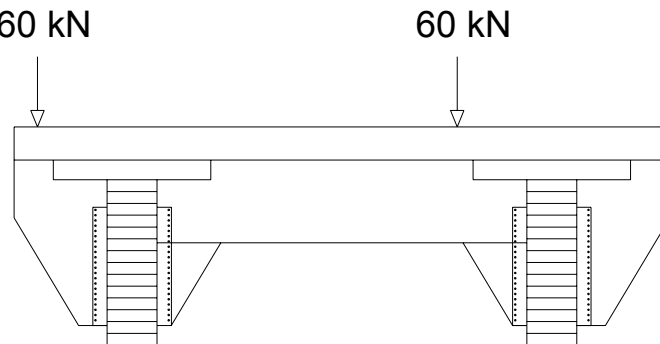
It follows the explanation of how these particular values (0.57 and 1.43) have been found.

By help of the Finite Element software SAP2000®, two different model of this problem have been studied: a simple supported beam and a fully-fixed beam.
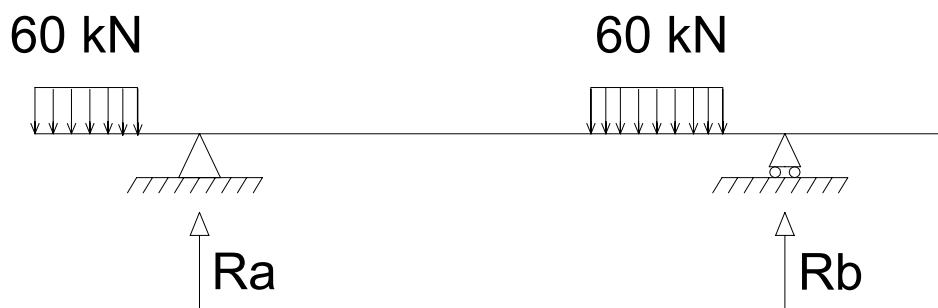
Simple supported beam:

The reactions Ra and Rb will represent the amount of load that is differently transferred to the two beams.

P = 60 kN

Ra * 1600mm= P *(1250mm+350mm) + P * 350 mm

$$Ra = \frac{2300mm}{1600mm} * P = 1,43 \qquad\qquad Rb = 0,57\ P$$

Using a model with short distributed loads that respects load treads (see also Appendix B), the following model can be studied:
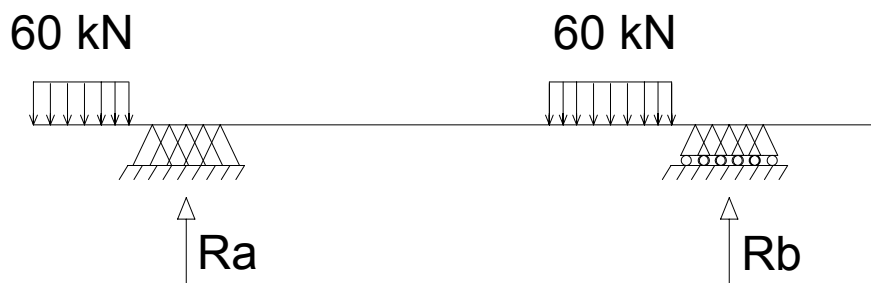

Using the Program SAP2000® the result is very similar to the one just found before with hand calculations:

Ra = 1.42 P   Rb = 0.58 P

Fully-fixed beam:

In another way, it is possible to model the connection deck-beams as a group of pins with the same length as the width of the beams. This kind of support is a fully-fix joint.


The result obtained by using the program SAP2000® is:

Ra = 1.1 P   Rb = 0.9 P

This second model with fully-fixed supports is less realistic than the previous one, because the upper sides of the glulam beams will be influenced by a rotation large enough to assume the model of the simple supported beam.

This fact is moreover proved by the results of another model of a stripe of the bridge performed with the Finite Element Program ABAQUS®. The model is similar to the one presented in Appendix A; it's a stripe of the bridge made of solid elements, with the lower side of the beams fixed to the ground. See the figure below.
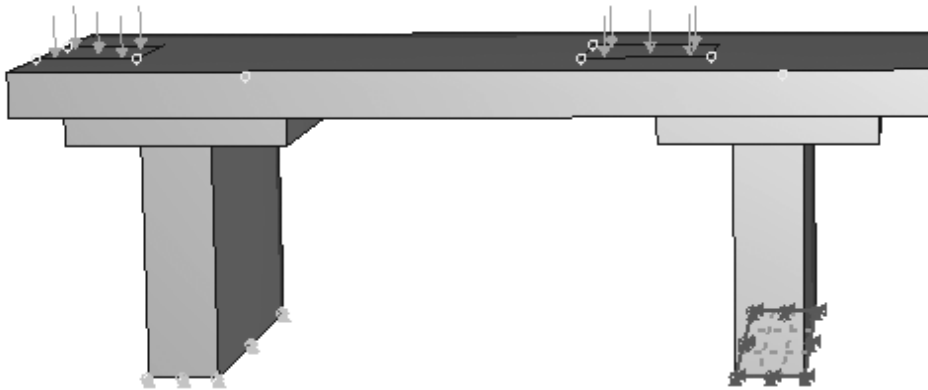
When this stripe is loaded it assumes the deformed shape presented as follow:
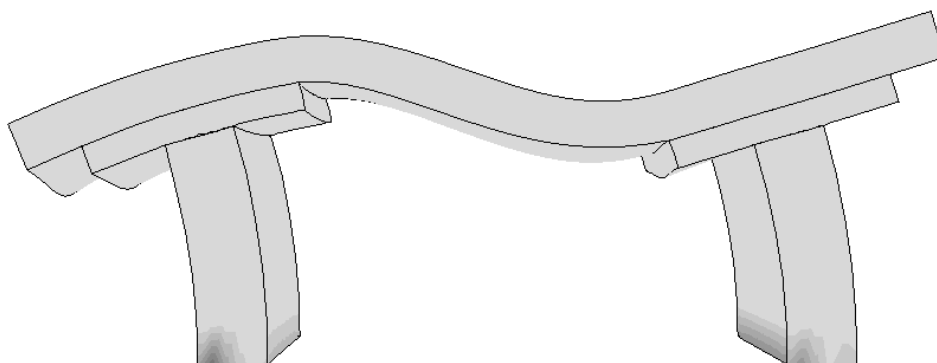
It's very clear how the stripe of deck can rotate over the two beams.
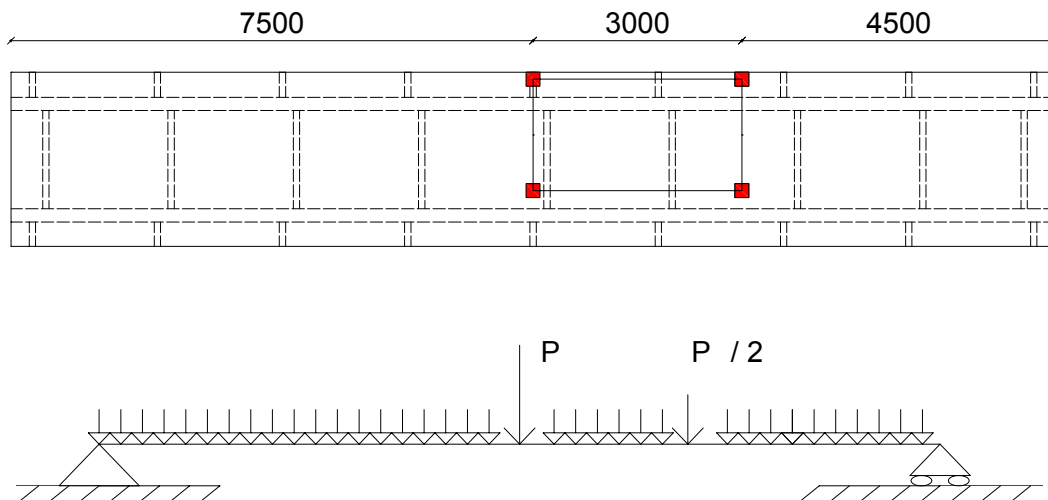
The reactions in the two supports are very close to the values found in the model of simple supported beam:

Ra = 1.42 P   Rb = 0.58 P

It was chosen to increase the most loaded beam by a factor equal to 1.43 compared to the situation with the vehicle in the center of the road.

Load combination 2 : Self-weight + Permanent load + Service vehicle load (placed in the middle of the span)

$$P_{max} = \frac{P_{rear} \cdot 1.5}{2} = 60kN = P \quad P_{min} = \frac{P_{front} \cdot 1.5}{2} = 30kN = \frac{P}{2}$$

Using the equilibrium equation for this statically-determinate structure is possible to obtain the values of M and V:

The reaction force on the right support R_B due to P/2 is equal to:

P/2 * 10.5 m = R_B * 15 m

R_B = 0.7 * P/2

The reaction force on the right supports due to P is equal to: P*0.5

The maximum shear force V_B at the right support due to the service vehicle load results:

V_B = P * 0.5 + P/2 * 0.7 = P/2 *1.7 = 51 kN

Furthermore, it should be taken into account the shear due to distributed loads:

$$V_B = \frac{ql}{2} = 50.63 \text{ kN} \qquad \text{(the value of q is 6.75 kN/m, see paragraph 5.1.4)}$$

The total shear force at the right support will be the sum of these two, remembering to use the coefficient **1.43** found before:

V = 51kN * **1.43** + 50.63 kN = 123.56 kN

The maximum moment in the middle span due to the vehicle load results:

$$M = \frac{P}{2} * 7.5m + \frac{P}{2} * 0.7 * 7.5m - \frac{P}{2} * 3m = 292.5 \text{ kNm}$$

The moment due to distributed loads must be added to the previous one:

$$M = \frac{ql^2}{8} = 189.84 \text{kNm}$$

The total moment in the middle span is calculated in a similar way as the total shear force:

M = 292.5 kNm ***1.43** + 189.84 kNm = 608.12 kNm

Load combination 3: Self-weight + Permanent load + Service vehicle load (placed over the support)

Following the the Eurocode 5, part 1-1, point 5.1.7.1:the heavy wheel axle is then located at a distance of 2h from the support. The depth of the effective section is equal to 831mm. $2 \cdot h = 1662mm$
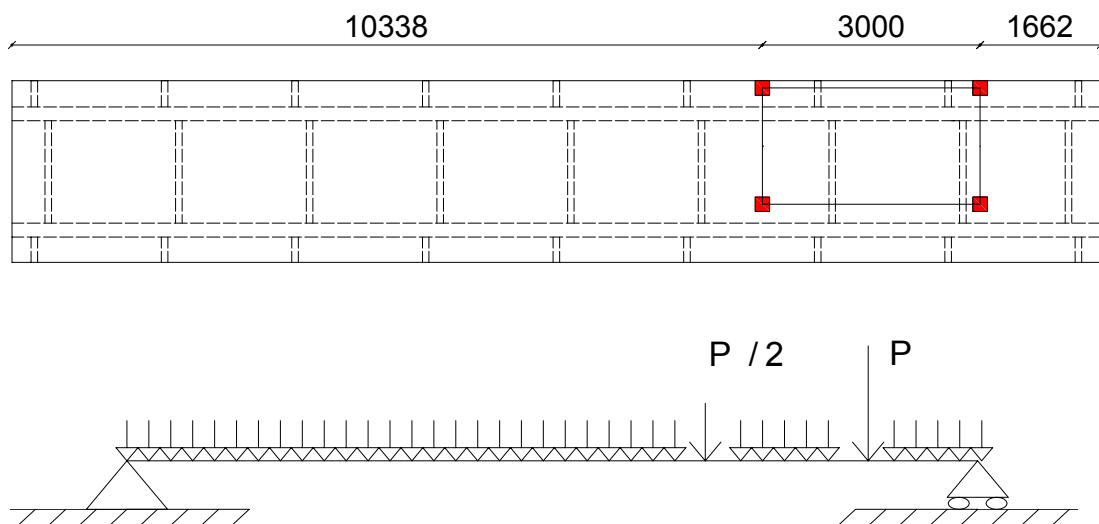
As before, it ca be used the equilibrium equation to get the values of M and V:

The reaction force on the right support R_B due to P is equal to:

P * (15 m – 1.66 m) = R_B * 15m R_B = 0.89 * P

The reaction force on the right support R_B due to P/2 is equal to:

P/2 * (15 m – 4.66 m) = R_B * 15m R_B = 0.69 * P/2

The maximum rakine force V_B at the right support due to the service vehicle load results:

$V_B = P * 0.89 + P/2 * 0.69 = P *1.235 = 74.4$ kN

Furthermore, it should be taken into account the shear due to distributed loads:
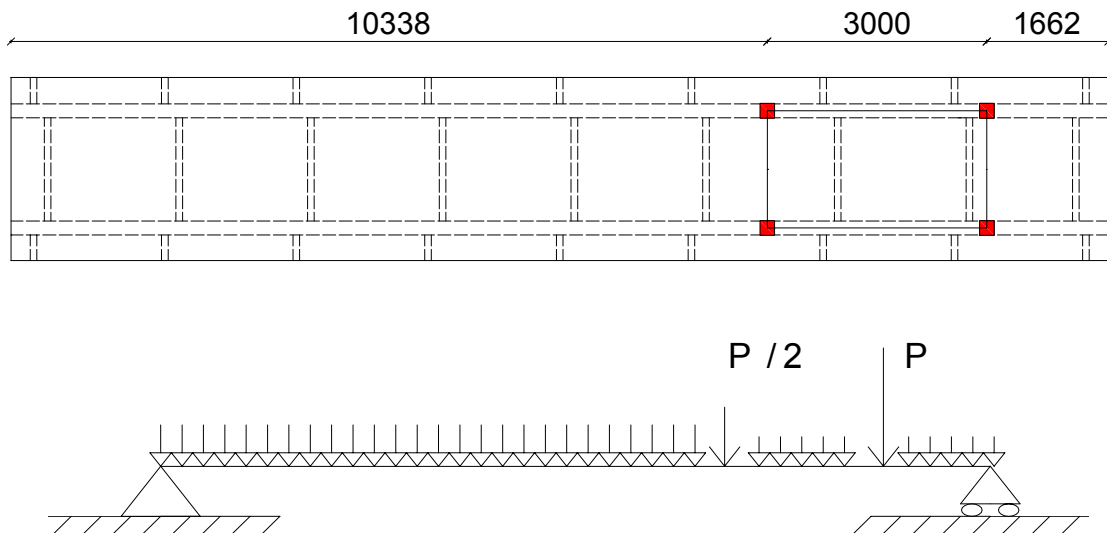
$$V_B = \frac{ql}{2} = 50.63 \text{ kN}$$

The total shear force at the right support will be the sum of these two, remembering to use the coefficient **1.43** found before:

V = 74.4 kN * **1.43** + 50.63 kN = 157 kN

The total moment in the middle span is calculated in a similar way as before:

M = 120 kNm * **1.43** + 189.84 kNm = 361 kNm

Load combination 4: Self-weight + Permanent load + Snow load + Service vehicle load

The maximum shear force V_B at the right support due to the service vehicle load results:

$V_B = P * 0.89 + P/2 * 0.69 = P *1.235 = 74.4$ kN

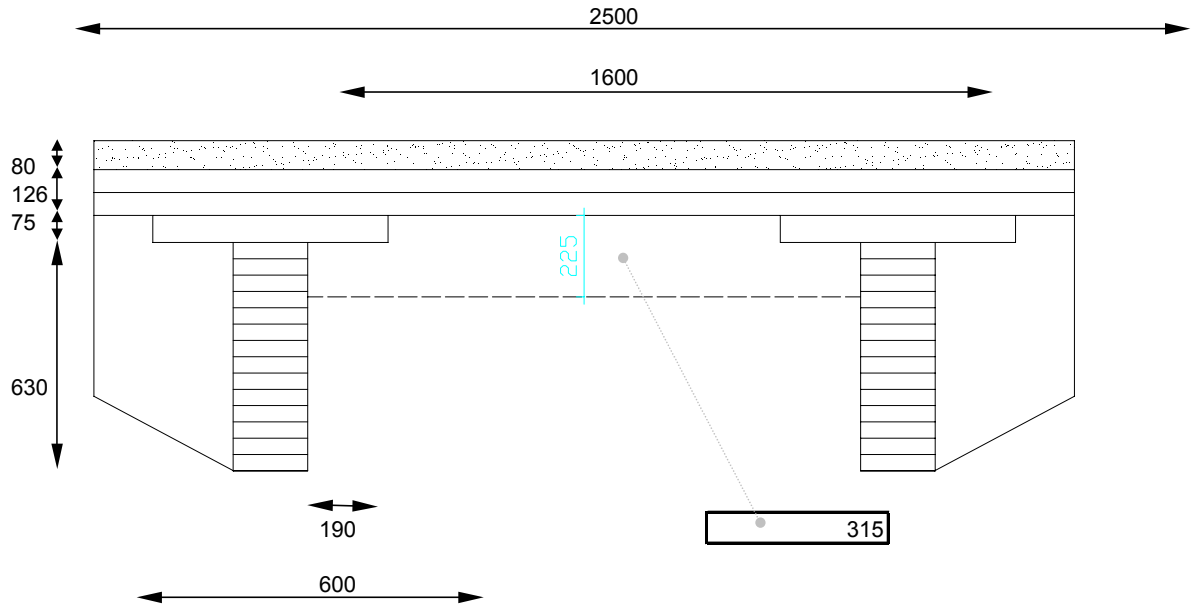The shear due to distributed loads:

$$V_B = \frac{ql}{2} = 74 \text{ kN}$$ (taking into account the snow, the value of q results 9.9 kN/m)

The total shear force at the right support is:

$V_B = 74.4$ kN * **1.00** + 74 kN = 148.25 kN

APPENDIX F: Inertia of the section

Lengh of beams =	L	15000	mm		H asphalt =	tasp	80	mm
H beams =	Hb	**630**	mm		Joists horiz dist =	i,j	3000	mm
B beams =	Bb	190	mm		H mid joists =	Hj,c	315	mm
Beams horiz dist =	i	1600	mm		H edge joists =	Hj,f	630	mm
Deck width =	td	2500	mm		B joists =	Bj	90	mm
H Kerto-Q =	tKQ	126	mm		Area Deck =	Ad	37,5	m^2
H Kerto-S =	tKS	75	mm		H tot =	Htot	831	mm
L Kerto-S =	LKS	600	mm					

Effective cross section

				Beff	750	mm
E$_{meanKertoQ}$=	10 500	MPa				
E$_{meanKertoS}$=	13 800	MPa				
E$_{meanEC5}$=	13 500	MPa				

Homogenisetion factors for resistence verification   <u>Kerto Q</u> n_1 Vtt=   1,00
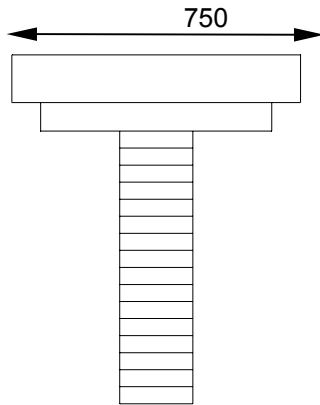
Kerto Q	Kerto Q	
Kerto S	<u>Kerto S</u>	n_2Vtt= 1,31
	Kerto Q	
Glulam	<u>Glulam</u>	n_3Vtt-EC5 = 1,29
	Kerto Q	

Effective cross section

A			**A Homog**		**d**		
A beam =	119700	mm^2	A beam =	153900 mm^2	Gb-G =	-206,98	mm
A KertoS=	45000	mm^2	A KertoS=	59142 mm^2	GKS-G=	145,52	mm
A KertoQ=	94500	mm^2	A KertoQ=	94500 mm^2	GKQ-G=	246,02	mm
A section=	259200	mm^2	A section=	307542 mm^2	Htot-G=	309,02	mm
I			**I Homog**		Inter Q/S G =	183,01	mm
I beam =	3,96E+09	mm^4	I beam =	5,09E+09 mm^4	Inter Glu/S- G =	108,01	mm
I KertoS=	2,11E+07	mm^4	I KertoS=	2,77E+07 mm^4			
I KertoQ=	1,25E+08	mm^4	I KertoQ=	1,25E+08 mm^4			

S		
S beam n=	3,09E+07	mm^3
S KertoS =	2,98E+07	mm^3
S KertoQ =	2,32E+07	mm^3

G		
G beam =	315,00	mm
G KertoS=	667,50	mm
G KertoQ=	768,00	mm
G sec hom=	521,98	mm

Isec=	1,88E+10	mm^4
x =	309,02	mm

Another procedure to calculate the inertia is presented below:
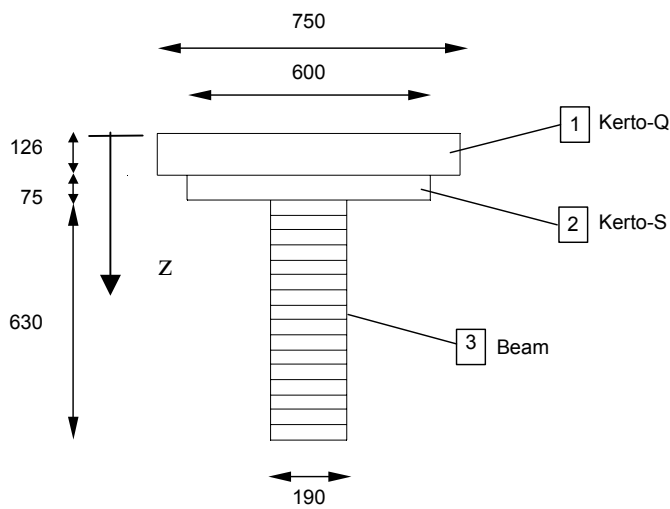
E_1 = 10500 Mpa   A_1 = 94500 mm2
E_2 = 13800 Mpa   A_2 = 45000 mm2
E_3 = 13500 Mpa   A_3 = 119700 mm2

                   A_TOT = 259200 mm2

z_1 = 63 mm
z_2 = 163,5 mm
z_3 = 516 mm

z_G = 309,016304

Part	h [mm]	b [mm]	A [mm2]	E [GPa]	EA [Mm]	z_i [mm]
1	126	750	94500	10,5	992250	63
2	75	600	45000	13,8	621000	163,5
3	630	190	119700	13,5	1615950	516

Total Values: 3,23E+06

Part	$E_i I_i$ [KN*m2]	EAz_i [MN*m]	$z_N - z_i$ [mm]	$(z_N - z_i)^2$ [mm2]	$EA (z_N - z_i)^2$ [KNm2]
1	1,31E+09	6,25E+07	246,0	60524	6,01E+10
2	2,91E+08	1,02E+08	145,5	21175	1,31E+10
3	5,34E+10	8,34E+08	-207,0	42842	6,92E+10

Total Values: 5,51E+10   9,98E+08   1,42436E+11

APPENDIX G: calculations regarding SLS, comparisons between codes

The load combination to adopt in the design in SLS is define as follow (Eurocode 5, part1-1, point 4.1):

(2) Combinations of actions for serviceability limit states should be calculated from the expression

$$\Sigma G_{k,j} + Q_{k,1} + \sum_{i>1} \psi_{1,i} \; Q_{k,i} \qquad (4.1a)$$

where the partial coefficients: $\gamma_Q = 1.00 \; \Psi_{1,1} = 0 \; \gamma_G = 1.00$

The same load combination is found following BKR at point 2:321

Table c. Prescribed combinations of actions 8 and 9 associated with the partial factor γ_f and with the values of actions for a structure in the serviceability limit states.

Action	Combination of actions	
	8	9
Permanent actions G_k	1.0 G_k	1.0 G_k
Variable action		
One variable action with the characteristic value Q_k	1.0 Q_k	–
Other variable actions with the frequent value ψQ_k	1.0 ψQ_k	–
All variable actions with the frequent value ψQ_k	–	1.0 ψQ_k

Combination of actions 8 shall be applied in design with respect to permanent damage in the serviceability limit states.

Swedish codes BKR

The deformation of a timber member is influenced by creep and moisture. In the calculations this is taken in account reducing the mean value of the modulus of elasticity by the factor k_s, which depends on the service class and the load duration class (BKR, 5:322):

:322[57] Design values of material properties

The design values in the serviceability limit states shall be determined in accordance with general formula (a) below:

$$E_d = \frac{\kappa_s\, E_k}{\gamma_m} \tag{a}$$

NOTATION

E_d	design value of material property
κ_s	modification factor which takes account of service class and the load duration class. Unless some other value is shown to be valid, the values of κ_s given in Tables (a) – (c) below for structural timber, glued laminated timber and structural boards shall be used
E_k	characteristic value for calculations in the serviceability limit states, e.g. E_k (or G_k) for calculations of deformations in accordance with Subsection 5:23
γ_m	partial factor for material properties which may be put equal to 1.0 in the serviceability limit states

Table a. Modification factor κ_s for calculation of the deformations of structural timber and glued laminated timber

Load duration class[1]	Service Classes 0 och 1	Service Class 2	Service Class 3
P	0.55	0.45	0.3
A	0.65	0.55	0.4
B	0.8	0.7	0.55
C	1.0	0.9	0.8

[1] P, A, B and C denote load duration classes as set out in Subsection 5:22.

Table b. Modification factor κ_s for calculation of the deformations of structural plywood

Load duration class[1]	Service Classes 0 och 1	Service Class 2	Service Class 3
P	0.55	0.5	0.3
A	0.65	0.6	0.4
B	0.8	0.7	0.55
C	1.0	0.9	0.8

---

[57] The amendment means inter alia that the last sentence in the definition of κ_s is deleted.

The values of k_s to use for the two types of load and the three different materials involved are:

	Kerto-Q®	Kerto-S®	Glulam
P loads :	0,5	0,5	0,45
C loads :	0,9	0,9	0,9

The modulus of elasticity E_d to use in the calculation of the deflection becomes:

	Kerto-Q®	Kerto-S®	Glulam
$E_{k,mean}$ [MPa]	10500	13800	13000
E_d - C loads [MPa]	5250	6900	5850
E_d - P loads [MPa]	9450	12420	11700

Three final deflections δ_p, δ_l and δ_v must be calculate.

δ_p is the final deflection due to permanent loads

δ_l is the final deflection due to variable live loads

δ_v is the final deflection due to variable service vehicle load

All of them must not be greater than the maximum value allowed $\delta_{max} = \dfrac{L}{400} = 37.5mm$, where L is the span of the bridge, which is equal to 15.00m.

The deflection due to evenly distributed loads is calculated by using the formula of Theory of elasticity: $\delta = \dfrac{5}{384} \cdot \dfrac{q \cdot l^4}{E \cdot I}$. In particular for the three deflections to consider:

$$\delta_p = \frac{5}{384} \cdot \frac{q \cdot l^4}{E_{d,KertoQ,P-loads} \cdot I_{P-loads}}$$

$$\delta_l = \frac{5}{384} \cdot \frac{q \cdot l^4}{E_{d,KertoQ,C-loads} \cdot I_{C-loads}}$$

The Inertia of the transformed section I depends on the modulus of elasticity of the three materials, and therefore is influenced by the duration of loads. Using values of Table 5.6, three modular ratios related to permanent loads and three modular ratios related to short-term loads are calculated:

P loads $\Longrightarrow$ $n_1 = \dfrac{KertoQ}{KertoQ} = 1,00$ $n_2 = \dfrac{KertoS}{KertoQ} = 1,31$ $n_3 = \dfrac{GL32c}{KertoQ} = 1,11$

C loads $\Longrightarrow$ $n_1 = \dfrac{KertoQ}{KertoQ} = 1,00$ $n_2 = \dfrac{KertoS}{KertoQ} = 1,31$ $n_3 = \dfrac{GL32c}{KertoQ} = 1,24$

Thus, inertias of the transformed section in Kerto-Q® are:

$$I_{P-loads} = 1.72E + 10mm^4$$

$$I_{C-loads} = 1.83E + 10mm^4$$

Leaving out at the moment the amount of deflection due to shear, δ_p and δ_l are verified:
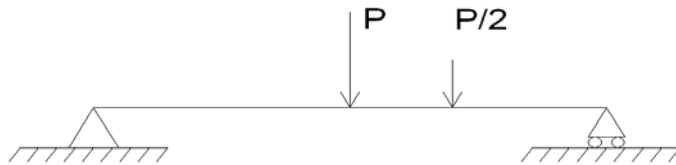
$$\delta_p = 36.34mm < 37.50mm \qquad \text{OK} \quad 96.91\%$$

$$\delta_l = 18.98mm < 37.50mm \qquad \text{OK} \quad 50.63\%$$

To calculate δ_v another formula is used: the maximum deflection of a simple supported beam due to a concentrated load applied in the middle of the span is:

$$\delta = \frac{1}{48} \cdot \frac{P \cdot l^3}{2 \cdot E \cdot I}$$

The significant load combination to assumed is the one with the service vehicle placed with the heavier wheel axle in the middle of the span:

In addition to the deflection caused by load P, the deflection caused by the load P/2 placed 4.5m from the right support should be counted. This second one can be expressed as:

$$\delta = \frac{4}{5} \cdot \frac{1}{48} \frac{(P/2) \cdot l^3}{2 \cdot E \cdot I}$$

Also in this case the amount of deflection due to shear is not taken in account. The vehicle load is placed symmetrically in the transversal direction, so that the load of each wheel axle is equally divided on the two beams. The deflection δ_v results:

$$\delta_v = 22.68mm < 37.50mm \qquad \text{OK} \quad 60.48\%$$

Deflection verification according to EC5

The increase of deformation due to creep and moisture are taken in account by the use of the factor k_{def} (Eurocode 5, part 1-1, point 4.1):

(4) The final deformation, u_{fin}, under an action should be calculated as

$$u_{fin} = u_{inst} (1 + k_{def})$$ (4.1b)

where k_{def} is a factor which takes into account the increase in deformation with time due to the combined effect of creep and moisture. The values of k_{def} given in Table 4.1 should be used.

When dealing with composite sections made by materials with different creep properties, each stiffness modulus should be reduced by the appropriate factor $(1 + k_{def})$ (Eurocode 5, part 1-1, point 4.1):

(5) The final deformation of an assembly fabricated from members which have different creep properties should be calculated using modified stiffness moduli, which are determined by dividing the instantaneous values of the modulus for each member by the appropriate value of $(1 + k_{def})$.

Furthermore, the contribution to the total deflection due to loads with different load-duration classes are to be calculated separately, because k_{def} depends on the load-duration class itself (Eurocode 5, part 1-1, point 4.1):

(6) If a load combination consists of actions belonging to different load duration classes, the contribution of each action to the total deflection should be calculated separately using the appropriate k_{def} values.

The values of k_{def} for glued laminated timber and plywood can be found in the following table (Eurocode 5, part 1-1, point 4.1):

Table 4.1 — Values of k_{def} for timber, wood-based materials and joints

Material/load-duration class	Service class		
	1	2	3
Solid timber[a] glued laminated timber			
Permanent	0,60	0,80	2,00
Long-term	0,50	0,50	1,50
Medium-term	0,25	0,25	0,75
Short-term	0,00	0,00	0,30
Plywood			
Permanent	0,80	1,00	2,50
Long-term	0,50	0,60	1,80
Medium-term	0,25	0,30	0,90
Short-term	0,00	0,00	0,40

Concerning this design, the service class is the second and the types of load to chose from are Permanent load and Short-term load. The mean values of stiffness modulus, the values of k_{def} for short load and permanent load, and the correspondent reduced values of stiffness modulus to be used in SLS calculations can be found in Table belove for all the three materials of interest:

	Glulam GL32c	Kerto-Q®	Kerto-S®
E_{mean}	13500 MPa	10500 MPa	13800 MPa
G_{mean}	845 MPa	600 MPa	600 MPa
K_{def} PERMANENT LOADS	0.80	1.00	1.00
K_{def} SHORT-TERM LOADS	0.00	0.00	0.00
E_d PERMANENT LOADS	7500 MPa	5250 MPa	6900 MPa
E_d SHORT-TERM LOADS	13500 MPa	10500 MPa	13800 MPa
G_d PERMANENT LOADS	469 MPa	300 MPa	300 MPa
G_d SHORT-TERM LOADS	845 MPa	600 MPa	600 MPa

Table above: Mean values of stiffness modulus, values of k_{def} for short loads and permanent loads, correspondent design values of stiffness modulus to be used in SLS calculations for glulam GL32c, Kerto-Q® and Kerto-S®

Comparing the factors that reduce the characteristic modulus of elasticity calculated following the two different codes: $\dfrac{1}{\left(1+k_{def}\right)}$ from the Eurocode with $\dfrac{k_s}{\gamma_m}$ from Swedish codes BKR

it can be noticed how they are very close:

		Eurocode 5	Swedish codes BKR
Glulam	PERMANENT LOADS	0.56	0.45
	SHORT-TERM LOADS	1.00	0.90
Plywood	PERMANENT LOADS	0.50	0.50
	SHORT-TERM LOADS	1.00	0.90

Table above: Comparison between the modification factors of the Eurocode and of the Swedish codes

The values of the deflection calculated with the two codes are therefore very close too. Instead the limitations imposed by Eurocode are less strict compared to those of the Swedish codes (eurocode 5, part 1-1, point 4.3.1):

4.3.1 Beams

(1) The components of deflection are shown in Figure 4.3.1, where the symbols are defined as follows:

u_0 precamber (if applied)

u_1 deflection due to permanent loads

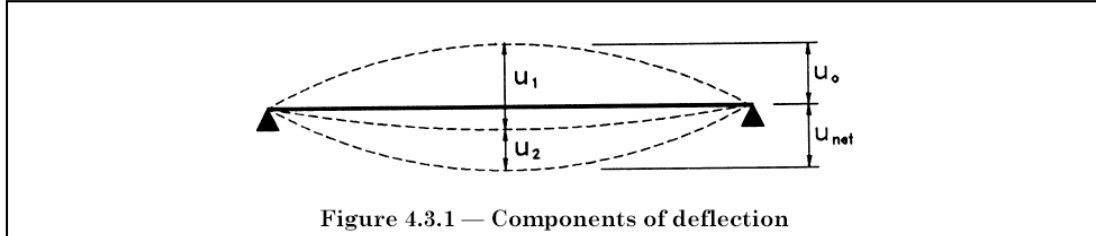u_2 deflection due to variable loads

Figure 4.3.1 — Components of deflection

The net deflection below the straight line joining the supports, u_{net}, is given by

$$u_{net} = u_1 + u_2 - u_0 \tag{4.3.1}$$

(2) In cases where it is appropriate to limit the instantaneous deflections due to variable actions, the following values are recommended unless special conditions call for other requirements:

$$u_{2,\,inst} \le \ell/300 \quad \text{(cantilever } \ell/150) \tag{4.3.2}$$

where ℓ is the beam span or the length of a cantilever.

(3) In cases where it is appropriate to limit the final deflection, u_{fin}, the following values are recommended unless special conditions call for other requirements:

$$u_{2,\,fin} \le \ell/200 \quad \text{(cantilever } \ell/100) \tag{4.3.3}$$

$$u_{net,\,fin} \le \ell/200 \quad \text{(cantilever } \ell/100) \tag{4.3.4}$$

Three verifications should be done:

final net-deflection must be lower than $\dfrac{L}{200} = 75mm$

final deflection only due to variable loads must be lower than $\dfrac{L}{200} = 75mm$

instantaneous deflection only due to variable loads must be lower than $\dfrac{L}{300} = 50mm$

Also the contribution due to shear is taken into account in the calculation of deflection. In case of uniformly distributed loads (permanent loads and live loads) it is used the formula: $\delta = \chi \cdot \dfrac{q \cdot l^2}{8 \cdot G \cdot A}$ (5.6)

where χ is equal to 1.20

In case of the service vehicle load, the deflection due to shear is taken as the 10% of the deflection due to bending.

To calculate the deflection appropriate values of Inertia and Area of the transformed composite section must be used. Therefore the values of modular ratios are needed:

Permanent load

$$\frac{E\ Kerto\ Q}{E\ Kerto\ Q} = 1,00 \qquad \frac{G\ Kerto\ Q}{G\ Kerto\ Q} = 1,00$$

$$\frac{E\ Kerto\ S}{E\ Kerto\ Q} = 1,31 \qquad \frac{G\ Kerto\ S}{G\ Kerto\ Q} = 1,00$$

$$\frac{E\ Glulam}{E\ Kerto\ Q} = 1,43 \qquad \frac{G\ Glulam}{G\ Kerto\ Q} = 1,56$$

Variable load

$$\frac{E\ Kerto\ Q}{E\ Kerto\ Q} = 1,00 \qquad \frac{G\ Kerto\ Q}{G\ Kerto\ Q} = 1,00$$

$$\frac{E\ Kerto\ S}{E\ Kerto\ Q} = 1,31 \qquad \frac{G\ Kerto\ S}{G\ Kerto\ Q} = 1,00$$

$$\frac{E\ Glulam}{E\ Kerto\ Q} = 1,29 \qquad \frac{G\ Glulam}{G\ Kerto\ Q} = 1,41$$

Final Deflection:

Permanent load

I section = 2,01E+10 mm^4

A section = 3,25E+05 mm^2 A section(shear amount) = 3,27E+05 mm^2

Variable load

I section = 1,88E+10 mm^4

A section = 3,08E+05 mm^2 A section(shear amount) = 3,08E+05 mm^2

Instantaneous Deflection:

I section = 1,88E+10 mm^4

A section = 2,59E+05 mm^2

Both in the final and instantaneous deflection variable loads are considered. Live load and service vehicle load must be taken into account, but in two different verifications.

Final net-deflection (variable load = live load)

u1,fin

u1,fin_bending =	31,28	mm
u1,fin_shear =	1,72	mm
u1,fin =	33,00	mm

u2,fin

u2,fin_bending =	19,47	mm
u2,fin_shear =	1,07	mm
u2,fin =	20,54	mm

Final deflection :

Utot,fin =	53,54	mm	**OK**	**<**	75,00	mm	71,39%

verified even without precambering

Final net-deflection (variable load = service vehicle load)

u1,fin

u1,fin_bending =	31,28	mm
u1,fin_shear =	1,72	mm
u1,fin =	33,00	mm

u2,fin

u2,fin_bending =	19,94	mm
u2,fin_shear =	1,99	mm
u2,fin =	21,93	mm

Final deflection :

Utot,fin =	54,94	mm	**OK**	**<**	75,00	mm	73,25%

verified even without precambering

The final deflections are verified even without considering the precambering. Therefore the final deflections $u_{2,fin}$ due only to variable loads are verified:

Final deflection only due to the variable load "live load"

u2,fin =	20,54	mm	**OK**	**<**	75,00	mm	27,38%

Final deflection only due to the variable load "Service vehicle load"

u2,fin =	21,93mm**OK<**75,00mm29,24%

Finally, the instantaneous verifications are considered:

Instantaneous deflection only due to the variable load "live load"

$u_{2,inst\_bending}$ =   19,50   mm

$u_{2,inst\_shear}$ =   1,27   mm

$u_{2,inst}$ =   20,77   mm   **OK**   <   50,00   mm   41,53%

Instantaneous deflection only due to the variable load "Service vehicle load"

$u_{2,inst\_bending}$ =   19,97   mm

$u_{2,inst\_shear}$ =   2,00   mm

$u_{2,inst}$ =   21,96   mm   **OK**   <   50,00   mm   43,93%

As for the Swedish codes BKR, also following the Eurocode the most significant verifications are those related to the final deflection.